
**Arsenic dispersion associated with the
Barbrook gold mine in the Mpumalanga
Province of South Africa**

by

Ruth Lanyon

BSc.(Hons) (La Trobe University), PhD. (University of Tasmania)

A dissertation submitted in partial fulfilment of the requirements
for the degree of Master of Science in Environmental Geochemistry
Department of Geological Sciences
University of Cape Town
December, 1996

[Faint, illegible text, likely a library stamp or archival mark]

The copyright of this thesis vests in the author. No quotation from it or information derived from it is to be published without full acknowledgement of the source. The thesis is to be used for private study or non-commercial research purposes only.

Published by the University of Cape Town (UCT) in terms of the non-exclusive license granted to UCT by the author.

ABSTRACT

Arseniferous sulphide-hosted gold deposits associated with the Barberton greenstone belt, located in the Mpumalanga province of South Africa, have been mined on various scales since late last century. The Barbrook mine is located close to the Swaziland border in an area of the Barberton mountainlands which forms part of the Kaap subcatchment of the Crocodile River. Scattered small communities depend on local streams and boreholes in the area for drinking and irrigation water. Hence, the prime motivation for this study was the potential risk to human health associated with enhanced As mobility as a result of the sulphide mineral weathering which accompanies gold mining and processing. Sampling of local waters, soils and sediments, as well as the ore and waste rock at Barbrook was undertaken during a week of fieldwork in August 1996. A range of chemical analyses were performed on the various samples, including As analysis by hydride generation-atomic absorption spectroscopy and inductively coupled plasma - mass spectrometry.

The Barbrook ore bodies are structurally controlled and hosted by banded iron formation, carbonaceous shales and carbonate-bearing schists. Within these ore bodies, As is mainly associated with auriferous arsenopyrite (FeAsS), although minor amounts also occur within pyrite (FeS_2) and ullmannite (NiSbS). Of the streams which flow through the mining lease, those at most risk of As contamination are Barbrook Creek, Low's Creek and Crystal Stream. Low's Creek flows through the main mine area, adjacent to the level 10 mine adit entrance, and past the processing plant before converging with Barbrook Creek. The latter receives water from the Shiyalongubo Dam which is the main water source for the area. Immediately downstream of the level 10 mine adit entrance, the steep eastern bank of Low's Creek is lined for several hundred metres with waste rock containing low grade ore. Tailings material from the processing plant is pumped to two tailings dams located about 5 km to the northwest of the plant and close to Crystal Stream.

High As concentrations (up to 4.12 mg/L), compared to the World Health Organisation's proposed upper limit of 0.01 mg As/L for drinking water, are mainly associated with bodies of standing water located on the tailings dams and the stream of tailings extending between them. Liming of the tailings during processing operations, plus the presence of carbonates within the host rocks, has resulted in neutral to alkaline pH values (7.0 to 11.0) for these waters, which are also highly enriched in SO_4^{2-} (>1100 mg/L) and have EC values ≥ 240 mS/cm. Seepage from the base of the slimes dam wall contains up to 1.64 mg As/L and the lowest pH values (6.0 to 6.7) recorded in the Barbrook area. Although it is highly unlikely that the tailings dam water bodies would be used by the local human

population for domestic purposes, their use as waterholes by cattle and birds was observed, and past contamination of Crystal Stream (up to 0.039 mg As/L) has been recorded.

By comparison with the tailings dam water, Barbrook Creek and Low's Creek are characterised by a more neutral pH (7.0 to 7.9), lower EC (≤ 7.5 mS/cm) and lower concentrations of As (≤ 0.007 mg/L), SO_4^{2-} , Na^+ , Mg^{2+} and Ca^{2+} . The only exception occurs immediately downstream of the gold processing plant, where Low's Creek has a slightly elevated EC value (18.5 mS/cm) and higher concentrations of As (0.011 mg/L) and other ionic constituents compared to the samples collected both upstream, within the mine site, and downstream, after the convergence with Barbrook Creek. Some discharge from the processing plant is suspected, although it appears to have been either diluted further downstream and/or attenuated by the Low's Creek sediments. Therefore, although the apparent discharge from the processing plant requires immediate attention, the Barbrook and Low's creek waters are currently suitable for domestic and agricultural use by the local population, in accordance with the South African water quality guidelines.

Groundwater in the vicinity of the tailings dams contains negligible amounts of As (≤ 0.002 mg/L). By comparison, the groundwater entering the level 10 mine adit in the vicinity of the Barbrook ore bodies is interpreted to have been naturally enhanced with As (0.012 mg/L) due to sulphide oxidation at depth. The abstraction of groundwater for local domestic use means that As levels need to be carefully monitored, particularly in view of the fact that fluctuating groundwater levels, possibly on a seasonal basis, have been reported in the scientific literature as causing variable As concentrations. At the time of sampling, in August 1996, one borehole in the tailings dam area did contain high NO_2^- (21.7 mg/L) and total N ($\text{NO}_2^- + \text{NO}_3^- = 8.22$ mg/L N), which would make it unsuitable for domestic use.

Arsenic and heavy metal contamination was detected in soils at the base of the slimes seepage pond, adjacent to the main slimes dam, and beneath the waste rock pile. The latter indicates that, contrary to the results of the standard toxicity characteristic leaching procedure (TCLP) which showed that leachate produced by two waste rock samples at pH 5 contained negligible As, downward leaching of As through the waste rock pile is occurring under the prevailing neutral to alkaline conditions. Since the sediment cores collected from the tailings dams comprise both tailings material and underlying soil, it is not possible to discern if leaching has occurred, and As and heavy metal enrichment is interpreted to be mainly due to the presence of primary sulphides. The occurrence of heavy metals, such as Zn, Mn, Fe and Ni within secondary sulphate, oxide and aluminosilicate mineral precipitates associated with the waste rock pile, however, suggests that heavy metals may also be associated with secondary mineralisation resulting from the oxidation of the tailings material. Since no As was detected in any of the secondary minerals analysed, despite being hosted by pyrite in the waste rock pile, the mobility of As may be more greatly enhanced under the current neutral to alkaline conditions than that of the heavy metals.

MINTEQA2 modelling of the data for Barbrook water samples with As contents ≥ 0.01 mg/L indicates that only the stream of tailings extending between the two tailings dams (4.12

mg As/L) is approaching equilibrium with respect to $\text{Ca}_3(\text{AsO}_4)_2$, which is stated in the literature to be the most stable arsenate mineral under oxidising, alkaline conditions. However, positive tentative correlations between the extractable As and total Ca and CaCO_3 contents of the Barbrook soils and sediments suggest that high As concentrations within the tailings dam sediments may be linked to the carbonate fraction. This would correlate with reports in the literature that As sorption by calcite increases from pH 6 to 12. The oversaturation of the tailings dam waters with respect to calcite and dolomite, as modelled by MINTEQA2, suggests that As could also be immobilised via coprecipitation with calcite.

Although Barbrook currently represents a well-buffered system, the lowered pH values associated with water seeping from the base of the main slimes dam wall could be an indication of the potential for acid mine drainage. The possible future occurrence of acid mine drainage from the tailings dams and waste rock pile will depend on their buffering capacity as progressive sulphide oxidation results in increasing acidification. Whereas an initial decrease in pH would be expected to result in increased heavy metal mobility, the maximum reported sorption of As(V) by Fe and Al oxides at pH 4 to 5 might result in decreased As mobility.

A tentative interpretation of pH and Eh data for the Barbrook water samples is that most of the As is present as As(V). Assuming that the Shortlands soil form is representative of the red, clay-rich soils which are common in the Barbrook area, an investigation into As(V) and P sorption by a Shortlands red-structured B horizon was undertaken in order to investigate its potential for As attenuation. The results indicated that both As and P sorption define similar H-shaped isotherms which can be mathematically described by either the Langmuir or the van Bemmelen-Freundlich equations. Therefore, whereas the Shortlands subsoil would have a high adsorptive capacity for As or P at low adsorbate concentrations, the soil surfaces would become swamped at high adsorbate concentrations resulting in reduced sorption. Although the high clay content of the Shortlands subsoil is dominated by kaolinite, the hematite and goethite detected by X-ray diffractometry would be expected to dominate anion sorption. Not only do the results of this study indicate a high loading capacity for As (3490 mg/kg) in the Shortlands soil, dictating its potential usefulness for the lining of effluent dams or seepage sites, but the similarity in the sorption behaviour of As and P means that abundant information regarding P sorption in a range of South African soils can potentially be used to predict their As sorption capacity.

Apart from the need to prevent further discharge from the processing plant into Low's Creek, the main concerns at Barbrook relate to the apparent As enrichment of the groundwater in the vicinity of the mine site, the intermittent As contamination of Crystal Stream and the planned cyanide heap leaching of the disused open cut mines, the latter representing a process already found to have caused gross environmental damage in the United States. Otherwise, most of the sites of potential As and heavy metal dispersion at Barbrook simply require careful monitoring during the lifetime of the mine and well-planned closure and remediation strategies.

ACKNOWLEDGEMENTS

I would like to thank the following people for their assistance and/or advice with regards to the completion of this dissertation:

- 🍏 The Caledonia Mining Corporation of Toronto, Canada, for funding this investigation and allowing me to undertake field work in the Barbrook area
- 🍏 My supervisor Dr. Martin Fey for his valued scientific input into this project and his enthusiastic assistance with fieldwork
- 🍏 Dr. Heather Jamieson for organising the project with the Caledonia Mining Corporation
- 🍏 Associate Professor James Willis for advice in the planning stages as well as with XRFS soil analyses
- 🍏 Mike Begg and Ronnie Masuku for assistance during fieldwork in the Barbrook area
- 🍏 Mike and Ann Begg for generously accommodating me in Nelspruit
- 🍏 Ernest Small and Shireen Govender for assistance with XRFS analyses
- 🍏 Patrick Sieas for assistance with HPIC analyses
- 🍏 Heather Dodds, Tom Nowicki and Antoinette Upton for advice and assistance as regards general laboratory work
- 🍏 Jake Pressly from the Anglo-American Research Laboratories for his information and patient assistance as regards the performance of the TCLP waste rock analyses
- 🍏 Dane Gerneke for his enthusiastic help and advice with the SEM analyses of the secondary mineral precipitates
- 🍏 Miranda Waldron and William Williams from assistance with SEM sample preparation and the development of the SEM photos, respectively
- 🍏 Bruce Cairns and Eric Bryce for enthusiastically organising vital bits and pieces for field and laboratory work
- 🍏 Hugh Ballard and John Tyler from the Scientific Services branch of the Cape Town City Council for performing the HG-AAS As analyses on the Barbrook water samples
- 🍏 Willem Kirsten and Mira Sobczyk from the Institute for Soil Climate and Water for promptly performing a range of soil analyses
- 🍏 Marian Mackay from the Chemistry Department at the University of Cape Town for performing ICP-AES on the Barbrook water samples
- 🍏 Suzanna Vasik from the Department of Chemical Engineering at the University of Cape Town for AAS and BET surface area analyses
- 🍏 David Wilson for making polished thin sections of the Barbrook ore rock at a moment's notice

- 🍏 Associate Professor Loewenthal from the Department of Civil Engineering at the University of Cape for his advice with redox measurements
- 🍏 Lewis McCaffrey for his expert advice as regards F^- analysis in the Barbrook water samples
- 🍏 Dick Rickard for his assistance with the electron microprobe analysis of the primary sulphide minerals
- 🍏 Leon van Heerden for helping me sort out my computer problems
- 🍏 Dr. Hartwig Frimmel for the use of his office during the writing-up stage
- 🍏 Isobelle Lathwaite for sorting out all the bills
- 🍏 Johann Lanz for his interpretation of the Barbrook soil textures
- 🍏 The computing centre for Water Research (CCWR) at the University of Natal, Pietermaritzburg, for access to MINTEQA2 software

In addition I would like to thank the 1996 Environmental Geochemistry MSc. class for an interesting year and an extremely enjoyable mid-year fieldtrip. The late night chat and coffee sessions with Justin Pooley and the friendship and "sisterhood" provided by Mieke van Tienhoven will be sorely missed. And finally my appreciation is extended to my friends and family for their enthusiasm regarding my return to study and their tolerance at my lack of spare time. To my parents, a special thank-you for your support and financial assistance (yet again!).

TABLE OF CONTENTS

ABSTRACT	i
ACKNOWLEDGEMENTS	iv
LIST OF FIGURES	xi
LIST OF TABLES	xiv

CHAPTER 1: Background information

1.1 Introduction.....	1
1.2 The Barbrook gold mine.....	2
1.2.1 Location and physiography.....	2
1.2.2 Local climate.....	3
1.2.3 Regional and local geology.....	3
1.2.4 Past and present mining and processing operations at Barbrook.....	6
1.3 Aims of this study.....	7

CHAPTER 2: When does arsenic in gold mine leachates represent a threat to human health and how can it be remediated?: A literature review

2.1 Introduction.....	8
2.2 Aims of this review.....	8
2.3 Arsenic chemistry.....	9
2.4 Arsenic occurrence in soils.....	9
2.4.1 Arsenic concentrations in natural and contaminated soils.....	9
2.4.2 Factors affecting the chemical behaviour of arsenic in soils.....	11
2.4.2.1 Redox potential and pH.....	11
2.4.2.2 Fe, Al and Mn oxide content.....	13
2.4.2.3 Clay and organic matter content.....	16
2.4.2.4 Microbial activity.....	16
2.5 Arsenic occurrence in aquatic sediments.....	17
2.5.1 Factors affecting the chemical behaviour of arsenic in aquatic sediments.....	17
2.5.2 The diagenetic cycling of arsenic in aquatic sediments.....	17
2.6 Arsenic occurrence in natural waters.....	18

2.6.1 Factors affecting the chemical behaviour of arsenic in water.....	19
2.6.1.1 Redox and pH conditions.....	19
2.6.1.2 Microbial activity.....	19
2.6.2 Factors causing thermodynamic disequilibrium of arsenic speciation in water.....	21
2.7 Environmental arsenic contamination associated with mining.....	22
2.7.1 The geochemistry of arsenic release during mining operations.....	22
2.7.2 Examples of arsenic dispersion from gold mining operations.....	23
2.7.3 Potential risks to human health from arsenic dispersion associated with mining.....	25
2.8 Human arsenic consumption.....	25
2.8.1 Arsenic as an essential element.....	25
2.8.2 Arsenic as a toxic element.....	26
2.8.2.1 Arsenic toxicity as a function of its chemical speciation.....	26
2.8.2.2 Arsenic toxicity as a function of its uptake in drinking water.....	27
2.8.2.3 Factors which may increase the toxic effects of arsenic.....	29
2.9 The remediation of environmental arsenic contamination.....	30
2.9.1 The removal of arsenic from water via coagulation, coprecipitation or adsorption.....	30
2.9.2 The treatment of arsenic-bearing mine wastes.....	31
2.10 Conclusions.....	32

CHAPTER 3: An assessment of arsenic release into the Barbrook environment

3.1 Introduction.....	33
3.2 Sampling sites.....	33
3.2.1 Barbrook tailings dam area.....	33
3.2.2 Barbrook mining area.....	43
3.3 Sampling and analytical methods.....	49
3.3.1 Water samples.....	49
3.3.2 Soil and sediment samples.....	50
3.3.3 Rock samples.....	50
3.4 Analytical results from the Barbrook area.....	51
3.4.1 Water samples.....	51
3.4.1.1 Tailings dam area.....	51
3.4.1.2 Mining area.....	56
3.4.1.3 Comparison of the results from the Barbrook tailings dam and mining areas.....	58
3.4.1.4 MINTEQA2 modelling of Barbrook water data.....	61

3.4.2 Soil and sediment samples.....	64
3.4.2.1 Tailings dam area.....	64
3.4.2.2 Mining area.....	65
3.4.3 Waste rock samples.....	66
3.4.4 Primary and secondary mineral samples.....	67
3.4.4.1 Primary sulphide minerals.....	67
3.4.4.2 Secondary minerals and precipitates.....	69
3.5 Discussion.....	76
3.5.1 Water quality in the Barbrook area.....	76
3.5.1.1 Tailings dam area.....	76
3.5.1.2 Mining area.....	78
3.5.2 The chemistry of the Barbrook soils and sediments.....	80
3.5.2.1 Tailings dam area.....	80
3.5.2.2 Mining area.....	82
3.5.3 The chemistry of the Barbrook waste rock pile.....	82
3.5.4 Arsenic in the Barbrook environment.....	83
3.5.4.1 Arsenic occurrence in the Barbrook water bodies.....	84
3.5.4.2 Arsenic speciation and toxicity in the Barbrook water bodies....	86
3.5.4.3 Arsenic occurrence in the Barbrook soils and sediments.....	89
3.5.4.4 Arsenic occurrence in association with the Barbrook waste rock pile	92
3.5.5 Is there a current or potential problem at Barbrook?.....	93
3.5.5.1 Acid mine drainage.....	93
3.5.5.2 Arsenic dispersion.....	95
3.5.5.3 Other potential problems.....	96
3.6 Conclusions and recommendations.....	97

CHAPTER 4: A preliminary assessment of the potential for arsenic sorption by the Shortlands soil in the Barbrook area

4.1 Introduction.....	100
4.2 Previous sorption studies.....	101
4.3 Sampling location and soil description.....	103
4.4 Analytical methods.....	104
4.4.1 Characterisation of the Shortlands soil in the Barbrook area.....	104
4.4.2 Phosphorus sorption experiment.....	105
4.4.3 Arsenic sorption experiment.....	105
4.5 Results and discussion.....	105
4.5.1 Characterisation of the Shortlands soil in the Barbrook area.....	105
4.5.2 Phosphorus sorption.....	110

4.5.3 Arsenic sorption.....	114
4.5.4 Comparison and interpretation of arsenic and phosphorus sorption.....	115
4.5.5 Implications for the mediation of As dispersion at Barbrook.....	120
4.6 Conclusions.....	122

REFERENCES.....	123
------------------------	------------

APPENDIX 1: Analytical methods used for the Barbrook water samples

A1.1 Electrical conductivity (EC).....	138
A1.2 pH measurements.....	139
A1.3 Alkalinity measurements.....	139
A1.4 Redox potential.....	140
A1.5 Cation and anion concentrations.....	141
A1.6 Silica concentrations.....	145
A1.7 Phosphorus concentrations.....	148
A1.8 ICP-AES analyses.....	150
A1.9 Arsenic concentrations.....	150
A1.10 Fluoride concentrations.....	152

APPENDIX 2: Analytical methods used for the Barbrook soil and sediment samples

A2.1 pH measurements.....	153
A2.2 Calcium carbonate content.....	153
A2.3 Extractable arsenic concentrations.....	154
A2.4 XRFs major and trace element determinations.....	155
A2.5 Exchangeable acidity and exchangeable cation concentrations.....	156
A2.6 Organic carbon content.....	158
A2.7 Soluble salt concentrations.....	160
A2.8 Separation of the clay fraction and XRD mineralogical analysis.....	161
A2.9 Soil water content.....	162
A2.10 Extractable Fe, Al and Mn.....	162
A2.11 Phosphorus sorption index.....	163
A2.12 Particle size distribution.....	164
A2.13 Specific surface area.....	165

APPENDIX 3: Analytical methods used for the Barbrook rock and mineral samples

A3.1 Calcium carbonate content.....	166
A3.2 XRFS major and trace element determinations.....	166
A3.3 Toxicity characteristic leaching procedure (TCLP).....	166
A3.4 Electron microprobe sulphide mineral analysis.....	167
A3.5 SEM secondary mineral analysis.....	167

APPENDIX 4: Analytical methods used for the arsenic and phosphorus sorption experiments

A4.1 Phosphorus sorption experiment.....	168
A4.2 Arsenic sorption experiment.....	171

LIST OF FIGURES

CHAPTER 1:

Figure 1.1 View of the Barbrook mining area.....	2
Figure 1.2 Maps showing the location of the Barbrook mine lease in southern Africa.....	4
Figure 1.3 Map showing the relative locations of the Barbrook gold mine and tailings areas.....	5

CHAPTER 2:

Figure 2.1 Sequence of reduction reactions involved in the biomethylation of As.....	10
Figure 2.2 Eh-pH diagram for the system As-H ₂ O.....	12
Figure 2.3 Eh-pH diagram for the system As-O-H.....	13
Figure 2.4 Relative stability of a range of metal arsenates under varying pH conditions... 14	
Figure 2.5 Effect of redox and pH on the stability of As(III) oxides and As(III) sulphides... 15	
Figure 2.6 Proposed transformations of Fe and As in the sediments of Lake Okahuri, New Zealand.....	18
Figure 2.7 Eh-pH diagram for As at 25°C and one atmosphere.....	20
Figure 2.8 Mole fraction distribution of arsenic acid species as a function of pH.....	21

CHAPTER 3:

Figure 3.1 Plan of the Barbrook calcine and slimes dams showing sampling localities.....	35
Figure 3.2 Pool of standing water on the calcine dam.....	36
Figure 3.3 Thickener overflow pond at Barbrook gold processing plant.....	37
Figure 3.4 Dual streams of black tailings material emerging from the calcine dam wall.....	37
Figure 3.5 Black stream of tailings extending between the calcine and slimes dams.....	38
Figure 3.6 View of the slimes dam looking south towards the calcine dam wall.....	39
Figure 3.7 Collection of sample of the slimes dam sediments in front of the southern slimes dam pond.....	39
Figure 3.8 View of the main slimes dam wall.....	40
Figure 3.9 Water seeping from broken clay pipe at the base of the slimes dam wall.....	40
Figure 3.10 Puddle of upwelling water near the base of the slimes dam wall.....	41
Figure 3.11 Sampling groundwater from boreholes located west of the base of the slimes dam wall.....	41
Figure 3.12 Collecting a sediment core from the slimes seepage pond.....	42

Figure 3.13 Collecting a sediment core from Crystal Stream.....	42
Figure 3.14 View of the slimes dam showing cattle drinking from the southern slimes dam pond as well as wind erosion of the tailings.....	43
Figure 3.15 Map of the Barbrook mining area showing the location of sampling sites.....	45
Figure 3.16 Entrance to the level 10 mine adit.....	46
Figure 3.17 Low's creek adjacent to the level 10 mine adit entrance.....	46
Figure 3.18 View of Shiyalongubo dam.....	47
Figure 3.19 View of Barbrook Creek, looking north.....	47
Figure 3.20 Low's Creek adjacent to the waste rock pile.....	48
Figure 3.21 Pond in the disused Clifford Scott open cut mine.....	48
Figure 3.22 XRD scans of copper thiocyanate precipitates.....	55
Figure 3.23 Plots of chemical parameters which distinguish the water samples from the tailings dam and mining areas.....	59
Figure 3.24 Piper diagram showing the relative compositions of the water samples from the tailings dam and mining areas.....	60
Figure 3.25 Photomicrograph of part of the Barbrook ore body showing pyrite, chalcopyrite, galena and ullmannite.....	68
Figure 3.26 Photomicrograph of part of the Barbrook ore body showing intergrown pyrite and arsenopyrite.....	68
Figure 3.27 Scanning electron microscopy EDS X-ray spectra for secondary minerals from the waste rock pile.....	70
Figure 3.28 Scanning electron microscopy backscattered electron image of a needle-like secondary sulphate mineral.....	73
Figure 3.29 Scanning electron microscopy backscattered electron image of secondary white anhydrous sulphate minerals and Fe oxides.....	74
Figure 3.30 Scanning electron microscopy backscattered electron image of an Fe and Mg-bearing aluminosilicate mineral.....	74
Figure 3.31 Scanning electron microscopy backscattered electron image of another aluminosilicate mineral.....	75
Figure 3.32 Scanning electron microscopy backscattered electron image of pyrite cubes.....	75
Figure 3.33 Measured Eh-pH values for the Barbrook water samples superimposed on an Eh-pH diagram.....	87
Figure 3.34 Plots of extractable As versus total As, Fe, Ca and Pb as well as %CaCO ₃ and pH(KCl).....	91

CHAPTER 4:

Figure 4.1 XRD pattern for the clay fraction of Shortlands soil sample BS5.....	109
Figure 4.2 Plot of sorbed P versus the pH and EC of each of the BS5 filtrates.....	111

Figure 4.3 Phosphorus sorption curve for Shortlands soil sample BS5.....	112
Figure 4.4 Linear expressions of the BS5 P sorption data according to the Langmuir and van Bemmelen-Freundlich equations.....	113
Figure 4.5 Plot of sorbed As versus the pH and EC of each of the BS5 filtrates.....	115
Figure 4.6 Arsenic sorption curve for Shortlands soil sample BS5.....	116
Figure 4.7 Linear expressions of the BS5 As sorption data according to the Langmuir and van Bemmelen-Freundlich equations.....	117
Figure 4.8 Phosphorus and arsenic sorption curves determined for the Barbrook Shortlands soil sample BS5.....	118

APPENDIX 1:

Figure A1.1 Silica calibration curve derived for the standard solutions.....	148
Figure A1.2 Phosphorus calibration curve derived for the standard solutions.....	149

APPENDIX 4:

Figure A4.1 Phosphorus calibration curve derived for the standard solutions.....	169
Figure A4.1 Phosphorus calibration curve derived for the second set of standard solutions.....	170

LIST OF TABLES

CHAPTER 2:

Table 2.1 The effects on human health of As intake in drinking water.....	29
---	----

CHAPTER 3:

Table 3.1 List of samples collected from the Barbrook tailings dam area and gold processing plant.....	34
Table 3.2 List of samples collected from the Barbrook mining area.....	44
Table 3.3 Electrical conductivity, total dissolved solids, pH and redox measurements for water samples collected from the Barbrook tailings dam area.....	52
Table 3.4 Cation concentration data for water samples collected from the Barbrook tailings dam area.....	53
Table 3.5 Anion concentration data for water samples collected from the Barbrook tailings dam area.....	53
Table 3.6 Total arsenic, fluoride and silica data for the water samples collected from the Barbrook tailings dam area.....	54
Table 3.7 ICP-AES elemental concentration data for the water samples collected from the Barbrook tailings dam area.....	54
Table 3.8 Electrical conductivity, total dissolved solids, pH and redox measurements for water samples collected from the Barbrook mining area.....	56
Table 3.9 Cation concentration data for water samples collected from the Barbrook mining area.....	57
Table 3.10 Anion concentration data for water samples collected from the Barbrook mining area.....	57
Table 3.11 Total arsenic, fluoride and silica data for the water samples collected from the Barbrook mining area.....	58
Table 3.12 ICP-AES elemental concentration data for the water samples collected from the Barbrook mining area.....	58
Table 3.13 Saturation indices calculated by MINTEQA2 for water samples collected from the Barbrook tailings dam area.....	62
Table 3.14 Saturation indices calculated by MINTEQA2 for water samples collected from the Barbrook processing plant.....	62
Table 3.15 Saturation indices calculated by MINTEQA2 for water samples collected	

from the Barbrook mining area.....	62
Table 3.16 Analytical data for the soils and sediment samples collected from the Barbrook tailings dam area.....	65
Table 3.17 Analytical data for the soils and sediment samples collected from the Barbrook mining area.....	66
Table 3.18 Analytical data for the waste rock samples collected from the Barbrook mining area.....	67
Table 3.19 Results of the toxicity characteristic leaching procedure for the waste rock samples.....	67
Table 3.20 Chemical analyses of sulphide minerals within the Barbrook ore bodies.....	69
Table 3.21 Summary of the water target quality guidelines for South Africa.....	77
Table 3.22 Summary of average concentrations of heavy metals in unpolluted soils.....	81
Table 3.23 Arsenic data for previous water analyses performed in the Barbrook mining area since February 1995.....	86

CHAPTER 4:

Table 4.1 Description of the Barbrook Shortlands soil sampling site.....	103
Table 4.2 Analytical data for the Shortlands subsoil.....	106
Table 4.3 Results of various extraction procedures performed on the Shortlands subsoil.....	108
Table 4.4 X-ray diffractometry results for the Shortlands soil sample BS5.....	109
Table 4.5 Phosphorus sorption results for the Shortlands soil sample BS5.....	110
Table 4.6 Phosphorus sorption data used in the Langmuir and van Bemmelen-Freundlich equations.....	114
Table 4.7 Arsenic sorption results for the Shortlands soil sample BS5.....	114
Table 4.8 Arsenic sorption data used in the Langmuir and van Bemmelen-Freundlich equations.....	116

APPENDIX 1:

Table A1.1 Results of triplicate electrical conductivity readings for the Barbrook water samples.....	138
Table A1.2 Results of triplicate pH readings for the Barbrook water samples.....	139
Table A1.3 Results of duplicate alkalinity measurements for the Barbrook water samples.....	140
Table A1.4 Comparison of the measured and expected HPIC results for four cation standard solutions.....	142
Table A1.5 Comparison of the measured and expected HPIC results for four anion standard solutions.....	143

Table A1.6 Repeat HPIC analyses of anion standard AN2.....	143
Table A1.7 Duplicate HPIC analyses for some Barbrook water samples.....	144
Table A1.8 Anion-cation charge balance results for the Barbrook water samples.....	144
Table A1.9 Silica results for the Barbrook water samples.....	147
Table A1.10 Results of duplicate ICP-AES analyses for Barbrook water sample BW10.....	150
Table A1.11 Results of replicate HG-AAS analyses of two As standard solutions.....	151
Table A1.12 Results of replicate HG-AAS As analyses of the Barbrook water samples.....	152

APPENDIX 2:

Table A2.1 Results of duplicate CaCO ₃ measurements for the Barbrook soil and sediment samples.....	154
Table A2.2 Results of the standard and duplicate As analyses by ICP-MS.....	155
Table A2.3 Instrumental conditions for routine XRF trace element analysis.....	156
Table A2.4 XRF trace element data for two international standard reference materials.....	156
Table A2.5 Results of replicate blank and sample KCl extractable acidity measurements on Shortlands soil sample BS5.....	157
Table A2.6 Measured and recalculated AAS base cation results for Shortlands soil sample BS5.....	158
Table A2.7 Results obtained for sample BS5 during the determination of soil organic C content.....	159
Table A2.8 Anion-cation charge balance results for the HPIC analyses of the BS5 saturated paste extract.....	160
Table A2.9 Soil water content results for sample BS5.....	162

APPENDIX 3:

Table A3.1 Results of duplicate CaCO ₃ measurements for the Barbrook waste rock samples.....	166
--	-----

APPENDIX 4:

Table A4.1 Measured P sorption results for the BS5 filtrates.....	169
Table A4.2 Measured P sorption results for the second set of BS5 filtrates.....	171
Table A4.3 Results of the standard As analyses by ICP-MS.....	172

CHAPTER 1

Background information

1.1 Introduction

Although there is growing evidence that arsenic (As) may be an essential trace element for humans (Emsley, 1985; Uthus, 1992), its toxic effects, including the fact that it is a recognised human carcinogen (Mass, 1992), mean that its ingestion in anything above normal background levels is highly undesirable. Due to the occurrence of As within over 200 naturally occurring minerals (Onken and Hossner, 1995), a range of human activities have the ability to enhance its release into the environment. Of increasing concern on a world-wide scale is the potential for environmental As contamination as a result of the mining of ore bodies which contain As-bearing minerals. The exposure and leaching, within tailings dumps, waste rock piles and mine workings, of this previously buried material means that the bioavailability of As may be increased within local soils, groundwaters and surface run-off. Such mining related environmental As pollution is of particular concern in terms of the long term deleterious health effects which may result from the ingestion of As-contaminated food and water supplies by the local inhabitants.

The common occurrence of As-bearing sulphide minerals within the gold deposits of the Barberton greenstone belt of northeastern South Africa means that this area is potentially subject to environmental As contamination as a result of gold mining activities. One such gold deposit within the Barberton area, the Barbrook deposit, forms the location for this investigation. Although small scale mining commenced in the area in the 1880's, the recent history of the Barbrook deposit has involved a series of larger scale operations interrupted by mine closures and subsequent takeovers. The 1995 acquisition of the Barbrook mining lease by the Canadian based Caledonia Mining Corporation, and their proposed early to mid-1996 resumption of on-site gold processing, necessitated the performance of an environmental management programme report (EMPR) under the South African Minerals Act of 1991. This report was completed in January 1996 according to the guidelines stipulated by the Department of Mineral and Energy Affairs in order to gain the necessary authorisation to mine and process gold. In keeping with their environmental concerns, the Caledonia Mining Corporation have also undertaken intermittent analyses of the various water bodies in the Barbrook mining area since February 1995. The results, revealing some consistently high levels of As relative to WHO (1993) drinking water standards, have prompted the instigation and funding of the current investigation.

1.2 The Barbrook gold mine

1.2.1 Location and physiography

The Barbrook gold mine lease extends over an area of approximately 40 km². Its location, within the Barberton mountainlands of northeastern South Africa (Figure 1.1), lies within the lowveld area of the province of Mpumalanga, immediately adjacent to the border of Swaziland (Figure 1.2). The nearest major towns in this area are Barberton, 55 km to the west, and Nelspruit, 65 km to the northwest. The Barberton area is one of deeply incised mountains and rolling hills which exceed heights of 1400 m in places and are dominated by vegetation types belonging to the Savanna biome (DWAF, 1995a). According to the Barbrook Mines EMPR (Ralph Morris and Associates, 1996), the dominant soil forms in the Barbrook area are Hutton, Glenrosa and Mispah, although the Shortlands form has also been identified during the course of the current study (Chapter 4).



Figure 1.1: View of the Barbrook mining area within the Barberton mountainlands; note the prominent chimney stack associated with the gold processing plant and the scars on the mountains produced by open cut mining activities.

The Barbrook mining lease, located within the Kaap subcatchment of the Crocodile River catchment (DWAF, 1995a) is drained by three major streams (Figure 1.3). Of particular interest to this study are the northward flowing Low's Creek and Crystal Stream. Low's Creek passes through the main mining area near the number 10 mine adit, joins with the Kaap River ~16 km below the mine lease, and then drains into the eastward flowing Crocodile River ~7 km further downstream. Crystal Stream drains the western part of the mine lease in the area of the tailings dam and joins the Kaap River ~12 km upstream from the Low Creek - Kaap River confluence. The third major stream, Mhlambangathi Stream, which flows in a northeasterly direction from the eastern part of the Barbrook mining area, was not sampled during the course of this study and therefore does not warrant further mention. Another minor creek which has been sampled, however, is the Barbrook Creek. This creek extends between the Shiyalongubo Dam, located in the mountains above the mine, and Low's Creek, draining into the latter just downstream of the gold processing plant at Barbrook (Figure 1.3).

Groundwater flow within the Barbrook region has been affected by past mining activities, resulting in lowered but variable water table levels (~500 to 670 m above mean sea level) throughout the area (Ralph Morris and Associates, 1996). Within the actual mine site, dewatering has generally occurred to the level of the number 10 mine adit, 597 m above mean sea level, from where discharge occurs into nearby Low's Creek. Water levels within boreholes around the Barbrook area vary from ~5 to 30 m below the land surface. Although the Shiyalongubo Dam supplies most of the irrigation and domestic water, via Barbrook and Low's Creeks, for the area immediately adjacent to, and downstream of, the mine, local groundwater is also abstracted for industrial and domestic purposes.

1.2.2 Local climate

The climate in the Barbrook Lowveld region (as summarised by Ralph Morris and Associates, 1996) is one of summer rains and high humidity with average daily temperatures of 18 to 30°C. Average daily temperatures for the winter months are 8 to 23°C with clear sunny days representing the norm. The average annual rainfall for the region is ~500 to 700 mm, falling mainly between November and March.

1.2.3 Regional and local geology

Both the regional geology of the Barberton area and the more localised geology of the Barbrook mine site have been documented by Houstoun (1990), a brief summary of which will be included here. The regional geology is dominated by the Archaean Barberton greenstone belt which comprises a fold and thrust belt of metamorphosed ultramafic, mafic

and silicic volcanic rocks, turbidites and shallow-water sediments ranging in age from 3.5 to 3.2 Ga. Gold mineralisation within the Barberton area is structurally-controlled such that the numerous ore deposits occur along shear zones. Due to the widespread association of submicroscopic gold with sulphides such as arsenopyrite and pyrite, the dominant gold precipitating mechanism is believed to be the sulphidation of Fe-rich wall rocks.

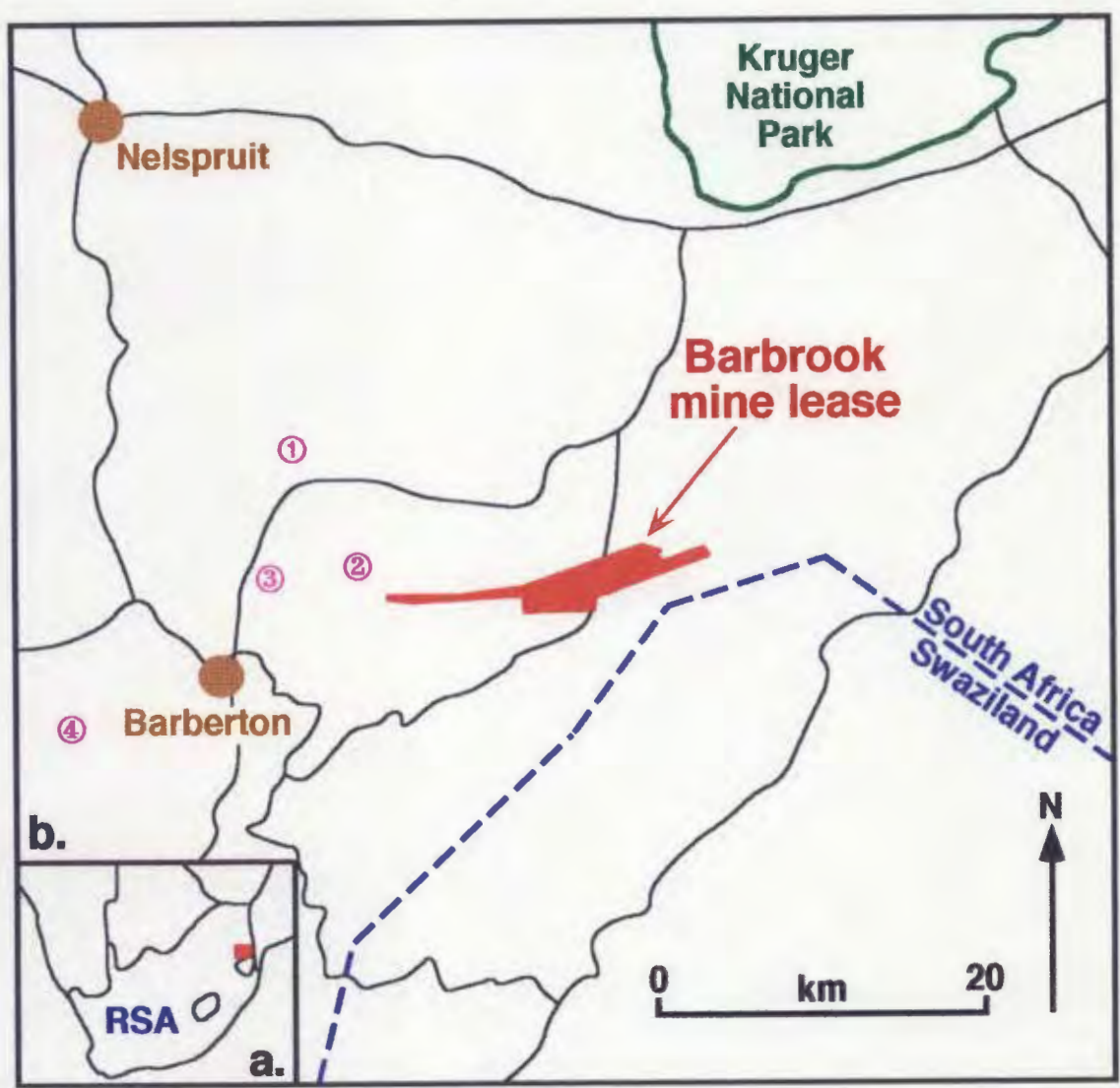


Figure 1.2: a) Map of southern Africa showing the location of the Barberton area in South Africa (RSA); and b) location of the Barbrook gold mine lease relative to the major towns, roads and other operating gold mines in the area: 1. Consort, 2. Sheba, 3. Fairview and 4. Agnes (modified after Ralph Morris and Associates, 1996).

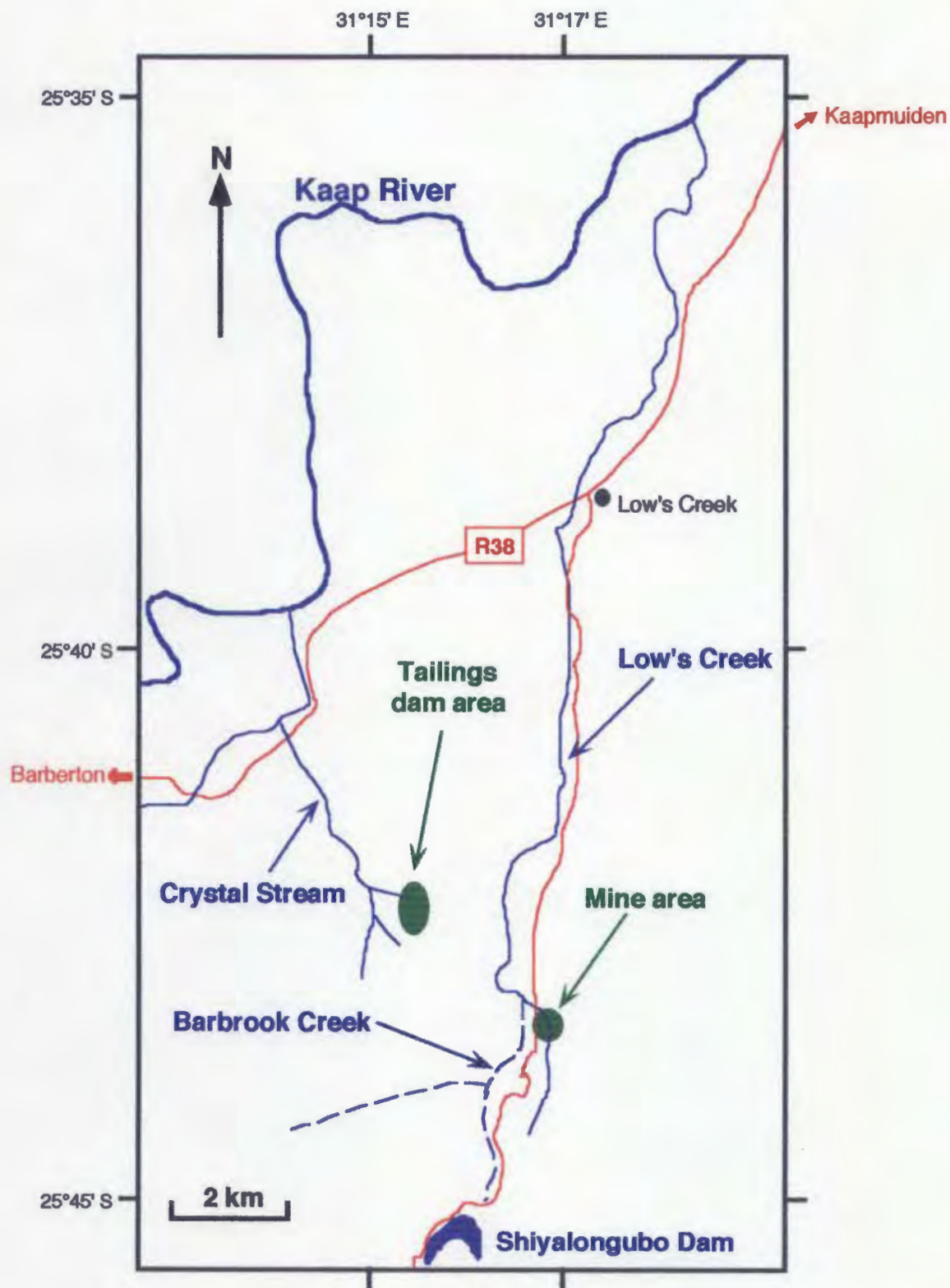


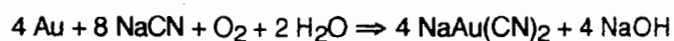
Figure 1.3: Location of the Barbrook gold mine and tailings dam areas relative to the major streams and roads in the area; adapted from the 1:50 000 topographic maps published by the South African Department of Surveys and Mapping - 2531CA Sheba (1984), 2531CB Kaapmuiden (1984) and 2531CD Shiyalongubo (1985).

The Barbrook deposit comprises two parallel east-northeast to west-southwest striking 'lines' of Archaean mesothermal gold mineralisation, the Barbrook Line and the Swartkoppie Line. These lines represent 500 to 600 m wide zones of intense deformation located at the contact between the meta-volcanics of the upper Onvervacht Group (Swartkoppie Formation) and the stratigraphically superior greywackes and shales of the lower Fig Tree Group (Sheba Formation), the latter forming a 700 m wide syndinal fold, the Barbrook syncline, in between the Barbrook and Swartkoppie lines. Gold mineralisation, occurring as pods and lenses along the Barbrook and Swartkoppie lines, is associated predominantly with disseminated arsenopyrite (FeAsS) plus, to a lesser extent, pyrite (FeS₂), pyrrhotite (Fe₇S₈ - FeS) and base metal sulphides including galena (PbS), sphalerite (ZnS), chalcopyrite (CuFeS₂) and minor stibnite (Sb₂S₃). The mineralisation is hosted by sheared and intercalated banded iron formation (BIF), carbonaceous shale, grey talc-carbonate and chlorite-carbonate±quartz schists, green fuchsite-carbonate-quartz schist and chert.

1.2.4 Past and present mining and processing operations at Barbrook

Past mining activities at Barbrook have included both open cut mining of the oxidised ore zone and underground mining of sulphide-hosted gold mineralisation. Open cut mines located in the mountains above the current mine site are now largely abandoned although plans for future heap leaching of these pits are outlined in the Barbrook Mines EMPR (Ralph Morris and Associates, 1996). Current mining activities are concentrated in the level 10 and 7 mine adits which intersect a number of distinct ore bodies associated with both the Barbrook and Swartkoppie Lines.

Although on-site gold processing at Barbrook previously involved roasting of the sulphide concentrate from the ore, this step has now been eliminated with the resumption of gold processing in mid-1996. The current method of mineral processing involves gold extraction via cyanide (CN⁻) leaching and gold recovery via the carbon-in-pulp (CIP) process. The general method, described by Funke (1990), involves the addition of NaCN and CaO to crushed rock from the ore pile. Whereas the lime is added to ensure protective alkalinity, the NaCN is added to oxidise and dissolve the gold. Although the CN⁻ ion is not actually an oxidant, it does complex with the gold to reduce its oxidation potential such that the dissolved O₂ in water can act as a strong enough oxidant to dissolve the gold (Edwards *et al.*, 1995). Therefore, the dissolution of the gold occurs via the reaction (Smith, 1994):



Following its dissolution and separation from the host rock, the gold is then precipitated out of solution via the addition of granulated activated carbon and the cyanide-bearing water and tailings are pumped to the tailings dam. Further extraction of the gold from the carbon is obtained using a combination of chemical and electrolytic processes.

1.3 Aims of this study

As a whole, this study has two main aims. The primary aim is to determine if past and present mining and/or processing operations at the Barbrook gold mine are resulting in the release of As into the surrounding environment at levels which may present a potential health threat to the local human population (Chapter 3). The second, and subordinate aim, is to assess the ability of one of the main soil types in the Barbrook area, the Shortlands soil form, to adsorb As and therefore potentially attenuate its dispersion into the local environment (Chapter 4). Background information regarding the complex chemistry of As and its effects on human health is included in the literature review presented in Chapter 2.

CHAPTER 2

When does arsenic in gold mine leachates represent a threat to human health and how can it be remediated? A literature review

2.1 Introduction

Arsenic (As) is known to be present within over 200 naturally-occurring minerals (Onken and Hossner, 1995). Some 60% of these minerals are arsenates whereas 20% are sulphides and sulphosalts (complex sulphides) and the remainder comprise a range of arsenides, arsenites, oxides and alloys (Baur and Onishi, 1978; Mitchell and Barr, 1995). Certain of these minerals, including arsenopyrite (FeAsS), orpiment (As₂S₃), realgar (AsS) and enargite (Cu₃AsS₄), may be mined specifically for the As which is used within pesticides and wood preservatives and as a growth promoter for pigs and poultry (O'Neill, 1995). However, the widespread association of a range of As-bearing sulphide minerals and oxidised metal arsenates (Irgolic, 1986) with Au, Ag, Pb, Zn and Cu deposits means that As may be released during the processing of these ores and is often present in mine waste and tailings dumps. The exposure and potential leaching of this previously buried As-bearing rock, within both the tailings dumps and the mines themselves, means that the bioavailability of As may be increased within local soils, groundwaters and surface run-off. However, the mobility, bioavailability and toxicity of As are all functions of its speciation and solubility, which are in turn dependent on a range of chemical, physical and biological factors.

2.2 Aims of this review

The complex chemistry of As dictates the need to examine how it behaves under a range of environmental conditions in order to assess and predict the possible impacts which may stem from the mining-related exposure of As-bearing material. The aims of this review, therefore, are:

1. to define the conditions under which As can be expected to be at its most mobile and toxic,
2. to examine the possible environmental and health risks associated with the release of As into the environment during mining, and
3. to examine possible remediation techniques for As-bearing aqueous leachates.

2.3 Arsenic chemistry

Arsenic, a metalloid element with an atomic number of 33, is represented by a single isotope of mass number 74.92. It has an outer electron configuration of $4s^2 4p^3$ and can occur in the 3+ (AsO_2^- = arsenite), 5+ (AsO_4^{3-} = arsenate), 0 (As(s) = metallic or solid arsenic) and 3- (AsH_3 = arsine gas) oxidation states (Baur and Onishi, 1978; Irgolic, 1986; McBride, 1994). The biological methylation of As involves a reduction sequence of As(V) to As(III) followed by the oxidative addition of one or more methyl (CH_3) species, as illustrated in Figure 2.1.

2.4 Arsenic occurrence in soils

2.4.1 Arsenic concentrations in natural and contaminated soils

In the absence of As contamination or mineralisation involving As-bearing minerals, O'Neill (1995) states that the natural levels of As in soils range from 1 to 40 mg/kg, with an average value of ~10 mg/kg, depending on the rock type from which that soil was derived. Chatterjee *et al.* (1993) present a similar range of 0.1 to 40 mg/kg in normal soils. Although most soils fall within the lower part of this range (O'Neill, 1995), with agricultural soils generally having As contents of between 1 and 20 mg/kg (Mitchell and Barr, 1995), it is possible, although rare, for several hundred ppm As to be present in uncontaminated soils (Mitchell, 1964; Schloemann, 1994). This may be due to the ranges of As within some rock types extending to quite high values: igneous and sedimentary rocks <1 to 15 mg/kg (average = 2 mg/kg), fine-grained argillaceous rocks (shales, mudstones and slates) <1 to 900 mg/kg (average = 10 to 15 mg/kg), sandstones and limestones <1 to 20 mg/kg, and phosphate rocks <1 to 200 mg/kg (O'Neill, 1995).

In a study of As contamination within soils associated with As-bearing gold-sulphide mineralisation at the Ashanti mine in Ghana, West Africa, Howell (1994) determined background levels for As in uncontaminated soils as 0.01 to 0.02 mg/kg and in soil porewater as 0.01 to 0.02 mg/L. Although these soil values are low compared to the average estimates for uncontaminated soils, O'Neill (1995) states that average soil porewater values are generally <0.01 mg/L. However, mineralisation involving As-bearing minerals or soil contamination resulting from As-containing pesticides, metal processing industrial effluents or mine wastes can significantly increase these levels such that As concentrations may exceed 1000 mg/kg soil (Howell *et al.*, 1994; Kavanagh *et al.*, 1996).

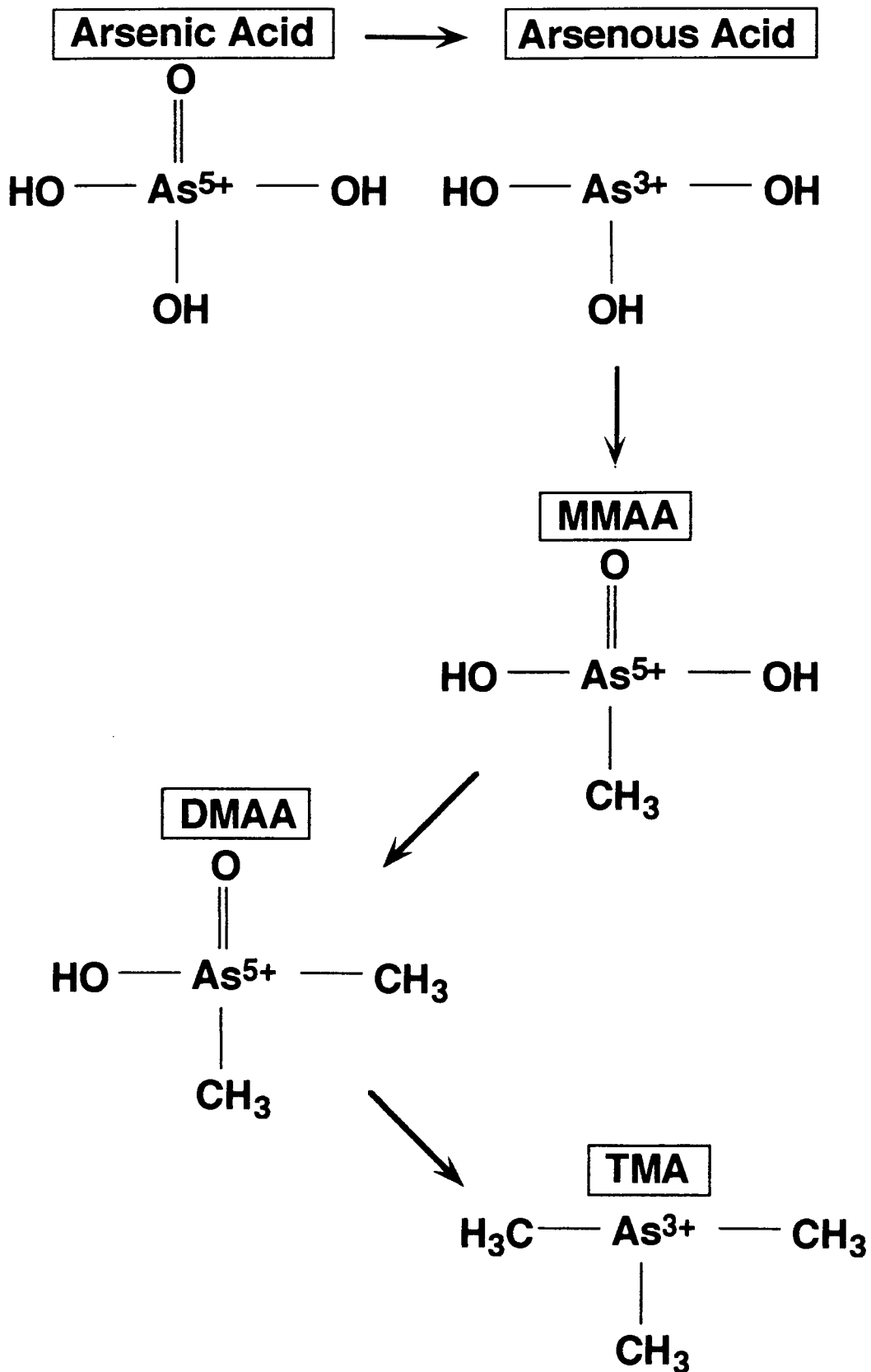


Figure 2.1: The sequence of reduction reactions involved in the biomethylation of As (after Thompson, 1993); MMAA = monomethylarsinic acid, DMAA = dimethylarsinic acid, TMA = trimethylarsine.

2.4.2 Factors affecting the chemical behaviour of arsenic in soils

The mobility, bioavailability and toxicity of As in soil depends on its solubility, which in turn reflects soil conditions such as redox potential, pH, clay content, organic matter content, microbial activity, and the presence and abundance of Fe, Al and Mn oxides and hydroxides (Pierce and Moore, 1982; Brannon and Patrick, 1987; Onken and Hossner, 1995). Complex interactions between this range of soil chemical and physical features means that no one factor can be treated in isolation when predicting the behaviour of As.

2.4.2.1 Redox potential and pH

According to the Eh-pH diagram of Masscheleyn *et al.* (1991) for the As-H₂O system (Figure 2.2), the most thermodynamically stable As species in soils within the pH range of 4 to 8, assuming that complexing species and methylating organisms are absent, are arsenous (As(III): H₃AsO₃) and arsenic (As(V): H₂AsO₄⁻, HAsO₄²⁻) acids, with As(s) representing the dominant species under the most reducing conditions. Arsine gas can only form if the soil solution is very reduced and acidic (Sadiq *et al.*, 1983). An Eh-pH diagram for the system As-O-H over a greater range of conditions (Bowell *et al.*, 1994) is presented in Figure 2.3. Whereas As(V) is the favoured oxidation state at higher redox potentials (Eh = +200 to +500 mV), such as occur under normal oxidising conditions at the Earth's surface (Haswell *et al.*, 1985; O'Neill, 1995), a decrease in redox potential results in the reduction of As(V) to As(III) via the reaction (Marin *et al.*, 1993):



In a series of experiments which involved equilibrating soil suspensions under controlled redox and pH conditions, Masscheleyn *et al.* (1991) found that the combination of an alkaline pH (pH = 8) and oxidising conditions resulted in a threefold increase in As solubility, almost all of which was As(V), as compared to its solubility at lower pH conditions. This was interpreted to be due to the increase in pH resulting in the replacement of As(V) by hydroxyl ions on the soil sorption sites, thereby releasing the negatively charged arsenic acid species (H₂AsO₄⁻ and HAsO₄²⁻) into solution. At the same alkaline pH but under reducing conditions, As(III) was the major dissolved species, although total As solubility was less than occurred during more acidic equilibrations. The increase in total As solubility which accompanies decreased pH is attributed to the increased dissolution of Fe oxides and hydroxides and the concurrent release of coprecipitated arsenate (Marin *et al.*, 1993).

The Eh-pH diagram of Masscheleyn *et al.* (1991) depicts the boundary between Fe(OH)₃ and Fe²⁺ to lie sub-parallel to the arsenic acid/arsenous acid boundary (Figure 2.2), thereby predicting that the reduction of Fe(III) to Fe(II) should be accompanied by the reduction of As(V) to As(III). However, as the rate of change in the oxidation state of As with

changes in Eh and pH conditions is variable, the measured proportions of As species in soil porewaters may not be as expected for those particular soil conditions (Marin *et al.*, 1993; O'Neill, 1995). Whereas As(III) can convert to As(V) within a matter of days under moderately oxidising conditions ($> +100$ mV) (Quastel and Scholefield, 1953; Deuel and Swoboda, 1972), the reduction of As(V) to As(III) may take several weeks (Takamatsu *et al.*, 1982). As a result, significant concentrations of thermodynamically unstable As(V) may be present under reducing conditions (Masscheleyn *et al.*, 1991). Therefore, although the increase in As solubility with decreased redox potential is often attributed solely to the reduction of As(V) to the generally more soluble As(III), it may actually be controlled by the reduction of ferric arsenates, and other forms of Fe(III) which are combined with arsenate, to a more soluble ferrous form rather than a change in the speciation of As itself (Deuel and Swoboda, 1972). Masscheleyn *et al.* (1991) also found that, under moderately reducing conditions (Eh = 0 to +100 mV), the solubility of As was controlled by the dissolution of Fe oxides and hydroxides.

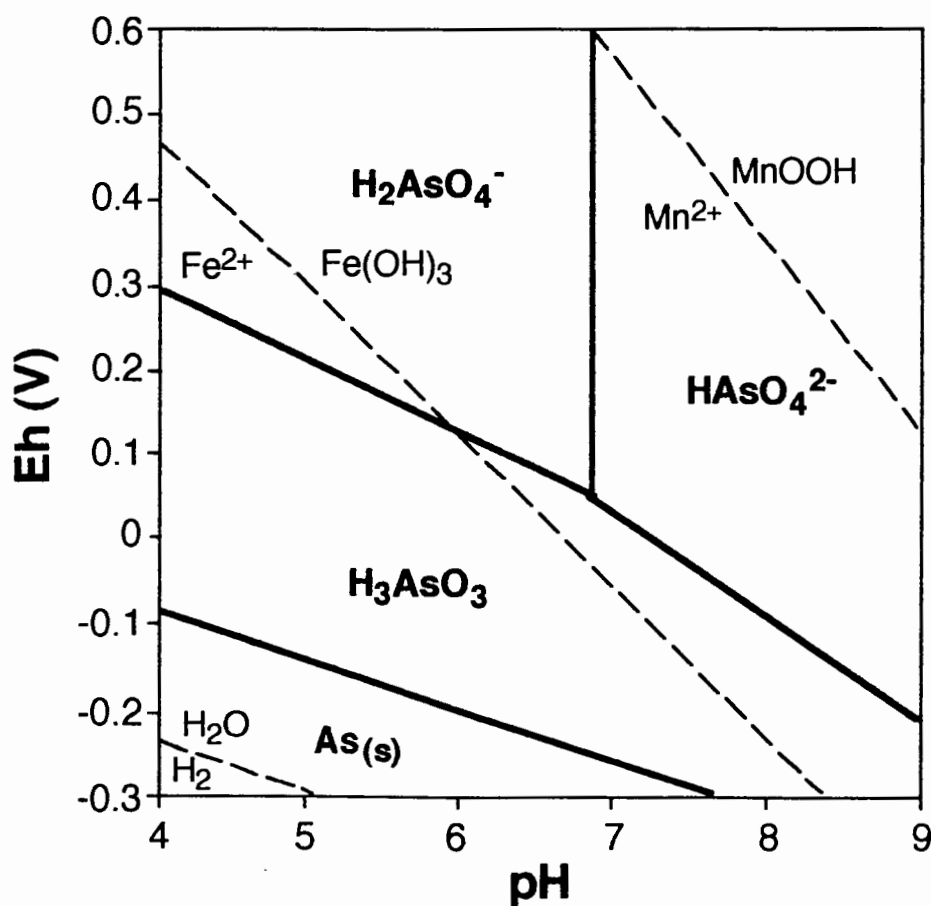


Figure 2.2: The Eh-pH diagram of Masscheleyn *et al.* (1991) for the system As-H₂O. The superimposed Mn and Fe redox couples are represented by dashed lines; activities of As, Mn and Fe were all taken to be 10⁻⁴ mol/L.

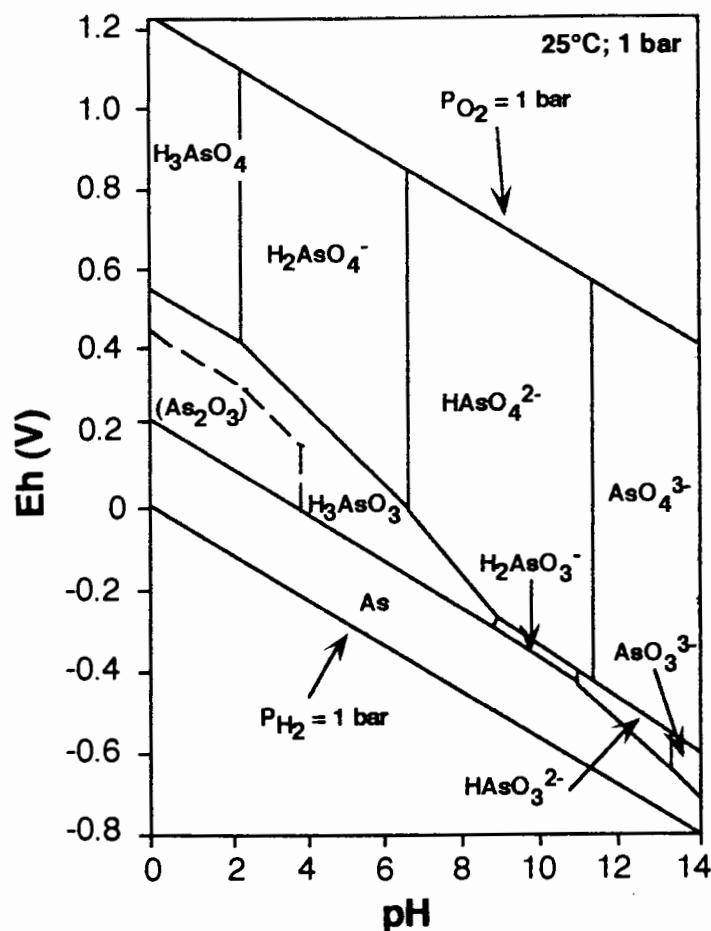


Figure 2.3: The Eh-pH diagram of *Bowell et al.* (1994) for the system As-O-H; the assumed activity of As is 10^{-5} mol/L.

2.4.2.2 Fe, Al and Mn oxide content

The fact that a significant correlation has been found between the K_d value¹ for As(III) and the dithionite²-extractable Fe content of a soil has been interpreted to show that the adsorption of As(III) within a soil, and therefore presumably the solubility of As, is controlled by the amorphous Fe oxide and hydroxide contents of the soil (Sakata, 1987). O'Neill (1995) states, however, that the sorption of As(V) is greater for both Al and Fe hydroxides than is the sorption of As(III). The sorption experiments of *Xu et al.* (1991), conducted over a pH range of 3 to 8, also showed that the overall adsorption of As(V) in soils was greater than that of As(III). Whereas the maximum sorption of As(III), as H_3AsO_3 , occurs at a pH of 7 to 8, the maximum adsorption of As(V), as H_2AsO_4^- , occurs at a significantly lower

¹ the K_d value (distribution coefficient) for As(III) is calculated as the ratio of the concentration of As(III) in solution relative to the concentration of adsorbed As(III)

² dithionite is used to extract metals bound specifically to Fe oxides (*Mitchell et al.*, 1994; cited in *Mitchell and Barr*, 1995)

pH of 4 to 5 (Gosh and Yuan, 1987; O'Neill, 1995). Yoshida *et al.* (1978; cited in Seyler and Martin, 1989) also cite an adsorption maximum for As(V) at a relatively low pH of 5.5, with a drastic decrease in sorption at both higher and lower pH values.

The behaviour of As in soil environments was examined by Sadiq *et al.* (1983) in terms of the thermodynamically predicted solubility relationships of a range of metal arsenates under changing soil solution conditions (Figure 2.4). They concluded that $\text{Ca}_3(\text{AsO}_4)_2$ was likely to be the most stable As mineral in well-oxidised, alkaline soils, followed by $\text{Mn}_3(\text{AsO}_4)_2$. The possibility that $\text{Mn}_3(\text{AsO}_4)_2$ may precipitate under more acidic and/or reducing soil conditions is predicted by both Sadiq *et al.* (1983) and Masscheleyn *et al.* (1991). In fact, Masscheleyn *et al.* (1991) state that where high concentrations of Mn are present under reduced soil conditions, the occurrence of thermodynamically unstable As(V) may also be due to the presence of a $\text{Mn}_3(\text{AsO}_4)_2$ phase. The association of As(V) with Mn under reducing conditions is a consequence of the extremely efficient oxidising ability of Mn for As(III) (Sullivan and Aller, 1996).

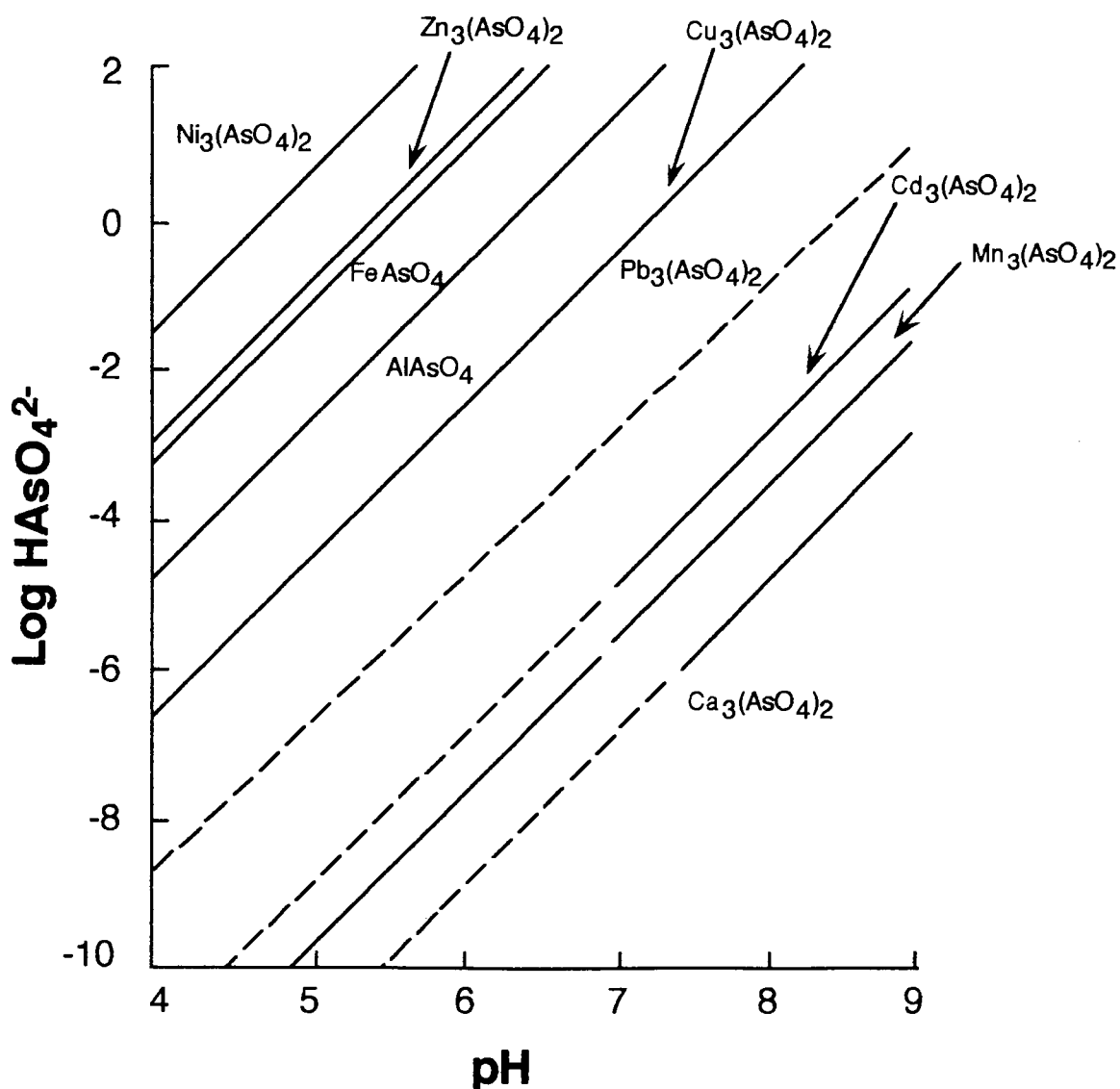


Figure 2.4: Diagram showing the relative stability of a range of metal arsenates under varying pH conditions, as determined by Sadiq *et al.* (1983); $\text{CO}_2(\text{g}) = 0.0003 \text{ atm}$.

The relative stabilities of As(III) oxides and As(III) sulphides in various soil environments were also examined by Sadiq *et al.* (1983), using $\text{Ca}_3(\text{AsO}_4)_2$ as an arsenate reference mineral (Figure 2.5). The results indicated that whereas As(III) oxides were relatively unstable at pH 7 as compared to the As(III) sulphides, even under reducing conditions, they are able to co-exist with sulphides at $\text{pH} \leq 6$. The As(III) sulphides, however, will only precipitate if the pH is >6 and the redox potential is low.

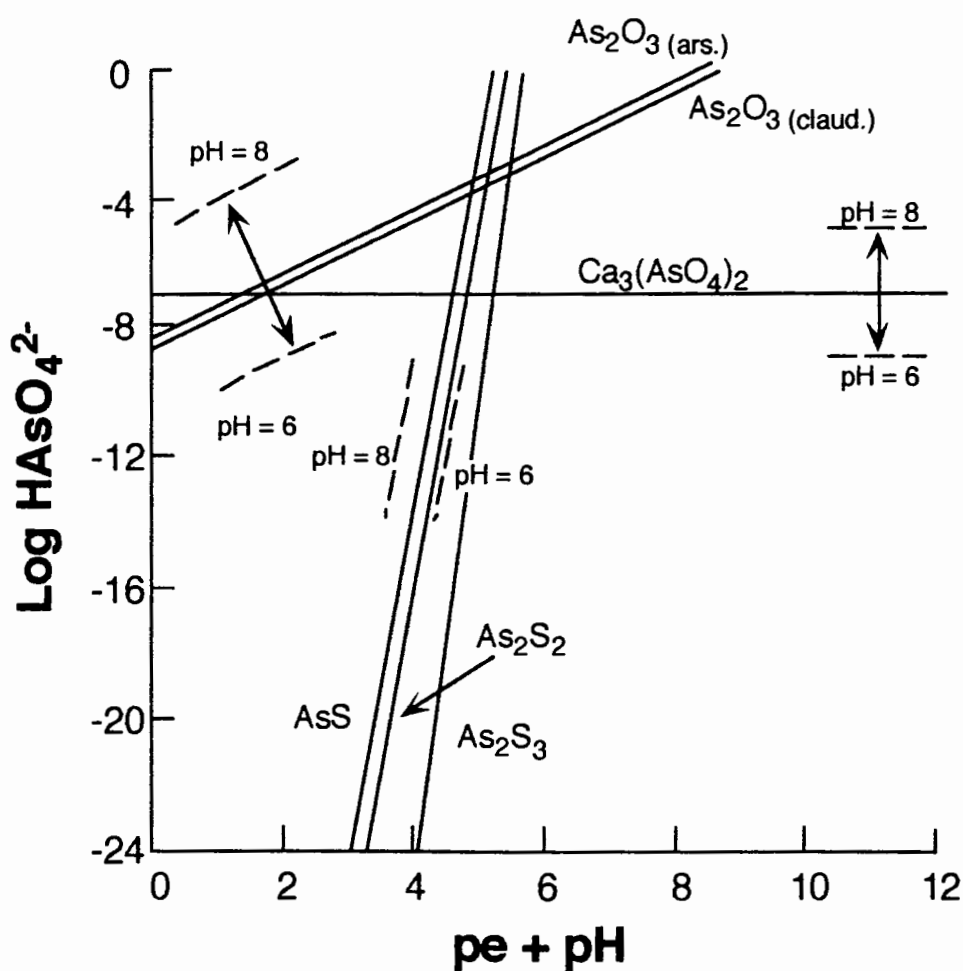


Figure 2.5: Diagram showing the effect of redox and pH on the stability of As(III) oxides and As(III) sulphides, as determined by Sadiq *et al.* (1983); $\text{CO}_2(\text{g}) = 0.003 \text{ atm}$. The As(III) oxides are arsenolite (ars.) and claudetite (claud.).

2.4.2.3 Clay and organic matter content

The fact that As can behave as an oxyanion with a similar adsorption behaviour to that of phosphate (O'Neill, 1995) means that it is easily adsorbed by minerals with Fe and Al coordination sites such as Al hydroxide, kaolinite, montmorillonite, goethite and ferrihydrite (Goldberg and Glaubig, 1988; Fuller *et al.*, 1993). Therefore the clay fraction (<2 µm particle size) of a soil is likely to be most enriched in As. However, As availability in soil is also partly controlled by organic matter content. The findings of Howell (1994), that high fulvic acid concentrations reduce As adsorption by Fe oxides, are consistent with the proposals that fulvic and humic acids increase the negative surface charge of Al and Fe oxides (Davis, 1982) and/or decrease As(V) adsorption by transforming the adsorbent minerals to organometallic complexes (Anderson *et al.*, 1982).

2.4.2.4 Microbial activity

Microbial activity in soils can result in a range of transformations involving As compounds. These transformations include the oxidation of As(III) to As(V) and the formation of a range of organoarsenical compounds via the biomethylation of As(III) (McBride, 1994; O'Neill, 1995). Although the biomethylation of As in soils is poorly studied, it appears that the activity of certain microorganisms and the type of As species they produce may be restricted by the pH conditions of the substrate (O'Neill, 1995). For example, whereas monomethylarsonic acid (MMAA) occurs mainly as monomethylarsonate ($\text{CH}_3\text{AsO}_2\text{OH}^-$) under normal soil pH conditions, the production of dimethylarsinic acid (DMAA) will change from its neutral form to its anionic form (dimethylarsinate: $(\text{CH}_3)_2\text{AsOO}^-$) at a pH close to 6. Although monomethylarsonates are sorbed by soil components in a similar way to arsenates, dimethylarsinates are less strongly sorbed (Gosh and Yuan, 1987). Hiroki (1993) found that the microbial population of As polluted soils under reducing conditions could actually be dominated by As(III) tolerant fungi. Whereas the bacterial strains isolated from these polluted soils appear unable to volatilise As(III), the fungal strains have the ability to produce a volatile As compound from As(III) (Hiroki and Yoshiwara, 1993). This same study suggested that under more oxidising conditions, certain fungal strains may be able to volatilise As as trimethylarsine (TMA) using organoarsenicals such as MMAA and DMAA.

2.5 Arsenic occurrence in aquatic sediments

2.5.1 Factors affecting the chemical behaviour of arsenic in aquatic sediments

Aquatic sediments can act as major sinks for As, containing up to 3600 mg/kg in the highly polluted Aberjona watershed of the eastern U.S.A. (Aurilio *et al.*, 1995). When conditions in the water body change such that As speciation is affected and/or its mobility is increased, possibly on a seasonal basis, this As can potentially be released back into solution (McLaren and Kim, 1995). Changes in factors such as Eh, pH, ionic strength, temperature, presence of competing anions or complexing ligands, status of Fe and Mn oxides, sediment sulphide content, adsorption density, microbial activity and/or water stratification have been proposed as possible controls on the mobilisation of As from aquatic sediments (Aggett and Kriegman, 1988; Reuther, 1992; McLaren and Kim, 1995). Aggett and O'Brien (1985) state that the mobility of As in aquatic sediments is not dependent, however, on the formation of methylated As species since demethylation is known to occur in anoxic sediments.

2.5.2 The diagenetic cycling of arsenic in aquatic sediments

In a series of leaching experiments under controlled pH conditions, Mok and Wai (1990) found that As solubility in sediment samples increased markedly at both high and low pH values, as a result of the change in As speciation with pH, and concluded that a near-neutral pH would be necessary to stabilise As within sediments. However, the redox potential of aquatic sediments also has a marked and well documented effect on As speciation and solubility. Within aquatic sediment profiles As tends to be correlated predominantly with Fe and Mn due to its immobilisation via either adsorption on, or coprecipitation with, Fe and Mn oxides and hydroxides in the oxic surface sediments (Brannon and Patrick, 1987; Mok and Wai, 1990; Loring *et al.*, 1995). This has been attributed to the fact that as sediments are buried or play host to intense biological activity, reducing conditions come to prevail and result in the reduction and subsequent dissolution at depth of As-bearing Fe(III) and Mn(IV) oxides. The upward migration of the solubilised As(III), Fe(II) and Mn(II) species in sediment pore waters redeposits them within the surface sediments, where, under oxidising conditions they will be reimmobilised as As(V)-bearing Fe(III) or Mn(IV) oxides or precipitated as FeAsO₄ (Aggett and O'Brien, 1985; Farmer and Lovell, 1986; Hunt and Howard, 1994; Sullivan and Aller, 1996). Due to this upward migration of As within aquatic sediments, the redox potential at the sediment-water interface may therefore determine whether the sediments will act as a sink or a source for As (Widerlund and Ingri, 1995). If the sediment-water interface is, in fact, reducing, possibly as a

consequence of a high degree of biological activity, the As will be released into solution rather than being oxidised and immobilised in the surface sediments (Reuther, 1992).

Moore *et al.* (1988) emphasise that there may be a role for diagenetic metal sulphides as As sinks in anoxic aquatic sediments. These metal sulphides, resulting from the microbially-mediated reduction of SO_4^{2-} in pore water to H_2S , may scavenge the As(III) released into the pore water of anoxic sediments following the reduction dissolution of As-bearing Fe(III) oxides. Subsequent exposure of such As-bearing sulphidic sediments to oxidising conditions, as a result of drainage of a water body or dredging, may therefore result in the increased mobility and release of As. The proposed diagenetic cycling of As in lake sediments is depicted in Figure 2.6.

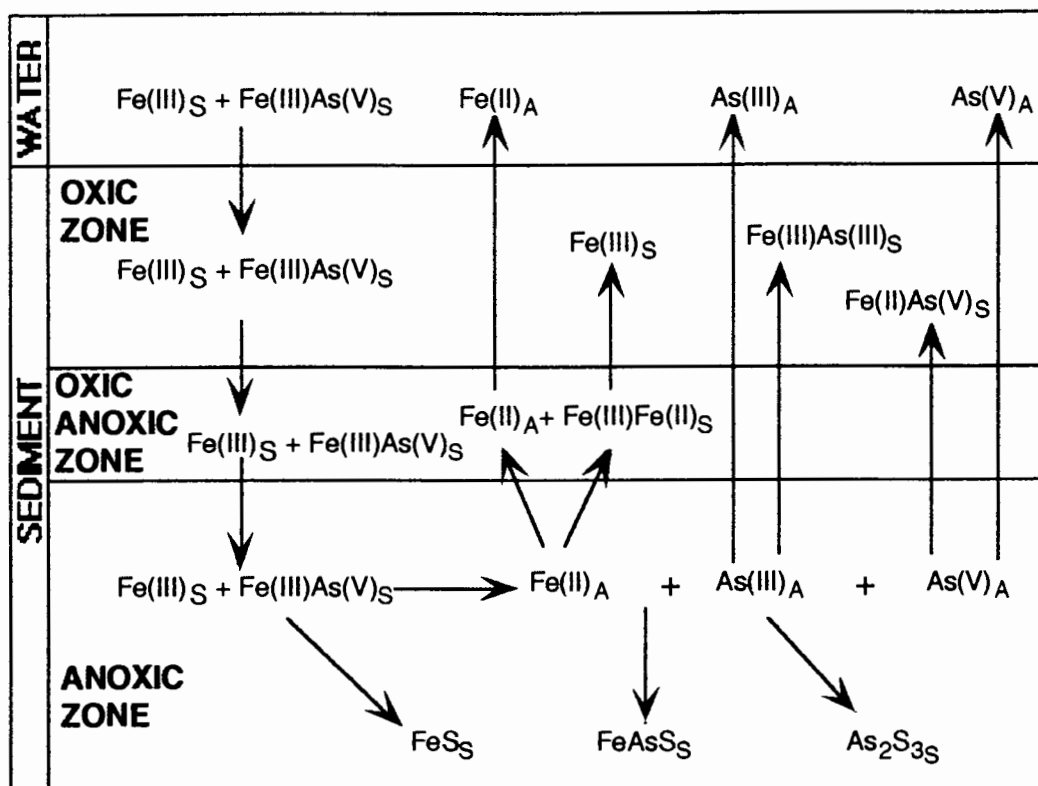


Figure 2.6: The proposed transformations of Fe and As in the sediments of Lake Ohakuri, New Zealand (Aggett and O'Brien, 1985). All solid Fe species are presumed to contain oxide and/or hydroxide groups; S = solid phase, A = aqueous phase.

2.6 Arsenic occurrence in natural waters

Chemical species such as As can be present in natural water systems as dissolved species or they may be transported via adsorption onto suspended particles or in association with colloidal matter (Babb *et al.*, 1985). In addition to the physical parameters controlling flow in such a water body, the transport of As and its presence in solution will also depend on the inter-related roles played by redox potential, pH and microbial activity (Del Razo *et al.*, 1990).

2.6.1 Factors affecting the chemical behaviour of arsenic in water

2.6.1.1 Redox and pH conditions

Although all four oxidation states of As are stable under the Eh conditions found in aquatic systems, the fact that As^{3-} and As(s) are only thermodynamically stable at very low Eh values means that the 5+ and 3+ oxidation states also dominate the speciation of As in water (Ferguson and Gavis, 1972). Whereas As(III) is generally more mobile than As(V), the latter is usually the dominant As species in natural waters due to the prevailing Eh-pH conditions (Pontius *et al.*, 1994). When organic As compounds are present, they normally constitute a very small percentage of the total As.

The similarities between the chemical behaviour of As in water and in soil solutions can be seen by comparing Figure 2.7 with Figure 2.3. The Eh-pH diagram (Figure 2.7) of Ferguson and Gavis (1972) indicates that the arsenic acids (H_3AsO_4 , H_2AsO_4^- , HAsO_4^{2-} and AsO_4^{3-}) are soluble in oxygenated waters. However, H_3AsO_4 and AsO_4^{3-} require pH values of <2 and >12 , respectively (Figure 2.8), and therefore lie outside the pH range of most natural waters (pH = 6 to 8: Dallas and Day, 1993). Under mildly reducing conditions, arsenous acid species (H_3AsO_3 , H_2AsO_3^- and HAsO_3^{2-}) are stable (Figure 2.7), but once again only H_3AsO_3 would occur in natural waters at pH <9 . Ferguson and Gavis (1972) state that although the arsenic oxides As_2O_5 and As_2O_3 are too insoluble to appear in their Eh-pH diagram, arsenic sulphides such as AsS and As_2S_3 have low solubilities and only occur as stable solids at pH <5.5 and Eh ~ 0 volts in the presence of S^{2-} . Under mildly reducing conditions, the only soluble As sulphide species are HAsS_2 , requiring a pH <4 , and AsS^{2-} , predominating at pH >3.7 . The two As species predicted to be stable under highly reducing conditions are As metal, which is considered to be extremely insoluble and has not been reported in water, and arsine (AsH_3), which is only slightly soluble.

2.6.1.2 Microbial activity

As with soils, several organic forms of dissolved As (organoarsenicals) can also occur in natural waters, and two of these, MMAA and DMAA, may at times dominate the dissolved As speciation of saline or freshwater systems (Anderson and Bruland, 1991). At natural water pH values MMAA and DMAA occur as anionic monomethylarsonate and dimethylarsinate, respectively, and DMAA can undergo abiotic degradation to As(V) (Anderson and Bruland, 1991). The factors which stimulate biomethylation of As are poorly understood, although it is thought to represent a possible detoxification process for the bacteria and fungi responsible. By virtue of the fact that As(III), MMAA and DMAA are all less strongly sorbed than As(V), the microbial activity responsible for the reduction, and subsequent methylation, of As(V) may actually result in increased As mobility in water (Aurilio *et al.*, 1994). Therefore, although the

occurrence of these natural organometalloids is not predicted by thermodynamic equilibrium models, they may still contribute to As availability.

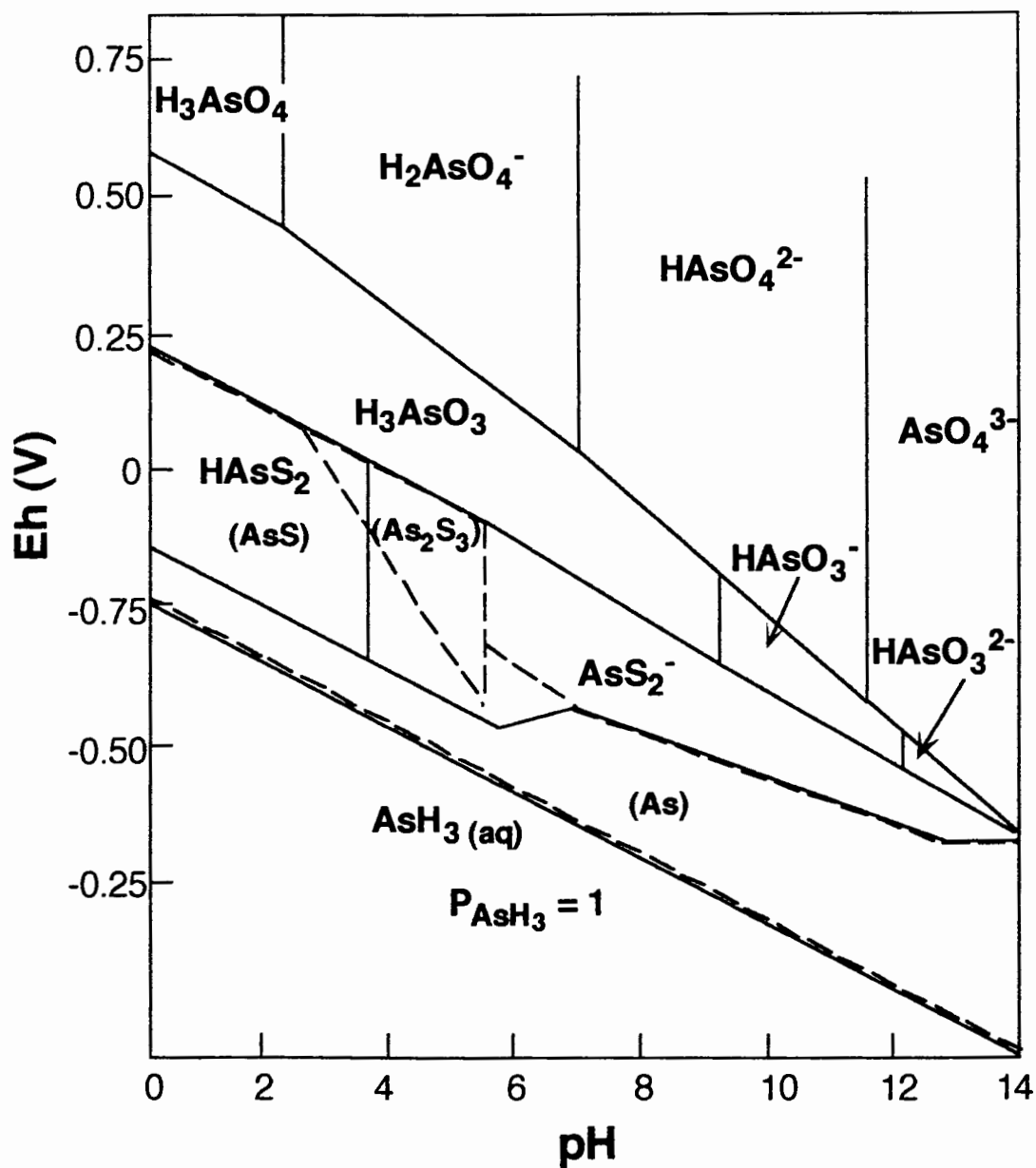


Figure 2.7: The Eh-pH diagram of Ferguson and Gavis (1972) for As at 25°C and one atmosphere; total As = 10^{-5} mol/L and total S = 10^{-3} mol/L. Solid species appear in parentheses in the dashed area which indicates solubility $< 10^{-5.3}$ mol/L.

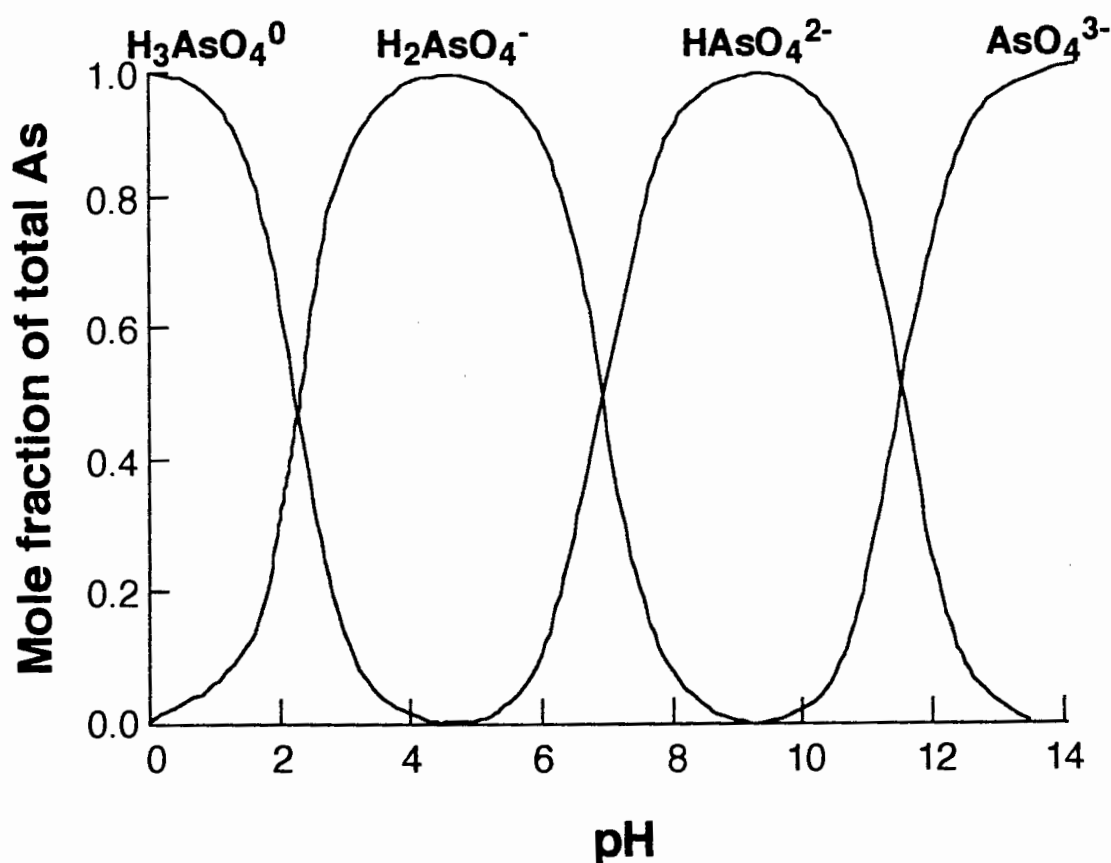


Figure 2.8: The mole fraction distribution of arsenic acid species in aqueous environments as a function of pH (Sadiq *et al.*, 1983).

2.6.2 Factors causing thermodynamic disequilibrium of arsenic speciation in water

A number of studies conducted on natural and contaminated water bodies around the world have revealed that, as with soil, inorganic As speciation is rarely at thermodynamic equilibrium (Aurilio *et al.*, 1994). Therefore, the speciation of As in water is complex, involving a number of possible contributing factors besides the prevailing pH and Eh conditions. A study of the depth distribution of As(III) and total As in oxic and anoxic waters of the Oslofjord, Norway, whereby the difference between them was assumed to be As(V), revealed that although As(V) dominated the oxygenated waters, As(III) was also present contrary to thermodynamic stability predictions (Abdullah *et al.*, 1995). The presence of As(III) in these oxic surface waters was interpreted to have resulted from run-off containing reduced As and/or seasonal planktonic As release. However, it is conceivable that, as with soil, slow oxidation-reduction mechanisms may be at least partly responsible. Thermodynamically unstable As speciation in a permanently stratified lake in central France was partly attributed to a slow and incomplete response of As to the prevailing redox conditions (Seyler and

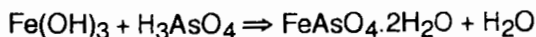
Martin, 1989), although the presence of As(V) in the bottom anoxic layer of the lake was also interpreted to be a possible consequence of both desorption from solubilising Fe oxides and hydroxides with decreasing pH and the possible release of biogenic As(V) from degrading diatom tests. The microbial reduction of As(V) to As(III), possibly by sulphate-reducing bacteria, has also been suggested as a possible cause for the presence of significant levels of As(III) in oxygenated surface waters of a dimictic lake in the eastern U.S.A., whereas slow reduction of As(V) and the differential scavenging of As(III) and As(V) by Fe and Mn oxides and hydroxides has been blamed for the presence of significant As(V) in the underlying anoxic layers (Spliethoff *et al.*, 1995). Fuller and Davis (1989) discovered that a daily pH fluctuation of up to 0.5 units within a creek in South Dakota, U.S.A., was induced by diurnal variations in photosynthetic activity and accompanied by variations in the concentration of As(V). Their interpretation that the sorption of As(V) by ferrihydrite was affected by variations in the pH of the creek water could have implications for other water bodies in which observed seasonal trace element cycling may be related to seasonal variations in photosynthetic rates in the oxic surface waters.

2.7 Environmental arsenic contamination associated with mining

The presence of high As concentrations in soils and groundwater can be a natural geological phenomenon (Matisoff *et al.*, 1982; Farmer and Lovell, 1986; Schloemann, 1994). However, that fact that elevated As levels are associated with many ore deposits, for which As may actually act as a pathfinder mineral (Grimes *et al.*, 1995), means that the mining of these ore deposits results in the production of potential environmental hazards. Such hazards may include wind dispersal and leaching into the groundwater of As from fine-grained waste rock piles, tailings dam material and from the mine workings themselves (Bowell *et al.*, 1994). Arsenic leaching into surface water bodies, particularly in high rainfall areas (Mitchell and Barr, 1995), must also be considered as a possible means of As dispersal.

2.7.1 The geochemistry of arsenic release during mining operations

The main source of As from most gold mining operations is the oxidation of arsenopyrite as a result of exposure, physical weathering and/or microbial activity (LaPerriere *et al.*, 1985; Chapman *et al.*, 1993). The oxidation of arsenopyrite results in the release of the arsenic acid H_3AsO_4 , which is mobile under highly acidic conditions (Wilson and Hawkins, 1978; Bottomley, 1984). However, As(V) is relatively immobile under weakly acidic or neutral conditions, due to co-precipitation with Fe oxides and hydroxides, and will ultimately form the mineral scorodite ($\text{FeAsO}_4 \cdot 2\text{H}_2\text{O}$), according to the equation (Wilson and Hawkins, 1978):



Under more alkaline conditions, As(V) is again quite mobile as the arsenic acid species HAsO_4^{2-} , which will, however, co-exist with Fe(OH)_3 and eventually coprecipitate with it. Depending on the prevailing redox potential, arsenic acid species may be reduced to arsenous acid species in solution. In acidic to neutral solutions, As(III) can exist as either As(OH)_2^+ or H_3AsO_3 , whereas in more alkaline solutions it may be present as H_2AsO_3^- , AsO_2^- or As(OH)_4^- (Wilson and Hawkins, 1978).

2.7.2 Examples of arsenic dispersion from gold mining operations

There are many examples in the scientific literature of gold mining operations posing a potential threat to the environment in terms of the high residual As content of their tailings and the oxidation of exposed mine workings. One incident, reported by Geyer (1977; cited in Frost *et al.*, 1993), occurred in western Poland in 1988 where 60 cases of chronic As poisoning were recognised in people living around a gold mine and deriving their drinking water from a spring that ran through the mine waste tailings. The As content of this water was measured as 25 mg/L. Another example involves the Berkeley Pit, an abandoned open pit/underground mine in the Butte Montana mining district of the U.S.A. Since 1983, this pit has been filling with an acidic metal sulphate solution due to contaminated surface run-off and groundwater inflow (Davis and Ashenberg, 1989). Arsenic contamination in this pit results mainly from the dissolution of arsenopyrite, with a minor contribution from the leaching of mine timbers which had been treated with As-bearing preservatives. The pH of the solution in the pit ranges from 2.7 at the surface to 3.17 at the bottom and the Eh conditions are oxidising, ranging from +450 mV to a surface high of +817 mV. Therefore, the dominant dissolved As species present is As(V), and total As concentrations of up to 0.7 mg/L have been measured. If, as predicted, the Berkeley Pit overflows by the year 2009, this acidic, As-contaminated solution could pose a potential environmental and human health risk.

At the Ashanti Au mine in Ghana, As occurs mainly within arsenopyrite, although it is also present as a trace element within tetrahedrite, pyrite, bournonite, pyrrhotite and aurostibite (Bowell *et al.*, 1994). Lateritic weathering results in increasing Eh conditions and the oxidation of these sulphide minerals to secondary arsenate and arsenate sulphate minerals which include bukovskyite, kankite, pitticite and scorodite. In the upper part of the saprolite and within the overlying soil profiles, the secondary As minerals are altered to goethite and haematite. Within these natural aerobic weathering profiles overlying areas of Au-As mineralised bedrock, soil As concentrations range between 189 and 1025 mg/kg and porewater As concentrations measure 0.086 to 0.557 mg/L, whereby $\geq 78\%$ of the total As present is As(V). The acidic condition of nearby soils contaminated by mine tailings from the Ashanti mine, however, means that As(III) is the dominant species present ($\leq 45\%$ of total As

in the aerobic soils and 79% of total As in the anaerobic soils). The As concentrations within these anthropogenically contaminated soils are: 40.5 to 1290 mg/kg in the soils, 0.07 to 0.11 mg/L in the aerobic porewaters and 0.07 to 0.60 mg/L in the anaerobic porewaters. Whereas MMAA and DMAA are also found within the aerobic soils, no methylated As species are detectable in the anaerobic soil porewaters.

Environmental As contamination also originates from the site of the abandoned Hillside Au-Ag mine and mill complex in an arid region of western Arizona (Rampe and Runnells, 1989). The tailings and waste rock dumps from past mining activities have been deposited on the bank of a stream, the Boulder Creek, which is often stagnant during summer and intermittently flooded during winter. Two As-contaminated seeps flowing into the creek have been located. Seepage originating from a collapsed mine adit was found to be weakly acidic (pH 5.4), low in oxygen and to contain 21 mg/L As, whereas drainage from the base of a tailings pile is oxygenated, extremely acidic (pH 2.4) and contains 34 mg/L As. Compared to the water in Boulder Creek upstream from the Hillside complex, which is alkaline (pH 8.4) and has a relatively low As concentration (0.03 mg/L), the water downstream from the two seepage sites has a significantly lower pH (7.3) and a much increased As concentration (1.2 mg/L). The effect of the alkaline waters on the mine drainage, therefore, appears to be similar to that of liming such that decreased As mobility is promoted via the sorption on As onto the river sediments at higher pH values. Rampe and Runnells (1989) concluded that the similarities between the patterns of total As and Fe concentrations in waters downstream from the mine site indicate that As adsorption involves Fe oxides and hydroxides. However, as high concentrations of Ca would be expected in these alkaline waters, there may also be a role for As precipitation as $\text{Ca}_3(\text{AsO}_4)_2$ (Figure 2.4). Rampe and Runnells (1989) also found that the transport of metals from the Hillside mine site by Boulder Creek is highly seasonal, with transport via dissolution dominating in summer whereas transport as particulate matter dominates during the winter floods. In addition, the high buffering capacity of the Boulder Creek water, as a consequence of the arid climate, means that pollution from the mine site does not extend more than 2.5 km downstream.

An attempt to examine the importance of sorption reactions in As partitioning between dissolved and sediment fractions in mine drainage waters using the computer modelling program MINTEQA2 confirmed the pH-dependence of As sorption (Smith *et al.*, 1992). The results of this study also suggested that whereas suspended Fe-rich particulates play an important role in the sorption of As in mine drainage waters with pH \gt 4, Fe-rich bed sediments may only play a limited role.

2.7.3 Potential risks to human health from arsenic dispersion associated with mining

Mitchell and Barr (1995) have reviewed public exposure to As in south west England as a consequence of prolonged mining and smelting operations involving As-bearing minerals. They foresee the major human health risks associated with mining to be As intake via water, the food chain and As-contaminated dust, the latter originating from mine spoils and presenting more of a problem in terms of ingestion by children playing in contaminated soils than via inhalation. Although As in contaminated soils is potentially available for plant and animal uptake, its bioavailability will be dependent on factors such as soil pH, redox potential, drainage, organic matter content, clay content and clay mineralogy. Even if the As is bioavailable, plant uptake is limited by factors such as seasonal effects, plant species characteristics and chemical factors at the soil-root and root-shoot interfaces. Therefore, the levels of As found in terrestrial plants, apart from a few known As-tolerant species, generally remain well below the levels within their soil substrates. Although the limited uptake of As by most plants prevents significant concentrations being passed up the soil-plant- human food chain, root vegetables grown in contaminated soils and not washed properly prior to being eaten could represent a potential source of As ingestion. Li and Thornton (1993) investigated the idea that As could also potentially enter the food chain, via meat or milk products, as a consequence of the direct ingestion of contaminated soil by livestock during grazing. Although it has been estimated that 34 to 90% of the As intake of cattle on contaminated land is due to soil ingestion (Mitchell and Barr, 1995), Li and Thornton (1993) concluded that only about 1% of this ingested As is actually absorbed. Therefore, apart from the problem of direct ingestion of contaminated dust and soil by children, the main risk to human health from environmental As contamination appears to be the drinking of contaminated water.

2.8 Human arsenic consumption

2.8.1 Arsenic as an essential element

Despite the notoriety gained by As through the use of arsenic trioxide ('white arsenic': As_2O_3) as a lethal poison, it may in fact be an essential trace element for humans in terms of stimulating haemoglobin production and influencing the metabolism of the essential amino acid arginine and the vital metals Zn and Mn (Emsley, 1985). Uthus (1992) suggests that As deprivation may also affect sulphur amino acid metabolism and states that there may be a possible human minimum As requirement in the order of 0.012 mg/day. A normal daily intake of As can be derived from water (0.01 to 1 mg/L), meat (0.06 to 1.1 mg/kg) and milk

(0.01 to 0.05 mg/L), whereby the values in parentheses represent the naturally-occurring or background levels presented by Schroeder and Balassa (1966).

The uptake of As by plants is relatively small (O'Neill, 1995), with the average concentration in grass being 0.30 mg/kg (Li and Thornton, 1993). Therefore, as marine organisms appear to accumulate and transform As compounds more efficiently than land-based organisms (Irgolic, 1986), the major source of dietary As for humans is seafood (10 to 40 mg/kg fresh weight; Pontius *et al.*, 1994). Arsenic occurs in marine organisms in the form of arsenobetaine ($(\text{CH}_3)_3\text{AsCH}_2\text{CO}_2$), an essentially non-toxic organoarsenical which is excreted in the urine unchanged (Chatterjee *et al.*, 1995), as well as arsenosugars (Le *et al.*, 1994). The World Health Organisation has recommended a maximum tolerable daily As intake of 0.002 mg/kg body mass (WHO, 1983), whereas Brown and Fan (1994) cite a United States Environmental Protection Agency (EPA) No-Observable-Adverse-Effect [intake] Level (NOAEL) for As of 0.0008 mg/kg bodyweight/day. The lethal dose for acute As poisoning is 1 to 4 mg/kg bodyweight (Pontius *et al.*, 1994).

2.8.2 Arsenic as a toxic element

2.8.2.1 Arsenic toxicity as a function of its chemical speciation

The toxicity of As to humans depends on its concentration, speciation and bioavailability. Arsenic is at its most toxic in the +3 and -3 oxidation states (Aurilio *et al.*, 1994) and inorganic forms are ~100 times more harmful than organic forms (Chatterjee *et al.*, 1993; Thomas, 1994; Chatterjee *et al.*, 1995; O'Neill, 1995). The order of decreasing toxicity of As species is cited as $\text{AsH}_3 > \text{As(III)} > \text{As(V)} > \text{MMAA} > \text{DMAA}$ (Matisoff *et al.*, 1982; Chatterjee *et al.*, 1995), whereby As(III) is between 2.6 and 59 times more toxic than As(V), depending on the test system used to evaluate toxicity (Del Razo *et al.*, 1990), and the -3 oxidation state (AsH_3) is only slightly soluble under highly reducing conditions (Ferguson and Gavis, 1972).

Most of the As ingested into the human body is extracted by the liver and excreted as DMAA in the urine (Emsley, 1985). This process suggests that As methylation represents a detoxification mechanism involving the following steps: $\text{As(V)} \Rightarrow \text{As(III)} \Rightarrow \text{MMAA} \Rightarrow \text{DMAA}$ (Chatterjee *et al.*, 1995). The reduction of As(V) to As(III) within the human body involves the enzyme glutathione (GSH), whereas subsequent methylation involves the enzyme-catalysed oxidative addition of a methyl group to As using S-adenosyl-1-methionine (SAME) as a methyl donor (Thompson, 1993). Although the inorganic As retained within the body has been implicated as a causal agent for cancers of the lung, bladder, kidney and liver the main cancer associated with the ingestion of As is skin cancer (Mass, 1992). Despite conclusive evidence that As is a human carcinogen, it represents a unique carcinogen in that there is no substantial supporting evidence linking it to the experimental induction of cancer in other animals (McKinney, 1992). There is also no evidence to show that organoarsenicals are carcinogenic, mutagenic or teratogenic to humans (Goldman and Dacre, 1991). However,

toxic effects have been recognised during the administration of dimethyl As to laboratory mice (Thomas, 1994), and Mass (1992) suggests that DNA damage during the actual methylation process within the human body may be cancer-inducing.

Thomas (1994) states that the discovery that the methylation capacity in humans becomes saturated at an As intake level of 0.5 mg/day means that once the methylation capacity for a particular As species (e.g. As(III)) has been saturated, it will accumulate within the body. This has led to speculation that As may represent a threshold carcinogen, whereby its carcinogenic potential is dependent on the metabolic capacity for its inactivation being exceeded. However, the methylation of As and its excretion in urine only accounts for ~50% of the As ingested into the human body. Whereas a small amount is also excreted in the faeces or bound to keratin in the skin, hair and nails (Das *et al.*, 1995), a substantial amount of ingested As is actually retained by the body (Chatterjee *et al.*, 1995). The results of a study by Hoppenhayn-Rich *et al.* (1993) also disagree with the methylation threshold hypothesis. These results indicated that an average of 20 to 25% of the inorganic As ingested by humans will remain unmethylated regardless of the exposure level.

2.8.2.2 Arsenic toxicity as a function of its uptake in drinking water

Since water usually represents the main source of inorganic As, the World Health Organisation has recommended a guideline value for As in drinking water. The original recommended maximum limit of 0.05 mg/L (WHO, 1984) underwent a significant reduction in 1993 to 0.01 mg/L (WHO, 1993) in recognition of the fact that the results of various research studies implicated As as a causative agent in a range of diseases including skin and internal cancers (Pontius *et al.*, 1994). However, despite this reduced limit, the WHO (1993) guidelines still fail to take into account that the toxicity of As is directly related to its speciation. Brown and Fan (1994) have calculated a Recommended Public Health Level (RPHL) for As in drinking water of 0.000002 mg/L (2 ppt) based on the lifetime risk of developing skin cancer at an As intake level of 0.05 mg/L. This RPHL assumes an average body weight of 70 kg, a daily water consumption of 2 L/day, a relative source contribution of 20% for As intake via drinking water, and a lifetime risk of 10^{-6} of contracting another form of cancer from As ingestion.

Chatterjee *et al.* (1995) cite the 1994 report of the COT (Committee on Toxicity of Chemicals in Food Consumer Products and the Environment) as stating that the daily intake of 1.5 mg of total inorganic As (equivalent to drinking 1.5 L of water containing a total inorganic As concentration of 1 mg/L) could produce signs of overt chronic arsenicism in humans. Natural As contamination of groundwater in West Bengal, India, is in the order of 0.05 to 3.7 mg/L total As, whereby As(III) may be present in concentrations of up to 2.6 mg/L. This contamination within the main drinking water supply for 30 million people has resulted in maximum ingestion rates in some districts of >1.5 mg/day of As(III) (Chatterjee *et al.*, 1995).

Long-term ingestion of this As-contaminated groundwater has been linked to a range of diseases (Das *et al.*, 1994; Chatterjee *et al.*, 1995) which Das *et al.* (1996) have subdivided into three clinical stages: *initial stage* - dermatitis, keratosis, conjunctivitis, bronchitis and gastroenteritis; *second stage* - peripheral neuropathies, hepatopathy, melanosis, depigmentation and hyperkeratosis; and *last stage* - gangrene in the limbs and malignant neoplasm. Within the victims of this chronic arsenicism, As was found to be abnormally high in the urine, nails, hair, skin-scales and liver, the latter being found to contain As levels of up to 2.6 mg/kg on biopsy compared to the normal liver concentration of only 0.005 to 0.015 mg/kg (Das *et al.*, 1996).

On the southwest coast of Taiwan, chronic As poisoning has manifested itself as a peripheral vascular disorder, known as 'blackfoot disease', which results in gangrene of the lower limbs (Lin *et al.*, 1995). This condition is due to the ingestion of high levels of As, mostly As(III) (Chen *et al.*, 1994), in artesian well water. Lin *et al.* (1995) believe that the As may cause lipid peroxidation (oxidative deterioration of polyunsaturated fatty acids) such that cellular injury and death occur. Water collected from one of three affected wells in the area had a pH of 8.1 ± 0.4 indicating that the soluble As(III) and As(V) species present should be H_2AsO_3 and HAsO_4^{2-} , respectively (Chen *et al.*, 1994). The fact that the ratio of As(III):As(V) within the aquifer averages 2.6:1 not only indicates a high toxicity of the water in this area, which averages 0.67 ± 0.015 mg/L total As, but, according to the thermodynamic equilibria of Ferguson and Gavis (1972; Figure 2.7), it also suggests the presence of a reducing environment. Methylated As species were below detection limit (0.001 mg/L) within this groundwater (Chen *et al.*, 1994).

In contrast to the above studies, which indicate that high levels of As within drinking water can prove to be extremely toxic to humans, a similar study by Varsányi *et al.* (1991) in the Southern Great Hungarian Basin concluded that a prolonged average As intake of 0.137 mg/L in drinking water, over ten times the WHO (1993) recommended limit, does not constitute a serious health risk. However, this study, which attempted to correlate high As intake, from the naturally contaminated Pleistocene groundwater used for drinking purposes, with mortality rates, failed to examine the speciation of the As. If the As was present within the water predominantly as As(V), the conclusions of Varsányi *et al.* (1991) may well be valid.

Other human health risks associated with the ingestion of high levels of inorganic As in drinking water include birth defects, possibly due to As acting as an oxidant within the placenta and again causing lipid peroxidation (Stone, 1994), neurological disturbances and hepatic abnormalities (Abernathy and Ohanian, 1992).

The South African Department of Water Affairs and Forestry (DWAF) have summarised the effects on human health of a range of As concentrations in drinking water (Table 2.1). They recommend that although the As concentration in potable water should ideally not exceed 0.01 mg/L, it should never exceed 0.2 mg/L, above which they state

"human health is seriously at risk". Once again, however, the DWAF (1995b) recommendations take no cognisance of the effect of As speciation on the level of toxicity.

Table 2.1: The effects on human health of As intake in drinking water, as stipulated by DWAF (1995b).

Arsenic Range (mg/L)	Effects
<i>Target Water Quality Range</i> 0 - 0.01	<i>No health effects expected; ideal concentration range.</i>
0.01 - 0.2	Tolerable concentration, but low risk of skin cancer in highly sensitive individuals over long term.
0.2 - 0.3	Increasing possibility of mild skin lesions over long term. Slight possibility of induction of skin cancer over long term.
0.3 - 0.6	Possible adverse, chronic effects in sensitive individuals; brief exposure has no effect; skin lesions, including hyperpigmentation, will begin to appear on long-term exposure.
0.6 - 1.0	Symptoms of chronic poisoning such as skin lesions, including hyperpigmentation, will appear on long-term exposure.
1.0 - 10	Cancer or death will result from chronic poisoning.
>10	Death will result from acute poisoning.

2.8.2.3 Factors which may increase the toxic effects of arsenic

The toxicity of As to humans appears to be enhanced by malnutrition. As reported by Das *et al.* (1996), Vitamin C and methionine have been found to reduce the toxicity of As whereas Vitamin A deficiencies increase sensitivity to the toxic effects of As. The failure to maintain a well balanced diet, such that it is excessively high in carbohydrate, protein or fat, also appears to increase the toxic effects of As. The fact that As has been found to inhibit the action of Se (Ohlendorf, 1989), whereby Se represents a component of the glutathione peroxidase enzyme (GSH-Px) and works in association with vitamin E to protect membranes from peroxidation (Rotruck *et al.*, 1973; Underwood, 1977; Diplock, 1981), may have implications for the occurrence of blackfoot disease in Taiwan. In a study of people affected by this disease, Lin and Yang (1988) did in fact find marked deficiencies in both Zn and Se.

2.9 The remediation of environmental arsenic contamination

Although research into the remediation of As from contaminated water bodies is continuing, several methods are already in use. Conventional methods of As removal at water treatment plants in the U.S.A. include coagulation with metal salts, Fe-Mn oxidation and 'softening', all of which can convert soluble As into insoluble As products prior to physical removal from the water body via filtration or sedimentation (Edwards, 1994; McNeill and Edwards, 1995).

2.9.1 The removal of arsenic from water via coagulation, coprecipitation or adsorption

Arsenic removal via coagulation involves the addition of Fe or Al coagulants to water in order to convert soluble As(III) and As(V) into insoluble products via processes of adsorption, precipitation or coprecipitation. Whereas adsorption involves the formation of surface complexes between As and a solid oxide/hydroxide, precipitation occurs when the solubility product of either FeAsO_4 or AlAsO_4 is exceeded, and coprecipitation involves the adsorption of As into a growing hydroxide phase via inclusion, occlusion or adsorption (Edwards, 1994). Arsenic removal via Fe-Mn oxidation involves similar mechanisms to coagulation, whereby oxidation to remove Fe(II) and Mn(II) results in the formation of Fe or Mn hydroxides ($\text{Fe}(\text{OH})_3$ and MnOOH , respectively) which also remove soluble As species via either coprecipitation or adsorption (Edwards, 1994). The method known as 'softening' involves the removal of As via adsorption onto either calcite or $\text{Mg}(\text{OH})_2$ solids. Fly ash, a by-product from coal-fired power stations, has also been proposed as an effective As(V) adsorbant although the degree of As removal from water by flyash is highly pH-dependent (Diamadopoulos *et al.*, 1993).

In a review of the methods used for arsenic removal from water in the U.S.A., McNeill and Edwards (1995) found that Al was not as effective a coagulant as expected, and that the oxidation of Mn(II), in isolation from Fe(II), failed to remove significant amounts of As from water. The enhanced coagulation method of As removal from water involves the use of FeCl_3 as a coagulant, which was found to be significantly more effective than Al (Cheng *et al.*, 1994). Pretreatment of the water with chlorine presumably oxidises the As(III) to As(V) and enhances the ability of the FeCl_3 to remove As (Scott *et al.*, 1995). During the 'softening' process, McNeill and Edwards (1995) found that whereas calcite precipitation removes less than 30% of the total As in solution, the precipitation of $\text{Mg}(\text{OH})_2$ can remove over 90% of the total As.

2.9.2 The treatment of arsenic-bearing mine wastes

Several methods have been proposed for treating As-bearing mine wastes, although most are still under investigation. For example, Peng and Di (1994) propose a method of adsorbing colloid flotation (ACF) for treating aqueous mine wastes. This method involves adding ferric hydroxide to the waste water in order to produce a floc which adsorbs and coprecipitates with the As. Sodium dodecyl sulphate (SDS) is then added as a surfactant and its adsorption onto the As-bearing $\text{Fe}(\text{OH})_3$ flocs renders them hydrophobic. Nitrogen microbubbles can then be used as a flotation technique in order to remove the flocs. Otte *et al.* (1995) have investigated the use of wetlands as sinks for As and other metalloids. Oxidation of the rhizosphere by wetland plants results in the precipitation of Fe oxides and hydroxides on the root surfaces of the plants which have the potential to accumulate As via adsorption or coprecipitation. Voigt *et al.* (1996) found that, although As within contaminated soils can be chemically fixated and immobilised using a combination of iron sulphate, portlandite and Portland cement, they were unable to identify the exact insoluble As-bearing phases formed during the process.

Ahmann *et al.* (1994) have recently discovered an anaerobic bacterium, known as MIT-13, which gains energy and grows from the electron transfer involved in reducing As(V) to As(III). This discovery suggests that bioremediation of As contamination may be possible in the future, whereby the microbially-mediated dissolution of As from sediments into water may allow for its subsequent removal via ion exchange or other remediating processes (Newman, 1995).

Ripley *et al.* (1996) report a case study in Ontario, Canada, where remediation methods are being successfully applied to As-contaminated Au mine tailings dams and drainage waters. At the abandoned Deloro Au mine and mineral processing site, crushed limestone has been spread over the tailings to reduce the acid drainage, and an on-site arsenic treatment plant has been installed to treat contaminated ground and surface waters. This water treatment, which removes 99.5% of the total As present, involves pumping the contaminated waters into clay-lined settling tanks, prior to the addition of FeCl_3 in order to precipitate the As as ferric arsenate. The resulting toxic sludge is retained in storage lagoons while the treated water is discharged into the adjacent Moira River. By 1989, 10 years after remediation began, the daily As contribution to the Moira River from the Deloro mine site had decreased from 35 kg to 6 kg. However, even though it is now more than 30 years since mining in the area ceased, a comparison of As concentrations in the Moira River upstream of the mine site (0.007 mg/L) with the concentration just downstream of the Deloro mine site (0.23 mg/L) indicates that the legacy remains (Azcue and Nriagu, 1995).

2.10 Conclusions

The risks to the environment and human health associated with the release of As during Au mining activities are dependent on the range of chemical, physical and biological factors which control the speciation, solubility and mobility of As. Those of most importance in determining the solubility of As in soil/sediment porewaters and aquatic systems include pH, redox potential and the amount and composition of the clay component within the soil or sediments. Although the concentration of total dissolved As is important in terms of its threat to human health, the speciation of the As present, whereby inorganic forms are significantly more toxic than organic forms and As(III) is substantially more toxic than As(V), dictates just how much of a risk this As contamination may represent.

Although it must be concluded that gold mining activities can result in increased human exposure to As, the degree to which this occurs will vary with each individual mining site. Therefore, in order to assess the risks and make recommendations regarding possible remediation requirements, detailed chemical analyses must be performed on leachates from the mine and tailings dumps, local surface and ground water bodies likely to have experienced inflow from mine seepages, as well as the local soils and aquatic sediments. The mineralogy of the tailings dumps, soils and aquatic sediments is also of considerable importance in assessing the potential for As sorption and attenuation considering the high sorption/coprecipitation capacity of any Fe, Al and Mn oxides/hydroxides which may be present within their clay fractions.

CHAPTER 3

An assessment of arsenic release into the Barbrook environment

3.1 Introduction

Gold mining and processing operations in the Barberton area of South Africa have the potential to cause severe degradation and pollution of the local environment if inadequate management and monitoring practices are employed. The decision to undertake the current investigation was based on the knowledge that the mining of a sulphide-hosted gold deposit such as Barbrook constitutes a particular threat to the environment in terms of potential As and heavy metal dispersion. Although this study is aimed at determining whether the current As levels and, to a lesser extent, heavy metal concentrations in the groundwater, surface waters, soils and sediments in the Barbrook area are of concern with respect to the health of the local population, the results also allow for speculation about the potential of the Barbrook operations to leave behind a legacy of future environmental hazards.

3.2 Sampling sites

Sampling within the area demarcated by the Barbrook gold mine lease was carried out in mid-August 1996. Two main areas were delineated for the purposes of this study, namely the tailings dam area and the mining area. Sampling was aimed at gathering representative samples from water bodies (BW samples) in each area, as well as accompanying sediments (BS samples) where possible. Several specimens of the Barbrook ore bodies (BOR samples) and waste rock pile (BR samples) were also collected.

3.2.1 Barbrook tailings dam area

Sampling locations for the water and sediment samples collected in the Barbrook tailings dam area, located ~5 km northwest of the Barbrook processing plant, are listed in Table 3.1. The tailings dam comprises two dams which will be referred to separately throughout this report as the calcine dam and the slimes dam (Figure 3.1). The calcine dam,

representing the smaller of the two tailings dams, was originally designed to receive the residue from the calcine circuit of the gold processing operation. This circuit was associated with the processing of the refractory sulphide-rich ore using the now defunct roaster, and these slimes were kept separate for possible later reprocessing. Water sample BW15 and sediment core BS7 were collected from a shallow greenish-coloured pond of standing water at the northwestern end of the calcine dam (Figure 3.2). Sample BW21 represents tailings material collected from residue tank three at the gold processing plant immediately preceding its discharge to the tailings dams. Sample BW20 was collected from the thickener overflow pond at the processing plant (Figure 3.3).

Discharge from the calcine dam emerges through two outlets in the dam wall (Figure 3.4) to form a shallow stream of black slimes (Figure 3.5: sample BW14) which includes visible fine-grained pyrite and enters the southern end of the main slimes dam. This slimes dam is located in a large valley immediately downslope from the small side valley occupied by the calcine dam (Figure 3.6). It was originally designed to receive the flotation plant residue which derived from the processing of the oxidised ore that did not require roasting. A pond at the southern end (Figure 3.7: water sample BW4 and sediment core BS3) acts as a sump from which water is pumped back to the processing plant. The main slimes dam comprises fine grey tailings material (sample BS4) which is covered in places by a white secondary efflorescence, the latter visible in Figure 3.7. Several shallow bodies of standing water were present on top of the slimes dam at the time of sampling. Sample BW13 was collected from one such water body, a greenish pond ≤ 30 cm deep at the northern end of the dam.

Table 3.1: List of samples collected from the Barbrook tailings dam area and gold processing plant.

Sample	Locality
Water samples:	
BW1	Pond located ~50 m east of Crystal Stream
BW2	Seepage from base of slimes dam wall
BW3	Seepage near base of slimes dam wall
BW4	Pond at southern end of slimes dam
BW9	Borehole below slimes dam wall - depth to water table = 19.5 m
BW10	Borehole below slimes dam wall - depth to water table = 14.9 m
BW11	Borehole below slimes dam wall - depth to water table = 22.9 m
BW12	Borehole below slimes dam wall - depth to water table = 17.3 m
BW13	Pond at northern end of slimes dam
BW14	Stream between calcine and slimes dams
BW15	Pond at northwestern end of calcine dam
BW20	Thickener overflow pond at processing plant
BW21	Residue tank at processing plant
Soil/sediment samples:	
BS1A	Crystal Stream sediment core (upper 12 cm)
BS1B	Crystal Stream sediment core (lower 8 cm)
BS2	Slimes seepage pond sediment core (17 cm)
BS3	Slimes dam southern pond sediment core (14 cm)
BS4	Slice through upper 0.5 m of slimes dam
BS7	Calcine dam pond sediment core (8.5 cm)

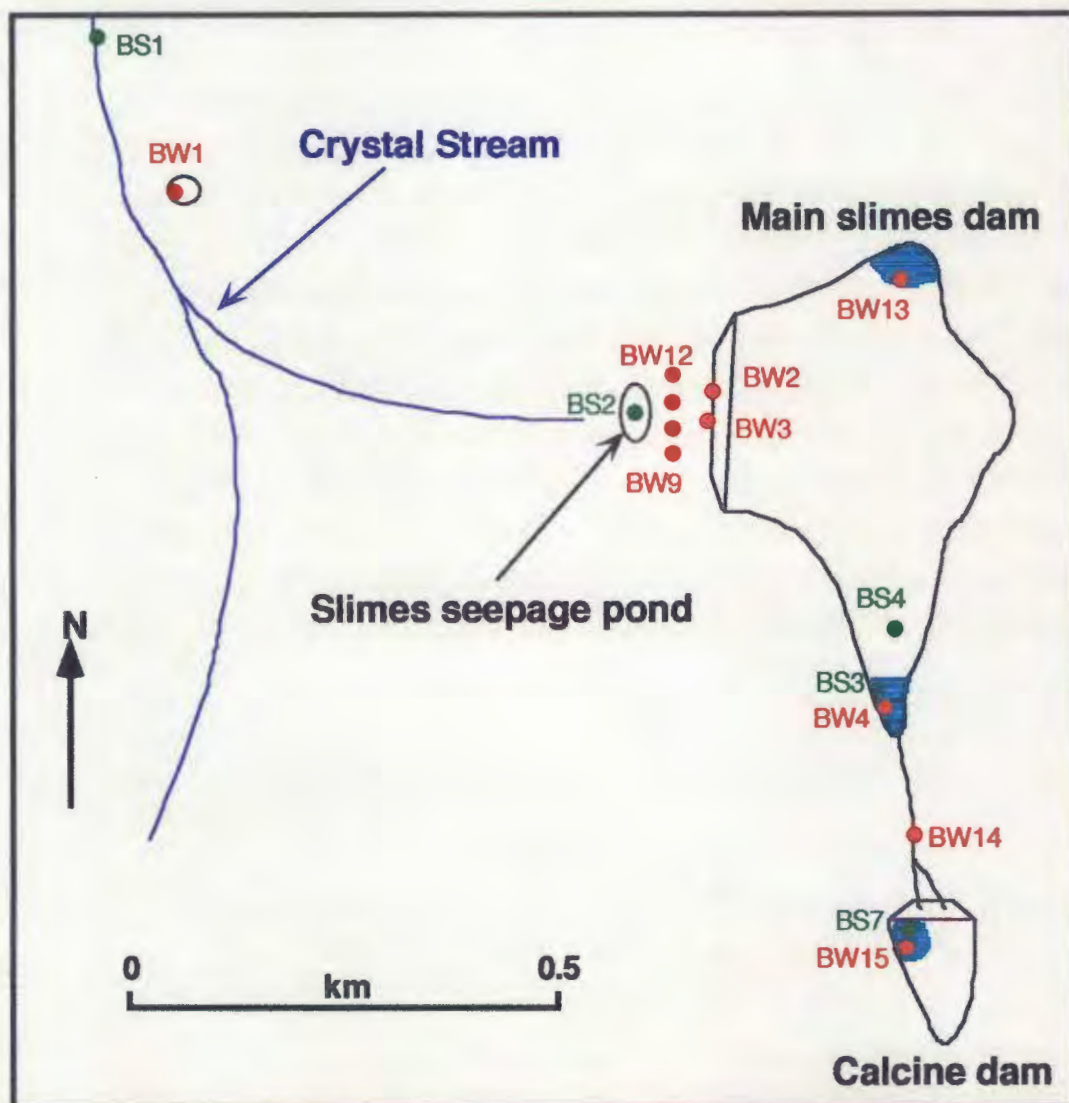


Figure 3.1: Plan of the Barbrook calcine and slimes dams showing the location of water and sediment sampling sites; adapted from the 1:10 000 orthophoto map series (2531 CB 21 Barbrook; 1988) published by the South African Department of Surveys and Mapping. Groundwater samples were collected from the row of boreholes labelled BW9 to BW12 - BW10 and BW11 are not individually labelled.

Sampling in the Barbrook tailings dam region included two areas of limited seepage from the base of the main slimes dam wall (Figure 3.8). Sample BW2 was collected from a small stream of clear water emerging from a broken clay pipe at the base of the wall (Figure 3.9), whereas sample BW3 was collected from a muddy puddle located ~5 m east of the wall (Figure 3.10). The latter was lined with a yellow, presumably Fe-rich precipitate, and appeared to have filled with upwelling water, possibly also from a broken pipe. Due to the lack of any pumping apparatus, the four boreholes located directly west of the slimes dam wall had to be sampled with the aid of a weighted sample bottle lowered on a length of string (Figure 3.11). The resulting water samples (BW9 to BW12) were extremely sediment-rich.

The slimes seepage pond is a depression, approximately 10 m deep, designed to collect water discharging from the underdrains located beneath the slimes dam as well as any seepage from the base of the slimes dam wall. It was empty and lined only with dry, cracked mud (sediment core BS2) and bullrushes at the time of sampling (Figure 3.12). Sample BW1 was collected from a muddy pond situated further to the west of the slimes dam and ~50 m east of Crystal Stream. Despite recent unseasonably heavy rains in the region, Crystal Stream was dry at the time of sampling apart from a few muddy depressions. Sediment core BS1 was collected in one such depression, immediately adjacent to the road crossing (Figure 3.13). All of the standing water bodies in the tailings dam area were surrounded by cattle hoof prints and were obviously used as drinking holes by the local animals and birds (Figure 3.14).



Figure 3.2: Pool of standing water on the calcine dam from which water sample BW15 and sediment core BS7 were collected.

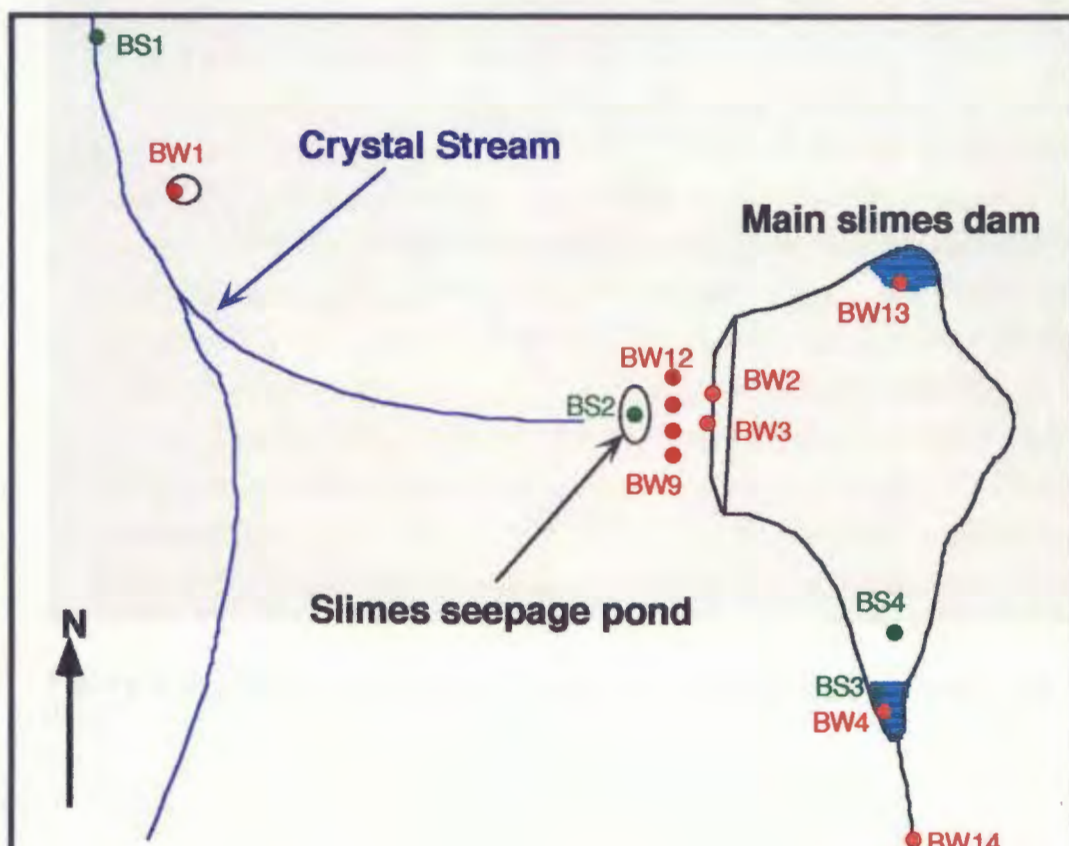




Figure 3.5: Black stream of tailings extending between calcine and slimes dam, from which sample BW14 was collected. The calcine dam wall is visible in the immediate background.



Figure 3.6: View of the slimes dam looking south towards the calcine dam wall in the background. The slimes dam wall is located in the far right of the photo.



Figure 3.7: Collection of slimes dam sample BS4 in front of the southern slimes dam pond from which water sample BW4 and sediment core BS3 were collected. The calcine dam wall is visible in the background.



Figure 3.8: View of the main slimes dam wall; Crystal Stream is located to the right of the area photographed.



Figure 3.9: Sample BW2 comprised water seeping from a broken clay pipe at base of the slimes dam wall.



Figure 3.10: Puddle of upwelling water near the base of the slimes dam wall from which sample BW3 was collected.



Figure 3.11: Sampling groundwater from four boreholes located west of the base of the main slimes dam wall. The slimes dam wall is visible in the background, on the right side of the photo.



Figure 3.12: Collecting sediment core BS2 from the slimes seepage pond.



Figure 3.13: Collecting sediment core BS1 from Crystal Stream.



Figure 3.14: Cattle drinking from the southern slimes dam pond. Wind erosion of the dry tailings material is visible in the background.

3.2.2 Barbrook mining area

Sampling locations for the water, sediment, rock and mineral samples collected in the Barbrook mining area are listed in Table 3.2 and depicted in Figure 3.15. Most of the current mining operations are concentrated around the level 10 mine adit (Figure 3.16). The water used during the mining operations at Barbrook is largely recycled, with ~70% of the groundwater which discharges into the level 10 mine adit (sample BW18) being re-used in the processing plant after clarification and filtration. The remaining fraction is pumped from the main drain in the mine adit (sample BW19) directly into Low's Creek. Low's Creek flows past the entrance to the level 10 mine adit, through the adjacent waste rock pile (Figure 3.17: samples BW7 and BW8) and alongside the gold processing plant before converging with Barbrook Creek (sample BW26). Additional Low's Creek samples were collected upstream of the mine site, adjacent to the explosives magazine (sample BW25), and downstream of the mine site and processing plant just prior to the confluence with Barbrook Creek (sample BW5). Barbrook Creek flows from the Shiyalongubo Dam (Figure 3.18: BW16), via an outlet tunnel/waterfall (BW17) and past, although not in direct contact with, the mine site (Figure 3.19: sample BW6). The Low's Creek Irrigation Board controls the amount of water released

from Shiyalongubo Dam at any one time in accordance with the domestic and agricultural requirements of the local population.

Table 3.2: List of samples collected from the Barbrook mining area.

Sample	Locality
Water samples:	
BW5	Low's Creek downstream of mine site before confluence
BW6	Barbrook Creek near mine site
BW7	Low's Creek at base of waste rock pile
BW8	Low's Creek just upstream of processing plant
BW16	Shiyalongubo Dam
BW17	Waterfall above Barbrook Creek
BW18	Diamond drill hole in side wall, level 10 mine adit - groundwater
BW19	Main drain in main haulage, level 10 mine adit
BW22	Main drain in main haulage, level 7 mine adit
BW23	Recycled mine water tanks above French Bob mine
BW24	Pond in disused Clifford Scott open cut mine
BW25	Low's creek at magazine and upstream from mine site
BW26	Below confluence of Barbrook and Low's Creeks
Soil/sediment samples:	
BS6	Low's Creek sediment core, adjacent to waste rock pile - 10 cm
BS8	Soil under waste rock pile
BS9	Clifford Scott open cut mine sediment core - 33 cm
Secondary mineral precipitates:	
BR1	Oxidised rock from base of waste rock pile
Rock samples:	
BR2	Waste rock pile - base of ~6 m high slope
BR3	Waste rock pile - half-way up 8 to 10 m high slope
BOR1 - BOR4	Samples from ore pile containing primary sulphide minerals

The waste rock resulting from underground mining in the level 10 adit extends for several hundred metres along the steep eastern bank of Low's Creek (Figure 3.20). Although it is largely a legacy of past mining activities at Barbrook, it remains the current site of waste rock disposal and is of particular concern in terms of potential As leaching into the local surface waters and underlying soil. Therefore, in addition to the water samples collected from Low's Creek, samples of the soil underneath the waste rock (BS8), the adjacent Low's Creek stream sediments (BS6) and the actual waste rock pile (BR2 and BR3) were also collected. Sample BR1 represents a chunk of oxidised waste rock collected from the base of the waste rock pile, the surface of which is covered by a range of fine-grained secondary minerals. In addition to sampling the waste rock pile, four rock samples were also collected from the ore pile adjacent to the processing plant in order to determine the primary sulphide mineralogy of the Barbrook ore bodies.

Although sample collection in the Barbrook mining area was concentrated around the level 10 mine adit entrance and adjacent waste rock pile, limited sampling was also undertaken around the upper mining levels at Barbrook. The main drain in the level 7 adit

contains water (sample BW22) derived from the recycled water tanks above the disused French Bob open cut mine (sample BW23) which in turn is derived from the groundwater discharging into the level 10 mine adit. The only one of the disused Barbrook open cut mines to contain water at the time of sampling was the Clifford Scott mine (Figure 3.21) from which water sample BW24 and sediment core BS9 were collected.

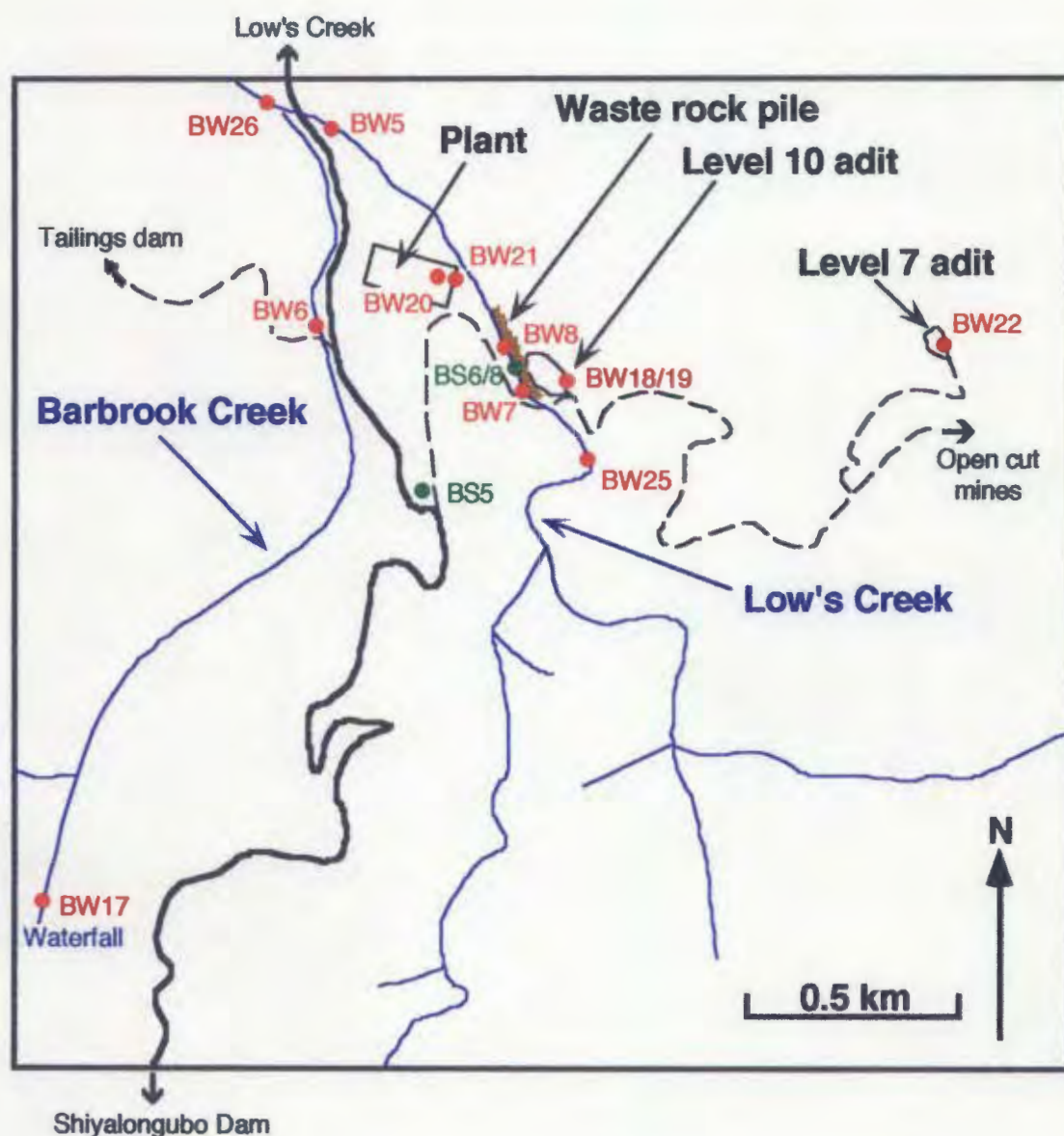


Figure 3.15: Location of water and sediment sampling sites associated with the Barbrook level 10 mine adit entrance area and nearby creeks; adapted from the 1:10 000 orthophoto map series (2531 CB 21 Barbrook; 1988) published by the South African Department of Surveys and Mapping.

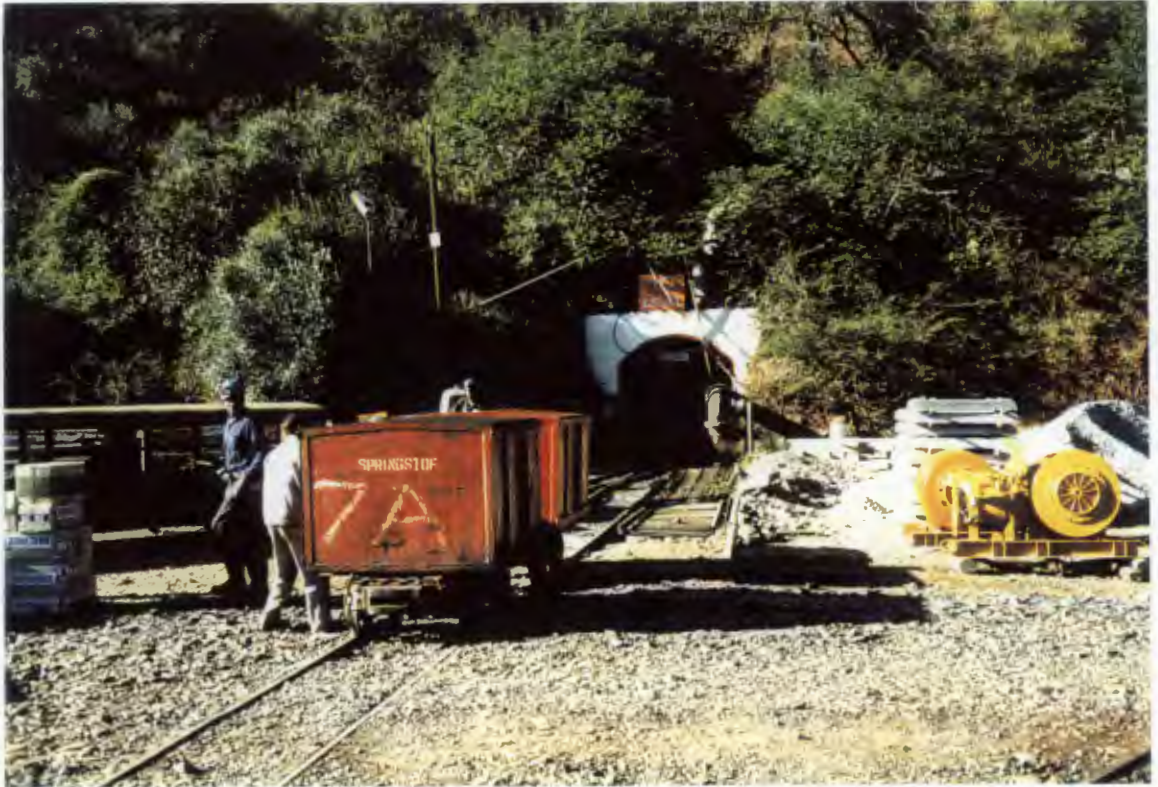


Figure 3.16: Entrance to the Barbrook level 10 mine adit.



Figure 3.17: Low's Creek immediately adjacent to the level 10 mine adit entrance and the waste rock pile at Barbrook.



Figure 3.18: Shiyalongubo dam located in the mountains above the Barbrook gold mine.



Figure 3.19: Location of Barbrook Creek sampling site BW6, looking north. The Barbrook gold mine and processing plant are located across the road on the right and a small settlement is located immediately adjacent to the left side of the creek at this site.



Figure 3.20: Low's Creek adjacent to the waste rock pile where sample BR3 was collected. Stream sediment core BS6 was also collected at this location.



Figure 3.21: Pond in the disused Clifford Scott open cut mine.

3.3 Sampling and analytical methods

3.3.1 Water samples

Triplicate 200 mL water samples were collected at each of 26 locations in the Barbrook area. Prior to sampling, each sample bottle was rinsed several times at the site in order to equilibrate it with the water to be collected. Where possible, samples were collected from approximately mid-depth and mid-stream within each of the water bodies, taking care to avoid disturbing the substrate in the immediate vicinity of the sampling site. Sample bottles were completely filled and sealed in order to exclude air. All samples were transported to the laboratory within five days of collection, after which they were refrigerated in an unfiltered, unacidified state until analysis so as to minimise the risk of chemical interaction (solute precipitation and/or adsorption) with the sample container. In order to calculate the mass discharge of individual chemical species from the Barbrook minesite, and thereby provide baseline data for future environmental monitoring in the area, it would have been desirable to measure the flow rate and cross-sectional dimensions of the individual streams from which the water samples were collected. Although time limitations precluded the gathering of such information, it should be considered an essential part of any future studies.

A brief description of the methods used to analyse the Barbrook water samples will be given here; further details are outlined in Appendix 1. The majority of water analyses were performed by the author in the Department of Geological Sciences at the University of Cape Town. Samples were initially analysed for pH and electrical conductivity (EC) using an automated Metrohm 691 pH meter and an automated CRISON microCM 2201 conductivity meter, respectively. Alkalinity was determined via a method of potentiometric titration to a preselected pH of 4.5 using 0.01M HCl and an automated Radiometer DTS 800 multi-titration system with a glass and calomel reference electrode pair attached. The redox potential of each water sample was determined using a platinum and saturated calomel electrode pair attached to the same Radiometer DTS 800 multi-titration unit operated in mV mode. The water samples were then filtered through 0.2 μm Millipore filters prior to analysis for their various constituents. The majority of the cation (K^+ , Na^+ , NH_4^+ , Ca^{2+} and Mg^{2+}) and anion (Cl^- , NO_2^- , NO_3^- and SO_4^{2-}) data were obtained via high performance ion chromatography (HPIC) using a Dionex ion chromatograph. The methods used to determine SiO_2 and F^- , namely the heteropoly blue colorimetric method and the ion selective electrode method, respectively, are as described in Standard Methods (1985). Phosphorus concentrations were determined using the ascorbic acid colorimetric method of Murphy and Riley (1962). Barbrook water samples were also analysed by inductively coupled plasma-atomic emission spectrometry (ICP-AES) for a range of elements, including Zn, Pb, Co, Ni, Si, Mn, Fe, Cr, Al and Cu. These analyses were performed on a Joby Yvon 70C (JY70C) spectrometer in the Chemistry Department at the University of Cape Town. Total As was determined using hydride generation-atomic absorption spectroscopy (HG-AAS) at the Scientific Services department of the Cape Town City Council.

3.3.2 Soil and sediment samples

Sediment cores were collected from nine sites in the Barbrook area using a hand corer. After their transportation to the laboratory in Cape Town, the cores were frozen within the outer casings. Following removal of the casings, the sediments were air-dried, gently crushed and passed through a 2 mm sieve. Core lengths ranged from 8 to 33 cm, with different horizons only recognisable in sample BS1. The main slimes dam was sampled by digging a pit and extracting a vertical slice through the upper 0.5 m of the sediments. A similar technique was employed to sample the soil underlying the waste rock pile, although the vertical slice was actually removed from the exposed surface on the slope next to Low's Creek (Figure 3.7). These samples were also air-dried, crushed and passed through a 2 mm sieve. The range of analytical techniques used to ascertain the chemical properties and constituents of the soil and sediment samples are detailed in Appendix 2 (Sections A2.1 to A2.4). Discussions of the expected precision and accuracy of the various methods are included where appropriate. The following section therefore represents only a brief synopsis of the techniques involved.

Soil and sediment pH values were determined using an automated Metrohm 691 pH meter on two separate soil solutions which were prepared for each sample using water and an electrolyte solution (1M KCl). The Karbonat-Bombe method of Birch (1981), whereby CO₂ pressure is measured following sample reaction with conc. HCl, was employed to determine the CaCO₃ content of each sample. Total concentrations of a range of major and trace elements were analysed by X-ray fluorescence spectrometry (XRFS) on pressed powder briquettes using a Philips PW1480 spectrometer in the Department of Geological Sciences at the University of Cape Town and the method described by Norrish & Chappell (1977). Arsenic extractions were undertaken using the NaHCO₃ method of Olsen and Sommers (1982) and As concentrations in the extractants were measured by inductively coupled plasma-mass spectrometry (ICP-MS) at the Institute for Soil, Climate and Water (ISCW) in Pretoria.

3.3.3 Rock samples

Two large (>2 kg) samples of waste rock (BR2 and BR3), comprising variably-sized and partly oxidised rock chips, were collected from different parts of the exposed face of the pile immediately adjacent to Low's Creek. Both samples were crushed in a jaw crusher and milled in a carbon steel swing mill prior to analysis. Detailed descriptions of the analytical techniques employed are presented in Appendix 3 (Sections A3.1 to A3.3). Analyses included XRFS determination of total major and trace element concentrations and determination of CaCO₃ content using the Karbonat-Bombe method (Birch, 1981). In order to determine the leachability of the waste rock for a range of elements including As, both

samples were also subjected to the toxicity characteristic leaching procedure (TCLP) at the Anglo American Research Laboratories in Johannesburg. This involved leaching the powdered samples for 24 hours using an acetate buffer solution at pH 5.0 and the rolling bottle technique (EPA, 1993), prior to multi-element analysis of the leachate via inductively coupled plasma - optical emission spectrometry (ICP-OES) and ICP-MS (As, Se and Te).

The methods used to analyse the primary and secondary minerals found at Barbrook are detailed in Appendix 3 (sections A3.4 to A3.5). Quantitative chemical analyses of the sulphide minerals present within the ore rock samples were obtained using the electron microprobe whereas secondary minerals were analysed semi-quantitatively by scanning electron microscopy (SEM).

3.4 Analytical results from the Barbrook area

3.4.1 Water samples

3.4.1.1 Tailings dam area

The complete results of the analyses performed on the Barbrook water samples collected from the tailings dam area and processing plant are presented in Tables 3.3 to 3.7. Apart from sample BW1, the EC values of the water samples from this area are all high relative to the South African Department of Water Affairs and Forestry (DWAf) water quality guidelines for domestic (≤ 70 mS/m; DWAf, 1995b) and agricultural (≤ 40 mS/m; DWAf, 1995c) use. In terms of their pH values and redox potential, these samples are all near-neutral to highly alkaline (pH 6.04 to 11.02), and span a limited range of Eh values (0.17 to 0.46 V). In terms of their ionic constituents, and consistent with their high EC and TDS values, all of the samples except BW1 contain high ionic concentrations. Compared to the WHO (1993) drinking water guideline value for As of ≤ 0.01 mg/L, most also contain high As levels.

The two samples collected from the Barbrook processing plant (BW20 and BW21) are characterised by high EC (> 250 mS/m), neutral to slightly alkaline pH values (6.92 to 7.68) and identical Eh measurements (0.32 V). These samples have particularly high concentrations of SO_4^{2-} (> 1400 mg/L), Ca^{2+} (> 300 mg/L) and Mg^{2+} (> 180 mg/L), all of which are slightly more enriched in BW21 than in BW20. Arsenic concentrations in both samples are approximately twice as high as the WHO (1993) drinking water guideline value.

The samples collected from the calcine dam pond (BW15), the stream of tailings extending between the calcine and slimes dams (BW14), and the pool of standing water at the southern end of the slimes dam (BW4) have the highest EC (> 300 mS/m) and pH (8.9 to 11.0) values, as well as the lowest Eh (0.17 to 0.24 V) measurements, of all samples collected within the tailings dam area. Although all three samples are high in SO_4^{2-} (> 1270 mg/L), Na^+ (> 280 mg/L), NH_4^+ (≥ 28 mg/L) and Ca^{2+} (≥ 230 mg/L), BW14 and BW15 are

particularly enriched in Na^+ (>600 mg/L) relative to BW4 (283 mg/L), whereas BW4 has particularly high Ca^{2+} (318 mg/L). All three samples have high As contents compared to the WHO (1993) drinking water guideline value, and sample BW14 has the highest value (4.12 mg/L) measured at Barbrook.

Table 3.3: Electrical conductivity (EC), total dissolved solids (TDS), pH and redox (Eh and pe) measurements for the water samples collected from the Barbrook tailings dam area.

Sample	EC (mS/m)	TDS (mg/L)	pH	Eh (V)	pe
BW1	28.1	186	7.28	0.34	5.74
BW2	211	1393	6.04	0.46	7.77
BW3	152	1003	6.74	0.27	4.60
BW4	319	2105	9.15	0.20	3.46
BW9	207	1366	7.86	0.35	5.92
BW10	274	1808	7.54	0.36	6.01
BW11	163	1076	7.94	0.35	5.92
BW12	182	1201	7.75	0.36	6.01
BW13	243	1604	7.04	0.31	5.26
BW14	519	3425	11.02	0.17	2.88
BW15	510	3366	8.93	0.24	4.00
BW20	255	1683	6.92	0.32	5.35
BW21	297	1960	7.68	0.32	5.34

Note: TDS (mg/L) = EC (mS/m) x 6.6 (Dallas and Day, 1993)

These same three calcine/slimes dam water samples are also anomalous in terms of their poor anion-cation charge balances, as a result of an excess of cations over anions (Section A1.5). The anion-cation charge balances of samples BW14 and BW15 are particularly poor, with differences of 19.7% and 16.1% respectively. These values lie well outside the acceptable limits (10%) for good quality data. Although sample BW4 has a charge balance which lies within the 10% acceptable limit, it has the next highest anion-cation charge difference of 9.8%. The addition of 10M HNO_3 to these three water samples during preparation for HG-AAS As analysis resulted in a drop in pH to values between 0.86 and 1.22 and the immediate formation of a white (BW4 and BW15) or pink (BW14) precipitate. The XRD analysis of this precipitate in samples BW14 and BW15 (Figure 3.22) revealed it to be copper thiocyanate ($\beta\text{-CuSCN}$). Therefore, the poor charge balance exhibited by these samples may be due to the presence of appreciable amounts of cyanide (CN^-) or thiocyanate (SCN^-) in solution which was not detected by HPIC but became insoluble with increased acidity. The pink colour of the BW14 precipitate is not explained by the XRD scan, which is identical to that of BW15, but it is presumed to be due to the presence of Mn.

Compared to the pond on the southern end of the slimes dam (BW4), the pool at the northern end (BW13) has a slightly lower EC, a substantially lower and neutral pH, lower Na^+ and SO_4^{2-} , higher Eh and Mg^{2+} , and a similar Ca^{2+} concentration. Although the As content of the water in this northern pond is over 100 times less than that in the southern pond, it is

still high (0.012 mg/L) and approximately equivalent to the WHO (1993) recommended upper limit for drinking water.

Table 3.4: Cation concentration data (mg/L) for the water samples collected from the Barbrook tailings dam area, as measured by HPIC; nd = not detected.

Sample	Na ⁺	NH ₄ ⁺	K ⁺	Mg ²⁺	Ca ²⁺
BW1	3.43	6.17	20.4	18.3	18.5
BW2	97.5	nd	14.6	84.0	338
BW3	119	20.4	7.14	61.6	99.9
BW4	283	27.6	43.3	101	318
BW9	191	nd	7.28	146	85.9
BW10	320	nd	7.63	152	131
BW11	131	nd	3.73	86.4	136
BW12	159	nd	2.83	109	45.5
BW13	47.8	10.1	38.6	155	299
BW14	642	67.1	150	89.9	236
BW15	673	37.6	34.0	99.9	230
BW20	42.3	11.5	38.2	182	322
BW21	30.8	13.3	38.5	217	410

Table 3.5: Anion concentration data (mg/L) for the water samples collected from the Barbrook tailings dam area, as measured by HPIC; *alkalinity is expressed as mg CO₃²⁻/L for sample BW14; nd = not detected.

Sample	Cl ⁻	NO ₂ ⁻	NO ₃ ⁻	HCO ₃ ⁻	SO ₄ ²⁻
BW1	20.7	nd	0.590	174	4.03
BW2	36.6	nd	74.8	44.4	1276
BW3	42.8	nd	nd	239	487
BW4	14.8	nd	60.9	83.3	1412
BW9	195	21.7	5.32	448	443
BW10	307	nd	2.91	560	469
BW11	101	nd	nd	304	432
BW12	140	nd	nd	340	442
BW13	11.9	nd	46.5	88.9	1128
BW14	17.3	76.9	43.0	118*	1436
BW15	32.6	9.64	63.4	156	1578
BW20	12.8	nd	82.7	64.3	1434
BW21	13.7	nd	68.8	142	1799

The lowest pH values (6.04 to 6.74) found in the Barbrook tailings dam area are associated with the water seeping from the base of the slimes dam wall (samples BW2 and BW3). Sample BW2, which constitutes clear water seeping directly from the base of the wall, has a slightly lower pH than BW3 as well as higher NO₃⁻, SO₄²⁻, K⁺ and Mg²⁺. The high Ca²⁺ concentration of BW2 is second only to processing plant sample BW21 in magnitude. However, sample BW3, which was collected from an upwelling puddle close to the base of the wall, has a substantially higher HCO₃⁻ content than BW2 and an As content (1.64 mg/L) which is similar to that of the southern slimes dam pond but approximately ten times higher

than that of sample BW2 (0.166 mg/L). In addition, sample BW3 was the only Barbrook sample found to contain detectable P (0.08 mg/L).

The four boreholes at the base of the slimes dam wall yielded groundwater samples (BW9 to BW12) which share near-neutral pH values (7.54 to 7.94), identical redox potentials (Eh = 0.35 to 0.36 V) and EC measurements which are high compared to DWAFF (1995b; 1995c) standards but at the lower end of the range measured within waters in the tailings dam area. These groundwaters are characterised by the highest HCO_3^- (304 to 560 mg/L), Cl^- (101 to 307 mg/L) and F^- (0.29 to 0.44 mg/L) values within the tailings dam area, as well as negligible As contents. Of the borehole samples, BW10 is distinct in that it has substantially higher Na^+ , HCO_3^- and Cl^- , plus slightly higher Mg^{2+} and SO_4^{2-} , compared to the other groundwater samples. Both BW10 and BW11 have higher Ca^{2+} than the other two groundwater samples. Only sample BW9 contains any detectable NO_2^- , whereas little if any NO_3^- is present within any of the borehole waters.

Table 3.6: Total arsenic, silica and fluoride data (mg/L) for the water samples collected from the Barbrook tailings dam area; nd = not detected

Sample	As	SiO_2	F^-
BW1	0.007	2.95	0.08
BW2	0.166	6.54	0.14
BW3	1.64	6.20	0.16
BW4	1.67	1.47	0.06
BW9	nd	3.51	0.44
BW10	0.003	7.61	0.34
BW11	nd	2.79	0.29
BW12	0.002	4.70	0.43
BW13	0.012	1.75	0.07
BW14	4.12	2.25	nd
BW15	0.423	1.22	nd
BW20	0.023	1.32	0.06
BW21	0.019	1.90	nd

Table 3.7: Elemental concentration data (mg/L) for the water samples collected from the Barbrook tailings dam area, as measured by ICP-AES; Zn, Pb, Cr, Al and Cu concentrations were all below detection limit; nd = not detected.

Element	BW2	BW3	BW10	BW21
Co	0.268	0.321	0.215	nd
Ni	0.312	0.223	0.257	nd
Mn	1.15	1.61	3.70	4.58
Fe	nd	nd	0.366	0.106

Sample BW1, collected from a small man-made pond close to Crystal Stream which is presumably filled by rainwater, is the only water body in this immediate area which has a low

EC value (28 mS/m). It contains negligible As and has the lowest concentrations of all the cations except K^+ and all the anions except Cl^- and HCO_3^- .

The SiO_2 concentrations of the water samples collected in the tailings dam area are variable. The highest values (6.2 to 7.6 mg/L) occur in the water seeping from the base of the slimes dam wall (BW2 and BW3) and in borehole sample BW10. The other borehole samples have SiO_2 concentrations of 2.8 to 4.7 mg/L. All other samples, apart from BW1 and BW14 (2.95 mg/L and 2.25 mg/L, respectively) have SiO_2 contents of <2 mg/L. Four of the water samples associated with the tailings dam and processing plant were analysed by ICP-AES for a range of elements in order to check for the presence of heavy metals. Only Co, Ni, Mn and Fe were above detection limit in these samples.

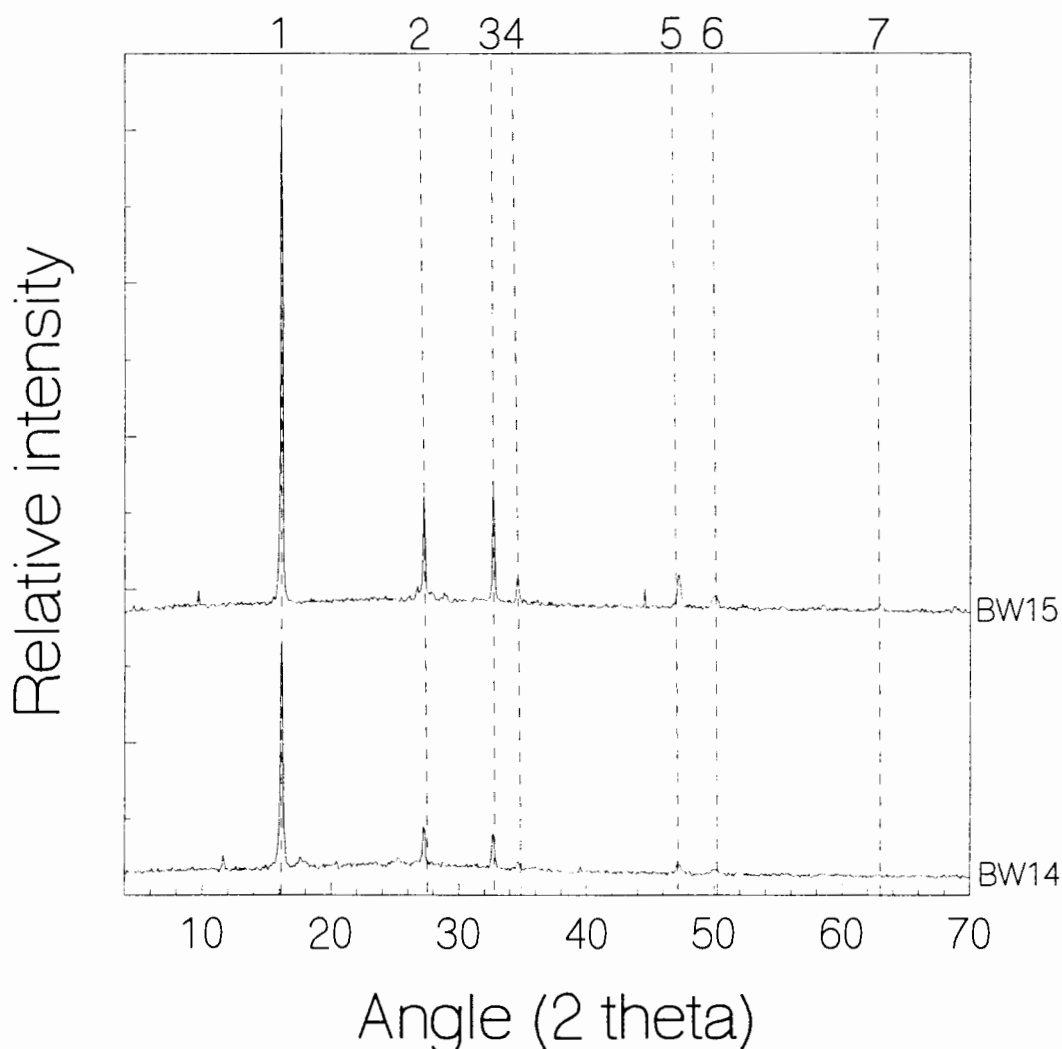


Figure 3.22: XRD scans for the copper thiocyanate precipitates formed during acidification of Barbrook water samples BW14 and BW15. The d-spacings (\AA) for the numbered peaks are as follows: 1 = 5.50, 2 = 3.27, 3 = 2.74, 4 = 2.59, 5 = 1.93, 6 = 1.82, and 7 = 1.58. Note that the intensity of the upper scan was increased in order to separate the two scans on the above plot.

3.4.1.2 Mining area

The complete results of the analyses performed on the water samples collected from the Barbrook mining area are presented in Tables 3.8 to 3.12. These water samples are characterised by neutral pH values (7.03 to 7.97), a limited range of Eh values (0.32 to 0.62 V) and generally low EC measurements. Ionic concentrations are also low and, apart from sample BW24, As levels are generally at or below the WHO (1993) drinking water guideline value of 0.01 mg/L.

Table 3.8: Electrical conductivity (EC), total dissolved solids (TDS), pH and redox (Eh and pe) measurements for the water samples collected from the Barbrook mining area.

Sample	EC (mS/m)	TDS (mg/L)	pH	Eh (V)	pe
BW5	18.5	122	7.29	0.32	5.42
BW6	6.3	41.6	7.87	0.42	7.09
BW7	7.5	49.5	7.47	0.41	7.01
BW8	7.1	46.9	7.60	0.41	6.90
BW16	6.0	39.6	7.03	0.59	10.0
BW17	5.6	37.0	7.37	0.62	10.5
BW18	26.7	176	7.97	0.34	5.74
BW19	136	898	7.44	0.39	6.52
BW22	95.4	630	7.88	0.38	6.40
BW23	106	700	7.73	0.39	6.57
BW24	19.4	128	7.15	0.40	6.68
BW25	6.1	40.3	7.58	0.38	6.43
BW26	7.3	48.2	7.60	0.39	6.52

Only samples BW19, BW22, and BW23, all of which represent recycled water used in the underground mining operations, have EC values (95 to 136 mS/m) greater than the 70 mS/m drinking water quality guideline value of DWAF (1995b). Compared to the other samples collected from the mining area, these three samples are also characterised by having the highest concentrations of every measured anion and cation and being the only samples to contain NO_2^- . They also contain the highest NO_3^- concentrations (91 to 188 mg/L) of all the Barbrook water samples. Sample BW19, from the main drain of the level 10 mine adit, has the highest ionic concentrations and is the only sample from this area to contain detectable F^- (0.05 mg/L).

Apart from sample BW5, the samples collected from Shiyalongubo Dam, Barbrook Creek and Low's Creek (BW6, BW7, BW8, BW16, BW17, BW25 and BW26) all share similarly low EC values (5.6 to 7.5 mS/m), low ionic concentrations and negligible As contents (<0.007 mg/L). However, sample BW5, collected from Low's Creek at a point downstream of the mine site and processing plant but prior to the confluence with Barbrook Creek, has a higher EC (18.5 mS/m), higher concentrations of all measured ionic constituents apart from K^+ , and an As content (0.011 mg/L) which is equivalent to the WHO (1993) suggested upper

limit for drinking water. Sample BW5 also has the lowest Eh value (0.32 V) of all the mine site water samples.

Table 3.9: Cation concentration data (mg/L) for water samples collected from the Barbrook mining area, as measured by HPIC; nd = not detected.

Sample	Na ⁺	NH ₄ ⁺	K ⁺	Mg ²⁺	Ca ²⁺
BW5	5.35	nd	0.529	11.5	12.9
BW6	3.73	nd	0.380	4.27	2.16
BW7	3.01	0.270	0.765	4.39	4.07
BW8	3.11	nd	0.196	3.71	5.85
BW16	2.29	nd	0.283	2.74	1.60
BW17	3.07	nd	0.323	1.44	4.61
BW18	8.51	nd	1.14	14.7	24.7
BW19	13.2	38.7	5.38	95.0	101
BW22	7.40	11.48	2.84	83.2	68.8
BW23	8.47	16.31	2.85	87.6	66.9
BW24	1.62	0.083	0.682	14.1	12.8
BW25	2.92	nd	0.091	4.31	3.50
BW26	3.53	nd	0.306	5.06	3.99

Table 3.10: Anion concentration data (mg/L) for water samples collected from the Barbrook mining area, as measured by HPIC; nd = not detected.

Sample	Cl ⁻	NO ₂ ⁻	NO ₃ ⁻	HCO ₃ ⁻	SO ₄ ²⁻
BW5	5.24	nd	7.52	50.6	29.6
BW6	4.34	nd	1.04	27.6	3.06
BW7	4.25	nd	0.249	32.6	5.51
BW8	4.52	nd	0.230	32.4	4.60
BW16	3.62	nd	0.591	17.1	0.916
BW17	3.88	nd	1.07	20.6	1.30
BW18	4.52	nd	0.483	157	9.43
BW19	7.96	7.68	188	110	370
BW22	5.02	1.44	91.3	88.0	342
BW23	5.56	1.25	158	112	349
BW24	2.38	nd	11.5	7.98	65.5
BW25	4.10	nd	0.113	27.0	2.62
BW26	4.18	nd	1.16	29.7	5.34

The standing water within the Clifford Scott open cut mine (BW24) is quite distinct from that found elsewhere within the Barbrook mining area. Compared to the surrounding creek waters (BW5 aside), it has higher concentrations of Mg²⁺, Ca²⁺, NO₃⁻ and SO₄²⁻ as well as a higher EC reading, although all of these values are lower than that found within the water samples collected from the underground mining operations. In addition, BW24 possesses the lowest Na⁺, Cl⁻, HCO₃⁻ and SiO₂ concentrations and the highest As content (0.021 mg/L) of all the mining area samples.

The only other sample collected from the Barbrook mining area was of the groundwater entering the level 10 mine adit (BW18). This water has the highest pH (7.97) and SiO₂ content (8.1 mg/L) of the mining area samples, a similarly low Eh to BW5 (0.34 V)

and an EC reading (26.7 mS/m) second only to that of the three recycled underground water samples (BW19, BW22 and BW23). In terms of its ionic constituents, BW18 has the highest HCO_3^- concentration, and higher cation concentrations than the surrounding creeks. The As content (0.011 mg/L) of this water is similar to that of the water in the main drain of the level 10 mine adit and equivalent to the WHO (1993) suggested upper limit for drinking water.

Only three samples from the Barbrook mining area were analysed by ICP-AES for a range of metals. Of the elements analysed, only Zn, Ni, Mn and Fe were above detection limit in some of these samples.

Table 3.11: Total arsenic and silica data (mg/L) for the water samples collected from the Barbrook mining area; nd = not detected.

Sample	As	SiO ₂
BW5	0.011	4.94
BW6	0.001	4.14
BW7	0.005	4.61
BW8	0.007	4.81
BW16	0.003	3.46
BW17	0.002	3.97
BW18	0.012	8.12
BW19	0.011	5.02
BW22	0.004	3.29
BW23	0.004	3.82
BW24	0.021	1.77
BW25	nd	4.40
BW26	0.002	4.13

Table 3.12: Elemental concentration data (mg/L) for the water samples collected from the Barbrook mining area, as measured by ICP-AES; Pb, Co, Cr, Al and Cu concentrations were all below detection limit; nd = not detected.

Element	BW6	BW7	BW19
Zn	nd	nd	0.167
Ni	nd	nd	0.347
Mn	0.047	nd	3.36
Fe	0.147	0.122	nd

3.4.1.3 Comparison of the results from the Barbrook tailings dam and mining areas

In terms of the majority of measured chemical parameters and constituents, the water samples collected from the Barbrook mining area are substantially different from the water samples collected around the tailings dam area, the latter including the processing plant samples (Figures 2.23 and 2.24). The plots presented in Figure 3.23 provide an indication of some of the major differences between the two areas. Apart from sample BW1, the tailings dam area samples have substantially greater EC, SO_4^{2-} , Na^+ , Mg^{2+} , and Ca^{2+} contents than the mining area samples, although the underground recycled water samples (BW19, BW22

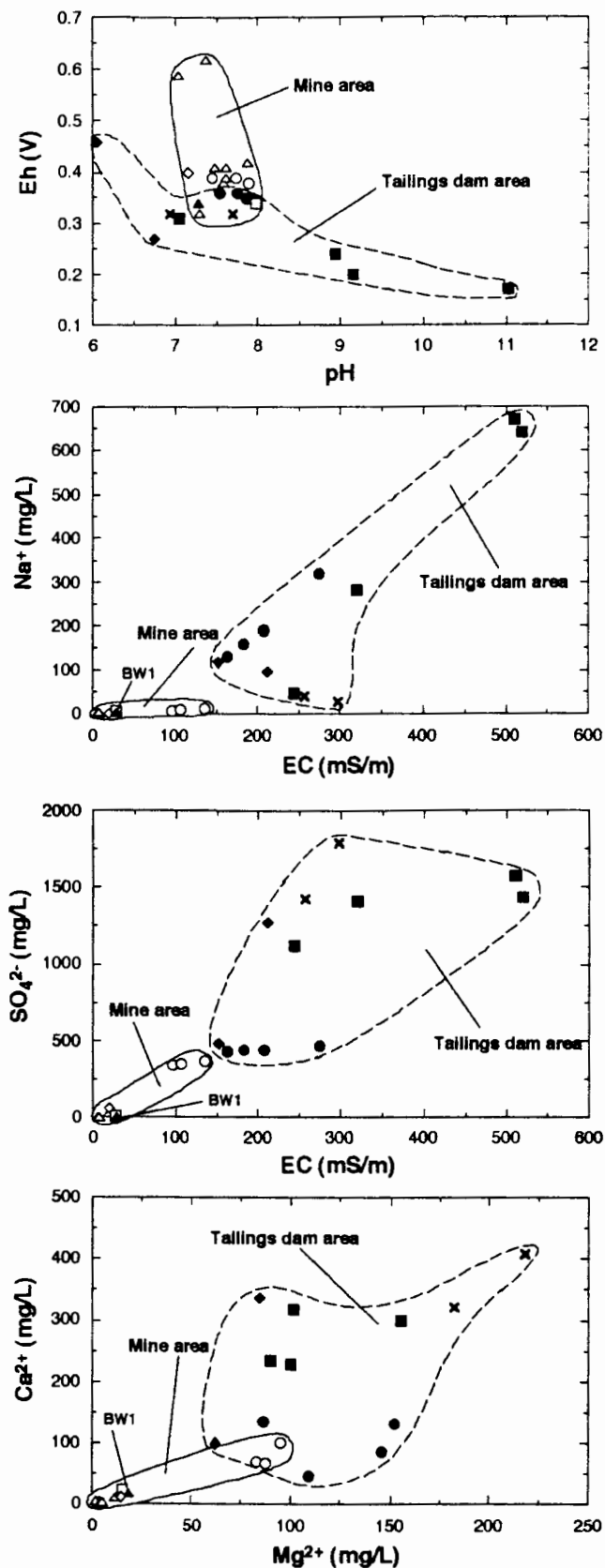


Figure 3.23: Plots of various chemical parameters which distinguish the water samples collected from the tailings dam area (filled circles = boreholes, filled squares = calcine/slimes dams, filled diamonds = seepage from base of slimes dam wall, filled triangle = dam near Crystal Stream (BW1), and crosses = processing plant) and the mining area (open circles = underground mining operations, open square = groundwater entering level 10 adit (BW18), open diamond = Clifford Scott open cut and open triangles = Barbrook and Low's creeks) at Barbrook.

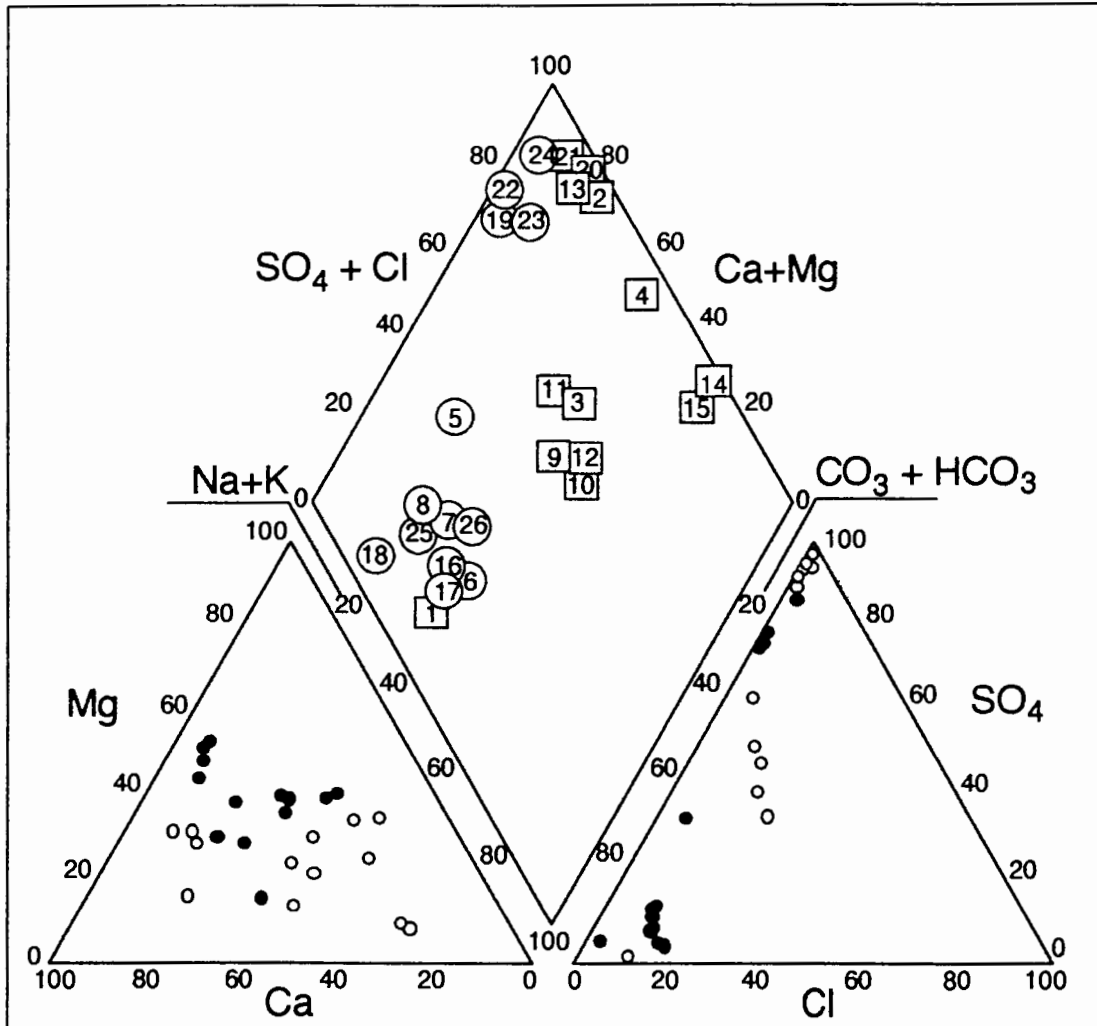


Figure 3.24: Piper diagram illustrating the relative anion and cation compositions (mg %) of the water samples collected from the Barbrook tailings dam (open circles) and mining (filled circles) areas. Numbers on the composite diamond plot represent BW sample numbers; numbers enclosed by squares are tailings dam samples whereas encircled numbers are mining area samples.

and BW23) are generally intermediate in composition between the two areas. The tailings dam area samples also have a greater range of pH values and extend to lower Eh values than the mining area waters. Sample BW1 has a greater chemical similarity to the surface waters and groundwater from the mining area than to any of the tailings dam area samples.

The Piper trilinear diagram of Figure 3.24 is a combined cation-anion plot which is useful for illustrating the fact that the various Barbrook water samples form distinct chemical groupings. This is particularly evident in terms of the similar position occupied by sample BW1 and the creek and groundwater samples from the mining area, whereas Low's Creek sample BW5 plots slightly separately. According to the hydrochemical facies subdivisions which can be applied to the Piper diagram (Freeze and Cherry, 1979), all of these waters can be described as the bicarbonate facies type in terms of their anion compositions, but no dominant type in terms of cations. A separate group of samples occupying the approximate centre of the diagonal plot represent the four borehole samples (BW9 to BW12) and the slimes dam wall seepage sample BW3. According to Freeze and Cherry (1979), these samples have no dominant geochemical facies type in terms of either their anion or cation compositions. The top end of the diagonal plot is occupied by the processing plant samples, the recycled waters from the underground mining operations, the water collected from the Clifford Scott open cut mine, the northern pond on the slimes dam and slimes dam seepage sample BW2. Although all of these samples conform to the sulphate facies type in terms of their anion compositions, those samples collected from the mining area approximate the magnesium facies type whereas the tailings dam area samples correspond to the calcium facies type in terms of their cation compositions. Samples BW4, BW14 and BW15 extend down the right side of the diamond plot and are once again different from the other Barbrook water samples in that they can be classified as sulphate, sodium facies waters.

3.4.1.4 MINTEQA2 modelling of Barbrook water data

The chemical data for Barbrook water samples with As concentrations ≥ 0.01 mg/L have been manipulated using the computer program MINTEQA2 (version 3.10: EPA, 1991) which represents a geochemical speciation model for dilute aqueous systems and is complemented by the PRODEFA2 interactive input program. This program allows As to be entered as either H_3AsO_3 or H_3AsO_4 , representing an As(III) and an As(V) species, respectively. The main aim of using MINTEQA2 is to investigate whether any secondary mineral phases resulting from the weathering of the waste rock and/or tailings material may be having an influence on water chemistry at Barbrook. Of particular interest is the possibility that As solution chemistry may be controlled by solid phases such as $\text{Ca}_3(\text{AsO}_4)_2$, stated by Sadiq *et al.* (1983) to be the most likely arsenate mineral to precipitate under oxidising, alkaline conditions.

Table 3.13: Saturation indices calculated for a range of representative mineral phases by MINTEQA2 for the water samples collected from the Barbrook tailings dam area.

Mineral:	Saturation Indices					
	BW2	BW3	BW4	BW13	BW14	BW15
Calcite (CaCO ₃)	-2.02	-0.68	1.58	-0.40	0.72	1.51
Dolomite (CaMg(CO ₃) ₂)	-4.36	-1.30	2.95	-0.81	1.29	2.94
Gypsum (CaSO ₄ ·2H ₂ O)	-0.04	-0.76	-0.07	-0.15	-0.21	-0.21
Quartz (SiO ₂)	0.11	0.08	-1.04	-0.65	-1.77	-1.40
Sepiolite(A) (Si ₆ Mg ₄ O ₁₅ (OH) ₂ ·4H ₂ O)	-12.2	-9.49	-3.05	-9.87	2.06	-5.10
Ca-arsenate (Ca ₃ (AsO ₄) ₂ ·6H ₂ O)	-13.0	-9.98	-3.85	-12.6	-0.25	-6.05

Note: Alkalinity was entered into MINTEQA2 as mg CO₃²⁻/L, SiO₂ was entered as mg H₄SiO₄/L and As was entered as either mg H₃AsO₃/L or mg H₃AsO₄/L. The saturation indices were calculated by MINTEQA2 based on the following relationship between the ion activity product (IAP) and the thermodynamic calculation for the solubility product (K_{sp}):

$$SI = \log_{10} \frac{[IAP]}{[K_{sp}]}$$

Table 3.14: Saturation indices calculated for a range of representative mineral phases by MINTEQA2 for the water samples collected from the Barbrook processing plant.

Mineral:	SI	
	BW20	BW21
Calcite (CaCO ₃)	-0.69	0.53
Dolomite (CaMg(CO ₃) ₂)	-1.35	1.07
Gypsum (CaSO ₄ ·2H ₂ O)	-0.07	0.07
Quartz (SiO ₂)	-1.17	-0.65
Sepiolite(A) (Si ₆ Mg ₄ O ₁₅ (OH) ₂ ·4H ₂ O)	-11.8	-7.18
Ca-arsenate (Ca ₃ (AsO ₄) ₂ ·6H ₂ O)	-12.2	-10.5

Table 3.15: Saturation indices calculated for a range of representative mineral phases by MINTEQA2 for the water samples collected from the Barbrook mining area.

Mineral:	Saturation Indices			
	BW5	BW18	BW19	BW24
Calcite (CaCO ₃)	-1.33	0.13	-0.19	-2.31
Dolomite (CaMg(CO ₃) ₂)	-2.44	0.30	-0.13	-4.31
Gypsum (CaSO ₄ ·2H ₂ O)	-2.41	-2.68	-0.86	-2.10
Quartz (SiO ₂)	-0.04	0.19	-0.02	-0.72
Sepiolite(A) (Si ₆ Mg ₄ O ₁₅ (OH) ₂ ·4H ₂ O)	-8.63	-5.07	-6.56	-11.1
Ca-arsenate (Ca ₃ (AsO ₄) ₂ ·6H ₂ O)	-14.6	-12.3	-12.5	-16.5

The calculated saturation indices (SI) for representative sulphate, carbonate, silicate and arsenate minerals within the Barbrook water samples are presented in Tables 3.13 to 3.15. An SI value which approaches zero indicates that the solution is approaching

equilibrium for a particular mineral phase, at which point it should neither precipitate nor dissolve it. A positive SI value implies that the water is supersaturated with respect to a mineral phase, such that the mineral could be expected to precipitate out of solution. However, not only does the MINTEQA2 model employed here disallow precipitation, but it also assumes thermodynamic equilibrium. Therefore, if the solution chemistry is being controlled by a metastable component, MINTEQA2 may indicate supersaturation with respect to that phase although in nature it would not actually precipitate out of solution.

The results of the MINTEQA2 modelling program indicate that all of the Barbrook samples with As contents ≥ 0.01 mg/L are undersaturated with respect to As minerals. If As is entered as H_3AsO_3 , MINTEQA2 calculates SI values for the As oxide (As_2O_3) minerals arsenolite and claudetite. However, if As is entered as H_3AsO_4 , SI values are calculated for the arsenic oxide As_2O_5 and calcium arsenate ($\text{Ca}_3(\text{AsO}_4)_2 \cdot 6\text{H}_2\text{O}$) instead. The only sample which approaches equilibrium with respect to calcium arsenate is BW14 (SI = -0.25), collected from the stream of tailings material traversing between the calcine and slimes dams. Although a negative SI value implies undersaturation with respect to a certain mineral phase, this could actually be a consequence of the contact time between the water and the mineral being too short for equilibrium to be reached.

The MINTEQA2 results for the water samples collected from the tailings dam area are presented in Table 3.13. Consistent with their relatively high SiO_2 concentrations, the samples collected from the base of the slimes dam wall (BW2 and BW3) are both oversaturated with respect to quartz, which is therefore the most likely mineral to precipitate out of solution. As a result of its higher Ca^{2+} and SO_4^{2-} contents, sample BW2 is only slightly undersaturated (SI = -0.04) with respect to the evaporitic sulphate mineral gypsum. An SI value so close to zero suggests that, within analytical uncertainty, this water could well be in equilibrium with gypsum. Calcine and slimes dams samples BW4, BW14 and BW15 have quite similar saturation indices which reflect their alkaline pH values. They are all oversaturated with respect to the carbonate minerals, calcite and dolomite, and undersaturated with respect to gypsum. In addition, sample BW14 is also oversaturated with respect to sepiolite. By comparison, the water collected from the northern end of the slimes dam (BW13) is undersaturated with respect to calcite and gypsum, reflecting its lower and more neutral pH.

The saturation indices of the two processing plant samples (BW20 and BW21) also reflect their different pH values. Whereas BW20, with a pH of 6.92, is undersaturated with respect to all of the representative phases presented in Table 3.14, sample BW21, with a more alkaline pH of 7.68, is oversaturated with respect to calcite, dolomite and gypsum.

The MINTEQA2 results for the water samples from the Barbrook mining area which contain significant As contents are presented in Table 3.15. Both the Low's Creek sample collected downstream of the processing plant (BW5) and the recycled mine water from the main drain in the level 10 adit (BW19) could be considered to be approaching equilibrium with quartz, with SI values of -0.04 and -0.02, respectively. In addition to quartz, however, the

groundwater entering the level 10 mine adit (BW18) is also oversaturated with respect to calcite and dolomite.

The results of the MINTEQA2 modelling also include proposed speciation for the various dissolved chemical components in solution. In terms of As, the speciation is primarily dependent on how As data were entered into the program as well as the pH of the solution. When the total As content was entered as H_3AsO_3 , it was speciated as either just H_3AsO_3 , a combination of H_3AsO_3 and H_2AsO_3^- , or, at still higher pH values (BW14: pH 11), as H_3AsO_3 , H_2AsO_3^- and HAsO_3^{2-} . However, when the total As content was entered as H_3AsO_4 , nominated species included either HAsO_4^{2-} alone or combinations of H_2AsO_4^- and HAsO_4^{2-} , or HAsO_4^{2-} and AsO_4^{3-} , once again depending on the measured pH of the solution. Therefore, although measured Eh values were also entered as part of the data input procedure, MINTEQA2 only speciates As on the basis of pH. In addition the results indicated that the As in solution would not combine with any of the other ionic species.

3.4.2 Soil and sediment samples

3.4.2.1 Tailings dam area

Analytical data for the sediment cores and slimes dam material from the Barbrook tailings dam area are presented in Table 3.16. The sediment cores collected from Crystal Stream (BS1) and the slimes seepage pond (BS2) are similar in terms of their near-neutral pH(H_2O) and slightly acidic pH(KCl) values, their low CaCO_3 contents ($\leq 3\%$) and their concentrations of elements such as Mn and Pb. However, compared to the BS1 sediments, sample BS2 does have higher concentrations of Fe, Al, Zn, Cu, Ni, Co and Cr. Both total and extractable As are also higher in BS2 than in BS1, the latter having a total As concentration within the usual range for unpolluted soils (≤ 40 mg/kg: Chatterjee *et al.*, 1993; O'Neill, 1995). The subdivision of the BS1 sediment core, primarily on the basis of colour, revealed an increase in pH (H_2O and KCl), Fe, Mn and extractable As with depth, although the concentrations of most other constituents were found to either remain the same (Co and V) or decrease slightly (Al, total As, Zn, Cu, Ni, Cr, and Pb) with depth.

By comparison with the Crystal Stream and slimes seepage pond sediments, the sediment cores and tailings material collected from the slimes (BS3 and BS4) and calcine (BS7) dams have substantially higher pH (H_2O and KCl) values, CaCO_3 contents ($\geq 5.8\%$) and concentrations of Fe, Zn, Cu, Mn and Pb. Total and extractable As concentrations are also substantially higher, with the highest values occurring in the calcine dam sediments.

Table 3.16: Analytical data for the soil and sediment samples collected from the tailings dam area at Barbrook; XRFS data represent total major and trace element contents analysed on powder briquettes, whereby the major elements were analysed as wt % Fe₂O₃, Al₂O₃ and CaO.

Parameter:	BS1A	BS1B	BS2	BS3	BS4	BS7
Munsell colour	yellowish brown 10YR5/6	dark yellow brown 10YR4/4	yellowish brown 10YR5/8	light grey 10YR7/2	greyish brown 2.5Y5/2	light grey 10YR7/2
Texture	clay loam	clay	clay	silty clay	fine sandy loam	silty clay loam
pH (H ₂ O)	6.28	7.11	6.52	8.25	8.18	8.67
pH (KCl)	5.27	6.22	5.79	7.92	7.86	8.54
CaCO ₃ (%)	3.0	2.8	3.0	6.8	5.8	7.6
Extractable As (mg/kg)	0.46	0.71	13.6	97.9	91.9	172
*Extractable As (%)	1.8	3.2	6.3	5.9	4.7	7.9
XRFS data (mg/kg):						
Fe	77637	80434	90226	115406	100718	104915
Al	75154	72507	88385	82563	57688	72507
Ca	2780	4560	3945	17096	13372	14673
As	25.2	22.2	217	1658	1964	2169
Zn	84.4	78.4	103	440	296	381
Cu	59.1	58.0	64.2	193	98.2	128
Ni	349	322	491	389	339	355
Co	41.9	42.2	60.5	43.7	47.2	45.4
Mn	1345	1461	1407	1716	1667	1889
Cr	865	799	1233	1109	862	1267
V	118	118	149	152	121	167
Pb	16.2	15.0	14.9	479	235	195

Note: Colour was determined according to the Munsell (1992) soil colour charts; textural class was determined according to the Soil and Irrigation Research Institute (SIRI, 1991) guidelines; *Extractable As (%) refers to the percentage of total As that was extracted using the NaHCO₃ method of Olsen and Sommers (1982).

3.4.2.2 Mining area

The analytical data for the sediment cores and soil collected from the Barbrook mining area are presented in Table 3.17. These samples are all characterised by near-neutral pH(H₂O) and slightly more acidic pH(KCl) values, low CaCO₃ contents ($\leq 3\%$) and high concentrations of total As relative to the range usually observed in unpolluted soils. Extractable As contents are intermediate to those observed in the Crystal Stream sediment core (BS1: 0.46 to 0.71 mg/kg) and the slimes seepage pond sediment core (BS2: 13.6 mg/kg) although both BS6, collected from Low's Creek adjacent to the waste rock pile, and BS9, collected from the Clifford Scott open cut mine, have higher total As than BS2. Therefore, the percentage of extractable As is more variable in the mining area sediments than the tailings dam area sediments.

The Clifford Scott open cut sediments (BS9) are characterised by having not only the highest total As content of the mining area sediments, but also the highest

concentrations of Fe, Al and Cr of all the Barbrook soil and sediment samples. However, the soil underlying the waste rock pile (BS8) has the highest concentrations of Zn, Cu, Ni, Co, Mn and Pb within the mining area samples and the concentrations of Zn, Ni, Co and Mn within this soil are substantially greater than the concentrations measured within any of the tailings dam area samples. The Pb contents of the mining area samples are up to ten times less than in the slimes/calcline dam sediments.

Table 3.17: Analytical data for the soil and sediment samples collected from the Barbrook mining area; XRF data represent total major and trace element contents analysed on powder briquettes, whereby the major elements were analysed as wt % Fe₂O₃, Al₂O₃ and CaO.

Parameter:	BS6	BS8	BS9
Munsell colour	Yellowish brown 10YR5/6	Reddish brown 5YR4/3	Yellowish red 5YR5/6
Texture	clay loam	clay	sandy loam
pH (H ₂ O)	6.46	7.31	6.66
pH (KCl)	5.38	6.62	6.11
CaCO ₃ (%)	2.9	3.2	2.9
Extractable As (mg/kg)	6.9	8.7	3.5
Extractable As (%)	1.9	6.5	0.56
XRF data (mg/kg):			
Fe	97920	94423	105614
Al	69861	84151	90502
Ca	6111	3259	3930
As	354	133	617
Zn	179	1085	168
Cu	75.9	116	93.7
Ni	314	544	334
Co	42.2	115	76.0
Mn	1248	4693	2183
Cr	782	582	1050
V	118	133	172
Pb	26.6	39.6	26.5

3.4.3 Waste rock samples

Analytical results for the two waste rock pile samples are presented in Table 3.18. Both of these samples have substantial CaCO₃ (≥10%) and total As contents. However, sample BR3, collected from a higher elevation within the waste rock pile than BR2, has a total As concentration twice as high as BR2 plus substantially greater concentrations of Zn, Cu, Ni, Co, Mn, Cr and Pb. The results of the Toxicity Characteristic Leaching Procedure (Table 3.19) indicate that although no detectable As was leached from the waste rock samples, substantial amounts of Fe and Mn were. The BR3 leachate contained higher concentrations of most of the measurable elements, apart from Ca and Mg. The higher Ca concentration in the BR2 leachate is consistent with the higher CaCO₃ content of BR2.

Table 3.18: Analytical data for the waste rock samples collected from the Barbrook mining area; XRFS data represent total major and trace element contents analysed on powder briquettes.

Parameter:	BR2	BR3
CaCO ₃ (%)	11.3	9.7
XRFS major element data (wt %):		
Fe	15.95	17.70
Al	12.38	12.02
Ca	4.04	2.83
XRFS trace element data (ppm):		
As	79.5	186
Zn	239	361
Cu	61.9	147
Ni	329	415
Co	31.9	48.4
Mn	1284	2256
Cr	798	802
V	124	123
Pb	6.23	34.1

Table 3.19: Results of the Toxicity Characteristic Leaching Procedure (TCLP) for the waste rock samples collected from the Barbrook mining area; Ag, As, B, Ba, Be, Cd, Mo, P, Sb, Se, Sn, Te were all below detection limit in the leachate.

Element	Leachate concentration (mg/L)	
	BR2	BR3
Al	24	48
Bi	0.7	0.8
Ca	720	650
Co	nd	1.0
Cr	nd	0.7
Cu	nd	1.0
Fe	188	316
Mg	205	205
Mn	30	61
Ni	0.7	3
Pb	nd	0.16
S	26	64
Si	8	18
Zn	1	5

3.4.4 Primary and secondary mineral samples

3.4.4.1 Primary sulphide minerals

Microscopic examination and analysis of four samples from the Barbrook ore pile revealed a range of primary sulphide minerals in varying associations (Figures 3.25 and 3.26). Representative mineral analyses are presented in Table 3.20. The dominant mineral association comprises aggregates of interlocking coarse-grained pyrite containing inclusions of chalcopyrite and galena. Intergranular spaces are mainly occupied by intergrown

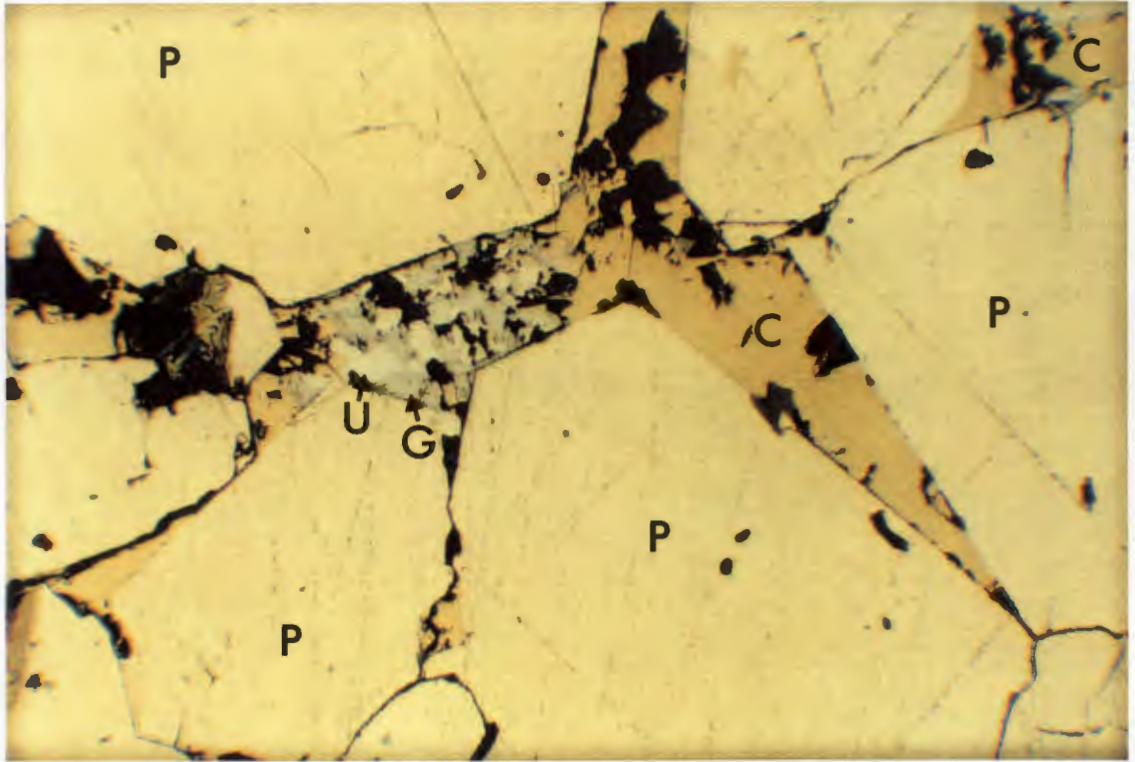


Figure 3.25: Photomicrograph of part of the Barbrook ore body showing intergrown grey galena (G) and white ullmannite (U), plus chalcopyrite (C), occupying intergranular spaces created by interlocking pyrite (P) grains; scale of photo: 4 cm = 1 mm.

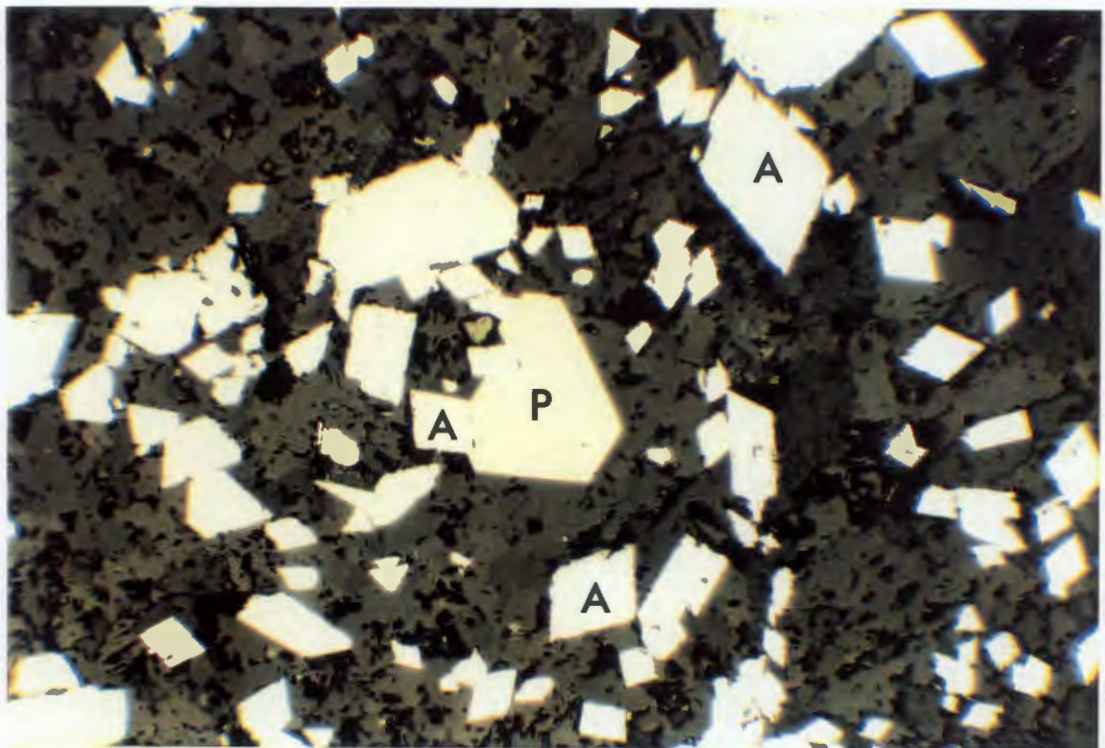


Figure 3.26: Photomicrograph of part of the Barbrook ore body showing intergrown pyrite (P) and arsenopyrite (A) in a matrix of scattered arsenopyrite and gangue (dark) minerals; scale of photo: 4 cm = 1 mm.

chalcopyrite and pyrrhotite, the latter often occurring as inclusions in chalcopyrite, as well as small patches of galena containing bleb-like intergrowths of ullmannite (Figure 3.25). The presence of ullmannite in the Barbrook ore bodies was not reported by Houstoun (1990). Where arsenopyrite is present it occurs as scattered fine-grained laths and coarser subhedral rhombs which are often intergrown with pyrite crystals (Figure 3.26). Arsenopyrite may also occur as fine inclusions within pyrite. Other occurrences of galena, apart from its intimate association with ullmannite, include large infrequent and irregularly-shaped aggregates, inclusions within chalcopyrite, or rims around chalcopyrite crystals. Sphalerite and stibnite were not identified in the four ore samples examined despite their reported presence within the Barbrook ore bodies (Houstoun, 1990).

Although the main source of As is arsenopyrite, small amounts are also present within ullmannite and some pyrite crystals. Within ullmannite, the As substitutes for Sb (Palache *et al.*, 1944) due to the fact that As is isostructural with, and displays similar behaviour to, Sb (Baur and Onishi, 1978). Within pyrite, As is only present in detectable amounts when arsenopyrite is present as inclusions or intergrown crystals.

Table 3.20: Chemical analyses (wt %) of sulphide minerals within the Barbrook ore bodies, as determined by electron microprobe.

	Pyrite (FeS ₂)	Pyrrhotite (Fe _{1-x} S)	Galena (PbS)	Chalcopyrite (CuFeS ₂)	Ullmannite (NiSbS)	Arsenopyrite (FeAsS)
S	52.70	39.47	12.84	35.00	15.04	22.24
Fe	46.22	59.93	0.50	30.94	0.21	35.84
Cu			0.69	35.06		
Ni					27.73	
Zn					0.11	
As	0.34				1.40	45.60
Pb			87.51			
Sb					56.03	
Total	99.26	99.40	101.54	101.00	100.52	103.68

3.4.4.2 Secondary minerals and precipitates

Five different secondary minerals, which had crystallised on the exposed and oxidised surfaces of waste rock sample BR1, were analysed semi-quantitatively using the scanning electron microscope. The EDS X-ray spectra are presented in Figure 3.27. The most abundant crystalline material consists of fine needle-like crystals (Figure 3.28) dominated by S, Al and O (Figure 3.27a) and therefore presumably representing an aluminium sulphate mineral. White fluffy-looking patches of an anhedral sulphate mineral (Figure 3.29) are also common, and individual grains contain minor amounts of Zn, Mn, Fe and Ni (Figure 3.27b). Dark irregular-shaped crystals of a mineral with apparently well-defined

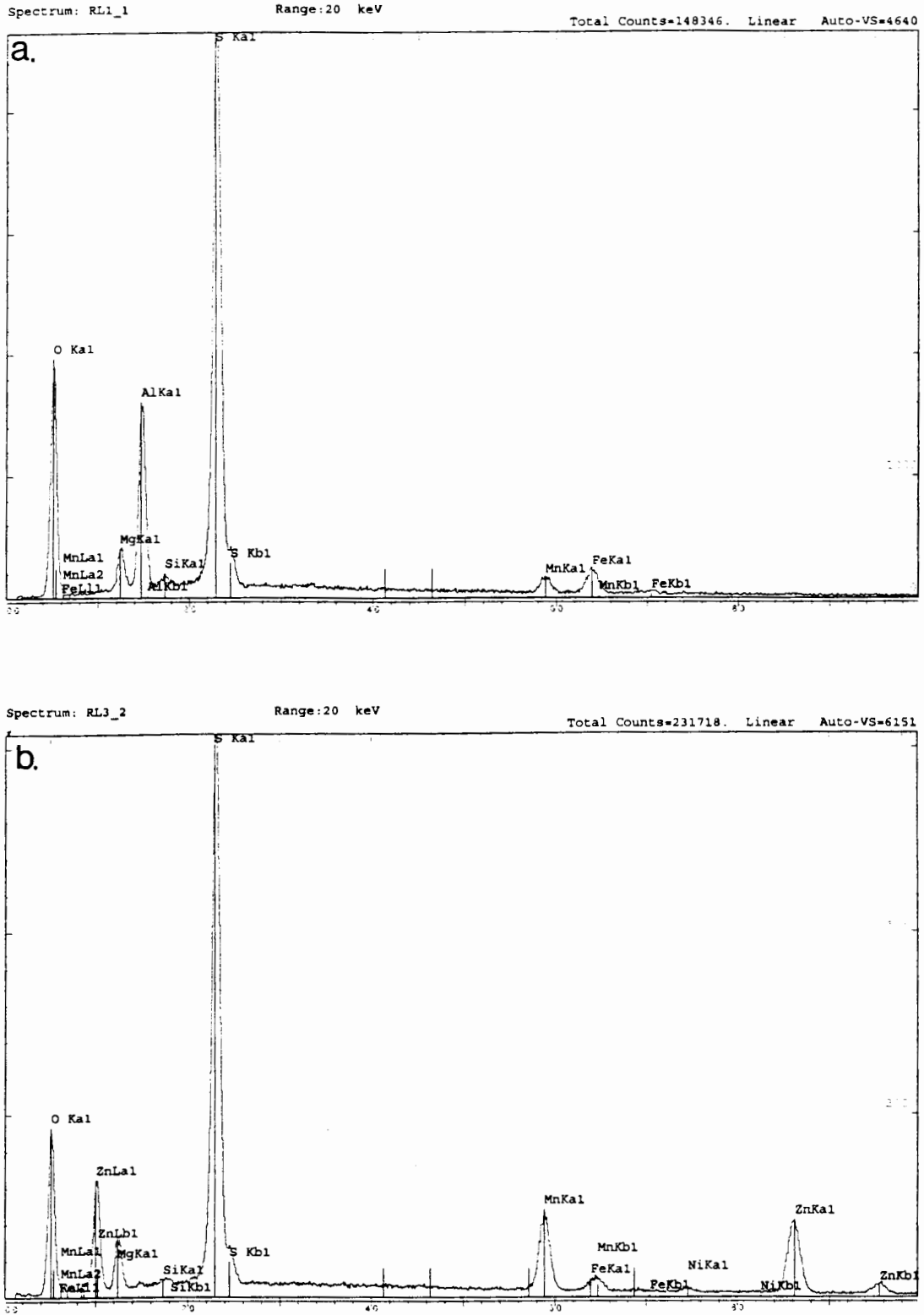


Figure 3.27: Scanning electron microscopy EDS X-ray spectra for single crystals of a range of secondary minerals found on the oxidised surfaces of Barbrook waste rock pile sample BR1: **a)** a needle-like secondary sulphate mineral; and **b)** a white anhedral sulphate mineral.

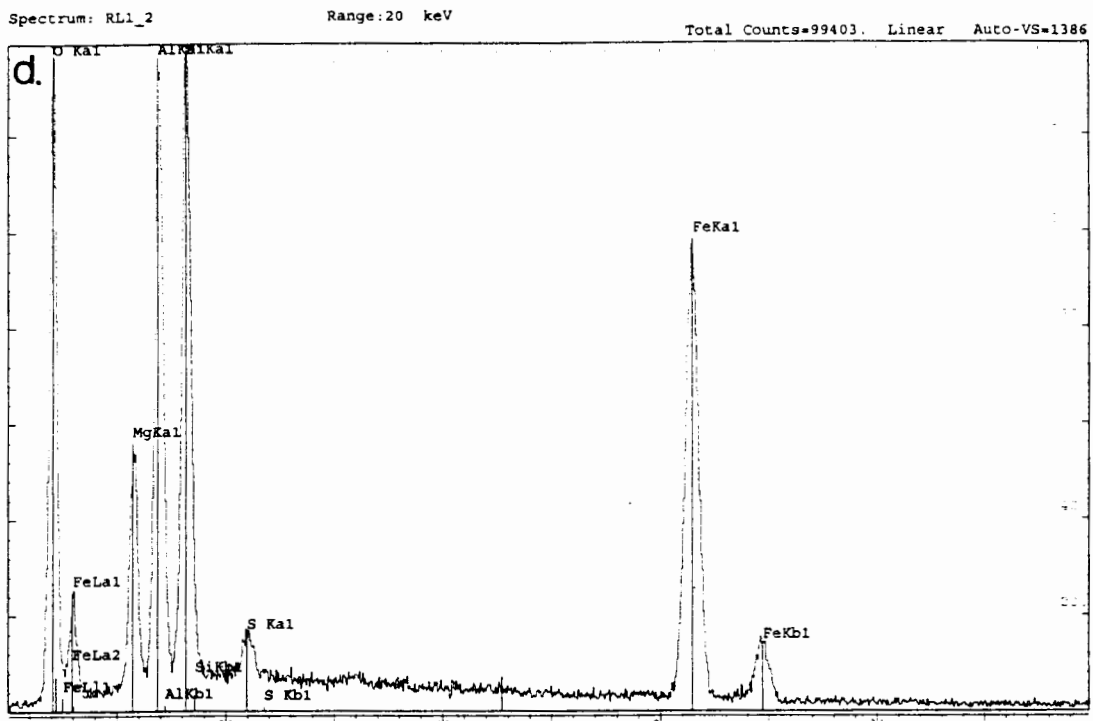
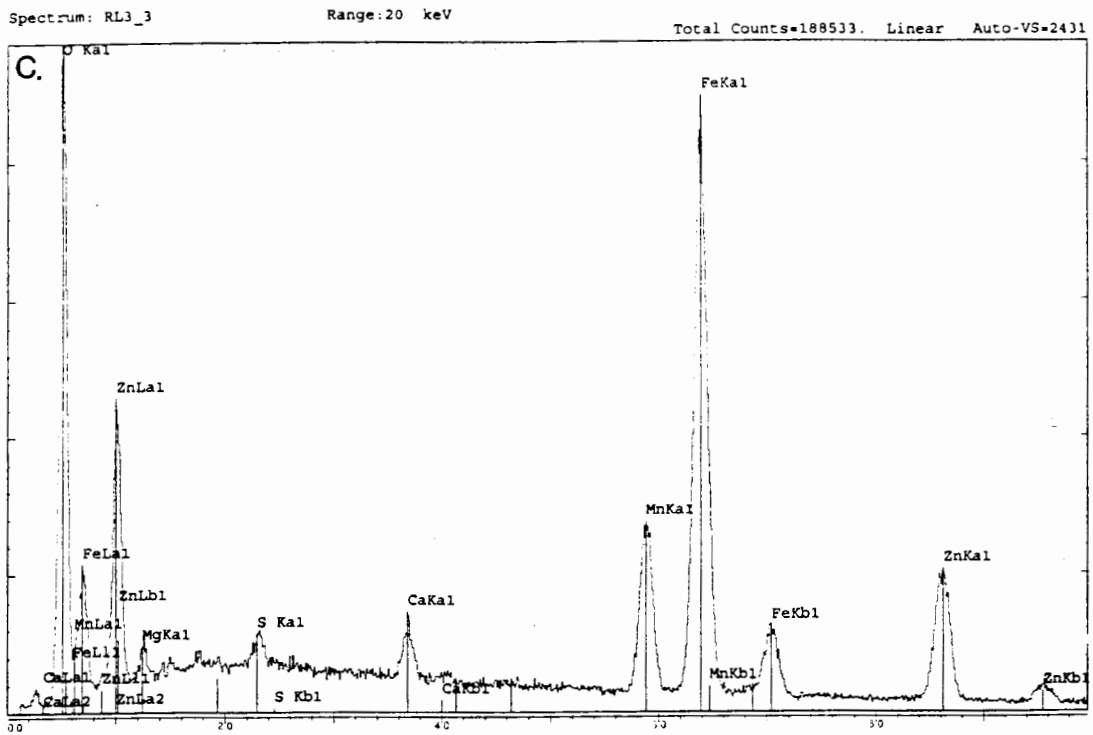


Figure 3.27 (continued): Scanning electron microscopy EDS X-ray spectra for single crystals of a range of secondary minerals found on the oxidised surfaces of Barbrook waste rock pile sample BR1: c) an Fe-oxide mineral; and d) an Fe and Mg-bearing aluminosilicate mineral.

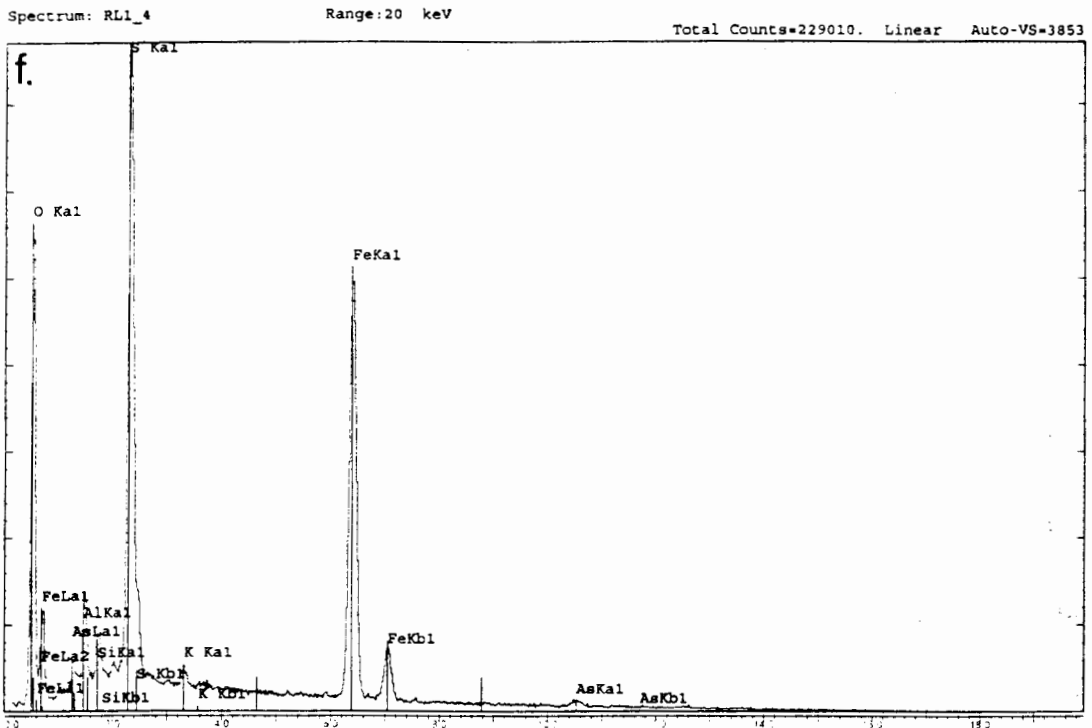
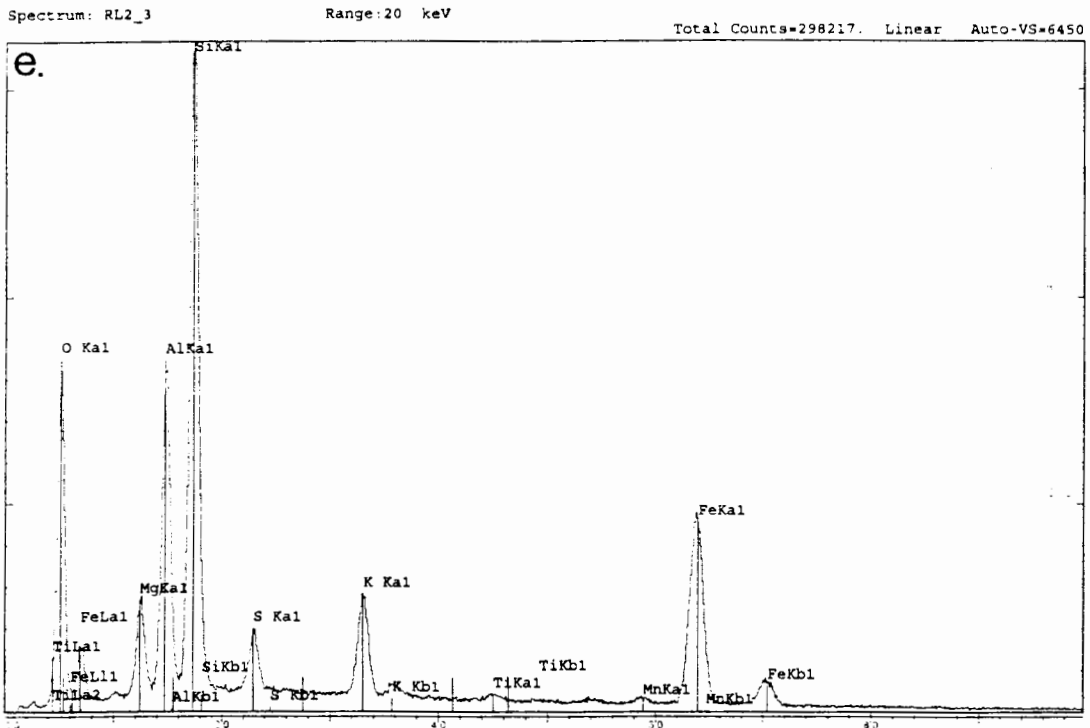


Figure 3.27 (continued): Scanning electron microscopy EDS X-ray spectra for single crystals of a range of secondary minerals found on the oxidised surfaces of Barbrook waste rock pile sample BR1: **e)** another secondary aluminosilicate mineral; and **f)** a pyrite crystal - the Si and Al in this scan represent refflorescence products as the pyrite crystal is $\leq 3 \mu\text{m}$ across (D. Gerneke, personal communication, 1996).

cleavage are scattered throughout the white precipitate (Figure 3.29). Chemical analysis suggests that this mineral is an Fe-oxide containing substantial amounts of Zn and Mn as well as minor amounts of Ca and S (Figure 3.27c). Two aluminosilicate minerals were also analysed. The first (Figure 3.30) contains substantial Fe and Mg (Figure 3.27d) whereas the second (Figure 3.31) is an aluminosilicate containing Fe, K and Mg plus minor S and Ti (Figure 3.27e).

Therefore, despite the fact that a single analysis of a pyrite crystal (Figure 3.32) from the same piece of waste rock did reveal a minor amount of As to be present (Figure 3.27f), As was not detected within any of the secondary sulphate, oxide or aluminosilicate minerals produced by oxidation of the waste rock.

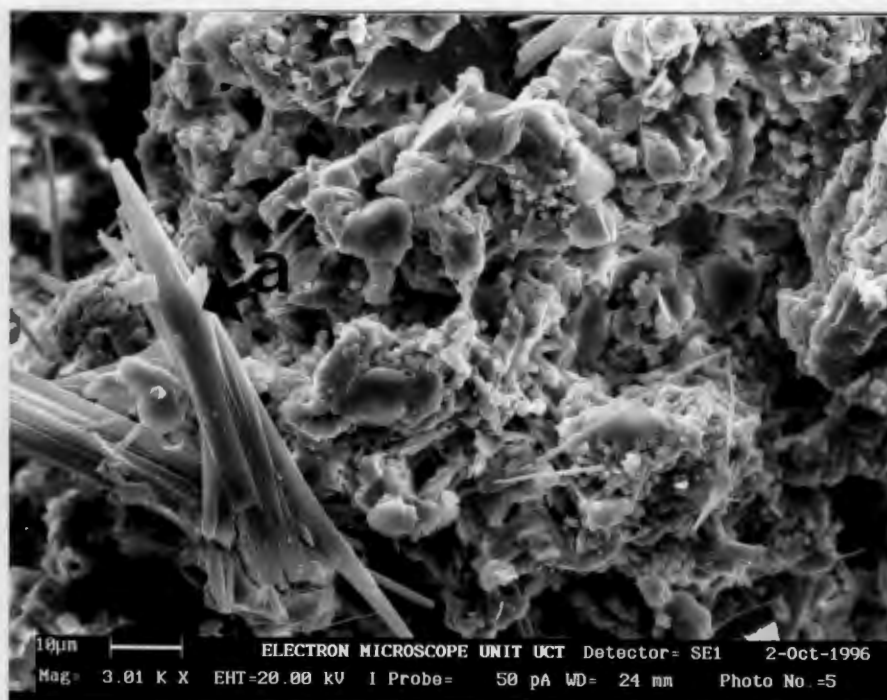


Figure 3.28: Scanning electron microscopy backscattered electron image showing abundant needle-like crystals of a secondary sulphate mineral (Figure 3.27a) within the Barbrook waste rock pile sample BR1. The analysed grain, to the left side of the photo, is indicated with an arrow.

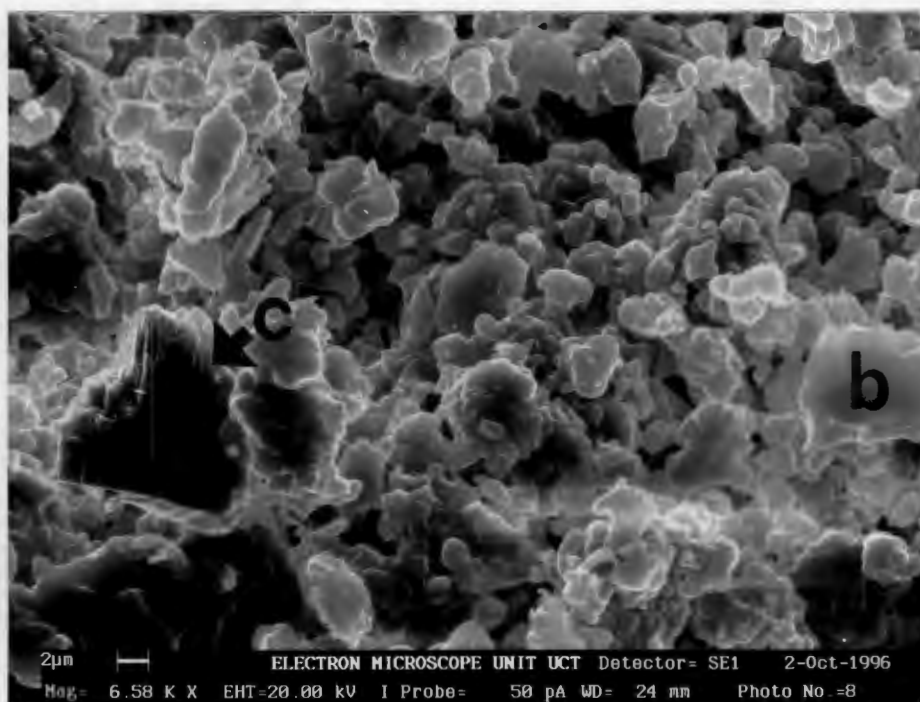


Figure 3.29: Scanning electron microscopy backscattered electron image of a patch of the white anhydrous sulphate minerals (Figure 3.27b) within the Barbrook waste rock pile sample BR1. Scattered dark irregular-shaped Fe-oxide crystals (Figure 3.27c) are also visible. Analysed crystals are marked b and c.

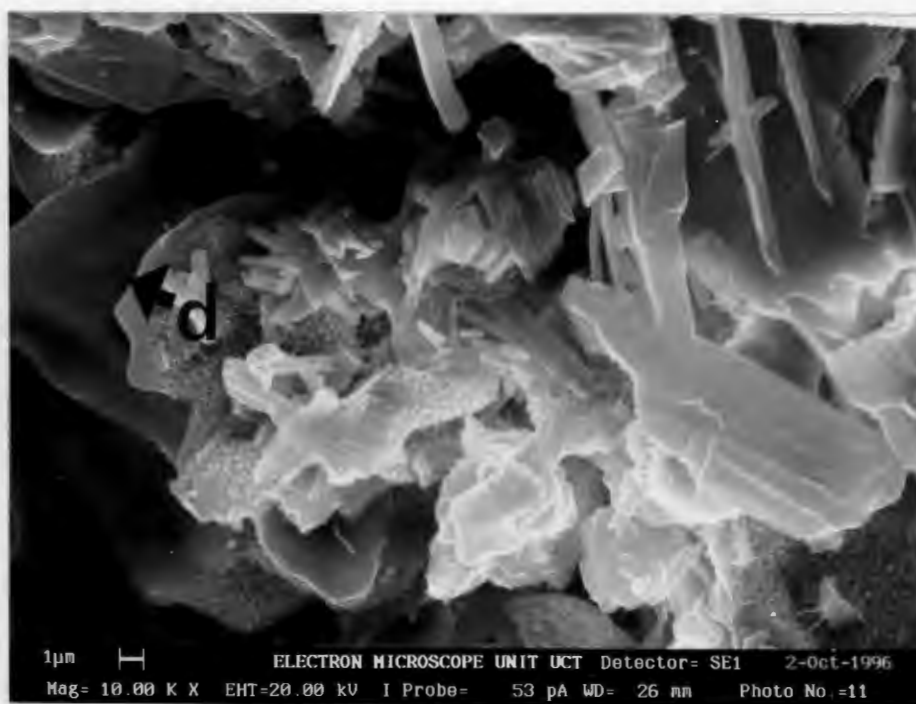


Figure 3.30: Scanning electron microscopy backscattered electron image of an Fe and Mg-bearing aluminosilicate mineral (Figure 3.27d) within the Barbrook waste rock pile sample BR1. The analysed grain, on the left side of the photo, is indicated with an arrow.

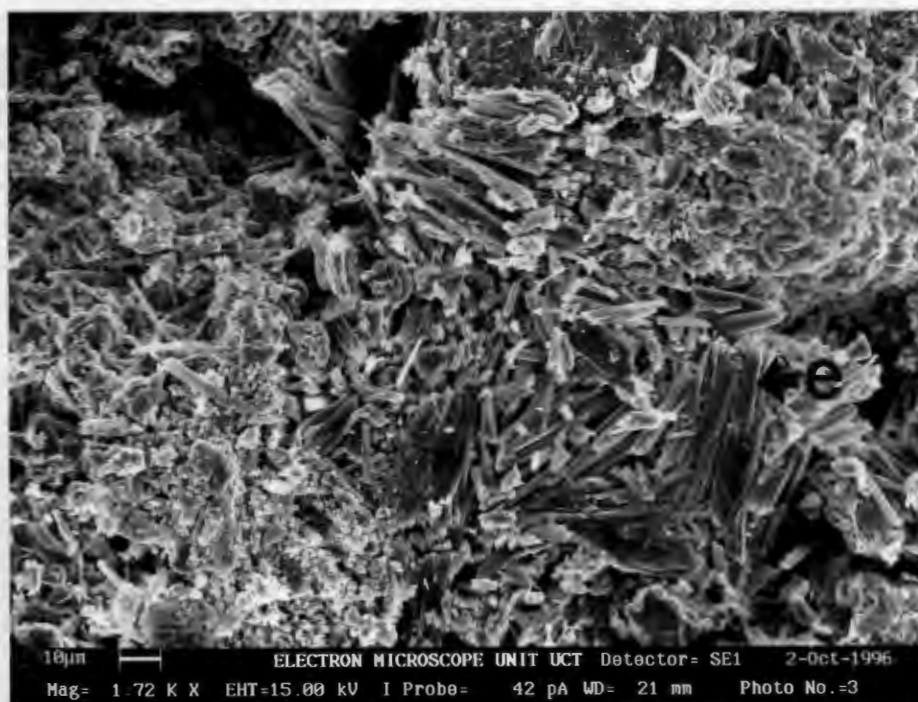


Figure 3.31: Scanning electron microscopy backscattered electron image of the second aluminosilicate mineral (Figure 3.27e) within the Barbrook waste rock pile sample BR1. The analysed grain (lower right) is indicated with an arrow.

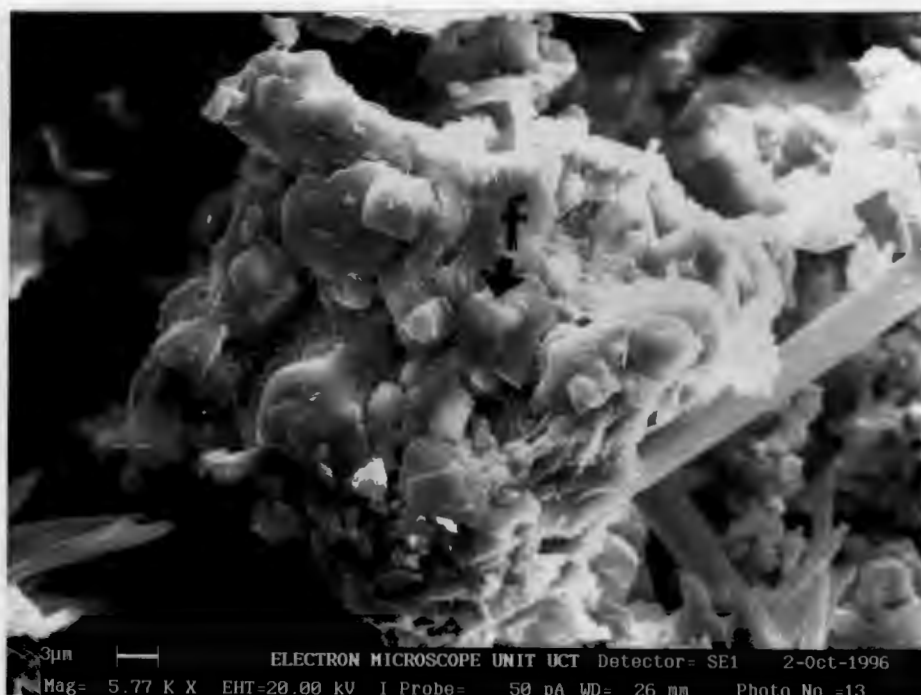


Figure 3.32: Scanning electron microscopy backscattered electron image of pyrite cubes within the Barbrook waste rock sample BR1. The analysed grain (Figure 3.27f) is located in the centre of the photo and indicated with an arrow.

sulphate-rich waters, and the fact that they do drink from the ponds on the slimes dam (Figure 3.14) suggests that they are also not affected by the poor palatability which normally accompanies such high SO_4^{2-} concentrations (DWAF, 1995d). However, the overall scarcity of water in the area at the time of sampling may have necessitated the consumption of the slimes dam water despite its poor quality. The Co, Ni and Mn contents of the water seeping from the base of the slimes dam wall do not constitute any problem for consumption by livestock in terms of the local guidelines (DWAF, 1995d).

Table 3.21: Summary of the target water quality guidelines for South Africa as stipulated by DWAF (1995b, 1995c, 1995d and 1995e).

Water Usage:	Domestic	Livestock	Irrigation	Industrial
pH	6 - 9		6.5 - 8.4	6.5 - 8.0
EC (mS/m)	≤70	≤300	≤40	≤30
SAR			<2.0	
Upper limit (mg/L):				
TDS	450	2000	264	200
Total hardness (CaCO_3)	50 - 100			100
As	0.01	1.0	0.1	
Si				10
Na^+	100	2000	70	
K^+	50			
NH_3 (as $\text{NH}_4^+ + \text{NH}_3$)	1.0			
Ca^{2+}	32	1000		
Mg^{2+}	30	500		
Cl^-	100	1500	100	40
F^-	1.0	2.0	2.0	
N as ($\text{NO}_3^- + \text{NO}_2^-$)	6.0			
Inorganic N			5.0	
NO_3^-		100		
NO_2^-		10		
SO_4^{2-}	200	1000		80
Co		1.0	0.05	
Ni		1.0	0.2	
Mn	0.05	10	0.02	0.1
Fe	0.1	10	5.0	0.2
Zn	3.0	20	1.0	

Note: Industrial guidelines refer to the values stipulated for category 2 industrial processes which require intermediate quality water; agricultural guidelines refer to the values required for cattle where different animal species were specified.

Total hardness (mg CaCO_3/L) = (2.497 x mg Ca^{2+}/L) + (4.118 x mg Mg^{2+}/L)

Sodium adsorption ratio (SAR) is calculated using mmol/L data and the equation (McBride, 1994):

$$\text{SAR} = \frac{\text{Na}^+}{(\text{Ca}^{2+} + \text{Mg}^{2+})^{0.5}}$$

Due to the fact that As contents of more than 1.5 mg/L in drinking water can cause adverse effects such as haemorrhagic diarrhoea and dehydration in cattle (DWAF, 1995d),

the ponds of standing water on the calcine dam (BW15) and southern end of the main slimes dam (BW4), as well as the stream of tailings (BW14) extending between them, must be deemed unsuitable for livestock watering. The high pH values associated with these waters could also constitute a problem for consumption in that a pH >9 can result in the deprotonation of species such as NH_4^+ to NH_3 , both of which can be microbially transformed into NO_3^- and NO_2^- (Schlesinger, 1991) within the rumen of cattle (DWAF, 1995d). The water in the stream of tailings extending between the two tailings dams (BW14) has both the highest pH and the highest NO_2^- content of all the Barbrook water samples. Although cattle can become adapted to relatively high NO_2^- levels, whereby it is reduced to NH_3 via a detoxification mechanism in the rumen, nitrite poisoning can cause methaemoglobinaemia as a result of NO_2^- combining with haemoglobin to prevent oxygen uptake. This is a particular danger where carbohydrate intake is poor and drinking water has high TDS and SO_4^{2-} contents (DWAF, 1995d).

The four groundwater samples collected from the tailings dam area are also classified as very hard water in terms of their total hardness values (>500 mg CaCO_3/L) and are unsuitable for domestic use in terms of their high EC, Na^+ , Mg^{2+} , Ca^{2+} and SO_4^{2-} contents. Although MgSO_4 can act as a laxative and induce diarrhoea in non-adapted individuals, the DWAF (1995b) guidelines state that high Na^+ is really only a problem in terms of taste and high Ca^{2+} in terms of getting soap to lather, rather than causing any adverse health effects. The main problem to human health associated with the groundwater in this area is the high NO_2^- content and total N content ($\text{NO}_2^- + \text{NO}_3^- = 8.22 \text{ mg/L N}$) of borehole sample BW9. According to DWAF (1995b), the presence of high NO_3^- in drinking water poses a problem in terms of its potential for microbial conversion to NO_2^- within the human body. High NO_2^- levels are unacceptable as they can result in methaemoglobinaemia. This constitutes a particular danger for infants under 3 months of age and is exacerbated by poor Vitamin C intake. The Mn and Fe concentrations in groundwater sample BW10 are high compared to the domestic guidelines of DWAF (1995b), although the effects would be mainly aesthetic and no adverse health effects should result from human consumption.

3.5.1.2 Mining area

The Shiyalongubo Dam, from which the local population ultimately derives water for domestic and agricultural purposes, contains high quality drinking water with low EC (6.0 mS/m), a neutral pH, and ionic concentrations well within the DWAF (1995) guidelines for domestic use, livestock watering, crop irrigation and industrial purposes. The overall quality of the water samples collected from the Barbrook and Low's Creeks, representing the conduits via which the Shiyalongubo water and surface run-off from the mountain catchment is transported through the Barbrook mining area, are also within the DWAF (1995) guidelines. Despite having higher concentrations of most constituents, the water sample

collected from Low's Creek just downstream from the processing plant but prior to the confluence with Barbrook Creek (BW5) is only questionable in terms of its suitability for drinking purposes as a result of its high As content (0.011 mg/L), which is approximately equivalent to the upper limit stipulated by both the WHO (1993) and DWAF (1995b) guidelines. The quality of the groundwater entering the level 10 mine adit (BW18) is also acceptable apart from its relatively high As (0.012 mg/L) content.

The DWAF (1995c) guidelines state that, although the target range for As in irrigation water is 0 to 0.1 mg/L, the maximum acceptable concentration for fine-textured neutral to alkaline soils is 0.1 to 2 mg/L. Therefore, the sampled waters from the Barbrook and Low's Creeks are all suitable for irrigation purposes in terms of their As contents. The calculated sodium adsorption ratios (SAR) for all of the Barbrook mining area waters are <1.0, indicating that these waters also have a low potential for inducing sodic conditions in soils during irrigation (DWAF, 1995c). The calculation of total hardness values reveals that most of the samples collected from the Barbrook and Low's Creeks, apart from the sample collected just downstream of the processing plant (BW5: 79.6 mg CaCO₃/L), are soft waters (<50 mg CaCO₃/L) whereas the groundwater entering the level 10 mine adit (BW18: 122 mg CaCO₃/L) constitutes moderately hard water. According to DWAF (1995b), the main problems associated with excessively soft water are its potential corrosive nature and its poor buffering capacity. Although the two Low's Creek samples (BW6 and BW7) analysed for heavy metals both have Fe contents above the target guideline value for domestic use, this will only affect the palatability of the water (DWAF, 1995b).

In contrast to the creek waters in the Barbrook mining area, the recycled water used in the mining and processing operations, and collected from the level 7 (BW22) and 10 (BW19) mine adits as well as the water tanks located above the French Bob open cut mine (BW23), have EC values ≥ 95 mS/m, and unacceptably high concentrations of NH₄⁺, Mg²⁺, Ca²⁺, N (as NO₂⁻ + NO₃⁻) and SO₄²⁻ relative to the DWAF (1995b) guidelines for domestic use. They are also classified as very hard (>300 mg CaCO₃/L) waters, with total hardness values >500 mg CaCO₃/L. Of these three water samples, however, only the water from the level 10 mine adit has a relatively high As (0.011 mg/L) content. Apart from As, the main problems with the compositions of these waters, in terms of human drinking water standards, are the high SO₄²⁻ and Mg²⁺ concentrations, due to the possible laxative effect of MgSO₄, plus the risk to infants associated with the high NO₂⁻ and NO₃⁻ contents. According to the DWAF (1995c) guidelines, the high Ni and Mn contents of the level 10 mine adit water (BW19) could constitute a potential problem in terms of crop yield if this water was to be used for irrigation purposes. However, although the Ni and Mn values are above the target values, the DWAF (1995c) guidelines do state that such concentrations are within the acceptable range for the irrigation of fine-textured, neutral to alkaline soils. Manganese contents >2 mg/L can be a problem in terms of industrial usage, however, resulting in the precipitation of Mn compounds which can interfere with processing operations and damage equipment (DWAF, 1995e). Although it is highly unlikely that these recycled mine waters will be used

3.5 Discussion

3.5.1 Water quality in the Barbrook area

Since the water bodies in the Barbrook tailings dams and mining areas could potentially be used for different purposes, it is important to examine them separately here in terms of how they compare to the South African water quality guidelines (Table 3.21). The surface waters in the Barbrook mining area are most likely to be used by the local human population for domestic and agricultural purposes, whereas the groundwater entering the level 10 mine adit is recycled for use in the mining and processing operations at Barbrook. In addition to the recycling of the surface waters from the tailings dams for further use in the processing plant, their other main use is as a source of drinking water for the local cattle and birds. These waters could only be expected to contribute to human domestic use as a result of possible surface run-off and incorporation into Crystal Stream during periods of flooding and/or via groundwater consumption.

3.5.1.1 Tailings dam area

The surface water bodies associated with the Barbrook tailings dam area are generally of poor quality in terms of the DWAF (1995) guidelines (Table 3.21) for human domestic use but appropriate for livestock watering in certain cases due to the less stringent guidelines applied. Most constituents within the water collected from the small pond (BW1) near Crystal Stream are within domestic quality guidelines but it does have a high NH_4^+ content, presumably as a result of the observed contamination by cattle dung. Although ammonia is not considered toxic in its ionic form (DWAF, 1995b), and the water can therefore be classified as suitable for livestock watering, the likely contamination by faecal coliforms, which are present within the faeces of a range of warm-blooded animals (WHO, 1984), may preclude its use by humans.

Whereas the total hardness value (122 mg CaCO_3/L) calculated for sample BW1 indicates that it is only slightly hard (DWAF, 1995b), all of the other surface waters in the tailings dam area have total hardness values of between 500 and 1400 mg CaCO_3/L and are classified as very hard and potentially problematic for industrial use due to scaling effects. The high As, N (as $\text{NO}_3^- + \text{NO}_2^-$), Na^+ , Mg^{2+} , Ca^{2+} and SO_4^{2-} concentrations of these waters preclude their use for domestic purposes and the high SO_4^{2-} concentrations of all samples, except for the upwelling water near the base of the main slimes dam wall (BW3), make the suitability of these water bodies for livestock watering questionable. Sulphate concentrations above 1000 mg/L, as occur in most of the tailings dam surface waters, can result in chronic diarrhoea, particularly in immature and/or non-adapted animals (DWAF, 1995d). However, the animals living in the tailings dam area may well be physiologically adapted to consuming these

intentionally and/or in an undiluted form as drinking water, the excessive hardness of these waters may constitute a particular problem for use in the Barbrook processing plant, whereby the high TDS values, and in particular the high concentrations of Mg^{2+} and Ca^{2+} , may result in scaling.

The standing water within the disused Clifford Scott open cut mine (BW24) is unlikely to be used for any particular purpose although it may eventually overflow and contribute to surface run-off. The quality of the water is good apart from its high As (0.021 mg/L) content.

3.5.2 The chemistry of the Barbrook soils and sediments

3.5.2.1 Tailings dam area

The sediment core collected from Crystal Stream (BS1) comprises alluvial clay-rich soil which appears to be relatively unpolluted compared to the other sediments collected in the Barbrook tailings dam area. Heavy metal concentrations within both the upper and lower sections of this core lie within the ranges for unpolluted soils presented in Table 3.22, and are therefore assumed to represent background concentrations for the soils of this area. The fact that the near-neutral pH values measured in soil solutions prepared with H_2O become more acidic when measured in KCl is a function of the cation exchange capacity (CEC) of the soil (Rowell, 1988). Due to the fact that water is a weak acid which barely dissociates, the exchange of H^+ ions in solution for cations on the surfaces of the clay particles is negligible compared to the cation exchange which occurs when a soil is swamped by an electrolyte solution such as KCl. The release of acidic cations such as H^+ and Al^{3+} during this cation swamping, whereby Al^{3+} is equivalent to the behaviour of three H^+ ions in terms of its effect on acidity, would therefore cause the lower pH values observed in the KCl generated soil solution. The difference between the measured $pH(H_2O)$ and $pH(KCl)$ values is greater for BS1A than for BS1B, suggesting that the upper horizon has a higher CEC. The higher concentrations of most heavy metals, except for Co, Mn and V, in the upper horizon may therefore possibly be related to different organic matter contents and the greater formation of organometallic complexes in the top section of the core.

By comparison with BS1, substantial heavy metal enrichment is present within the sediment samples collected from the tailings dams. This enrichment is most evident in terms of the high Zn, Cu, Mn, Cr and Pb contents of the slimes (BS3 and BS4) and calcine (BS7) dam samples. Jambor (1994) describes the tailings material produced from the processing of sulphide-rich ore bodies as the "ground mill-processed gangue in which the ore minerals occurred". However, "because recoveries of the valuable minerals are never 100%, the tailings always contain small amounts of ore minerals". Therefore, the elevated heavy metal concentrations in the mine tailings and associated sediments can be explained in terms of the sulphide and gangue minerals associated with the Barbrook ore bodies which were

Table 3.22: Summary of average concentrations of heavy metals in unpolluted soils.

Element	Range (mg/kg)	Average (mg/kg)	Reference
As	0.1 - 40	10	Chatterjee <i>et al.</i> (1993); O'Neill (1995)
Zn	10 - 300	50	Kiekens (1995)
Cu	2 - 100	20 - 30	Baker and Senft (1995)
Ni	≤5000	24 - 53	McGrath (1995)
Co	0.05 - 300	10 - 15	Smith and Paterson (1995)
Mn	50 - 11 500		Smith and Paterson (1995)
Cr	≤10 000	41 - 200	McGrath (1995)
V	20 - 500	100	Edwards <i>et al.</i> (1995)
Pb	<20		Davies (1995)

Note: References cited are not necessarily primary references, but have often compiled the results of numerous studies to ascertain average soil compositions.

crushed and oxidised during ore processing and transported as fine-grained residuals to the tailings dams. The ore minerals contributing to the heavy metal concentrations would include chalcopryite (Cu), galena (Pb), ullmannite (Ni) and, although it was not observed within the ore samples examined during the course of this study, the sphalerite (Zn) reported by Houstoun (1990). Although Sb was not included within the element analyses performed on the Barbrook soils and sediments during the course of this study, the identification of ullmannite and the reported presence of stibnite (Houstoun, 1990) within the ore bodies indicate that Sb could also be present in elevated concentrations. The main gangue mineral which appears to contributing to elevated heavy metal concentrations is the Cr-muscovite, fuchsite, within the green fuchsite-carbonate-quartz schists (Houstoun, 1990) which host the Barbrook ore bodies. The high concentrations of Fe, As and Ca in the tailings dams sediments can also be explained in terms of the Barbrook processing operations. Whereas Fe is present in a range of sulphides, including pyrite, pyrrhotite and arsenopyrite, As would be present mainly as arsenopyrite. The elevated Ca concentrations of the tailings material are not only due to the carbonate minerals present within the gangue material, but also to the fact that CaO is added during ore processing. The similar concentrations of Co, V and Al in BS1 and the tailings material suggests that these elements are not present in elevated concentrations within the Barbrook ore bodies.

The coarser grainsize of the tailings material, in comparison to the clay-rich cores collected from Crystal Stream and the slimes seepage pond, is consistent with the findings of Jambor (1994) that most mine tailings contain sand- or silt-sized particles. The alkaline pH (H₂O and KCl) values obtained for the tailings material are a function of both the abundance of CaCO₃ (up to 8%), as a result of the carbonate-rich host rocks at Barbrook, and the liming which occurs as part of the gold processing operation. Due to the fact that heavy metal mobility generally decreases markedly under neutral to alkaline pH conditions (McBride, 1994), any leachate seeping from the tailings dams could be expected to contain relatively low heavy metal concentrations.

Despite the prevailing alkaline conditions in the tailings dam material, some heavy metal contamination is evident in the sediment core collected from the slimes seepage pond (BS2). This seepage pond is lined with a similar clay-rich alluvial soil to that found in the Crystal Stream core (BS1). It also has a similar CaCO_3 content, and pH(H₂O and KCl) values which are intermediate between the BS1 upper and lower horizons. Compared to the Crystal Stream core, however, the slimes seepage pond core has elevated levels of Fe, Zn, Ni, Cr, As and, to a lesser extent, Cu. This implies some heavy metal and As contamination due to seepage from the tailings dams.

3.5.2.2 Mining area

Although the original intention was to collect sediment cores from the Barbrook and Low's Creeks at the same sites from which water was sampled, this was not possible due to the scarcity of sediment within the creek beds at the time of sampling. Therefore, the sediment core collected from Low's Creek immediately adjacent to the waste rock pile (BS6) and the soil from underneath the waste rock pile (BS8) provide the only indication of whether leachate from the waste material is actually contaminating the sediments and soils in the immediate area. The chemical composition of an uncontaminated soil (BS5), sampled near the main entrance to the Barbrook mine site (Chapter 4), provides possible background levels for this area. By comparison with BS5 and the Low's Creek core (BS6), the soil underneath the waste rock pile is highly contaminated with respect to Zn, Ni, Co, Mn, and Pb, thereby implying that heavy metals are being leached downwards from the overlying waste material. Although most of this waste material would be expected to comprise gangue minerals, waste rock piles can contain substantial amounts of low-grade ore material due to the dependence of cut-off grade on the prevailing market gold prices (Funke, 1990). The presence of primary sulphides is indicated by the high heavy metal concentrations within the underlying soil. Significant As contamination is also evident in the soil and sediments in the immediate vicinity of the waste rock pile.

The sediment core collected from the Clifford Scott open cut mine is also contaminated with respect to As and Pb, but particularly so with respect to Cr which is presumably derived from the fuchsite in the host rocks.

3.5.3 The chemistry of the Barbrook waste rock pile

Although the waste rock pile at Barbrook constitutes a definite aesthetic problem for the Caledonia Mining Company (Figures 3.17 and 3.20), the analytical results obtained in an attempt to determine whether or not it constitutes a current or future geochemical problem are somewhat contradictory. The two waste rock pile samples (BR2 and BR3) have

substantially different concentrations of Fe, As and certain heavy metals, including Zn, Cu, Ni, Mn, and Pb, suggesting that the distribution of primary sulphide minerals within the waste rock pile is highly heterogeneous. Consistent with the higher concentrations of most elements in sample BR3, the leachate produced from this sample during TCLP analysis also contained higher concentrations of heavy metals and Fe than the BR2 leachate. However, neither leachate contained any detectable As.

It is difficult to interpret the TCLP results in terms of water quality guideline values due to the fact that they were extracted in a pH 5 solution and are therefore not representative of what would occur with simple leaching by rainwater in such a well buffered system. In addition, any leachate produced is likely to be either diluted by the adjacent Low's Creek waters or interact with the underlying soil. According to the EPA (1993) guidelines, the maximum allowable As concentration in a standard TCLP leachate extracted from As-bearing wastes is 5 mg/L. Despite the lack of As at anywhere near this level in the Barbrook TCLP leachates, several elements are present in high enough concentrations to be potentially problematic. These elements include Fe, Mn, Ca and Mg as well as certain heavy metals. Whereas the Fe is likely to derive predominantly from the Fe-sulphide minerals and the Mg and Ca from carbonate and talc gangue minerals, both Fe and Mg are also present in chlorite. The source of the Mn is not so obvious, although it is likely to occur in minor amounts in the Fe-sulphide minerals, due to solid solution substitution for the Fe, and it may also be present within some of the carbonates, namely ankerite and siderite, the latter also in a solid solution scenario. Although the heavy metals would presumably be leached from the primary sulphide minerals present within the waste rock pile, SEM analyses performed on a number of secondary minerals from waste rock sample BR1 also revealed the presence of Zn, Mn, Fe, and Ni within secondary sulphate and oxide minerals (Section 3.4.4.2).

The aforementioned contradiction which occurs in relation to the waste rock pile analytical results stems from the fact that although the heavy metal contamination of the soil underneath the waste rock pile (BS8) is in agreement with the TCLP leachates containing heavy metals, substantial As is also present within the underlying soil but undetectable in the TCLP leachates. This will be discussed further in Section 3.5.4.4.

3.5.4 Arsenic in the Barbrook environment

The results of this study indicate that As is present in significant concentrations within some of the water bodies, soils and sediments in the immediate vicinity of the Barbrook mining and tailings dams areas. The chemical analysis of the primary sulphide minerals within the Barbrook ore bodies has revealed that although arsenopyrite is the main As-bearing sulphide mineral, containing ≥ 45 wt% As, the presence of minor amounts of As in pyrite, which is the most abundant sulphide mineral at Barbrook (Houstoun, 1990), and ullmannite means that their oxidation will also release As.

3.5.4.1 Arsenic occurrence in the Barbrook water bodies

Despite the fact that not all of the sampled water bodies with the Barbrook area would be considered or even available for human domestic use (Section 3.5.1), the fact that the Barbrook and Low's Creeks have low As concentrations (≤ 0.007 mg/L) suggests that background levels are below the drinking water guideline value of ≤ 0.01 mg/L (WHO, 1993; DWAf, 1995b).

In terms of the various water bodies sampled in the Barbrook area in August 1996, the highest As levels were detected in the surface waters located in the tailings dam area. However, substantial amounts of As were also measured in some of the mining area waters, including Low's Creek downstream from the processing plant (BW5), the groundwater entering the level 10 mine adit (BW18) and present within the main drain at this level (BW19), as well as the water in the Clifford Scott open cut mine (BW24). Although the results of this study represent the state of the Barbrook water bodies at a single point in time, analyses performed by the Caledonia Mining Company since February 1995 (Table 3.23) confirm that certain water bodies in the Barbrook area do contain consistently high As concentrations. Such As-contaminated waters include the slimes seepage pond (0.05 to 5.18 mg/L), which was completely dry and therefore not sampled during the course of this study, and the main drain in the level 10 mine adit (0.12 to 0.45 mg/L), although the latter was only sampled twice prior to August 1996. Other water bodies which have revealed intermittently high As levels since February 1995 include Crystal Stream just west of the slimes dam (up to 0.78 mg/L), Low's Creek downstream from the processing plant (up to 0.022 mg/L) and Low's Creek adjacent to the explosives magazine and upstream of the main mining area (up to 0.015 mg/L).

Compared to the tailings slurries sampled at the processing plant (BW20 and BW21), which contain As levels of ~ 0.02 mg/L, water bodies associated with the calcine and slimes dams have considerably higher As contents of up to 4.12 mg/L. Therefore, it appears that although substantial amounts of As are being pumped to the tailings dams from the processing plant, this As is becoming increasingly concentrated within the pools of water on the two dams and within the waters leaching from the base of the slimes dam wall. Climatic data for the Barbrook area include high monthly evaporation rates of between 115 and 195 mm (Ralph Morris and Associates, 1996), suggesting that evaporation is a likely mechanism for increasing As concentrations within the tailings dam area waters. The other possible mechanism involves further oxidation of the primary sulphide minerals present within the tailings material subsequent to discharge from the processing plant, thereby resulting in increased As release.

Although the water in the small pond (BW1) located west of the main slimes dam wall and close to Crystal Stream had a negligible As content at the time of sampling, the high As concentrations determined for Crystal Stream on previous occasions (Table 3.23) suggest that it may be intermittently subject to contamination from tailings dam leachates. This implies

that surface run-off, possibly involving the seepage from the base of the slimes dam wall, may be occurring during periods of heavy rainfall. However, little is known about the prevailing conditions associated with previous sampling periods.

Despite the high As concentrations within the surface waters in the tailings dam area, the water samples collected from the four boreholes (BW9 to BW12) recently drilled below the main slimes dam wall indicate that no groundwater contamination has yet occurred in this area. In contrast, the groundwater entering the level 10 mine adit (BW18) does contain substantial As. The fact that the recycled water used in the mining operations, and sampled from the water tanks above the French Bob open cut mine (BW23) and the main drain in the level 7 mine adit (BW22), contains negligible As, suggests that the groundwater may be naturally contaminated with As rather than contaminated by leachate associated with the mining operations. If this is the case, the relatively high As content of the water in the main drain of the level 10 mine adit (BW19) may be due to direct contamination by the groundwater entering at this level, whereas subsequent dilution may be responsible for the lower As contents of the recycled mine waters.

With the exception of the water sample collected from Low's Creek just downstream of the processing plant (BW5), the As contents of the Barbrook and Low's Creeks in August 1996 were ≤ 0.007 mg/L. Since the usual As contents of unpolluted rivers have been reported as ≤ 0.01 mg/L (Ferguson and Gavis, 1972), the creeks in the Barbrook region could be considered to have been unpolluted at the time of sampling. By comparison, the slightly elevated EC value and higher concentrations of As (0.011 mg/L) and other ionic constituents in the water collected from the vicinity of the Barbrook processing plant (BW5), indicate that Low's Creek was experiencing contamination from the processing plant. However, below the point where the Barbrook and Low's Creeks converge, just downstream of the BW5 sampling site, the As content of the Low's Creek water was found to be a much more acceptable 0.002 mg/L (BW26). This downstream decrease in the As concentration of Low's Creek may simply be due to dilution by the converging Barbrook Creek waters or it may be due to the removal of As from solution. Although As sorption onto Fe and Mn oxides and hydroxides in aquatic surface sediments is a well-documented phenomenon (Brannon and Patrick, 1987; Mok and Wai, 1990; Loring *et al.*, 1995), the creek beds in this area are quite rocky and relatively devoid of surface sediments. In a study of the effects of mixing between As-bearing seepage from mine tailings and surface stream waters, Babb *et al.* (1985) found that the influx of oxidising waters resulted in the oxidation of Fe(II) to Fe(III) in stream sediments and the precipitation, via subsequent hydrolysis, of colloidal hydrous oxides which scavenged As. Jackson and Bistricki (1995) found that As in mine polluted lakes is also scavenged by plankton which have outer coatings of FeOOH. A comparison of dilution factors for the various elements analysed in samples BW5 and BW26 indicate that the As, SO_4^{2-} and NO_3^- concentrations of sample BW26 are more than five times less than sample BW5, whereas Ca^{2+} is about three times lower and the other elements are all ≤ 2 times more dilute. The greater dilution of As, SO_4^{2-} and NO_3^- suggests that, in addition to dilution by the

converging creek waters, some sort of anion sorption may also be occurring within Low's Creek.

The water in the bottom of the Clifford Scott open cut mine (BW24) also has a high As content compared to the other water bodies in the area. Prior to its closure, this mine operated within the oxidised ore zone, and high As levels could therefore naturally be expected within any water collecting in or leaching from this site.

Table 3.23: Arsenic data tabulated from the results of water analyses performed in the Barbrook mining area by the Caledonia Mining Corporation since February 1995; numbers in parentheses represent corresponding sample numbers from this study.

Date:	Arsenic (mg/L):				
	21/2/95	23/3/95	23/4/95	24/5/95	21/6/95
Sampling location:					
Slimes seepage pond	0.053	0.580	0.360	1.30	0.550
Crystal Stream	0.010	<0.010	0.039	nd	nd
Waterfall (BW17)	nd	nd	0.008	nd	<0.050
Low's Creek below plant (BW5)	nd	0.017	0.008	0.022	0.018
Low's Creek at Magazine (BW25)	nd	nd	0.008	0.015	nd
No. 10 adit (BW19)					

Date:	Arsenic (mg/L):			
	21/8/95	8/11/95	13/2/96	21/5/96
Sampling location:				
Slimes seepage pond	5.18	0.40	0.80	0.78
Crystal Stream	0.017			0.009
Waterfall (BW17)	nd	nd	0.008	nd
Low's Creek below plant (BW5)	0.007	0.007	nd	0.016
Low's Creek at Magazine (BW25)	nd	nd	nd	nd
No. 10 adit (BW19)			0.12	0.45

Note: nd <0.005 mg/L

3.5.4.2 Arsenic speciation and toxicity in the Barbrook water bodies

The measured Eh and pH values for the Barbrook water samples with As contents ≥ 0.01 mg/L are plotted in Figure 3.33 relative to the thermodynamic stability fields calculated by Ferguson and Gavis (1972). Since the As within the Barbrook water samples is assumed to be predominantly inorganic (Section A1.9), no allowances have been made for any organic As species. This diagram indicates that, although elevated As levels occur in some of the Barbrook water bodies, this inorganic As should be present as the less toxic As(V), with arsenic acid speciation primarily dependent on pH. Whereas the alkaline waters from the tailings dam area (BW4, BW14 and BW15) all plot within the stability field for HAsO_4^{2-} , the more neutral pH samples cluster around the dividing line between HAsO_4^{2-} and HAsO_4^- .

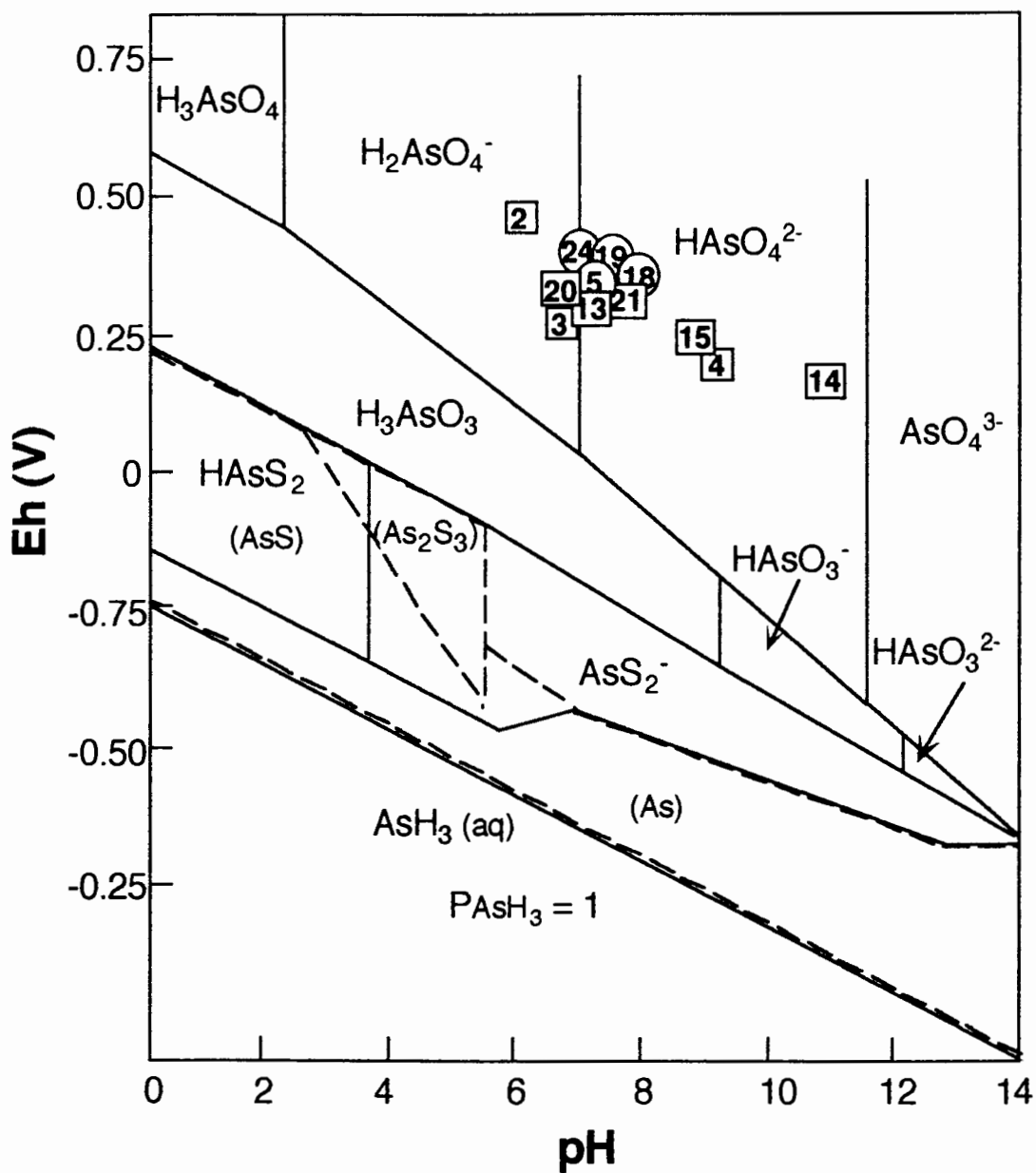


Figure 3.33: Plot of measured Eh and pH values for the Barbrook water samples with As contents ≥ 0.01 mg/L superimposed on the As Eh-pH diagram of Ferguson and Gavis (1972); Barbrook samples are represented by sample numbers and distinguished as tailings dam area (squares) and mining area (circles) samples.

indicating that both species would be present in solution. The sample with the lowest pH, comprising seepage from the base of the slimes dam wall (BW2), plots in the HAsO_4^- stability field. The As speciation assigned during MINTEQA2 modelling of the Barbrook water samples, when all of the As was entered into the program in the pentavalent state as H_3AsO_4 , is similar to that observed in Figure 3.33 although the samples which plot well within a stability field on this diagram are assigned significant amounts of the adjoining As species via MINTEQA2. For example, sample BW14 is listed as containing 57% of its As content as HAsO_4^{2-} and 43% as AsO_4^{3-} .

The validity of using a diagram like Figure 3.33 to predict the As speciation of the Barbrook water samples is highly questionable. One reason for this is the uncertainty associated with the method (Section A1.4) which was used to measure redox potential in the water samples. Sposito (1989) states that the determination of redox potential using the platinum electrode method is subject to such uncertainty that any derived Eh values can be considered to provide only a qualitative indication of pe. Drever (1988) also questions any quantitative interpretation of data derived for oxidising waters via this method due to the fact that such measurements can rarely be related to a specific redox pair. In addition to the uncertainty associated with the actual method, the fact that the measurements were performed several weeks after sample collection, albeit on sealed and refrigerated samples, also places doubt on the analytical results. A third reason to question the validity of plotting the Barbrook data directly onto Figure 3.33 is the fact that As speciation is complex and rarely in thermodynamic equilibrium (Aurilio *et al.*, 1994). As discussed in Chapter 2, a number of factors, besides just the prevailing pH and Eh conditions, can contribute to determining the speciation of As in water.

The quantitative determination of As speciation is highly desirable as a means to assess the relative toxicity of elevated As levels in different water bodies. Although the scientific literature lists numerous methods via which various inorganic and/or organic As species can be measured, many of which are summarised in Van Loon and Barefoot (1995), time constraints precluded such measurements during the course of this study. Therefore, the tentative interpretation of the measured Eh and pH values of the various Barbrook water samples, taking cognisance of the concerns outlined above, is that most of the As in these waters is present as arsenic acids and therefore not as toxic as the arsenous acid species which could form under more reducing conditions.

According to the stability diagrams of Sadiq *et al.* (1983) presented in Chapter 2 (Figures 2.4 and 2.5), the most likely arsenate mineral to precipitate under oxidising, alkaline conditions is $\text{Ca}_3(\text{AsO}_4)_2$. The results of the MINTEQA2 modelling, however, indicated that only the stream of tailings extending between the two tailings dams (BW14), which constitutes the sample with the highest As content, was approaching equilibrium with $\text{Ca}_3(\text{AsO}_4)_2$. Based on these results, it appears unlikely that As would be removed from these waters via the precipitation of any arsenate minerals under the conditions prevailing at Barbrook.

3.5.4.3 Arsenic occurrence in the Barbrook soils and sediments

The background concentration of As in the soils and sediments of the Barbrook area appears to be ~20 mg/kg, based on the sediment core (BS1) collected from Crystal Stream and a sample of uncontaminated soil (BS5) collected from outside the main entrance to the mine site (refer to Chapter 4 for a discussion of this soil). This value is within the range (1 to 40 mg/kg) stated by O'Neill (1995) to normally occur in unpolluted soils, but higher than his average value of ~10 mg/kg. By comparison, all of the other soil and sediment samples collected from the Barbrook area contain substantially higher total As concentrations of up to 2170 mg/kg.

Although the Barbrook soils and sediments in the vicinity of the tailings dams, waste rock pile and Clifford Scott open cut mine all share some degree of heavy metal contamination, their near-neutral to alkaline pH values mean that the mobility of these metals would be greatly reduced as compared to a more acidic environment (McBride, 1994). As discussed in Chapter 2, the behaviour of As is not as simple since its mobility is highly dependent on its speciation which is in turn dependent on redox potential (Masscheleyn *et al.*, 1991). The pH(H₂O) values obtained for the As-contaminated Barbrook soils and sediments range from 6.5 to 8.7 which covers the range (pH 7 to 8) at which maximum As(III) sorption occurs (Gosh and Yuan, 1987; O'Neill, 1995). However, surface sediments, and presumably the tailings dam material down to a depth of ~2 m (Funke, 1990), could be expected to represent relatively oxidising environments whereby most of the As would be present as As(V). If most of the As is present in the pentavalent state, the fact that the sorption of As(V) peaks strongly at pH 4 to 5 (Gosh and Yuan, 1987; O'Neill, 1995) means that it may be more mobile at these higher pH(H₂O) values than if it was present in the more toxic As(III) state. This As(V) mobility may be a particular problem as regards the calcine and slimes dams sediments with their pH(H₂O and KCl) values of ≥7.9, since the results of experimental studies have shown that the combination of oxidising conditions and an alkaline pH can result in a substantial increase in the mobility of As due to the replacement of As(V) on soil sorption sites by hydroxyl ions (Masscheleyn *et al.*, 1991). Despite the dependence of As mobility on redox potential, however, the fact that total As solubility is highest under acidic conditions due to the dissolution of Fe oxides and hydroxides (Masscheleyn *et al.*, 1991; Marin *et al.*, 1993) suggests that, as is the case with heavy metals, the neutral to alkaline conditions present within the Barbrook soils and sediments will help to reduce As mobility. In addition, the possible precipitation of Ca₃(AsO₄)₂ under oxidising, alkaline conditions (Sadiq *et al.*, 1983), and the presumed presence of calcite which sorbs As under alkaline conditions (Goldberg and Glaubig, 1988), may also help to reduce As mobility within the alkaline tailings dam material.

Since the total concentration of As in a soil is a poor indication of how much is actually available or potentially mobile (Sheppard, 1992), As was extracted from the Barbrook soils and sediments using a 0.5M NaHCO₃ solution in order to obtain an index of As availability. In

a review of the relative effectiveness of a range of different solutions for extracting As from soil, Johnston and Barnard (1979) state that 0.5M NaHCO₃ has a low As-releasing potential. However, they also state that it is the preferable method for use in extracting P from alkaline soils. This is due to the fact that in calcareous, neutral or alkaline soils, where Ca phosphates are present, the Ca precipitates as CaCO₃ during the extraction procedure and releases P (Olsen and Sommers, 1982). If a more acidic extractant were to be used, there is the possibility that rapid neutralisation of the acid by CaCO₃ will occur, thereby limiting P extraction. Since As is considered to behave in a similar manner to P (Johnston and Barnard, 1979), the use of a NaHCO₃ solution can also be justified for As extraction in calcareous, neutral or alkaline soils.

The amount of extractable As in the contaminated Barbrook soils and sediments ranges from 3.5 to 172 mg/kg, but is always less than 8% of the total As concentration. Although extractable As (mg/kg soil) appears to be positively correlated with the total As content and pH(KCl) values of the soils and sediments, observed correlations between extractable As and the Ca and percentage CaCO₃ contents are of doubtful validity due to the fact that they simply comprise lines extending between two point clusters (Figure 3.34). Whereas a correlation between total and extractable As would be expected, in that the more As there is present the more that can be extracted, any correlation between CaCO₃ content and total and extractable As concentrations may suggest some link in terms of As mobility within the Barbrook soils and sediments. Since As sorption by calcite increases from pH 6 to pH 12 (Goldberg and Glaubig, 1988), higher pH(KCl) samples would also be expected to correlate with higher As concentrations if As is being sorbed by calcite. The MINTEQA2 results for the calcine and slimes dams water samples (BW4, BW14 and BW15) indicate oversaturation with respect to calcite and dolomite, suggesting that another possible mechanism controlling As mobility under such alkaline conditions may be coprecipitation with calcite. Although the correlation between extractable As and the total Ca content of the soils and sediments is questionable, it is also possible that As has precipitated as Ca₃(AsO₄)₂ within the tailings dam sediments. The MINTEQA2 results indicated that none of the tailings dam area waters were in equilibrium with Ca₃(AsO₄)₂, although sample BW14 was only slightly undersaturated (SI = -0.25) and therefore interpreted to be approaching equilibrium. However, if Ca₃(AsO₄)₂ has precipitated, it may be that the analysed waters have not been in contact with the sediments long enough to establish equilibrium.

Since inorganic As forms anionic species, the presence of Fe, Mn and Al oxides and hydroxides within the clay content of a soil is of particular importance. The fact that the anion exchange capacity (AEC) of these amphoteric oxides and hydroxides is greatest under acidic pH conditions (McBride, 1994) has already been alluded to when discussing the pH dependent sorption of the different As species. Although no linear correlation exists between extractable As and the total Fe (Figure 3.34), Al and Mn (not shown) contents of the Barbrook soils and sediment, this does not preclude a significant role for the oxides and hydroxides in terms of As sorption at Barbrook. The work of Sakata (1987) suggests that a

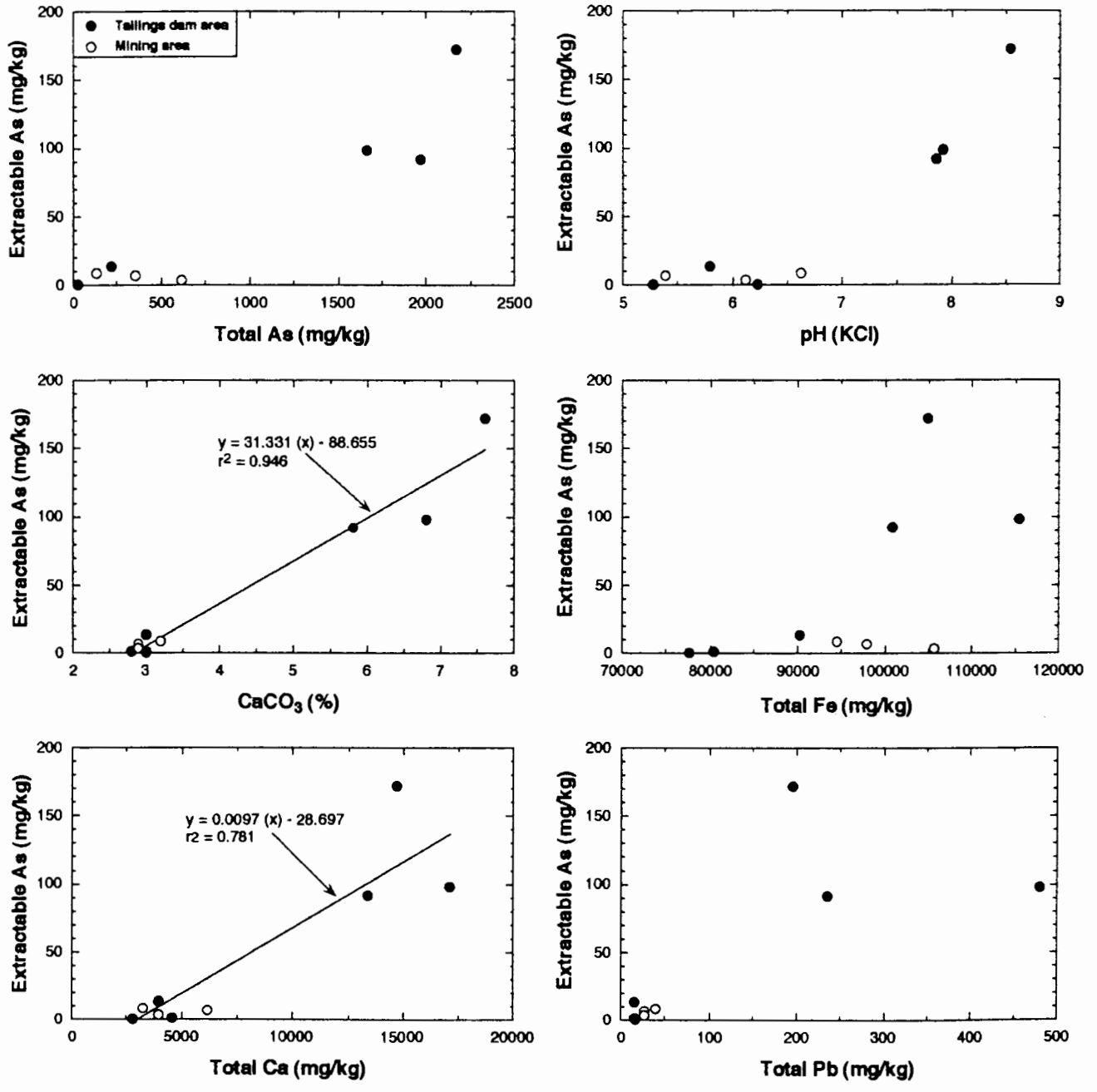


Figure 3.34: Plots of extractable As versus total As, Fe, Ca and Pb as well as % CaCO₃ and pH(KCl) in the Barbrook soil and sediment samples.

more valid method of investigating a possible correlation between these factors would have been to determine the concentrations of extractable Fe, Al and Mn using the dithionite-citrate-bicarbonate method (Appendix A2.10) in order to examine the possible role of free oxides in As sorption.

The presence of primary sulphide minerals within the calcine and slimes dam sediments necessarily complicates any discussion of purported correlations between extractable As and the range of variables which may influence As mobility. Whereas the primary sulphides may well be responsible for the high total As, Fe and Pb concentrations (Figure 3.34) of the calcine and slimes dam sediments, the presence of carbonates within the host rocks and the liming of the tailings material during ore processing could be responsible for the high CaCO₃ contents such that little, if any, sorptive relationship exists between them. Therefore, the combination of soil and overlying tailings material within the sediment cores collected from the calcine and slimes dams makes it difficult to interpret the behaviour of As except to state that substantial amounts are present and extractable.

3.5.4.4 Arsenic occurrence in association with the Barbrook waste rock pile

Despite the fact that no As was detected in the TCLP leachates from the waste rock pile samples, high As concentrations are present in both the soil underlying the waste rock pile and the immediately adjacent Low's Creek sediments. Although the sediments could have accumulated As as a result of the discharge into Low's Creek of As-bearing water from the level 10 mine adit, it seems most likely that the soil underneath the waste rock pile was directly contaminated by leaching of the waste rock. The fact that the concentrations of various heavy metals are also enriched in the underlying soil, implies that the waste rock pile is contributing to the contamination of the immediate environment.

Although the TCLP is a standard procedure designed by the U.S. Environmental Protection Agency "to determine the mobility of both organic and inorganic analytes present in [a range of] liquid, solid or multiphase wastes" (EPA, 1993), its applicability to the Barbrook environment is questionable. The prevailing neutral to alkaline conditions at Barbrook, due to the high degree of buffering provided by the carbonate minerals present in the host schists, make it highly unlikely that a pH 5 leachate will form within the foreseeable future, despite the fact that rainwater in equilibrium with atmospheric CO₂ has a pH of 5.6 (Drever, 1988). This stance was also adopted by Sadler *et al.* (1994) who performed a modified TCLP on As contaminated soil using pH 7 distilled water for much the same reason. In addition, the presence of As in such an acidic leachate is likely to be decreased by the fact that arsenopyrite oxidation results in the release of an arsenic acid (H₃AsO₄) species (Wilson and Hawkins, 1978; Bottomley, 1984), and As(V) is strongly sorbed at pH 4 to 5 (Gosh and Yuan, 1987; O'Neill, 1995). Davis and Ashenberg (1989) note that the mineral scorodite (FeAsO₄·2H₂O) actually controls As solubility at pH 4 to 5 in an oxic environment.

The two samples from the Barbrook waste rock pile were collected mainly to provide an indication of the total and leachable As contents of the waste rock. However, the limited size of these samples means that they are by no means representative of the waste rock pile as a whole. In fact, the substantial variation in the chemical compositions of these samples indicates a high degree of heterogeneity in the waste rock pile, particularly in terms of the distribution of sulphide minerals. This heterogeneity may be due to variations in ore cut-off grades over the lifetime of the mine. As a result, the concentrations of As and heavy metals in leachates emanating from along the length of the waste rock pile could vary substantially depending on the relative distribution of residual primary sulphide minerals and gangue material.

3.5.5 Is there a current or potential problem at Barbrook?

3.5.5.1 Acid mine drainage

Sulphide oxidation is a naturally-occurring, microbially-mediated process which may be enhanced by activities such as mining. The exposure of previously buried and reduced sulphide material to the atmosphere, and subsequent leaching by water, can result in the formation of an acidic, sulphate-rich effluent known as acid mine drainage (Jambor, 1994). Depending on the original composition of the gangue and ore minerals, this effluent may contain high concentrations of heavy metals, the mobility of which is enhanced by the acidic conditions (McBride, 1994). Although the potential for acid mine drainage is of major concern in many mining operations involving sulphide minerals, the abundance of carbonate minerals within the intercalated banded iron formation, shales and schists which host the Barbrook ore bodies (Houstoun, 1990) means that the formation of any acidic effluent is buffered in much the same way that liming is used as a remediation mechanism for acid mine drainage. A similar situation is described by Bottomley (1984) for an area of Nova Scotia where auriferous arsenopyrite is closely associated with calcite in quartz veins. Past mining of these veins has resulted in As contamination of the groundwaters due to arsenopyrite oxidation but the accompanying oxidation of the calcite serves to consume any acidity generated by this process, thereby preventing the acidification of the groundwater.

The actual mechanism involved in the carbonate-driven neutralisation of acid mine drainage is described by Blowes and Ptacek (1994). They state that the H^+ ions released during sulphide oxidation are most effectively consumed by calcite, the most soluble of the carbonate minerals, to produce Ca^{2+} and HCO_3^- . This accords with the high concentrations of these ions in many of the tailings dam waters at Barbrook. When calcite is present, the pH is buffered in the range of 6.5 to 7.5. As the dissolution of other carbonate minerals proceeds more slowly than that of calcite, the order of carbonate depletion, which begins with calcite, is followed by dolomite, ankerite and siderite, all of which are present in the Barbrook country rock. Once the calcite is consumed, the pH range at which the acid

leachate is buffered is lowered. According to Blowes and Ptacek (1994), the dissolution of calcite and the generation of intermediate pH values results in the precipitation of amorphous and crystalline metal hydroxides which decrease heavy metal mobility.

The seepage from the base of the main slimes dam wall (BW2) and the nearby puddle of upwelling water (BW3) have the lowest pH values (6.04 to 6.74) of all the Barbrook samples and, as such, are the closest that Barbrook currently comes to generating acid mine drainage. Whereas the saturation indices calculated by MINTEQA2 for the tailings dams surface waters (BW4, BW14 and BW15) indicate oversaturation with respect to calcite and dolomite, both BW2 and BW3 are undersaturated with respect to both. Assuming that the seepage was in equilibrium with the matrix which generated it, this suggests that in certain areas of the main slimes dam, an acid leachate is being generated which is resulting in carbonate dissolution. The fact that sample BW2 has a pH value which is at least one whole pH unit lower than any of the surface water bodies associated with the tailings dams, and lower than the calcite-buffering pH range of 6.5 to 7.5 (Blowes and Ptacek, 1994), combines with its extremely high Ca^{2+} and SO_4^{2-} concentrations to suggest that seepage from the base of the slimes dam wall is approaching the composition of acid mine drainage.

Although the Barbrook system represents a highly buffered system at this point in time, the sheer volume of tailings material which has already been dumped and the proposal to continue gold processing at the Barbrook site until at least the year 2000 (Ralph Morris and Associates, 1996) makes it difficult to predict whether the buffering capacity of the system will be exhausted before all of the primary sulphide material has been oxidised. Blowes and Ptacek (1994) state that sulphide oxidation within mine tailings, and the consequent release of acid mine drainage, can actually last for tens to hundreds of years. Therefore, the character of future leachates from the Barbrook slimes dam will depend to a certain extent on the treatment of the area during the decommissioning period, and the subsequent, if any, maintenance and monitoring undertaken. According to the Barbrook Mines EMPR (Ralph Morris and Associates, 1996), the current plan is to undertake "shaping of the slimes dam in order to minimise penetration of the rainfall". Although it is assumed that this will involve the use of an impermeable cover to prevent both water and oxygen infiltration, no specific details are provided. In the meantime though, the tailings currently being deposited may be subject to immediate oxidation upon exposure, which Jambor (1994) cites as a "vivid demonstration" that the generation of acid mine drainage may start long before the decommissioning stage. Funke (1990) states that sulphide oxidation in a tailings impoundment is limited to periods between the application of successive layers of slime, due to the pore volumes within the tailings being filled with water at other times. However, the Barbrook tailings dams were extremely dry and exposed in August 1996 and therefore potentially susceptible to large amounts of sulphide oxidation.

The waste rock pile and the underground mine workings are also possible contenders for future generation of acid mine drainage. Whereas the Barbrook Mines EMPR (Ralph Morris and Associates, 1996) states that the underground mine adits will eventually

be sealed in order to prevent contaminated groundwater from discharging into the local streams, there appear to be no future plans for the ever-increasing waste rock pile. The fact that the soil underlying the waste rock pile is already subject to heavy metal contamination suggests that even though the leachate is not acidic at the stage, it is still able to transport and disperse heavy metals into the surrounding environment.

3.5.5.2 Arsenic dispersion

Although the possible future generation of acid mine drainage at Barbrook has major implications for heavy metal mobility and dispersion into the surrounding environment, the implications for As dispersion are not quite as straightforward due to the complex interactions which control As mobility (Chapter 2). In the Barbrook area, the main concern associated with possible As dispersion from mining operations involves contamination of the Barbrook and Low's Creeks which provide drinking and irrigation water for the local population. Therefore, although the highest As concentrations have been detected in the tailings dam area, high levels of As in the mining area may be of greater concern in terms of the health of the local human population. Crystal Stream, which was dry during the August 1996 sampling period, did experience elevated As levels during 1995 and could also possibly contribute to downstream contamination of local drinking water.

In August 1996, As dispersion into the Barbrook and Low's Creeks as a result of the underground mining operations was negligible. However, some sort of discharge or seepage of As-contaminated material was entering Low's Creek in the vicinity of the processing plant. The lack of any appreciable sediment lining either the Barbrook or Low's Creeks means that As is unlikely to accumulate to any great extent in these creek beds and the processing plant discharge appears to be diluted once the two creeks converge downstream. The degree of dilution which occurs will depend, however, on both the current rainfall and the amount of water being released from the Shiyalongubo Dam into Barbrook Creek.

The fact that background As levels may be enhanced as a result of the natural exposure and oxidation of As-bearing sulphide minerals must also be taken into account when examining mining-related As dispersion. This appears to be the case for the groundwater entering the level 10 mine adit in the vicinity of the Barbrook ore bodies, although subsequent dilution by the recycled mine waters results in negligible As discharge from the mine into Low's Creek. Natural As contamination of groundwater in an area of West Bengal, India, has also been attributed to the oxidation of As-bearing pyrite in borehole sediments (Das *et al.*, 1996). Since pyrite is insoluble in water, Das *et al.* (1996) have suggested that the withdrawal of large amounts of groundwater from three interconnected and largely unconfined aquifers may have resulted in oxidation of the As-rich pyrite such that it decomposed and released the As. This interpretation is supported by the fact that each

year an increasing area of West Bengal, dependent on different parts of this same aquifer system, is affected by high As levels within the groundwater, suggesting that the progressive withdrawal of water from the system is resulting in increasing pyrite exposure and oxidation. The fact that As levels of up to 0.45 mg/L have been detected within the level 10 mine adit water at Barbrook within the last two years could also indicate that the rate at which the sulphide minerals are oxidising at depth fluctuates with changing groundwater levels. Seasonal fluctuations in the As concentrations of borehole waters in the western United States have also been documented by Frost *et al.* (1993). These seasonal fluctuations were a problem in this case as water was abstracted directly from the boreholes for domestic use following single As determinations which, it eventually became apparent, were not temporally representative of water quality. A similar problem could occur in the Barbrook area as groundwater is abstracted for drinking water purposes close to the mine site (Ralph Morris and Associates, 1996). Unfortunately, no information is available regarding the As concentrations of the groundwater in these boreholes, but fluctuations in groundwater As concentrations at the actual mine site could also result in varying degrees of As contamination of Low's Creek.

3.5.5.3 Other potential problems

Two other potential environmental problems associated with the Barbrook tailings dams are wind dispersal of the fine-grained tailings material and cyanide dispersion. According to Mitchell and Barr (1995), aerial dispersal of tailings material, such as that observed at Barbrook during the August 1996 sampling period (Figure 3.14), can result in the downwind contamination of soils, vegetation and surface waters. Although present circumstances make it difficult to prevent such wind-dispersal of the dry tailings, the decommissioning of Barbrook must include a procedure for stabilisation of the tailings material, possibly involving the use of vegetative cover using tolerant plant species (Runke, 1990).

The presence of cyanide within some of the surface waters associated with the Barbrook tailings dams is indicated by the precipitation of copper thiocyanate (CuSCN) upon water acidification. Although this cyanide, derived from the leaching of the ore at the processing plant, will eventually volatilise upon exposure to ultraviolet radiation, the photo-oxidation process can take up to nine or ten months to occur, depending on the ambient temperature (Ripley *et al.*, 1996). In the meantime though, the cyanide is available for dispersion via seepage from the tailings dams, and the deposition of subsequent slime layers could potentially inhibit the photo-oxidation of previously deposited cyanide. As stated by Ripley *et al.* (1996), residual cyanide within tailings material could represent a long-term problem due to periodic flushing from the system as equilibrium conditions within the tailings material change. The presence of cyanide in solution as the thiocyanate (SCN⁻) ion

can occur as a direct result of the cyanidation process due to production of labile sulphur atoms from the attack of cyanide or lime on pyrrhotite or the air oxidation of sulphide ions during ore processing (Smith, 1994). Although SCN^- is reported to be somewhat less toxic than the CN^- form, it is still an environmental hazard in terms of the general toxicity of both cyanide and its breakdown products (Smith, 1994). The presence of high amounts of NH_4^+ , one of the breakdown products of cyanide, within many of the Barbrook tailings dam area waters suggests that photo-oxidation of cyanide is occurring. However, the fact that NH_4^+ can itself be deprotonated to form NH_3 , both of which can be microbially transformed into NO_3^- and NO_2^- , indicates that cyanide breakdown can still result in toxicity.

The proposal to re-open the currently disused open cut mines at Barbrook for heap leaching (Ralph Morris and Associates, 1996) may cause a severe impact on the surrounding environment. Although heap leaching, whereby a cyanide solution is sprayed over heaps of crushed ore, is an economically efficient method for gold dissolution and removal, it is also a potentially damaging procedure. Hammond *et al.* (1993) state that the use of the heap leaching technique in the U.S.A. has been widely criticised due to the severe environmental damage it has caused as a result of cyanide leakage into waterways. Although the report states that the main effect has been the extensive mortality of the aquatic life within these contaminated streams, a similar leakage at Barbrook could result in cyanide contamination of the drinking and irrigation water used by the local population. Ripley *et al.* (1996) also criticise the practice of heap leaching due to the dangers of cyanide dispersion into the environment.

3.6 Conclusions and recommendations

The results of this investigation indicate that past and present mining and processing operations at the Barbrook gold mine are responsible for As and heavy metal dispersion into the local environment. The main danger associated with this type of environmental dispersion is contamination of the local water sources used for drinking and agricultural purposes. This is of particular concern for the area around the level 10 mine adit entrance and waste rock pile at Barbrook due to the proximity of the Barbrook and Low's Creeks to the mining and processing operations. Despite the fact that Low's Creek receives discharge directly from the level 10 mine adit and flows through, and adjacent to, the waste rock pile, the only evidence for As contamination in August 1996 was found downstream of the Barbrook processing plant. Although elevated As levels were not detected further downstream, possibly due to either dilution by the converging Barbrook Creek waters or As adsorption by stream sediments or colloidal matter, the fact that As-bearing discharge is emanating from the processing plant requires immediate attention. This is particularly so as the processing plant was only just being recommissioned at the time of sampling and might therefore result in even greater discharge levels once full operation is in progress. The added danger that cyanide could be present within this discharge, due to its extensive use

within the gold processing operations, indicates that the investigation of this area should constitute a high priority for the Caledonia Mining Company. By comparison with Low's Creek, there is no evidence, and no likely source, of As contamination in Barbrook Creek.

Contamination of the groundwater in the vicinity of the Barbrook mining area is also of concern since locally-abstracted groundwater is used for domestic purposes. Although no information is available regarding the quality of the water pumped directly from these boreholes, the groundwater in actual contact with the Barbrook ore bodies and discharging into the level 10 mine adit has an elevated As concentration. Since this appears to be a natural phenomenon resulting from sulphide oxidation within the aquifer, As concentrations could be influenced by changing groundwater levels and differing degrees of sulphide exposure and oxidation. The contamination of groundwater distant to the actual ore bodies will depend on the direction and rate of groundwater flow, but there is a distinct need for regular monitoring of the quality of the groundwater abstracted for use by the local population.

The waste rock pile, located outside the entrance to the level 10 mine adit and alongside the eastern bank of Low's Creek, constitutes a major eyesore in the Low's Creek valley. In addition, the As and heavy metal contamination of the underlying soil and adjacent Low's Creek sediments indicates that it is producing a potentially harmful leachate. The association of the Barbrook ore bodies with carbonate bearing country rocks has resulted in a well buffered system, however, which currently mediates heavy metal mobility. The lack of any discernible As contamination of the Low's Creek water in the vicinity of the waste rock pile is most likely a function of the low residence times of the water as it passes through the waste rock as well as the sorption capacity of the soil (Chapter 4). Although the Barbrook waste rock pile is largely a legacy of past mining activities at Barbrook, its location beside a stream which is ultimately a domestic water source for the local communities, added to the fact that sufficient low grade ore material is present within it to produce a heavy metal and As contaminated leachate, make it a future environmental risk for the area. Based on the results of this study, it is suggested that the current owners of Barbrook should discontinue the practice of waste rock disposal at this site and consider including a management strategy for the waste rock pile within their decommissioning phase plans.

The high As content of the water in the disused Clifford Scott open cut mine is not of serious concern at present. The only obvious danger would involve flooding of this quarry such that, as part of the mountain catchment area, it contributed to surface run-off into nearby streams. The intention to heap-leach the abandoned open cut mines at Barbrook using a cyanide solution should be re-examined, however, in the light of problems and concerns which have been documented in the scientific literature regarding the dispersion of highly toxic cyanide into the environment.

The location of the tailings dams was deliberately chosen to be quite remote from human settlements in order to lessen the prospect of contaminating local water sources. However, the use of the tailings dams waters, particularly during the drier months when other

surface water sources are depleted or non-existent, by cattle, birds and possibly also native animals, means that the quality of these waters and any leachates seeping from the main slimes dam is also important. The possible contamination of Crystal Stream, located within the Kaap subcatchment of the Crocodile River catchment (DWAF, 1995a), by tailings dam leachates is also of concern in terms of affecting the quality of the water used downstream for domestic and agricultural purposes. Previous analyses of Crystal Stream water have indicated that As contamination does occur, but whether the source of this contamination is aqueous or particulate, the latter due to wind-dispersal of fine-grained tailings material, is unknown.

Although acid mine drainage is not currently a problem at Barbrook, there is evidence, based on the composition and lowered pH of the water seeping from the base of the slimes dam wall, that it would occur if it were not for the buffering provided by the carbonate minerals present within the tailings material and derived from the host rocks. The risk of producing heavy metal-laden acid mine drainage in the future will depend largely on the overall buffering capacity of the carbonates as well as the strategy adopted for dealing with the tailings dam area in the long term. The need to stabilise and isolate the tailings material, in order to minimise exposure to both air and water, is dictated by the risks of both acid mine drainage production and wind-dispersal of contaminated material.

In conclusion, the Caledonia Mining Company faces a number of environmental challenges at Barbrook. Some of these, such as the discharge of As-bearing material from the processing plant into Low's Creek, the apparent intermittent contamination of Crystal Stream, and the possibility that As-bearing waters may be abstracted from the local boreholes for domestic use, require immediate attention. However, in most cases, careful monitoring over the lifetime of the mine and well planned closure and remediation strategies are probably the only requirements. The plan to use the heap leaching technique in order to derive full economic benefit from the disused open cut mines should also be carefully re-examined.

CHAPTER 4

A preliminary assessment of the potential for arsenic sorption by the Shortlands soil in the Barbrook area

4.1 Introduction

As discussed in Chapter 3, the mining and processing operations at Barbrook are resulting in As release into the local environment due primarily to the enhanced exposure and oxidation of As-bearing sulphide minerals derived from the Barbrook ore bodies. Since the main danger, in terms of human health, involves potential As contamination of the groundwater and surface streams used by local communities for domestic purposes, the capacity of the soil at Barbrook to sorb As and thereby mediate its dispersion is of prime importance when investigating its potential environmental impact.

Several different soil forms, some of which appear to be alluvial in origin, have been identified in the Barbrook area. Although the Barbrook Mines EMPR (Ralph Morris and Associates, 1996) only reports the presence of the Hutton, Glenrosa and Mispah soil forms, the Shortlands form was also identified during the course of this study. Due to the predominance of red, clay-rich soils in the Barbrook area, and the apparent abundance of the Shortlands soil form within the actual mining area, it was chosen as a representative soil for the area. The Shortlands soil is a sesquioxidic, kaolinitic clay (M.V. Fey, personal communication, 1996) which would be expected to have a relatively strong capacity to sorb anions, such as those formed by As. Quantifying this capacity is considered desirable as a preliminary basis for assessing the potential value of such soils in the Barbrook area for the disposal and attenuation of arsenical wastes.

A concurrent investigation into the P sorption capacity of this same soil was aimed at investigating reports in the scientific literature that As and P display similar sorption behaviour due to their shared tendency to form oxyanions (e.g. Woolson and Kearney, 1973; O'Neill, 1995). Compared to As sorption, P sorption has been extensively studied in a wide range of South African soils (Bainbridge *et al.*, 1995). Similar sorption behaviours by As and P could therefore potentially enable predictions to be made regarding As sorption in soils for which P sorption information is already available.

4.2 Previous sorption studies

According to Sposito (1989), the term sorption refers to the uptake of a solute from solution via adsorption, absorption or co-precipitation. Natural As sorption is considered to be dominated by three processes, which include: (i) adsorption by hydrous Fe, Al and Mn oxides, (ii) coprecipitation with Fe oxides, and (iii) replacement of phosphate with isomorphous arsenate within certain minerals (Bodek *et al.*, 1988; cited in McLaren and Kim, 1995). In addition, limited anion sorption by layer silicates within the clay fraction of a soil can occur due to the presence of dangling protonated hydroxyl ions associated with particle edges at relatively low pH (Frost and Griffin, 1977). In contrast, the coating of Fe oxides by adsorbed organic matter may result in reduced anion sorption due to the competition for negatively charged sites and the resultant increase in the negative surface charge resulting from the adsorption of fulvic and humic acids (Davis, 1982; Xu *et al.*, 1991). It has been suggested, however, that both As(V) and phosphate may be adsorbed by humic substances via Al or Fe bridging (Gustafsson and Jacks, 1995).

To reiterate some of the information presented in Chapter 2, the sorption behaviour of As depends primarily on its oxidation state and the dominant sorption sites in soil are considered to be provided by the Fe and Al oxide and hydroxide minerals (Pierce and Moore, 1982; Sakata, 1987; Hunt and Howard, 1994). The fact that these are amphoteric minerals, with valence-unsatisfied surface hydroxyl ions, means that when the soil pH is less than their individual point of zero charge (pzc) values the development of a positive surface charge favours anion sorption (Xu *et al.*, 1988). Therefore, pH is a dominant factor controlling As sorption in soils (Blakey, 1984). Whereas maximum As(III) sorption occurs at a pH of 7 to 8, maximum As(V) sorption occurs at a pH of 4 to 5 (Frost and Griffin, 1977; Pierce and Moore, 1982; Gosh and Yuan, 1987; O'Neill, 1995). In terms of organic As, MMAA and DMAA sorption peaks at pH 4 (Xu *et al.*, 1991). According to Xu *et al.* (1991), different mechanisms may be responsible for the sorption of the different As species. Whereas the major mechanism for As(III) sorption appears to be specific adsorption, As(V) sorption may involve both specific adsorption and electrostatic attraction. Specific adsorption or chemisorption differs from simple electrostatic attraction in that it involves ligand exchange reactions whereby the As anion displaces surface $-OH^-$ or $-OH_2$ groups (McBride, 1994). As opposed to non-specific electrostatic attraction, chemisorption also shows a high degree of specificity toward particular anions and is either non-reversible or involves only very slow desorption (McBride, 1994). The fact that arsenate diffuses slowly in and out of adsorbent aggregates, in a similar manner to phosphate, means that the attainment of sorption equilibrium is a slow process (Fuller and Davis, 1989; Fuller *et al.*, 1993). However, experimental studies into As sorption have shown that equilibrium can be achieved within 24 hours (Elkhatib *et al.*, 1984a; Sakata, 1987).

Pierce and Moore (1982) found that As(III) and As(V) sorption by Fe oxides involves two processes. Whereas initial As sorption can be described by a Langmuir-type adsorption

isotherm, higher sorption densities require a linear isotherm. The Langmuir-type isotherm describes a homogeneous adsorption situation where the surfaces of the soil solids have an array of adsorption sites of equal energy, each of which can adsorb one species (O'Neill, 1995). By comparison, the subsequently derived linear isotherm was interpreted by Pierce and Moore (1982) as describing a heterogeneous adsorption situation where sorption was not confined to the Fe oxide surfaces as would be expected with a crystalline solid. Langmuir isotherms were also found to best describe the specific adsorption of As(V), MMAA and DMAA on activated alumina (Gosh and Yuan, 1987), as well as As sorption on bauxite and carbon (Gupta and Chen, 1978). By comparison with these mineral sorption studies, Elkhatib *et al.* (1984b) found that As(III) sorption in five different soil types was best described by a Freundlich isotherm over an initial As concentration range of 5 to 1000 mg/L. This type of isotherm indicates that surface heterogeneity comprises groups of homogeneous adsorptive sites of differing energy, each of which describes Langmuir-type sorption behaviour (O'Neill, 1995). The definition of Freundlich isotherms by the soils of Elkhatib *et al.* (1984b) was interpreted to result from the presence of a range of different minerals with individual surface properties and possible Fe, Al and Mn hydroxide surface coatings (O'Neill, 1995).

In their study into the sorption of arsenate on a calcareous (14.7% CaCO₃), montmorillonitic soil under a range of pH conditions, Goldberg and Glaubig (1988) found that maximum sorption by the clay minerals, montmorillonite and kaolinite, occurred at a pH of ~5 whereas sorption by calcite increased from pH 6 to 10, peaked at pH 10 to 12, and decreased above pH 12. Although Brannon and Patrick (1987) found that As release was significantly correlated with the CaCO₃ equivalent of sediments, Glaubig and Goldberg (1988) state that this may be a function of the carbonates having hydrous Al or Fe oxide coatings.

Discussions of P adsorption in soils refer to the chemisorption of ionic P (H₂PO₄⁻, HPO₄²⁻) from solution onto clays, oxides and hydroxides of Fe and Al, calcium carbonates and organic matter (Pierzynski *et al.*, 1994). In addition, P sorption can also involve coprecipitation (McBride, 1994). The chemical similarities between As and P, both of which belong to the nitrogen group (N, P, As, Sb, Bi) of elements, form oxyanion species in solution and have very similar dissociation constants, have been used by some researchers to predict that similarly charged As and P species will compete for sorption sites on soil solids (O'Neill, 1995). Compared to arsenate, the smaller size associated with the phosphate species are thought to result in stronger sorption, such that sorbed As can be displaced by phosphate and leach down through the soil profile before being re-adsorbed within a subordinate horizon (Woolson and Kearney, 1973). Peryea (1991) also found that As mobility, phytoavailability and phytotoxicity was enhanced by the addition of a phosphate-containing fertiliser to As-contaminated soil. However, this is a relatively contentious issue as Pierce and Moore (1982) found that, although arsenate and phosphate compete for sorption sites, the addition of phosphate after arsenate has already been adsorbed does not have a

significant effect on As sorption. Pierce and Moore (1982) did find, however, that at low As concentrations the adsorption of As can be significantly affected by previously sorbed phosphate.

4.3 Sampling location and soil description

A large (several kg) soil sample (BS5) was collected from a road cutting located immediately outside the main entrance gate to the Barbrook mine complex (Figure 3.15). The actual sampling site was chosen on the basis that it was devoid of any obvious source of contamination. The sample was taken from a depth of approximately 30 to 50 m within the B horizon of a soil profile classified (M.V. Fey, personal communication, 1996) as belonging to the Empangeni family of the Shortlands soil form (Soil Classification Working Group, 1991). The Shortlands classification is based on the presence of a red-structured B horizon overlain by an orthic A horizon. The more tentative classification of BS5 into the Empangeni family is based on the fact that the dystrophic or mesotrophic B horizon is luvic, containing significantly more clay than the A horizon, and has a fine subangular structure. A description of the sampling site is presented in Table 4.1. The following description of the actual soil was prepared according to SIRI (1991) guidelines, with soil colours determined according to the Munsell (1992) soil colour charts:

Moist; yellowish red 5YR4/6 (dusky red 2.5YR3/4 when moist); clay; strong, fine, subangular blocky; hard, firm, slightly sticky; non-plastic; many very fine to fine pores; many fine cracks; no cementation or slickensides; many clay cutans; few angular gravel rock fragments.

Table 4.1: Description of the Barbrook Shortlands soil sampling site, prepared according to SIRI (1991) guidelines.

Profile No:	BS5
Soil form:	Shortlands (Sd)
Soil family:	Empangeni (1210)
Latitude and Longitude:	25°43'23"S / 31°16'45"E
Locality:	Adjacent to road, immediately outside main entrance to Barbrook mine site
Elevation (above sea level):	620 m
Annual rainfall:	500 to 700 mm
Annual average temperature range:	8 to 30°C
Terrain unit:	Midslope - southeastern aspect
Parent material:	Dolerite colluvium
Vegetation:	Valley bushveld
Land use:	Cattle grazing

Note: Soil form and family classifications are according to the Soil Classification Working Group (1991) guidelines. Annual temperature and rainfall information was summarised by Ralph Morris and Associates (1996). Latitude, longitude and elevation were determined from the 1:50 000 Topographic Series map (2531CB Kaapmuiden, 1984) published by the Chief Directorate, Surveys and Land Information.

4.4 Analytical methods

4.4.1 Characterisation of the Shortlands soil in the Barbrook area

The following range of analytical techniques was used to ascertain the physical properties and chemical constituents of the Shortlands soil sample BS5. Detailed descriptions of these techniques, including discussions of their expected precision and accuracy, are presented in Appendix 2. The following section presents a brief synopsis of the techniques involved.

Many of the analyses were performed by the author in the Department of Geological Sciences at the University of Cape Town on aliquots of air-dried and sieved (≤ 2 mm) soil. The determination of pH in two soil solutions, prepared using either water or 1M KCl, involved the use of a Metrohm 691 pH meter, whereas the CaCO_3 concentration was measured using the Karbonat-Bombe method of Birch (1981). A range of major and trace element concentrations were analysed by XRF on pressed powder briquettes using a Philips PW1480 spectrometer and the method described by Norrish & Chappell (1977). Exchangeable acidity was determined by saturating an aliquot of the soil with a 1M KCl solution prior to undertaking an automated potentiometric titration with 0.01M NaOH to an end-point pH of 8.3. This was achieved using an automated Radiometer DTS 800 multi-titration system. Soluble salt concentrations were determined in an aqueous saturated paste extract which was prepared according to the method of Rhoades (1982a). Cation (Ca^{2+} , Mg^{2+} , Na^+ and K^+) and anion (SO_4^{2-} , Cl^- and NO_3^-) concentrations within the saturated paste extract were measured by high performance ion chromatography (HPIC) using a Dionex ion chromatograph. The rapid dichromate oxidation-titration method of Walkley and Black (1934) was used to determine soil organic C content. Soil water content was determined gravimetrically by overnight oven-drying of a soil aliquot at 110°C. X-ray diffractometry (XRD) was used in order to determine the minerals present within the clay fraction of sample BS5 following separation of this fraction by dispersion in a dilute Na_2CO_3 solution and sedimentation.

A number of analyses were also performed in other departments at the University of Cape Town on soil extracts prepared by the author. Exchangeable cation (Ca^{2+} and Mg^{2+}) concentrations in the 1M KCl extract were determined by flame atomic absorption spectroscopy (AAS) in the Department of Chemical Engineering, whereas the concentrations of Zn, Pb, Co, Ni, Si, Mn, Fe, Cr, Al and Cu in the aqueous saturated paste extract were analysed by ICP-AES in the Chemistry Department. The specific surface area was determined in the Department of Chemical Engineering using nitrogen gas and the BET equation (Carter *et al.*, 1986). Analyses performed by the Institute for Soil, Climate and Water (ISCW) in Pretoria included the ICP-MS determination of the concentration of As extracted from BS5 using the NaHCO_3 method of Olsen and Sommers (1982), the determination of particle size distribution by the hydrometer method, and the measurement of extractable Fe and Al and Mn using the dithionite-citrate-bicarbonate and sodium pyrophosphate methods

(Non-Affiliated Soil Analysis Work Committee, 1990). The P sorption index (%) of BS5 was also measured at ISCW using a method which involved equilibrating an aliquot of soil with a known quantity of P by shaking on an end-over-end shaker. Following filtration, the P content of the supernatant was determined via the ascorbic acid colorimetric method of Murphy and Riley (1962) and the amount of sorbed P was expressed as a percentage of the initial amount added to the soil.

4.4.2 Phosphorus sorption experiment

A detailed description of the method used to determine the P sorption characteristics of Shortlands soil sample BS5 is presented in Appendix 4. The method involved 24 hour equilibrations of a series of ground, sieved (<2 mm) and air-dried 2.5 g soil sub-samples with 25 mL of a solution containing one of a range of phosphate concentrations (0 to 500 mg/L P as Na_2HPO_4 in 0.1M NaCl). The equilibration procedure involved shaking for 24 hours on a horizontal shaker, followed by centrifugation and filtration of the supernatant prior to analysis. The P concentration of each filtrate was determined using the ascorbic acid colorimetric method of Murphy and Riley (1962). The equilibrium P concentration was then subtracted from the initial concentration of P added to the soil in order to derive the amount sorbed.

4.4.3 Arsenic sorption experiment

A similar procedure, to that described above, was employed in order to determine the As sorption characteristics of Shortlands soil sample BS5. Individual sample aliquots were equilibrated with solutions containing a range of As concentrations (0 to 1209 mg/L As as $\text{Na}_2\text{HAsO}_4 \cdot 7\text{H}_2\text{O}$ in 0.1M NaCl) which extended over the same concentration (mmol/L) range used for the P sorption study. The equilibrium As concentrations in the filtrates were determined by ICP-MS at ISCW. A detailed description of the procedure is included in Appendix 4.

4.5 Results and discussion

4.5.1 Characterisation of the Shortlands soil in the Barbrook area

The results obtained from a range of whole-soil chemical analyses performed on Shortlands soil sample BS5 are presented in Table 4.2, whereas the results of various extraction procedures are presented in Table 4.3. Texturally, sample BS5 can be classified as a clay. It has low organic C, H_2O and CaCO_3 contents, a high specific surface area, a

neutral pH(H₂O) value and a slightly more acidic pH(KCl) value. The high total Fe and Al contents of this soil, as compared to the other Barbrook soils and sediments discussed in Chapter 3, are presumably derived from the primary mineralogy (pyroxene, plagioclase ± olivine) of the dolerite parent rock, fragments of which are present within the soil. Basic igneous rocks are also relatively enriched in elements such as Zn, Cu, Ni, Co, Cr and V. This is due to the fact that these elements are all compatible with respect to the major mineral phases within dolerite since they possess the appropriate ionic radii and valence charges to enable their substitution within the crystalline mineral structures (Barker, 1983). Therefore, although a comparison of the composition of sample BS5 with other Barbrook soil samples could suggest some heavy metal contamination of the former, the fact that it has total As and Pb contents within the ranges predicted for uncontaminated soils (O'Neill, 1995; Davies, 1995) indicates that the high heavy metal concentrations are probably accounted for by the mafic composition of its parent rock type.

Table 4.2: Analytical data for the Shortlands subsoil; XRF data represent total major and trace element contents analysed on powder briquettes, whereby the major elements were analysed as wt % Fe₂O₃, Al₂O₃ and CaO.

Parameter:	BS5
Clay (%)	65
Silt (%)	25
Sand (%)	10
Organic C (%)	0.46
H ₂ O (%)	0.45
CaCO ₃ (%)	2.6
Surface area (m ² /g)	68
P sorption (%)	53
pH (H ₂ O)	6.94
pH (KCl)	5.45
XRFS data (mg/kg):	
As	20.9
Fe	148279
Ca	1437
Al	124903
Zn	212
Cu	167
Ni	367
Co	54.2
Mn	1491
Cr	786
V	274
Pb	19.2

The Soil and Irrigation Research Institute (SIRI)¹ conducted an investigation into the P sorption/fixation ability of 50 selected South African soils, following their equilibration with an initial P concentration of 250 mg/kg. Since the red-structured B horizon belonging to the Shortlands soil form sorbed 100% of the added P, it was classified as an extremely high P-sorbing soil (Group I). In contrast to these findings, the Shortlands soil sample collected from the Barbrook area sorbed only 53% of the added P and would therefore be classified as a medium-sorbing soil (Group III). As the soil family was not specified in the SIRI report, this obvious difference in anion sorbing properties may be due to the Barbrook soil belonging to a different family than the Shortlands soil used in the sorption study.

The CEC of a soil is most effectively measured by using a technique which involves a salt solution containing divalent ions (Arnold, 1978), such as the BaCl₂-MgSO₄ method described by Rhoades (1982b). However, an indication that the Shortlands soil has a high CEC was obtained by determining the concentrations of the KCl extractable cations Ca²⁺ and Mg²⁺. Although Thomas (1982) states that Ca²⁺ is generally present in higher concentrations than Mg²⁺, the high exchangeable Mg²⁺ content of sample BS5 may once again be attributable to the presence of pyroxene ± olivine within the parent dolerite material. In contrast, the exchangeable acidity, which is a measure of the exchangeable concentrations of the acidic cations H⁺ and Al³⁺ on the surfaces of the soil solids (Thomas, 1982), is low. This is consistent with the near-neutral pH of the soil (Table 4.2).

The negligible concentrations of heavy metals within the saturated paste extract (Table 4.3), as compared to the total amounts measured by XRFs, indicate that their solubility in water, and therefore their mobility, is low. This is not surprising, considering the near-neutral pH of the saturated paste extract and the fact that the heavy metals are relatively immobile at pH >6 (McBride, 1994). The EC_e value is low, in terms of the range encountered for soils by Ayers and Westcot (1985), confirming that most ionic constituents are bound up in the soil in a relatively insoluble state and that the soil is non-saline.

The amount of As extracted from sample BS5 using the NaHCO₃ method of Olsen and Sommers (1982) constituted 2.7% of the total As concentration of the soil. This is comparable to the results obtained for the uncontaminated clay-textured sediment core samples (BS1A and BS1B) collected from Crystal Stream in the Barbrook tailings dam area (Chapter 3).

The concentrations of Na pyrophosphate- and CBD-extractable Fe and Al indicate that organically bound forms of these metals are negligible and that the free Fe and Al content of the Shortlands subsoil is relatively small, as compared with other soils derived from basic igneous rocks in subtropical weathering environments (Allen and Hajek, 1989). While the red colour of the Shortlands soil is indicative of the presence of hematite, XRD analysis also indicated the presence of some goethite (Table 4.4; Figure 4.1) in the clay fraction. However, the dominant clay mineral within the Shortlands soil is kaolinite, with goethite,

¹ Final report on the P sorption/fixation investigation on 50 selected soils and recommendation for further (routine) work on the remaining 4000 soils of the natural resources survey. *Unpublished Soil and Irrigation Research Institute Report.*

hematite, mica, quartz and an undifferentiated 2:1 layer silicate representing only minor constituents. The undifferentiated 2:1 layer silicate represented by peak 1 (d-spacing = 14.85 Å) could be chlorite, vermiculite or smectite. Unfortunately, an attempt to distinguish between these possibilities by saturating the phyllosilicate exchange sites with Mg prior to solvating with a 15% glycerol solution (Whittig and Allardice, 1986) was not successful due to the weakened intensity of reflections caused by glycerol solvation.

Table 4.3: Results of the various extraction procedures performed on the Shortlands subsoil.

Sample No.:	BS5
KCl extraction (cmol_c/kg):	
Acidity	0.03
Ca ²⁺	5.54
Mg ²⁺	11.5
Effective CEC	17.1
Saturated paste extract (mg/L):	
EC _e (mS/m)	4.92
pH	6.35
F ⁻	0.06
Cl ⁻	5.76
NO ₃ ⁻	7.54
SO ₄ ²⁻	1.79
Na ⁺	5.29
K ⁺	0.47
Ca ²⁺	1.34
Mg ²⁺	2.20
Zn	0.06
Pb	0.39
Co	0.06
Ni	0.14
Si	2.94
Mn	0.05
Fe	0.32
Cr	0.05
Al	0.34
Cu	0.05
CBD extraction (%):	
Fe	3.62
Al	0.17
Mn	0.10
Na pyrophosphate extraction (%):	
Fe	0.09
Al	0.13
NaHCO₃ extraction (mg/kg):	
As	0.56

Note: Effective CEC represents an estimate based on the sum of the KCl exchangeable acidity and base cation (Ca + Mg) concentrations, and was calculated according to the summation method of Rhoades (1982b).

The fact that the clay fraction of BS5 is dominated by kaolinite, a dioctahedral 1:1 phyllosilicate often found within highly weathered soils (Greenland and Hayes, 1978), has implications for both the exchange capacity of the soil and the BET specific surface area measurement. The limited isomorphous substitution which occurs within the crystal structure

Table 4.4: X-ray diffractometry results for the Shortlands soil sample BS5.

Peak No.	Mineral	d-spacing (Å)
1	Undifferentiated 2:1 layer silicate	14.85
2	Mica (10)	10.11
3	Kaolinite (10)	7.19
4	Chlorite (8) or mica (2-5)	4.97
5	Goethite (10)	4.18
6	Kaolinite (8) + chlorite (7-10)	3.57
7	Quartz (10) + mica (10)	3.34
8	Mica (10)	2.79
9	Hematite (7)	2.50
10	Goethite (6)	2.45
11	Kaolinite (6)	2.00

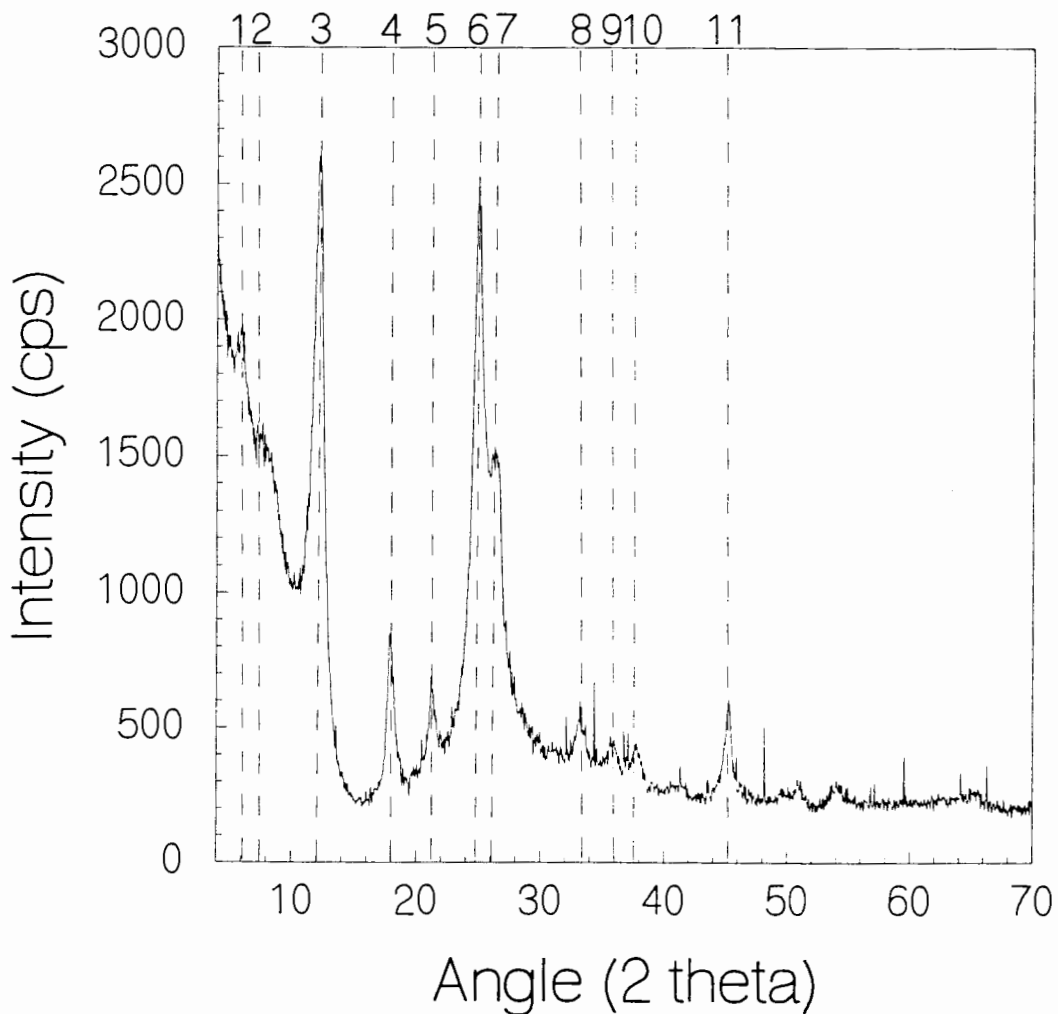


Figure 4.1: X-ray diffractometry pattern for the clay fraction of Shortlands soil sample BS5.

of kaolinite results in only a slight permanent negative surface charge and a low swelling propensity in water (Wild, 1993). In addition to the fact that these properties will result in limited contribution to the CEC of the soil, the predominance of kaolinite within the clay fraction of sample BS5 means that although the BET measurement of surface area relates specifically to external surface area only (Carter *et al.*, 1986), this value may actually be a good approximation of reactive surface area (Greenland and Mott, 1978) in this soil. Ultimately, the nature of the silicates in the clay fraction will play a subordinate role in terms of anion sorption due to the presence of Fe oxides (goethite and hematite) within the clay fraction of the Shortlands soil. This is a function of the high specific surface area of submicroscopic Fe oxide particles, such that they usually dominate the anion sorption behaviour of the soils in which they occur (Schwertmann and Taylor, 1989).

4.5.2 Phosphorus sorption

The results of the P sorption experiment are presented in Table 4.5. The pH values of the BS5 filtrates gradually increased with increasing P concentrations despite the corresponding increase in EC. The latter would normally result in a decreased pH for much the same reason that pH(KCl) is always less than pH(H₂O) in this soil. These trends are plotted in Figure 4.2 and provide a clear indication of the ligand exchange mechanism of P sorption whereby phosphate displaces hydroxyl ions from sorbing surfaces (Mott, 1988).

Table 4.5: Phosphorus sorption results for the Shortlands soil sample BS5.

Initial P (mg/L)	EC (mS/cm)	pH	Equilibrium P (mg/L)	Sorbed P (mg/kg soil)
0	9.23	5.46	0	0
0*	9.22	5.51	0	0
5	9.34	5.66	0	50
10	9.40	5.76	0	100
20	9.43	5.86	0	200
40	9.43	6.15	0.165	398
60	9.54	6.37	0.778	592
80	9.62	6.56	2.49	775
100	9.59	6.67	5.77	942
150	9.56	6.86	26.6	1234
200	9.72	7.03	55.2	1448
250	9.89	7.12	93.2	1568
250*	9.75	7.13	99.5	1505
300	9.93	7.21	134	1664
400	10.14	7.34	223	1770
500	10.51	7.43	317	1831
500*	10.40	7.44	286	2135

Note: * indicates a duplicate sample

The P sorption isotherm plotted in Figure 4.3 can be classified as a high affinity H-curve isotherm (Sposito, 1989), the best mathematical expression of which is provided by the Langmuir equation. This equation is expressed by Pierce and Moore (1982) as follows:

$$\Gamma_A = \frac{\Gamma_{A,max} C_{equil}}{(K_L + C_{equil})}$$

where Γ_A is the adsorption per unit mass adsorbent (sorbed P in mmol/kg), C_{equil} is the equilibrium concentration of P in solution (mmol/L), $\Gamma_{A,max}$ is maximum adsorption per unit mass adsorbent, and K_L is the Langmuir constant. A linear relationship is derived by plotting the equilibrium P concentration versus $K_d (= C_{equil} \text{ versus } \frac{C_{equil}}{\Gamma_A})$ (Figure 4.4a), using the data presented in Table 4.6. This indicates that P sorption by the Shortlands soil can be successfully described by the Langmuir equation, according to which the slope of the line in Figure 4.4a is equivalent to $\frac{1}{\Gamma_{A,max}}$ and the y-intercept is equivalent to $\frac{K_L}{\Gamma_{A,max}}$.

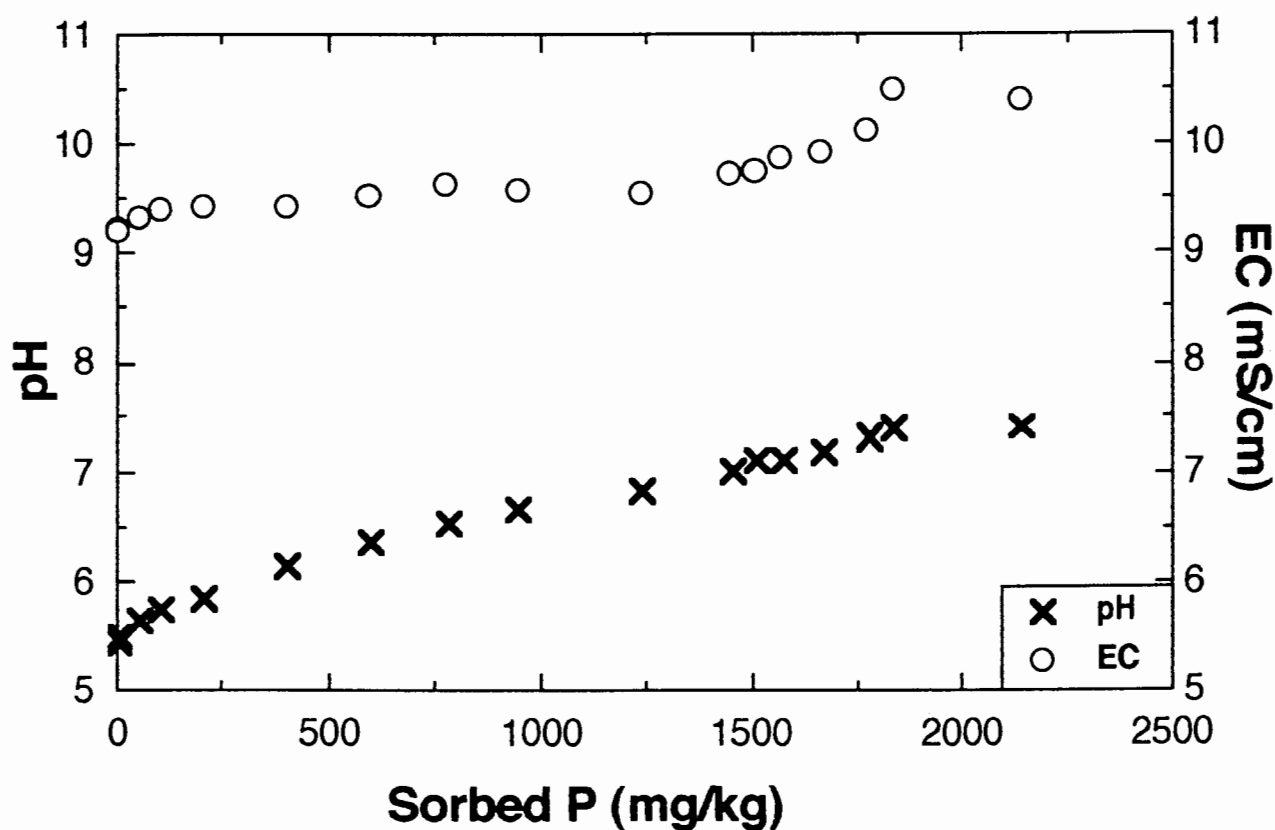


Figure 4.2: Plot of sorbed P (mg/kg soil) versus the pH and EC of each of the BS5 filtrates generated during the P sorption experiment.

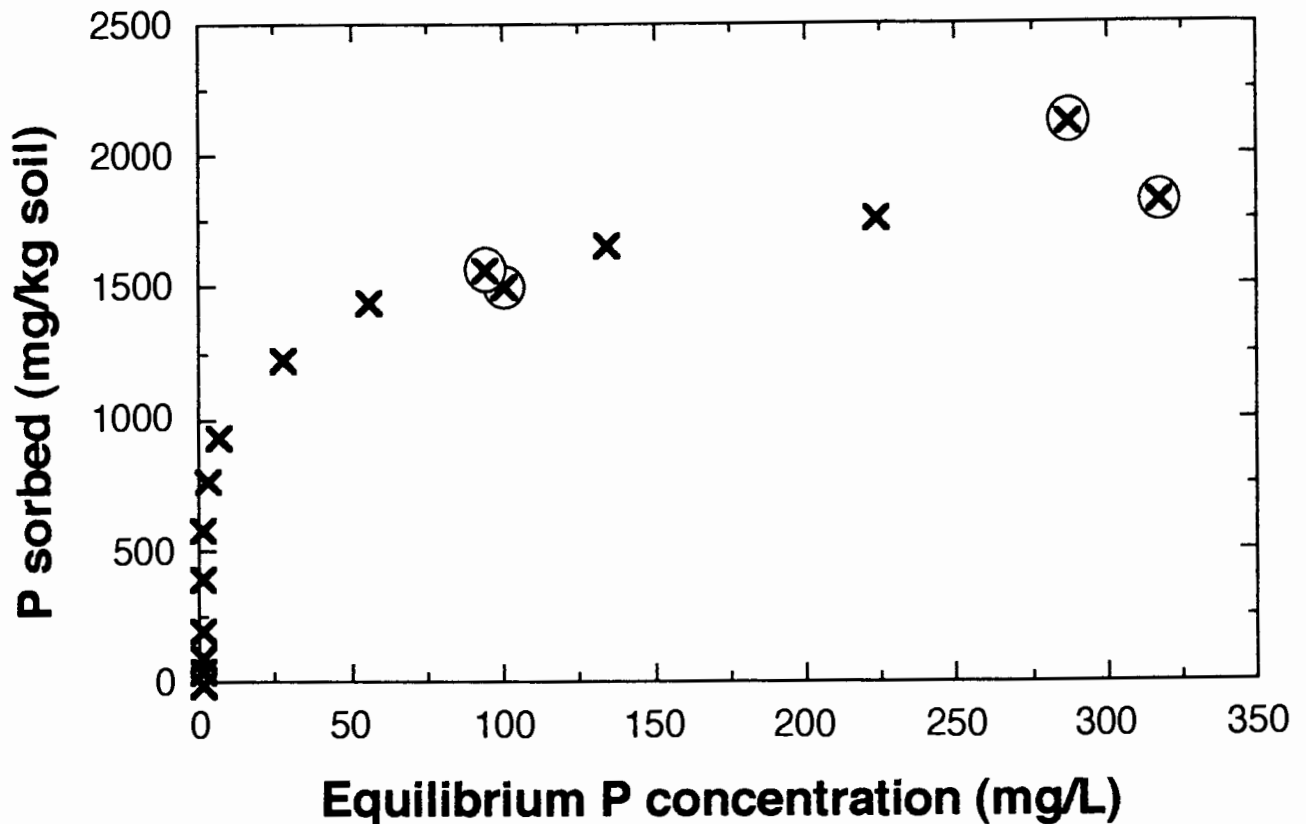


Figure 4.3: Phosphorus sorption curve determined for the Barbrook Shortlands soil sample BS5; circled values represent duplicate samples with initial P concentrations of 250 mg/L and 500 mg/L.

In addition to the Langmuir equation, the van Bemmelen-Freundlich isotherm equation has also been used to mathematically describe P sorption (Sposito, 1989):

$$q_i = A c_i^\beta$$

where q_i is surface excess of a chemical species (sorbed P in mmol/kg), c_i is the equilibrium concentration of P in solution (mmol/L) and A and β are positive-valued adjustable coefficients. A log plot of q_i versus c_i (Figure 4.4b) shows an excellent linear relationship, indicating that P sorption by the Shortlands soil at Barbrook is equally well described by the van Bemmelen-Freundlich isotherm equation. The slope of the line in Figure 4.4b is equivalent to $\log A$ in the equation and the y-intercept is equivalent to β .

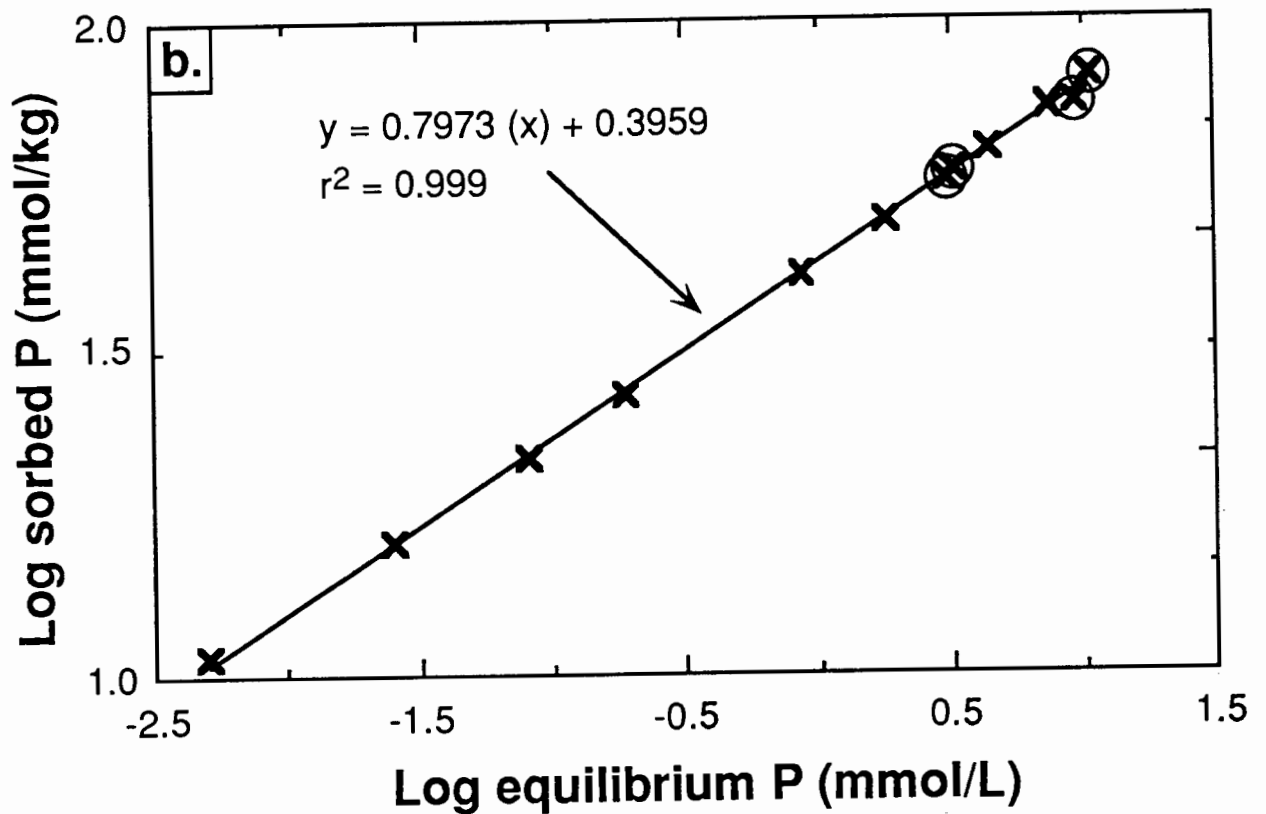
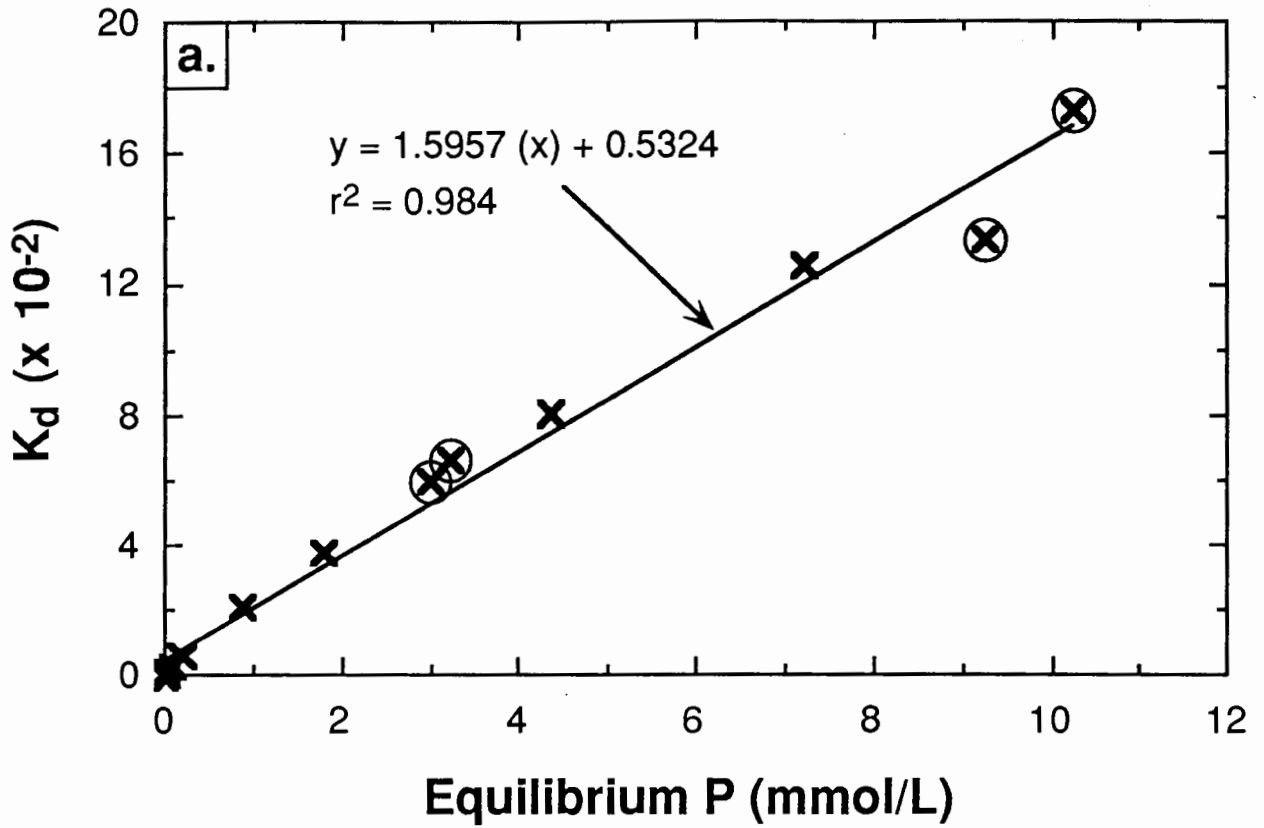


Figure 4.4: Linear expressions of the P sorption data derived for the Barbrook Shortlands soil sample BS5 according to **a)** the Langmuir equation, and **b)** the van Bemmelen-Freundlich equation. Circled values represent duplicate samples with initial P concentrations of 250 mg/L and 500 mg/L.

Table 4.6: Phosphorus sorption data converted from Table 4.5 for use in the Langmuir and van Bemmelen-Freundlich equations.

Initial P (mmol/L)	Equilibrium P (mmol/L)	Sorbed P (mmol/kg soil)	K_d ($\times 10^{-2}$)
0	0	0	0
0*	0	0	0
0.161	0	1.61	0
0.323	0	3.23	0
0.646	0	6.46	0
1.29	0.005	12.9	0.039
1.94	0.025	19.1	0.131
2.58	0.080	25.0	0.320
3.23	0.186	30.4	0.612
4.84	0.859	39.8	2.16
6.46	1.78	46.7	3.81
8.07	3.01	50.6	5.95
8.07*	3.21	48.6	6.60
9.69	4.33	53.7	8.06
12.9	7.20	57.1	12.6
16.1	10.23	59.1	17.3
16.1*	9.23	68.9	13.4

Note: * indicates a duplicate sample; $K_d = \frac{\text{equilibrium P}}{\text{sorbed P}}$ or $\frac{C_{\text{equil}}}{\Gamma_A}$

4.5.3 Arsenic sorption

The results of the As sorption experiment conducted on the Shortlands soil are presented in Table 4.7. Since sorption can be affected by changes in pH and ionic concentration, it was ensured that the 1209 mg/L As standard solution used throughout the As sorption experiment had virtually identical initial pH and EC values (pH = 8.94; EC = 11.19 mS/cm) to the standard solution using during the P sorption experiment. Consistent with the P sorption results, the pH and EC values obtained for the various filtrates are all lower than the starting values, and display a gradual increase with the increasing addition and sorption of As (Figure 4.5). Similar mechanisms to those detailed for the P sorption study are considered to be responsible.

Table 4.7: Arsenic sorption results for the Shortlands soil sample BS5.

Initial As (mg/L)	EC (mS/cm)	pH	Equilibrium As (mg/L)	Sorbed As (mg/kg soil)
0	9.14	5.99	0.036	0
43.38	9.19	6.16	0.072	433
96.75	9.34	6.63	0.764	960
145.1	9.27	6.88	4.25	1409
193.5	9.53	6.79	17.4	1761
241.9	9.59	6.84	32.8	2091
362.8	9.56	7.02	108	2544
483.8	9.81	7.14	217	2665
604.7	9.90	7.22	324	2810
725.7	9.95	7.29	428	2972
967.6	10.30	7.39	653	3143
1209	10.55	7.47	829	3807

Also consistent with the P sorption results, the As sorption data (Table 4.8) define a H-curve isotherm (Figure 4.6), which can be mathematically described by both the Langmuir and van Bemmelen-Freundlich equations (Figure 4.7).

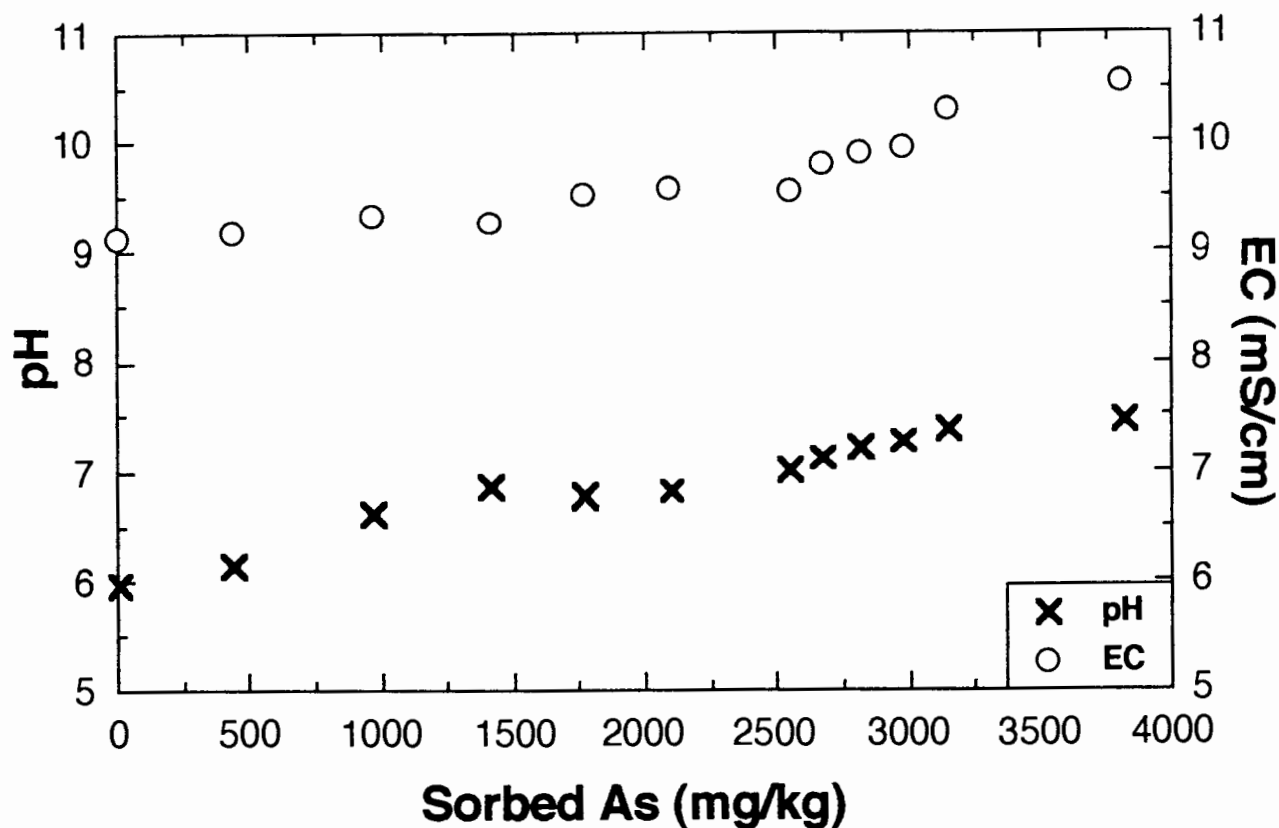


Figure 4.5: Plot of sorbed As (mg/kg soil) versus the pH and EC for each of the BS5 filtrates generated during the As sorption experiment.

4.5.4 Comparison and interpretation of arsenic and phosphorus sorption

The As and P sorption data derived for Shortlands soil sample BS5 describe similar H-curve isotherms (Figure 4.8), which represent extreme versions of the L-curve isotherm (Sposito, 1989; McBride, 1994) and can be mathematically described by either the Langmuir or the van Bemmelen-Freundlich isotherm equations. According to Sposito (1989), the large initial slope of the H-curve isotherm indicates that the soil has a very high affinity for the adsorbate, possibly due to inner sphere surface complexation or significant van der Waals interactions. The characteristic concave shapes of both the H- and L-curve isotherms are explained, however, by the fact that at low adsorbate concentrations, the soil has a high adsorptive capacity but as the concentration of the adsorbate in solution increases, the soil surfaces become swamped and the amount of adsorbing surface therefore decreases. McBride (1994) states that the success of the Langmuir equation in describing the P

sorption capacity of a soil means that phosphate solubility is controlled by the degree of saturation of limited sorption sites such that, as the soil approaches its saturation limit for adsorption, solubility will abruptly increase and anions are much more likely to be leached out of the soil. Mott (1988) describes the Freundlich expression as "being produced by a set of Langmuir sites with a log normal spread of energy levels".

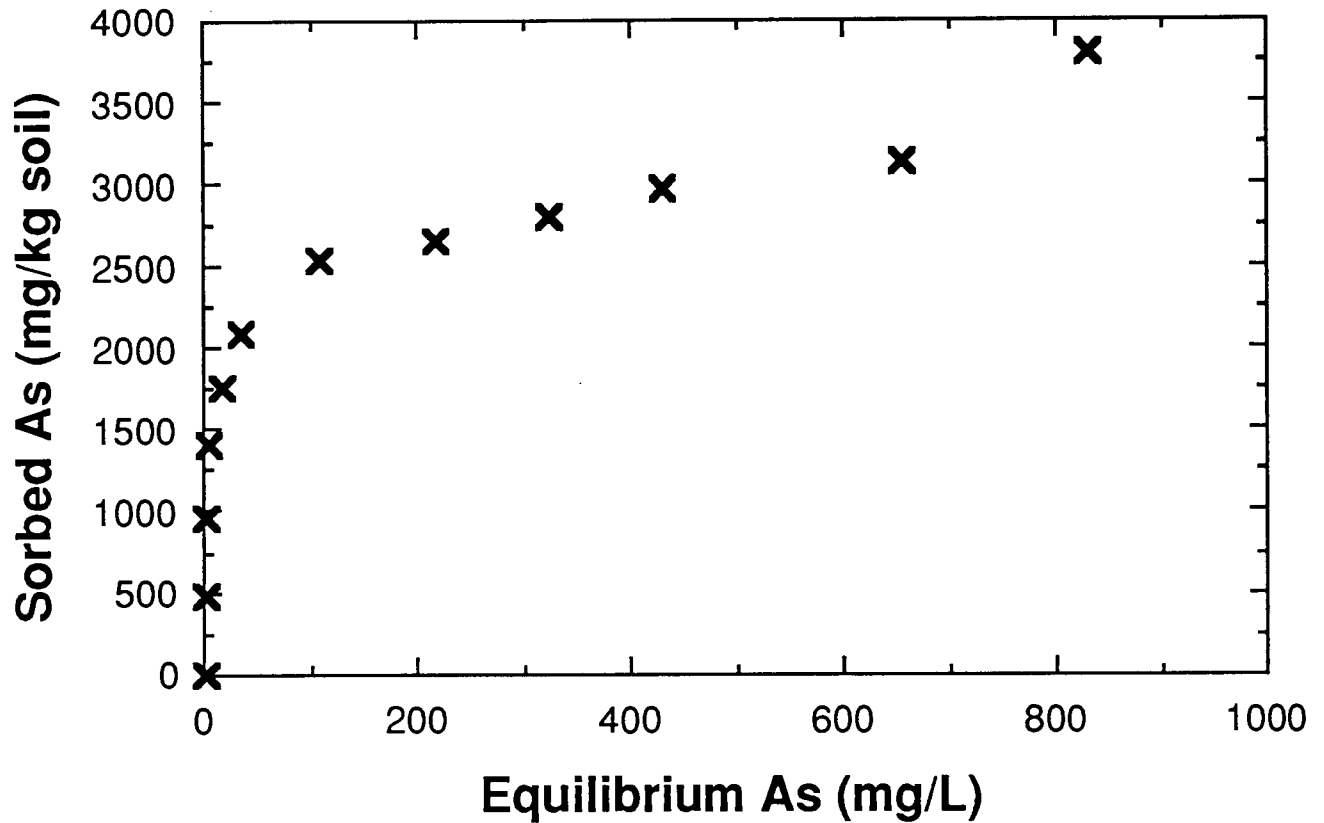


Figure 4.6: Arsenic sorption curve determined for the Barbrook Shortlands soil sample BS5.

Table 4.8: Arsenic sorption data converted from Table 4.7 for use in the Langmuir and van Bemmelen-Freundlich equations.

Initial As (mmol/L)	Equilibrium As (mmol/L)	Sorbed As (mmol/kg soil)	K_d ($\times 10^{-2}$)
0	0.0005	0	0
0.579	0.001	5.78	0.017
1.29	0.010	12.8	0.078
1.94	0.057	18.8	0.303
2.58	0.232	23.5	0.987
3.23	0.438	27.9	1.57
4.84	1.44	34.0	4.24
6.46	2.90	35.6	8.15
8.07	4.33	37.5	11.5
9.69	5.71	39.7	14.4
12.9	8.72	42.0	20.8
16.1	11.07	50.8	21.8

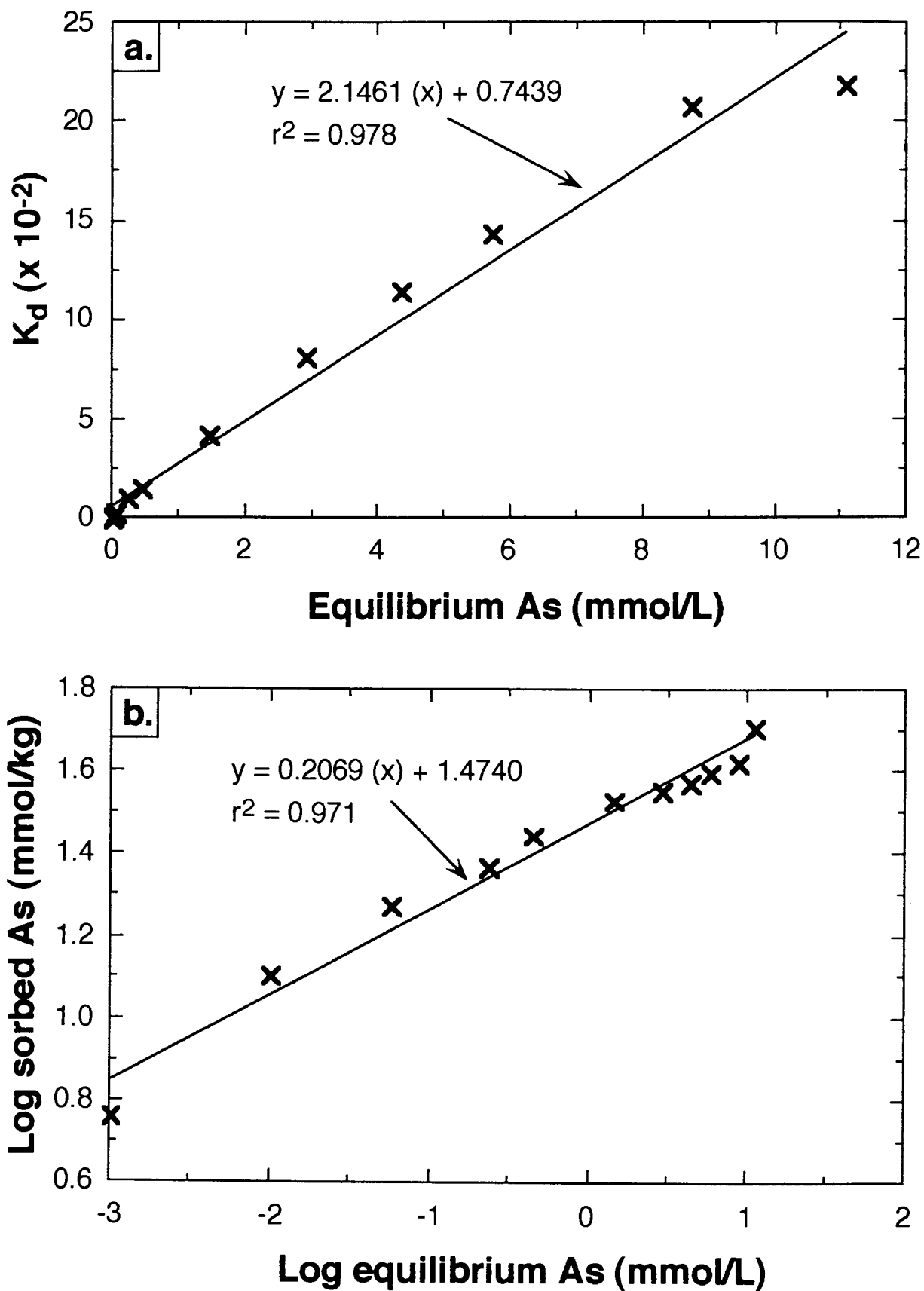


Figure 4.7: Linear expressions of the As sorption data derived for the Barbrook Shortlands soil sample BS5 according to a) the Langmuir equation, and b) the van Bemmelen-Freundlich equation.

The fact that the P sorption curve has a greater initial slope than the As sorption curve suggests that at low adsorbate concentrations, the adsorptive capacity of the Shortlands soil is greater for P than for As. MINTEQA2 modelling at pH 6, using equivalent equilibrium concentrations of As and P, entered as H_3AsO_4 and PO_4^{3-} , respectively, indicates that the different sorption behaviours exhibited in Figure 4.8 could well be a function of the relative speciation of the two elements in solution. The results of the MINTEQA2 modelling showed that, under the specified conditions, 92.5% of the P in solution would be present as the monovalent species H_2PO_4^- , whereas only 81.5% of the As would be in the monovalent state, as H_2AsO_4^- . The fact that the Shortlands soil is characterised by high effective CEC, confirmed by the markedly lower $\text{pH}(\text{KCl})$ than $\text{pH}(\text{H}_2\text{O})$ value, indicates that it has an overall negative charge. Therefore, any positive charge associated with sesquioxides, possibly occurring as surface coatings on other minerals, and/or protonated hydroxyl ions associated with phyllosilicate particle edges, is likely to be swamped by the overall negative charge. Since the resulting electrostatic repulsion of the As and P oxyanions from the surfaces of the soil solids would be greatest for the divalent ions, the presence of a greater proportion of monovalent ions for P, as compared to As, may be responsible for the enhanced P sorption at low adsorbate concentrations. In addition, the smaller size of the phosphate, as compared to arsenate, ions (Woolson and Kearney, 1973) means that a denser packing of phosphate ions around positively-charged surface sites may be possible.

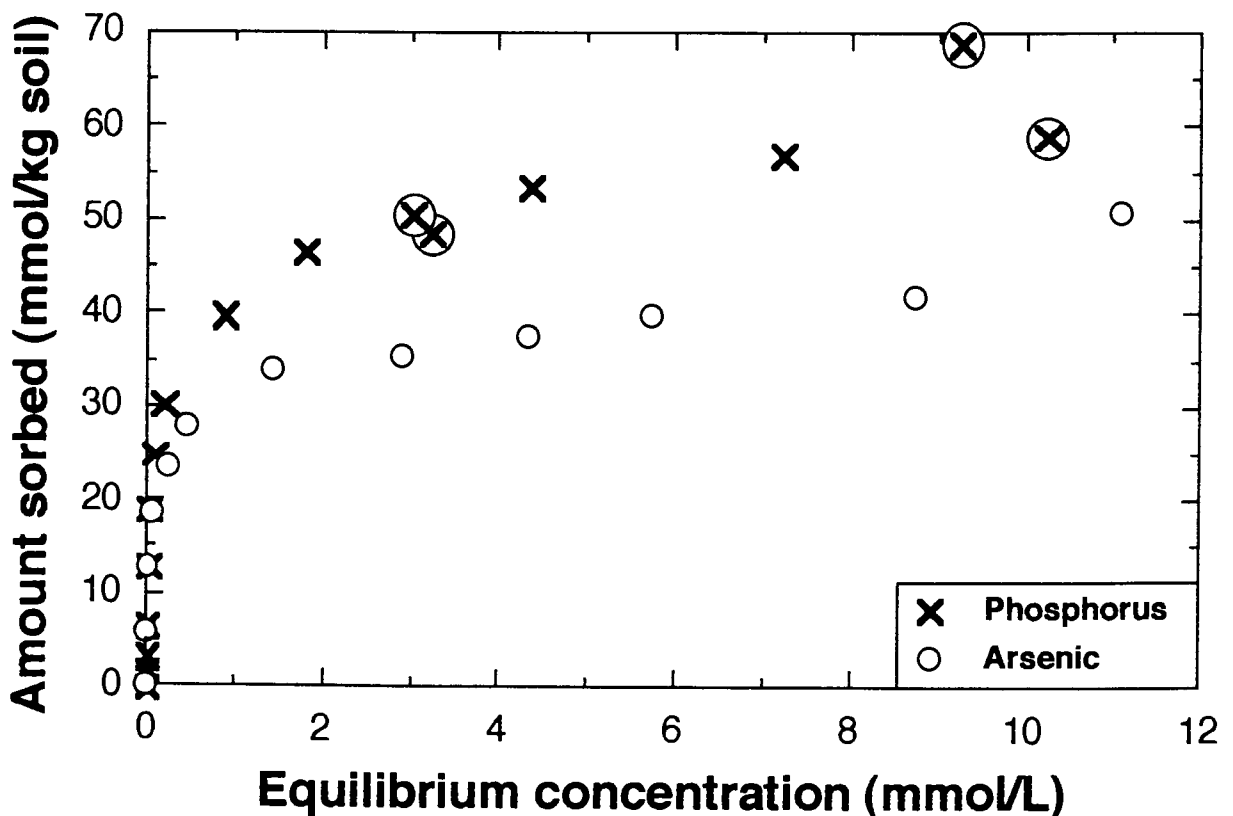


Figure 4.8: Phosphorus and arsenic sorption curves determined for the Barbrook Shortlands soil sample BS5; circled values represent duplicate samples with initial P concentrations of 250 mg/L and 500 mg/L.

It is difficult in a study such as this, whereby only one soil type has been examined, to establish which soil properties are actually controlling sorption. In an investigation into the As(III) sorption capacity of five different soil types, Elkhatib *et al.* (1984a) observed that whereas Fe oxide content was correlated with sorption at high initial As concentrations, total clay content was correlated with sorption at low initial concentrations. This implied that the phyllosilicate minerals within the clay fraction were involved in As sorption at low adsorbate concentrations. For kaolinite, high P adsorption at low concentrations has been related to the presence of two different types of sorption sites on the crystal structure, both of which differ energetically and correlate with different regions of an adsorption isotherm (Dixon, 1989). The first type, correlated with the steep initial slope of a P sorption isotherm, is a protonated hydroxyl site associated with Al at the edge of the octahedral sheets within the kaolinite crystal structure. These sites have a very high affinity for phosphate ions and result in largely irreversible sorption. Although the second type of sorption site, correlated with the point at which the sorption isotherm becomes convex to the y-axis, is also a protonated hydroxyl site, it is associated with Al at the exchange sites in kaolinite. Sorption at these sites is still high, but it is also reversible. The high clay content of the Shortlands soil, and its dominance by kaolinite, suggest that the high affinity of this soil for As and P at low initial concentrations could be, at least partly, related to the strong sorption associated with the kaolinite edge effects. In addition, the possible presence of chlorite within the clay fraction of this soil may also contribute to anion sorption, to a small extent, due to the presence of a positively-charged metal hydroxide sheet within the chlorite structure (McBride, 1994). The micas which form part of the clay fraction of sample BS5 could be expected to contribute very little to anion sorption since any positive charge is restricted to the broken O and OH bonds associated with crystal edges (Fanning *et al.*, 1989).

In a comparison of As sorption during the flooding of two different soil types, Onken and Hossner (1996) found that sorption was greater within the soil which had the higher clay and Fe oxide contents. The latter is often cited within the scientific literature as being largely responsible for As sorption in soils (Jacobs *et al.*, 1970; Pierce and Moore, 1982; Elkhatib *et al.*, 1984b; Sakata, 1987; Hunt and Howard, 1994). The Fe oxides in the Shortlands soil are therefore likely to have contributed substantially to both As and P sorption.

Le Mare (1981) discusses a number of studies in which the BET surface area of a range of soils was correlated with P sorption. However, the soil leaching experiments of Korte *et al.* (1976) indicated that the attenuation of elements present in their leachates as anions was more strongly correlated with Fe oxide content than with surface area. Korte *et al.* (1976) describe a Davidson soil from North Carolina, U.S.A. as containing a large (61%) clay fraction dominated by kaolinite, a surface area of $51.3\text{m}^2/\text{g}$ and 17% free Fe oxides. By comparison, the Shortlands subsoil has a higher clay content (65%), also dominated by kaolinite, a substantially lower free Fe oxide content (3.6%) and a greater specific surface area ($68\text{m}^2/\text{g}$). Therefore, the high surface area measured for the Shortlands soil may be largely a function of the phyllosilicate minerals. The fine-texture of the Shortlands soil

appears to be an important property in terms of sorption behaviour since As is reported to be more mobile, and therefore more easily extracted and potentially phytotoxic, in coarse-textured (sandy and loamy) soils as compared to fine-textured soils (Jacobs *et al.*, 1970; Korte *et al.*, 1976; Merwin *et al.*, 1994).

4.5.5 Implications for the mediation of As dispersion at Barbrook

The results of this study indicate that the As(V) sorption capacity of the Shortlands soil is particularly high at low concentrations, but is limited by the number of available sorption sites at higher As concentrations. The highest As value (4.12 mg/L) obtained for any of the Barbrook water bodies sampled during August 1996 was associated with the stream of tailings extending between the calcine dam and the main slimes dam (Chapter 3). Although the Shortlands soil is well equipped to mediate As dispersion at these concentrations, the continual exposure of the soil to As-bearing leachates from the tailings dams and waste rock pile mean that the sorption sites could eventually become saturated. Saturation of the sorption sites would enhance the possibility of As-bearing leachates reaching the groundwater.

McBride (1994) states that it is possible to estimate the loading capacity of a soil for a certain chemical once the sorption capacity of the soil is known. For the Shortlands soil at Barbrook, the maximum sorption of As per unit mass adsorbent ($\Gamma_{A,max}$) can be estimated from the slope of the line ($= \frac{1}{\Gamma_{A,max}}$) defined by the Langmuir equation (Figure 4.7a) as 3490 mg/kg. By comparison, the estimated loading capacity of this same soil for P is 1940 mg/kg. Although, at first glance, this seems contrary to the relative sorption results plotted in Figure 4.8 and interpreted as indicating a greater capacity for P sorption at high adsorbate concentrations, this is simply a function of the mass difference between P and As. Whereas sorption results expressed as mmol/kg provide information regarding the inherent chemical receptiveness of a soil for As versus P ions, the expression of the soil loading capacity in mg/kg relates to the relative maximum mass volumes of As and P that can be sorbed by the soil. According to McBride (1994), slow chemical reactions and diffusion processes within a soil can result in a regeneration of the sorption capacity of a soil with time. Therefore, the fact that the sorption capacity of a soil is not a temporally fixed parameter means that the mobility of a particular element can actually be overestimated, particularly when long time periods are involved.

The predominance of red clay-rich soils in the area covered by the Barbrook gold mine lease means that the estimation of the As loading capacity of the Shortlands soil may have implications for the environmental management of the Barbrook site. One implication of this work is that the Shortlands soil would be suitable for use in the attenuation of As-bearing wastes such that it could be used to line slimes dams or possible sites of waste spillage. For maximum advantage, the pH of any effluent to be disposed of on such soils should be

adjusted to ensure maximum As adsorption. The recognition of at least three other soil forms within the area covered by the Barbrook gold mine lease (Ralph Morris and Associates, 1996) means that this study can only be considered to represent a very preliminary investigation of the potential for As sorption by the local soils. However, the fact that the sorption behaviour of As and P within the Shortlands soil has proved to be quite similar means that information regarding P sorption in a range of other South African soils (Bainbridge *et al.*, 1995), including the Hutton, Glenrosa and Mispah forms found at Barbrook, can be used to estimate their As sorption capacity. Combining this information with detailed mapping of the distribution of the various soils in relation to the sites, such as the tailings dams and the waste rock pile, known to produce As-bearing leachates at Barbrook would then enable an estimation to be made regarding the potential for As dispersion through the soils and into the underlying groundwater.

Although phosphate is unlikely to be a problem in the Barbrook area, in terms of competition for soil sorption sites, the high sulphate concentrations within many of the Barbrook waters may provide some competition for the As anions. Xu *et al.* (1988) found that, at pH <7, the presence of relatively low concentrations of SO_4^{2-} caused a decrease in As(V) adsorption on alumina. As the concentration of SO_4^{2-} increased, however, the effect on As sorption became negligible, indicating that different sorption mechanisms were involved. Sulphate interference with As(V) adsorption on Fe and Al oxides has also been reported by Gustafsson and Jacks (1995).

The potential for the future formation of acid mine drainage in the Barbrook mining and tailings dams areas was discussed in Chapter 3. The fact that As(V) sorption by kaolinite, the dominant phyllosilicate mineral within the clay fraction of the Shortlands soil, peaks at a pH of 5 (Goldberg and Glaubig, 1988) and As(V) sorption by Fe and Al oxides and hydroxides reaches a maximum between pH 4 and 5 (Frost and Griffin, 1977; Pierce and Moore, 1982; Gosh and Yuan, 1987; O'Neill, 1995) could have implications for the mobility of arsenate species within such an acidic leachate. Although heavy metal mobility will increase with the onset of acidic conditions (McBride, 1994), the increased sorption of As(V) at lower pH values would decrease its mobility as long as sorption sites were available. In addition to enhanced adsorption with a slight reduction in pH, some precipitation/co-precipitation with Fe could further reduce As(V) mobility (Xu *et al.*, 1991). Although it is difficult to distinguish between the effects of adsorption and precipitation during sorption experiments, precipitation is more likely to occur and influence anion mobility at medium to high concentrations (McBride, 1994). If acid mine drainage does eventuate at Barbrook, further lowering of the pH to values less than pH 4 could be predicted to increase not only heavy metal solubility, but also the mobility of As(V).

4.6 Conclusions

An investigation into As dispersion in the area covered by the Barbrook gold mine lease (Chapter 3) has revealed that As-bearing leachates and bodies of standing water are present within both the mining and tailings dams area. The measured pH and Eh conditions of these waters suggest that inorganic As is dominated by As(V). Although the predominance of red clay-rich soils, such as the Shortlands form, within the Barbrook area may help to attenuate this As(V) dispersion into the local environment, its effectiveness will be dependent on a number of factors. Since pH is considered to be of primary importance in controlling As sorption by soil solids, the prevailing conditions at Barbrook and the way in which they change with time may greatly influence As mobility. Although the current near neutral to alkaline conditions associated with the Barbrook water bodies are more likely to favour As(III) sorption, the potential future formation of acid mine drainage and the accompanying initial reduction in pH is likely to favour As(V) sorption.

Although the P sorption capacity of a range of South African soils has already been established, there is a lack of published information regarding As sorption. Therefore, the characterisation of the Shortlands subsoil, in relation to its sorption capacity for both P and As, may provide reference data for future studies. In addition, the confirmation of reports in the scientific literature that the sorption behaviour of As is very similar to that of P may enable the As sorption and loading capacities of a range of South African soils to be predicted from the results of P sorption studies, such that appropriate soils can be used effectively in the attenuation of arsenical wastes.

REFERENCES

- Abdullah M.I., Shiyu Z. and Mosgren K. (1995) Arsenic and selenium species in the oxic and anoxic waters of the Oslofjord, Norway. *Marine Pollution Bulletin* **31**, 116-126.
- Abernathy C.O. and Ohanian E.V. (1992) Non-carcinogenic effects of inorganic arsenic. *Environmental Geochemistry and Health* **14**, 35-41.
- Aggett J. and Kriegman M.R. (1988) The extent of formation of arsenic(III) in sediment interstitial waters and its release to hypolimnetic waters in Lake Ohakuri. *Water Research* **22**, 407-411.
- Aggett J. and O'Brien G.A. (1985) Detailed model for the mobility of arsenic in lacustrine sediments based on measurements in Lake Ohakuri. *Environmental Science and Technology* **19**, 231-238.
- Ahmann D., Roberts A.L., Krumholz L.R. and Morel F.M.M. (1994) Microbe grows by reducing arsenic. *Nature* **371**, 750.
- Allen B.L. and Hajek B.F. (1989) Mineral occurrence in soil environments. In: Dixon J.B. and Weed S.B. (editors) *Minerals in Soil Environments* (2nd edition). Soil Science Society of America, Inc., U.S.A. p. 199-278.
- Anderson H.A., Berrow M.L., Farmer V.C., Hepburn A., Russell J.D. and Walker A.D. (1982) A reassessment of podzol formation processes. *Journal of Soil Science* **33**, 125-136.
- Anderson L.C.D. and Bruland K.W. (1991) Biogeochemistry of arsenic in natural waters: the importance of methylated species. *Environmental Science and Technology* **25**, 420-427.
- Arnold P.W. (1978) Surface-electrolyte interactions. In: Greenland D.J. and Hayes M.H.B. (editors) *The Chemistry of Soil Constituents*. John Wiley & Sons, Ltd. U.K. p. 355-404.
- Aurilio A.C., Durant J.L., Hemond H.F. and Knox M.L. (1995) Sources and distribution of arsenic in the Aberjona watershed, eastern Massachusetts. *Water, Air and Soil Pollution* **81**, 265-282.
- Aurilio A.C., Mason R.P. and Hemond H.F. (1994) Speciation and fate of arsenic in three lakes of the Aberjona watershed. *Environmental Science and Technology* **28**, 577-585.

- Ayers R.S. and Westcot D.W. (1985) *Water Quality for Agriculture*. United Nations Food and Agriculture Organisation Irrigation and Drainage paper 29 (Rev. 1). 174 p.
- Azcue J.M. and Nriagu J.O. (1995) Impact of abandoned mine tailings on the arsenic concentrations in Moira Lake, Ontario. *Journal of Geochemical Exploration* **52**, 81-89.
- Babb J.M., Enger S.K. and Pagenkopf G.K. (1985) Chemical changes in a receiving stream due to oxygenation and dilution of mine tailings seep waters. *Water, Air and Soil Pollution* **26**, 219-224.
- Bainbridge S.H., Miles, N. Praan R. and Johnston M.A. (1995) Phosphorus sorption in Natal soils. *South African Journal of Plant and Soil* **12**, 59-64.
- Baker D.E. and Senft J.P. (1995) Copper. In: Alloway B.J. (editor) *Heavy Metals in Soils* (2nd edition). Blackie Academic & Professional, U.K. p. 179-205.
- Barker D.S. (1983) *Igneous Rocks*. Prentice Hall Inc., U.S.A. 417 p.
- Baur W.H. and Onishi H. (1978) Arsenic. In: Wedepohl K.H. (editor) *Handbook of Geochemistry* (Vol. II/3). Springer Verlag, Germany.
- Birch G.F. (1981) The Karbonat-Bombe: a precise, rapid and cheap instrument for determining calcium carbonate in sediments and rocks. *Transactions of the Geological Society of South Africa* **84**, 199-203.
- Blakey N.C. (1984) Behavior of arsenical wastes co-disposed with domestic solid wastes. *Journal of the Water Pollution Control Federation* **56**, 69-75.
- Blowes D.W. and Ptacek C.J. (1994) Acid-neutralization mechanisms in inactive mine tailings. In: Jambor J.L. and Blowes D.W. (editors) *Short Course Handbook on Environmental Geochemistry of Sulphide Mine-Wastes*. Mineralogical Association of Canada, Waterloo, Ontario. p. 271-292.
- Bottomley D.J. (1984) Origins of some arseniferous groundwaters in Nova Scotia and New Brunswick, Canada. *Journal of Hydrology* **69**, 223-257.
- Bowell R.J. (1994) Sulphide oxidation and arsenic speciation in tropical soils. *Environmental Geochemistry and Health* **16**, 84.
- Bowell R.J., Morley N.H. and Din V.K. (1994) Arsenic speciation in soil porewaters from the Ashanti Mine, Ghana. *Applied Geochemistry* **9**, 15-22.
- Brannon J.R. and Patrick W.H. Jr. (1987) Fixation, transformation, and mobilization of arsenic in sediments. *Environmental Science and Technology* **21**, 450-459.

- Brown J.P. and Fan A.M. (1994) Arsenic: risk assessment for California drinking water standards. *Journal of Hazardous Materials* **39**, 149-159.
- Carter D.L., Mortland M.M. and Kemper W.D. (1986) Specific surface. In: Klute A. (editor) *Methods of Soil Analysis, Part 1. Physical and Mineralogical Methods* (2nd edition). Agronomy Monograph **9**, 413-423.
- Chapman J.T., Marchant P.B., Lawrence R.W. and Knopp R. (1993) Bio-oxidation of a refractory gold bearing high arsenic sulphide concentrate: A pilot study. *FEMS Microbiology Reviews* **11**, 243-252.
- Chatterjee A., Das D. and Chakraborti D. (1993) A study of ground water contamination by arsenic in the residential area of Behala, Calcutta due to industrial pollution. *Environmental Pollution* **80**, 57-65.
- Chatterjee A., Das D., Mandal B.K., Chowdhury T.R., Samanta G. and Chakraborti D. (1995) Arsenic in ground water in six districts of West Bengal, India: the biggest arsenic calamity in the world. Part 1. Arsenic species in drinking water and urine of the affected people. *Analyst* **120**, 643-650.
- Chen S.-L., Dzung S.R., Yang M.-H., Chiu K.-H., Shieh G.-M. and Wai C.M. (1994) Arsenic species in groundwaters of the blackfoot disease area, Taiwan. *Environmental Science and Technology* **28**, 877-881.
- Cheng R.C., Liang S., Wang H.-C. and Beuhler M.D. (1994) Enhanced coagulation for arsenic removal. *American Water Works Association Journal* **86**, 79-90.
- Dallas H.F. and Day J.A. (1993) *The Effect of Water Quality Variables on Riverine Ecosystems: A Review*. Water Research Commission, South Africa. 240 p.
- Das D., Chatterjee A., Mandal B.K., Samanta G., Chakraborti D. and Chanda B. (1995) Arsenic in ground water in six districts of West Bengal, India: the biggest arsenic calamity in the world. Part 2. Arsenic concentration in drinking water, hair, nails, urine, skin-scale and liver tissue (biopsy) of the affected people. *Analyst* **120**, 917-924.
- Das D., Chatterjee A., Samanta G., Mandal B., Chowdhury T.R., Samanta G., Chowdhury P.P., Chanda C., Basu G., Lodh D., Nandi S., Chakraborty T., Mandal S., Bhattacharya S.M. and Chakraborti D. (1994) Arsenic contamination in groundwater in six districts of West Bengal, India: the biggest arsenic calamity in the world. *Analyst* **119**, 168N-170N.
- Das D., Samanta G., Mandal B.K., Chowdhury T.R., Chanda C.R., Chowdhury P.P., Basu G.K. and Chakraborti D. (1996) Arsenic in groundwater in six districts of West Bengal, India. *Environmental Geochemistry and Health* **18**, 5-15.

- Davies B.E. (1995) Lead. In: Alloway B.J. (editor) *Heavy Metals in Soils* (2nd edition). Blackie Academic & Professional, U.K. p. 206-223.
- Davis A. and Ashenberg D. (1989) The aqueous geochemistry of the Berkeley Pit, Butte, Montana, U.S.A. *Applied Geochemistry* **4**, 23-36.
- Davis J.A. (1982) Adsorption of natural dissolved organic matter at the oxide/water interface. *Geochimica et Cosmochimica Acta* **46**, 2381-2393.
- Del Razo L.M., Arellano M.A. and Cebrian M.E. (1990) The oxidation states of arsenic in well-water from a chronic arsenicosis area of northern Mexico. *Environmental Pollution* **64**, 143-153.
- Deuel L.E. and Swoboda A.R. (1972) Arsenic solubility in a reduced environment. *Soil Science Society of America Proceedings* **36**, 276-278.
- Diamadopoulos E., Ioannidis S. and Sakellariopoulos G.P. (1993) As(V) removal from aqueous solutions by fly ash. *Water Research* **27**, 1773-1777.
- Diplock A.T. (1981) Metabolic and functional defects in selenium deficiency. *Philosophical Transactions of the Royal Society of London* **B294**, 105-117.
- Dixon J.B. (1989) Kaolin and serpentine group minerals. In: Dixon J.B. and Weed S.B. (editors) *Minerals in Soil Environments* (2nd edition). Soil Science Society of America, Inc., U.S.A. p. 467-526.
- Drever J.I. (1988) *The Geochemistry of Natural Waters* (2nd edition). Prentice Hall, U.S.A. 437 p.
- DWAF (1995a) *Crocodile River catchment, Eastern Transvaal: Water Quality Situation Assessment*. Department of Water Affairs and Forestry, Extended Executive Summary, 60 p.
- DWAF (1995b) *Draft of South African Water Quality Guidelines* (2nd edition). Vol. 1. *Domestic Use*. Department of Water Affairs and Forestry, Pretoria, South Africa.
- DWAF (1995c) *Draft of South African Water Quality Guidelines* (2nd edition). Vol. 5 *Agricultural Use: Irrigation*. Department of Water Affairs and Forestry, Pretoria, South Africa.
- DWAF (1995d) *Draft of South African Water Quality Guidelines* (2nd edition). Vol. 4 *Agricultural Use: Livestock Watering*. Department of Water Affairs and Forestry, Pretoria, South Africa.
- DWAF (1995e) *Draft of South African Water Quality Guidelines* (2nd edition). Vol. 3 *Industrial Use*. Department of Water Affairs and Forestry, Pretoria, South Africa.

- Edwards M. (1994) Chemistry of arsenic removal during coagulation and Fe-Mn oxidation. *American Water Works Association Journal* **86**, 64-78.
- Edwards R., Lepp N.W. and Jones K.C. (1995) Other less abundant elements of potential environmental significance. In: Alloway B.J. (editor) *Heavy Metals in Soils* (2nd edition). Blackie Academic & Professional, U.K. p. 306-352.
- Elkhatib E.A., Bennett O.L. and Wright R.J. (1984a) Kinetics of arsenite sorption in soils. *Soil Science Society of America Journal* **48**, 758-762.
- Elkhatib E.A., Bennett O.L. and Wright R.J. (1984b) Arsenite sorption and desorption in soils. *Soil Science Society of America Journal* **48**, 1025-1030.
- Emsley J. (1985) Whatever happened to arsenic? *New Scientist* **19**, 10-14.
- EPA (1991) *MINTEQA2/PRODEFA2, A Geochemical Assessment Model for Environmental Systems: Version 3.10 User's Manual*. United States Environmental Protection Agency, Government Printing Agency. 106 p.
- EPA (1993) Method 1311 Toxicity Characteristic Leaching Procedure (TCLP). In: *Identification and Listing of Hazardous Waste*. United States Environmental Protection Agency, Title 40 of the Code of Federal Regulations (CFR), Part 261, Appendix II. p. 66-82.
- Fanning D.S., Keramidas V.Z. and El-Desoky M.A. (1989) Micas. In: Dixon J.B. and Weed S.B. (editors) *Minerals in Soil Environments* (2nd edition). Soil Science Society of America, Inc., U.S.A. p. 551-634.
- Farmer J.G. and Lovell M.A. (1986) Natural enrichment of arsenic in Loch Lomond sediments. *Geochimica et Cosmochimica Acta* **50**, 2059-2067.
- Ferguson J.F. and Gavis J. (1972) A review of the arsenic cycle in natural waters. *Water Research* **6**, 1259-1274.
- Freeze R.A. and Cherry J.A. (1979) *Groundwater*. Prentice-Hall Inc., U.S.A. 604 p.
- Frost F., Frank D., Pierson K., Woodruff L., Raasina B., Davis R. and Davies J. (1993) A seasonal study of arsenic in groundwater, Snohomish County, Washington, USA. *Environmental Geochemistry and Health* **15**, 209-214.
- Frost R.R. and Griffin R.A. (1977) Effect of pH on adsorption of arsenic and selenium from landfill leachate by clay minerals. *Soil Science Society of America Journal* **41**, 53-57.
- Fuller C.C. and Davis J.A. (1989) Influence of coupling of sorption and photosynthetic processes on trace element cycles in natural waters. *Nature* **340**, 52-54.

Fuller C.C., Davis J.A. and Waychunas G.A. (1993) Surface chemistry of ferrihydrite: Part 2. Kinetics of arsenate adsorption and coprecipitation. *Geochimica et Cosmochimica Acta* **57**, 2271-2282.

Funke J.W. (1990) *The Water Requirements and Pollution Potential of South African Gold and Uranium Mines*. Water Research Commission Report No. KV 9/90, 172 p.

Garrels R.M. and Christ C.L. (1965) *Solutions, Minerals and Equilibria*. Freeman, Cooper & Company, U.S.A. 450 p.

Gee G.W. and Bauder J.W. (1986) Particle-size analysis. In: Klute A. (editor) *Methods of Soil Analysis, Part 1. Physical and Mineralogical Methods* (2nd edition). Agronomy Monograph **9**, 383-411.

Goldberg S. and Glaubig R.A. (1988) Anion sorption on a calcareous montmorillonitic soil - arsenic. *Soil Science Society of America Journal* **52**, 1297-1300.

Goldman M. and Dacre J.C. (1991) Inorganic arsenic compounds: are they carcinogenic, mutagenic, teratogenic? *Environmental Geochemistry and Health* **13**, 179-191.

Gosh M.M. and Yuan J.R. (1987) Adsorption of inorganic arsenic and organoarsenicals on hydrous oxides. *Environmental Progress* **6**, 150-157.

Greenland D.J. and Hayes M.H.B. (1978) Soils and soil chemistry. In: Greenland D.J. and Hayes M.H.B. (editors) *The Chemistry of Soil Constituents*. John Wiley & Sons, Ltd. U.K. p. 1-27.

Greenland D.J. and Mott C.J.B. (1978) Surfaces of soil particles. In: Greenland D.J. and Hayes M.H.B. (editors) *The Chemistry of Soil Constituents*. John Wiley & Sons, Ltd. U.K. p. 321-353.

Grimes D.J., Ficklin W.H., Meier A.L. and McHugh J.B. (1995) Anomalous gold, antimony, arsenic, and tungsten in ground water and alluvium around disseminated gold deposits along the Getchell Trend, Humboldt County, Nevada. *Journal of Geochemical Exploration* **52**, 351-371.

Gupta S.K. and Chen K.Y. (1978) Arsenic removal by adsorption. *Journal of the Water Pollution Control Federation* **50**, 493-506.

Gustafsson J.P. and Jacks G. (1995) Arsenic geochemistry in forested soil profiles as revealed by solid-phase studies. *Applied Geochemistry* **10**, 307-315.

Hammond A., Mast T.S. and Silver C.S. (1993) *The 1994 Information Please Environmental Almanac*. World Resources Institute, U.S.A. 704 p.

- Haswell S.J., O'Neill P. and Bancroft K.C.C. (1985) Arsenic speciation in soil-pore waters from mineralized and unmineralized areas of south-west England. *Talanta* **32**, 69-72.
- Hiroki M. (1993) Effect of arsenic pollution on soil microbial population. *Soil Science and Plant Nutrition* **39**, 227-235.
- Hiroki M. and Yoshiwara Y. (1993) Arsenic fungi isolated from arsenic-polluted soils. *Soil Science and Plant Nutrition* **39**, 237-243.
- Hopenhayn-Rich C., Smith A.H. and Goeden H.M. (1993) Human studies do not support the methylation threshold hypothesis for the toxicity of inorganic arsenic. *Environmental Research* **60**, 161-177.
- Horwitz W. and Albert R. (1993) Experience with the IUPAC - 1987 harmonized protocol for method-performance studies: suggestions for revision and application to internal quality control systems. In: Parkany M. (editor) *Quality Assurance for Analytical Laboratories*. The Royal Society of Chemistry Special Publication No. 130, p. 80-95.
- Houstoun S. (1990) *Controls on Gold Deposition at the Barbrook Mining Centre, Barberton Greenstone Belt, South Africa*. Unpublished PhD. thesis, University of Western Australia.
- Hunt L.E. and Howard A.G. (1994) Arsenic speciation and distribution in the Carnon Estuary following the acute discharge of contaminated water from a disused mine. *Marine Pollution Bulletin* **28**, 33-38.
- Irgolic K. (1986) Arsenic in the environment. In: Xavier A.V. (editor) *Frontiers in Bioinorganic Chemistry*. VCH Publishers, U.S.A. p. 399-408.
- Jackson T.A. and Bistricki T. (1995) Selective scavenging of copper, zinc, lead and arsenic by iron and manganese oxyhydroxide coatings on plankton in lakes polluted with mine and smelter wastes: results of energy dispersive X-ray micro-analysis. *Journal of Geochemical Exploration* **52**, 97-125.
- Jacobs L.W., Syers J.K. and Keeney D.R. (1970) Arsenic sorption by soils. *Soil Science Society of America Journal* **34**, 750-754.
- Jambor J.L. (1994) Mineralogy of sulphide-rich tailings and their oxidation products. In: Jambor J.L. and Blowes D.W. (editors) *Short Course Handbook on Environmental Geochemistry of Sulphide Mine-Wastes*. Mineralogical Association of Canada, Waterloo, Ontario. p. 59-102.
- Johnston S.E. and Barnard W.M. (1979) Comparative effectiveness of fourteen solutions for extracting arsenic from four western New York soils. *Soil Science Society of America Journal* **43**, 304-308.

Kavanagh P.J., Farago M.E., Thornton I., Fernandes S.C. and Freire I. (1996) Arsenic, antimony and bismuth concentrations in soils of the Tamar Valley area, south west England. *Society for Environmental Geochemistry and Health 14th European conference*, London (abstract), p. 47.

Kiekens L. (1995) Zinc. In: Alloway B.J. (editor) *Heavy Metals in Soils* (2nd edition). Blackie Academic & Professional, U.K. p. 284-305.

Korte N.E., Skopp J., Fuller W.H., Niebla E.E. and Alesii B.A. (1976) Trace element movement in soils: influence of soil physical and chemical properties. *Soil Science* **122**, 350-359.

Lajunen L.H.J. (1992) *Spectrochemical Analysis by Atomic Absorption and Emission*. The Royal Society of Chemistry, U.K. 241 p.

LaPerriere J.D., Wagener S.M. and Bjerklie D.M. (1985) Gold-mining effects on heavy metals in streams, Circle Quadrangle, Alaska. *Water Resources Bulletin* **21**, 245-252.

Le Mare P.H. (1981) Phosphorus sorption and release. In: Greenland D.J. (editor) *Characterization of Soils*. Oxford University Press, U.K. p. 97-134.

Le S.X.C., Cullen W.R. and Reimer K.J. (1994) Speciation of arsenic compounds in some marine organisms. *Environmental Science and Technology* **28**, 1598-1604.

Li X. and Thornton I. (1993) Arsenic, antimony and bismuth in soil and pasture herbage in some old metalliferous mining areas in England. *Environmental Geochemistry and Health* **15**, 135-144.

Lin S.M. and Yang M.H. (1988) Arsenic, selenium, and zinc in patients with Blackfoot disease. *Biological Trace Element Research* **15**, 213-221.

Lin T.-H., Huang Y.-L. and Tseng W.-C. (1995) Arsenic and lipid peroxidation in patients with blackfoot disease. *Bulletin of Environmental Contamination and Toxicology* **54**, 488-493.

Loring D.H., Næs K., Dahle S., Matishov G.G. and Illin G. (1995) Arsenic, trace metals, and organic micro contaminants in sediments from the Pechora Sea, Russia. *Marine Geology* **128**, 153-167.

Marin A.R., Masscheleyn P.H. and Patrick W.H. Jr. (1993) Soil redox-pH stability of arsenic species and its influence on arsenic uptake by rice. *Plant and Soil* **152**, 245-253.

Mass M.J. (1992) Human carcinogenesis by arsenic. *Environmental Geochemistry and Health* **14**, 49-54.

Masscheleyn P.H., Delaune R.D. and Patrick W.H. Jr. (1991) Effect of redox potential and pH on arsenic speciation and solubility in a contaminated soil. *Environmental Science and Technology* **25**, 1414-1419.

Matisoff G., Khourey C.J., Hall J.F., Varnes A.W. and Strain W.H. (1982) The nature and source of arsenic in northeastern Ohio groundwater. *Ground Water* **20**, 446-456.

McBride M.B. (1994) *Environmental Chemistry of Soils*. Oxford University Press Inc., New York. 406 p.

McCaffrey L.P. (1996) *Distribution and Causes of High Fluoride Groundwater in the Western Bushveld Area of South Africa*. Unpublished PhD. thesis, University of Cape Town.

McGrath S.P. (1995) Chromium and nickel. In: Alloway B.J. (editor) *Heavy Metals in Soils* (2nd edition). Blackie Academic & Professional, U.K. p. 152-178.

McKinney J.D. (1992) Metabolism and disposition of inorganic arsenic in laboratory animals and humans. *Environmental Geochemistry and Health* **14**, 43-48.

McLaren S.J. and Kim N.D. (1995) Evidence for a seasonal fluctuation of arsenic in New Zealand's longest river and the effect of treatment on concentrations in drinking water. *Environmental Pollution* **90**, 67-73.

McLean E.O. (1982) Soil pH and lime requirement. In: Page A.L., Miller R.H. and Keeney D.R. (editors) *Methods of Soil Analysis, Part 2. Chemical and Microbiological Properties* (2nd edition). Agronomy Monograph **9**, 199-224.

McNeill L.S. and Edwards M. (1995) Soluble arsenic removal at water treatment plants. *American Water Works Association Journal* **87**, 105-113.

Merwin I., Pruyne P.Y., Ebel J.G.Jr., Manzell K.L. and Lisk D.J. (1994) Persistence, phytotoxicity, and management of arsenic, lead and mercury residues in old orchard soils of New York state. *Chemosphere* **29**, 1361-1367.

Mitchell P. and Barr D. (1995) The nature and significance of public exposure to arsenic: a review of its relevance to South West England. *Environmental Geochemistry and Health* **17**, 57-82.

Mitchell R.L. (1964) Trace elements in soil. In: Bear F.E. (editor) *Chemistry of the Soil*. Reinhold Publications Corporation, New York. p. 320-368.

Mok W.-M. and Wai C.M. (1990) Distribution and mobilization of arsenic and antimony species in the Coeur D'Alene River, Idaho. *Environmental Science and Technology* **24**, 102-108.

- Moore J.N., Ficklin W.H. and Johns C. (1988) Partitioning of arsenic and metals in reducing sulfidic sediments. *Environmental Science and Technology* **22**, 432-437.
- Mott C.J.B. (1988) Surface chemistry of soil particles. In: Wild A. (editor) *Russell's Soil Conditions and Plant Growth*. Longman Scientific and Technical, U.K. p. 239-281.
- Munsell (1992) *Soil Colour Charts* (revised edition). Macbeth Division of Kollmorgen Instruments Corp., New York.
- Murphy J. and Riley J. (1962) A modified single solution method for the determination of phosphate in natural waters. *Analytica Chimica Acta* **27**, 31-36.
- Murray K. and Wade P. (1996) Checking anion-cation balance of water quality analyses: limitations of the traditional method for non-potable waters. *Water SA* **22**, 27-32.
- Nelson D.W. and Sommers L.E. (1982) Total carbon, organic carbon, and organic matter. In: Page A.L., Miller R.H. and Keeney D.R. (editors) *Methods of Soil Analysis, Part 2. Chemical and Microbiological Properties* (2nd edition). Agronomy Monograph **9**, 539-579.
- Newman A. (1995) Microbe thrives on arsenic. *Environmental Science and Technology* **29**, 70A.
- Nicholson K. and Duff E.J. (1981) Rapid sample pre-treatment for removal of aluminium from aqueous solutions prior to fluoride determination using a fluoride-selective electrode. *Analyst* **106**, 904-906.
- Non-Affiliated Soil Analysis Work Committee (1990) *Handbook of standard soil testing methods for advisory purposes*. Soil Science Society of South Africa.
- Norrish K. and Chappell B. W. (1977) X-ray fluorescence spectrometry. In: Zussman J. (editor) *Physical Methods in Determinative Mineralogy* (2nd edition). Academic Press, London, p. 254-272.
- Norrish K. and Hutton J. T. (1969) An accurate X-ray spectrographic method for analysis of a wide range of geological samples. *Geochimica et Cosmochimica Acta* **33**, 431-454.
- O'Neill P. (1995) Arsenic. In: Alloway B.J. (editor) *Heavy Metals in Soils* (2nd edition). Blackie Academic & Professional, U.K. p. 105-121.
- Ohlendorf H.M. (1989) Bioaccumulation and effects of selenium in wildlife. In: Jacobs L.W. (editor) *Selenium in Agriculture and the Environment*. *Soil Science Society of America Special Publication* **23**, 133-177.

Olsen S.R. and Sommers L.E. (1982) Phosphorus. In: Page A.L., Miller R.H. and Keeney D.R. (editors) *Methods of Soil Analysis, Part 2. Chemical and Microbiological Properties* (2nd edition). Agronomy Monograph **9**, 403-430.

Onken B.M. and Hossner L.R. (1995) Heavy metals in the environment: Plant uptake and determination of arsenic species in soil solution under flooded conditions. *Journal of Environmental Quality* **24**, 373-381.

Onken B.M. and Hossner L.R. (1996) Determination of arsenic species in soil solution under flooded conditions. *Soil Science Society of America Journal* **60**, 1385-1392.

Otte M.L., Kearns C.C. and Doyle M.O. (1995) Accumulation of arsenic and zinc in the rhizosphere of wetland plants. *Bulletin of Environmental Contamination and Toxicology* **55**, 154-161.

Palache C., Berman H. and Frondel C. (1944) *Dana's System of Mineralogy* (7th edition). Volume 1. John Wiley and Sons, U.S.A. 834 p.

Peng F.F. and Di P. (1994) Removal of arsenic from aqueous solution by adsorbing colloid flotation. *Industrial Engineering Chemical Research* **33**, 922-928.

Peryea F.J. (1991) Phosphate-induced release of arsenic from soils contaminated with lead arsenate. *Soil Science Society of America Journal* **55**, 1301-1306.

Pierce M.L. and Moore C.B. (1982) Adsorption of arsenite and arsenate on amorphous iron hydroxide. *Water Research* **16**, 1247-1253.

Pierzynski G.M., Sims J.T. and Vance G.F. (1994) *Soils and Environmental Quality*. CRC Press Inc., U.S.A. 313 p.

Pontius F.W., Brown K.G. and Chen C.-J. (1994) Health implications of arsenic in drinking water. *American Water Works Association Journal* **86**, 52-63.

Potts P.J. (1987) *A Handbook of Silicate Rock Analysis*. Blackie & Son Ltd., U.K. 622p.

Quastel J.H. and Scholefield P.G. (1953) Arsenite oxidation in soils. *Soil Science* **75**, 279-285.

Ralph Morris and Associates (1996) *Barbrook Mines Limited Environmental Management Programme Report*.

Rampe J.J. and Runnells D.D. (1989) Contamination of water and sediment in a desert stream by metals from an abandoned gold mine and mill, Eureka district, Arizona, U.S.A. *Applied Geochemistry* **4**, 445-454.

- Reuther R. (1992) Geochemical mobility of arsenic in a flowthrough water-sediment system. *Environmental Technology* **13**, 813-823.
- Rhoades J.D. (1982a) Soluble salts. In: Page A.L., Miller R.H. and Keeney D.R. (editors) *Methods of Soil Analysis, Part 2. Chemical and Microbiological Properties* (2nd edition). Agronomy Monograph **9**, 167-179.
- Rhoades J.D. (1982b) Cation exchange capacity. In: Page A.L., Miller R.H. and Keeney D.R. (editors) *Methods of Soil Analysis, Part 2. Chemical and Microbiological Properties* (2nd edition). Agronomy Monograph **9**, 149-165.
- Ripley E.A., Redmann R.E. and Crowder A.A. (1996) *Environmental Effects of Mining*. St. Lucie Press, Florida, U.S.A. 356 p.
- Rotruck J.T., Pope A.L., Ganther H.E., Swanson A.B., Hafeman D.G. and Hoekstra W.G. (1973) Selenium: Biochemical role as a component of glutathione peroxidase. *Science* **179**, 588-590.
- Rowell D.L. (1988) Soil acidity and alkalinity. In: Wild A. (editor) *Russell's Soil Conditions and Plant Growth*. Longman Scientific and Technical, U.K. p. 844-898.
- Sadiq M., Zaidi T.H. and Mian A.A. (1983) Environmental behaviour of arsenic in soils: theoretical. *Water, Air and Soil Pollution* **20**, 369-377.
- Sadler R., Olszowy H., Shaw G., Biltoft R. and Connell D. (1994) Soil and water contamination by arsenic from a tannery waste. *Water, Air and Soil Pollution* **78**, 189-198.
- Sakata M. (1987) Relationship between adsorption of arsenic (III) and boron by soil and soil properties. *Environmental Science and Technology* **21**, 1126-1130.
- Schlesinger W.H. (1991) *Biogeochemistry. An Analysis of Global Change*. Academic Press, Inc. U.S.A. 443 p.
- Schloemann H. (1994) *The Geochemistry of Some Common Western Cape Soils (South Africa) with Emphasis on Toxic and Essential Elements*. Unpublished PhD. thesis, University of Cape Town.
- Schollenberger C.J. (1927) A rapid approximate method for determining soil organic matter. *Soil Science* **24**, 65-68.
- Schroeder H.A. and Balassa J.B. (1966) Abnormal trace elements in man: arsenic. *Journal of Chronic Diseases* **19**, 85-106.

Schwertmann U. and Taylor R.M. (1989) Iron oxides. In: Dixon J.B. and Weed S.B. (editors) *Minerals in Soil Environments* (2nd edition). Soil Science Society of America, Inc., U.S.A. p. 379-438.

Scott K.N., Green J.F., Do H.D. and McLean S.J. (1995) Arsenic removal by coagulation. *American Water Works Association Journal* **87**, 114-126.

Seyler P. and Martin J.-M. (1989) Biogeochemical processes affecting arsenic species distribution in a permanently stratified lake. *Environmental Science and Technology* **23**, 1258-1263.

Sheppard S.C. (1992) Summary of phytotoxic levels of soil arsenic. *Water, Air and Soil Pollution* **64**, 539-550.

SIRI (1991) A procedure for describing soil profiles. *Soil and Irrigation Research Institute Report No. GB/A/91/67*, 20 p.

Smith A. (1994) The geochemistry of cyanide in mill tailings In: Jambor J.L. and Blowes D.W. (editors) *Short Course Handbook on Environmental Geochemistry of Sulphide Mine-Wastes*. Mineralogical Association of Canada, Waterloo, Ontario. p. 293-332.

Smith K.A. and Paterson J.E. (1995) Manganese and cobalt. In: Alloway B.J. (editor) *Heavy Metals in Soils* (2nd edition). Blackie Academic & Professional, U.K. p. 224-244.

Smith K.S., Ficklin W.H., Plumlee G.S. and Meier A.L. (1992) Metal and arsenic partitioning between water and suspended sediment at mine-drainage sites in diverse geologic settings. In: Kharaka Y.K. and Maest A.S. (editors) *Water-Rock Interaction*. AA Balkema, Rotterdam. p. 443-447.

Soil Classification Working Group (1991) *Soil Classification. A Taxonomic System for South Africa*. Memoirs on the Agricultural Natural Resources of South Africa No. 15.

Spliethoff H.M., Mason R.P. and Hemond H.F. (1995) Interannual variability in the speciation and mobility of arsenic in a dimictic lake. *Environmental Science and Technology* **29**, 2157-2161.

Sposito G. (1989) *The Chemistry of Soils*. Oxford University Press Inc., New York. 277 p.

Standard Methods (1985) *Standard Methods for the Examination of Water and Wastewater* (16th edition). American Public Health Association, Washington D.C. 1268 p.

Stone R. (1994) Trail of toxins leads through conference rooms in Dallas. *Science* **264**, 204.

- Sullivan K.A. and Aller R.C. (1996) Diagenetic cycling of arsenic in Amazon shelf sediments. *Geochimica et Cosmochimica Acta* **60**, 1465-1477.
- Takamatsu T., Aoki H. and Yoshida T. (1982) Determination of arsenate, arsenite, monomethylarsonate and dimethylarsinate in soil polluted with arsenic. *Soil Science* **133**, 239-246.
- Thomas D.J. (1994) Arsenic toxicity in humans: research problems and prospects. *Environmental Geochemistry and Health* **16**, 107-111.
- Thomas G.W. (1982) Exchangeable cations. In: Page A.L., Miller R.H. and Keeney D.R. (editors) *Methods of Soil Analysis, Part 2. Chemical and Microbiological Properties* (2nd edition). Agronomy Monograph **9**, 159-165.
- Thompson D.J. (1993) A chemical hypothesis for arsenic methylation in mammals. *Chemical-Biological Interactions* **88**, 89-114.
- Underwood E.J. (1977) *Trace Elements in Human and Animal Nutrition* (4th edition). Academic Press Inc., New York. 545 p.
- Uthus E.O. (1992) Evidence for arsenic essentiality. *Environmental Geochemistry and Health* **14**, 55-58.
- Van Loon J.C. and Barefoot R.R. (1995) Trends and developments. In: Ure A.M. and Davidson C.M. (editors) *Chemical Speciation in the Environment*. Blackie Academic & Professional, U.K. p. 335-388.
- Varsányi I., Fodré Z. and Bartha A. (1991) Arsenic in drinking water and mortality in the Southern Great Plain, Hungary. *Environmental Geochemistry and Health* **13**, 14-22.
- Voigt D.E., Brantley S.L. and Hennessey J.-C. (1996) Chemical fixation of arsenic in contaminated soils. *Applied Geochemistry* **11**, 633-643.
- Walkley A. and Black I.A. (1934) An examination of the Degtjareff method for determining soil organic matter and a proposed modification of the chromic acid titration method. *Soil Science* **37**, 29-38.
- Whittig L.D. and Allardice W.R. (1986) X-ray diffraction techniques. In: Klute A. (editor) *Methods of Soil Analysis, Part 1. Physical and Mineralogical Methods* (2nd edition). Agronomy Monograph **9**, 331-362.
- WHO (1983) *27th Report of the Joint FAO/WHO Expert Committee on Food Additives*. World Health Organisation, Geneva, Switzerland.

WHO (1984) *Guidelines for Drinking Water Quality, Vol. 1. Recommendations*. World Health Organisation, Geneva, Switzerland.

WHO (1993) *Guidelines for Drinking Water Quality, Vol. 2. Health Criteria and Other Supporting Information*. World Health Organisation, Geneva, Switzerland.

Widerlund A. and Ingri J. (1995) Early diagenesis of arsenic in sediments of the Kalix River estuary, northern Sweden. *Chemical Geology* **125**, 185-196.

Wild A. (1993) *Soils and the Environment: An Introduction*. Cambridge University Press, U.K. 287 p.

Willis J.P. (1996) Instrumental parameters and data quality for routine major and trace element determinations by WDXRFS. *Department of Geological Sciences, University of Cape Town Information Circular No. 14*.

Wilson F.H. and Hawkins D.B. (1978) Arsenic in streams, stream sediments, and ground water, Fairbanks area, Alaska. *Environmental Geology* **2**, 195-202.

Woolson E.A. and Kearney P.C. (1973) Persistence and reactions of ¹⁴C-cacodylic acid in soils. *Environmental Science and Technology* **7**, 47-50.

Xu H., Allard B. and Grimvall A. (1988) Influence of pH and organic substance on the adsorption of As(V) on geologic materials. *Water, Air and Soil Pollution* **40**, 293-305.

Xu H., Allard B. and Grimvall A. (1991) Effects of acidification and natural organic materials on the mobility of arsenic in the environment. *Water, Air and Soil Pollution* **57-58**, 269-278.

APPENDIX 1

Analytical methods used for the Barbrook water samples

A1.1 Electrical conductivity (EC)

The electrical conductivity of each water sample was determined using a CRISON microCM 2201 conductivity meter. The meter comprises a conductivity cell (cell constant: $C = 1.03/\text{cm}$) and a temperature probe, the latter to provide automatic temperature compensation. Electrical conductivity standards (12.88 mS/cm and 1433 $\mu\text{S}/\text{cm}$ at 25°C) were measured prior to triplicate sample analysis at room temperature (18°C). Individual measurements as well as mean and sample standard deviation (SD) values, where appropriate, are listed in Table A1.1. Relative standard deviation (RSD) values of $<2\%$ for all replicate analyses indicate good precision.

Table A1.1: Results of triplicate electrical conductivity (EC) readings for the Barbrook water samples.

Sample	EC readings (mS/cm)			Mean	SD	% RSD
	1	2	3			
BW1	0.279	0.281	0.283	0.281	0.002	0.71
BW2	2.10	2.11	2.11	2.11	0.01	0.47
BW3	1.52	1.52	1.52	1.52		
BW4	3.19	3.19	3.19	3.19		
BW5	0.185	0.185	0.185	0.185		
BW6	0.063	0.063	0.063	0.063		
BW7	0.075	0.075	0.075	0.075		
BW8	0.071	0.071	0.071	0.071		
BW9	2.06	2.07	2.07	2.07	0.01	0.48
BW10	2.73	2.74	2.76	2.74	0.02	0.73
BW11	1.63	1.63	1.63	1.63		
BW12	1.81	1.82	1.82	1.82		
BW13	2.43	2.43	2.43	2.43		
BW14	5.16	5.19	5.21	5.19	0.03	0.58
BW15	5.07	5.11	5.12	5.10	0.03	0.59
BW16	0.060	0.060	0.061	0.060	0.001	1.70
BW17	0.055	0.056	0.056	0.056	0.001	1.79
BW18	0.266	0.266	0.269	0.267	0.002	0.75
BW19	1.35	1.36	1.36	1.36	0.01	0.74
BW20	2.54	2.54	2.56	2.55	0.01	0.39
BW21	2.95	2.97	2.98	2.97	0.02	0.67
BW22	0.953	0.954	0.956	0.954	0.002	0.21
BW23	1.06	1.06	1.06	1.06		
BW24	0.194	0.194	0.194	0.194		
BW25	0.061	0.061	0.061	0.061		
BW26	0.073	0.073	0.073	0.073		

A1.2 pH measurements

Determination of pH was achieved using a Metrohm 691 pH meter which comprises a combined electrode (glass indicator electrode plus reference electrode). The pH meter was calibrated before use with buffer solutions of pH 7.02 and 4.00. Triplicate sample measurements were performed at room temperature (18.3°C). Individual measurements as well as mean and standard deviation SD values are listed in Table A1.2. The <1% RSD values presented in Table A1.2 indicate good analytical precision.

Table A1.2: Results of triplicate pH readings for the Barbrook water samples.

Sample	pH readings			Mean	SD	% RSD
	1	2	3			
BW1	7.26	7.28	7.29	7.28	0.02	0.27
BW2	6.05	6.04	6.03	6.04	0.01	0.17
BW3	6.74	6.74	6.74	6.74		
BW4	9.12	9.16	9.17	9.15	0.03	0.33
BW5	7.28	7.29	7.31	7.29	0.02	0.27
BW6	7.90	7.85	7.87	7.87	0.03	0.38
BW7	7.44	7.47	7.49	7.46	0.02	0.27
BW8	7.56	7.62	7.62	7.60	0.04	0.53
BW9	7.85	7.87	7.87	7.86	0.01	0.13
BW10	7.53	7.54	7.54	7.54	0.01	0.13
BW11	7.94	7.94	7.95	7.94	0.01	0.13
BW12	7.75	7.74	7.75	7.75	0.01	0.13
BW13	7.05	7.04	7.04	7.04	0.01	0.14
BW14	11.00	11.02	11.03	11.02	0.02	0.18
BW15	8.95	8.92	8.92	8.93	0.02	0.22
BW16	7.06	7.04	6.98	7.03	0.04	0.57
BW17	7.32	7.36	7.42	7.37	0.05	0.68
BW18	7.95	7.96	7.99	7.97	0.02	0.25
BW19	7.43	7.44	7.44	7.44	0.01	0.13
BW20	6.93	6.91	6.91	6.92	0.01	0.14
BW21	7.66	7.69	7.70	7.68	0.02	0.26
BW22	7.86	7.88	7.89	7.88	0.02	0.25
BW23	7.72	7.73	7.74	7.73	0.01	0.13
BW24	7.17	7.15	7.14	7.15	0.02	0.28
BW25	7.56	7.56	7.61	7.58	0.03	0.40
BW26	7.57	7.61	7.62	7.60	0.02	0.26

A1.3 Alkalinity measurements

Alkalinity was measured by potentiometric titration to a preselected pH using a Radiometer DTS 800 multi-titration system comprising a TTT 85 titrator and an ABU 80 autoburette to which was attached a PHG201 glass electrode and a REF401 calomel reference electrode. The procedure involved determining the volume of 0.01M HCl required to titrate 10 mL of each sample to an end-point pH of 4.5. As HCO_3^- is the dominant carbonate species in waters at pH 6.4 to 10.33 (Drever, 1988), all alkalinity readings, apart

from sample BW14 (pH 11.02), were recalculated from mmol_c/mL of H⁺ used in the titration to mg HCO₃⁻/L using the following formula:

$$\text{mg HCO}_3^-/\text{L} = \text{mmol}_c \text{ H}^+/\text{mL} \times \text{atomic wt HCO}_3^- \times 1000$$

The alkalinity reading for sample BW14 was recalculated to mg CO₃²⁻/L as follows:

$$\text{mg CO}_3^{2-}/\text{L} = \frac{\text{mmol}_c \text{ H}^+/\text{mL}}{2} \times \text{atomic wt CO}_3^{2-} \times 1000$$

Table A1.3: Results of duplicate alkalinity measurements for the Barbrook water samples.

Sample	Alkalinity (mg HCO ₃ ⁻ /L)		Mean ± SD
	1	2	
BW1	175.8	171.2	173.5 ± 3.25
BW2	44.35	44.38	44.37 ± 0.02
BW3	237.8	240.8	239.3 ± 2.12
BW4	82.72	83.87	83.30 ± 0.81
BW5	49.84	51.36	50.6 ± 1.07
BW6	27.19	28.03	27.61 ± 0.59
BW7	32.27	32.97	32.62 ± 0.49
BW8	32.42	32.24	32.33 ± 0.13
BW9	450.6	444.4	447.5 ± 4.38
BW10	560.3	558.6	559.5 ± 1.20
BW11	301.6	305.2	303.4 ± 2.55
BW12	336.1	343.5	339.8 ± 5.23
BW13	85.71	92.17	88.94 ± 4.57
BW15	155.3	156.1	155.7 ± 0.57
BW16	17.63	16.59	17.11 ± 0.73
BW17	20.64	20.50	20.57 ± 0.10
BW18	156.1	158.8	157.4 ± 1.91
BW19	110.4	110.5	110.4 ± 0.07
BW20	64.4	64.2	64.3 ± 0.14
BW21	135.2	148.4	141.8 ± 9.33
BW22	87.29	88.69	87.99 ± 0.99
BW23	110.6	114.3	112.4 ± 2.62
BW24	7.99	7.96	7.98 ± 0.02
BW25	26.75	27.15	26.95 ± 0.28
BW26	29.80	29.52	29.66 ± 0.20

Sample	Alkalinity (mg CO ₃ ²⁻ /L)		Mean ± SD
	1	2	
BW14	120.9	114.3	117.6 ± 4.67

A1.4 Redox potential

The redox potential of each water sample was measured upon initial opening of the sealed and completely-filled sample bottles. This was achieved using an M21Pt platinum electrode and a REF401 saturated calomel reference electrode pair attached to the same Radiometer DTS 800 multi-titration system used for the alkalinity measurements. Measured sample redox values were adjusted relative to the hydrogen electrode by adding the Eh

value of the saturated calomel electrode (0.2444 V) to each reading (Garrels and Christ, 1965). In order to check the calibration of the platinum-calomel electrode pair, the potential of a redox buffer solution, comprising 100 mmol/L each of ferrous and ferric ammonium sulphate in 1M H₂SO₄, was measured prior to sample analysis. According to Sposito (1989), the accepted redox value for this solution (0.430 V at 298 K) represents the formal potential of a solution containing both the oxidised and reduced species. Repeat measurements of this solution over the period of sample analysis ranged from 0.429 to 0.435 V at room temperature. The equation relating Eh (volts) to pe is given by Sposito (1989) as:

$$Eh \text{ (volts)} = \frac{RT \ln 10}{F} = 0.05916 \text{ pe}$$

where R = molar gas constant, T = 298 K and F is the Faraday constant.

The validity of measuring the redox potential of water samples using this method is discussed in Chapter 3.

A1.5 Cation and anion concentrations

Cation (K⁺, Na⁺, NH₄⁺, Ca²⁺ and Mg²⁺) and anion (Cl⁻, NO₂⁻, NO₃⁻ and SO₄²⁻) concentrations within the Barbrook water samples were determined by high performance ion chromatography (HPIC). Analyses were performed on a Dionex ion chromatograph within the Department of Geological Sciences at the University of Cape Town. The samples were initially filtered through 0.2 μm Millipore filter membranes to remove suspended solids and then diluted with Milli-Q deionised water to obtain EC values of between 50 and 100 μS/cm. Immediately prior to analysis, the samples were also passed through a Dionex onguard-P cartridge containing a polyvinylpyrrolidone (PVP) polymer designed for removing the phenolic fraction of humic acids, tannic acids, lignins, anthocyanins and azo dyes. Within the ion chromatograph, anions were separated on a HPIC-AS4A anion exchange column using an eluant comprising 1.8mM Na₂CO₃ and 1.7mM NaHCO₃. Cations were separated on a HPIC-CS12A cation exchange column using a 22mMMSA (methanesulfonic acid) eluant.

In order to assess accuracy during sample measurement, four standards were analysed at the start of each analytical session and Milli-Q deionised water was included as a blank. Tables A1.4 and A1.5 present a comparison of expected and measured results for the cation and anion standards, respectively, on each of the days that Barbrook water samples were analysed. The difference between expected and measured values was always ≤5% for the cation standards and generally ≤6% for the anion standards. However, the difference between expected and measured values for some of the anion standards during the final analytical session (October 14, 1996) increased to 7% for NO₂⁻ and 15% for NO₃⁻.

Table A1.6 presents the results of ten repeat analyses of anion standard AN2 performed over three consecutive days in early September 1996. A comparison of the measured and expected RSD values provides an indication of the within-laboratory precision

of the analytical procedure. Only SO_4^{2-} has a slightly higher RSD than expected, due predominantly to a single high measurement on the second day of analysis. Data for duplicate sample analyses (Table A1.7) shows that the difference between duplicates was generally $<3\%$. Considered together, the data presented in Tables A1.6 and A1.7 indicate good within-laboratory precision during HPIC analysis.

As a measure of the quality of the Barbrook analytical data, the anion-cation charge balance of each water sample (Table A1.8) was calculated using the method of Murray and Wade (1996). Fluoride (Section A1.10) and alkalinity (Section A1.3) measurements were also included in the charge balance calculations, the latter as either HCO_3^- or CO_3^{2-} (BW14). Phosphorus (Section A1.7) was included as PO_4^{3-} for sample BW3. Measured ionic concentrations (mg/L) were converted to mmol_c/L prior to calculating the percentage difference:

$$\text{mmol}_c/\text{L} = \frac{\text{mg/L}}{\text{atomic or molecular weight}} \times \text{ionic charge}$$

$$\% \text{ difference} = 100 \times \left(\frac{\text{sum of cations} - \text{sum of anions}}{\text{sum of cations} + \text{sum of anions}} \right)$$

Table A1.4: Comparison of the expected and measured results (mg/L) for the four cation standards analysed on each of the days that Barbrook water samples were analysed. Numbers in parentheses represent the % difference between the expected and measured values.

	AK2	AK3	AK4	AK5
Na⁺				
Expected concentration	6.25	12.5	25	50
October 10, 1996	6.02 (1.9)	12.7 (0.8)	24.1 (1.8)	48.6 (1.4)
October 11, 1996	5.96 (2.4)	12.4 (0.4)	24.2 (1.6)	47.2 (2.9)
NH₄⁺				
Expected concentration	1.25	2.5	5	10
October 10, 1996	1.17 (3.3)	2.45 (1.0)	4.78 (2.2)	9.59 (2.1)
October 11, 1996	1.16 (3.7)	2.39 (2.3)	4.77 (2.4)	9.57 (2.2)
K⁺				
Expected concentration	1.25	2.5	5	10
October 10, 1996	1.22 (1.2)	2.55 (1.0)	4.76 (2.5)	9.79 (1.1)
October 11, 1996	1.18 (2.9)	2.43 (1.4)	4.68 (3.3)	9.51 (2.5)
Mg²⁺				
Expected concentration	1.25	2.5	5	10
October 10, 1996	1.13 (5.0)	2.47 (0.6)	4.87 (1.3)	9.95 (0.3)
October 11, 1996	1.22 (1.2)	2.44 (2.0)	4.85 (1.5)	9.49 (2.6)
Ca²⁺				
Expected concentration	6.25	12.5	25	50
October 10, 1996	6.25 (0.0)	13.2 (2.7)	25.1 (0.2)	50.0 (0.0)
October 11, 1996	5.79 (3.8)	12.1 (1.6)	24.1 (1.8)	47.9 (2.1)

Table A1.5: Comparison of the expected and measured results (mg/L) for the four anion standards analysed on each of the days that Barbrook water samples were analysed. Numbers in parentheses represent the percentage difference between the expected and measured values.

	AN2	AN3	AN4	AN5
Cl⁻				
Expected concentration	0.94	1.88	4.69	9.38
September 17, 1996	0.88 (3.3)	1.80 (2.2)	4.66 (0.3)	9.39 (0.1)
September 27, 1996	0.95 (0.5)	1.83 (1.3)	4.93 (2.5)	9.30 (0.4)
October 14, 1996	0.84 (5.6)	1.70 (5.0)	4.64 (0.5)	8.66 (4.0)
NO₂⁻				
Expected concentration	0.5	1	2.5	5
September 17, 1996	0.46 (4.2)	0.94 (3.1)	2.40 (2.0)	4.87 (1.3)
September 27, 1996	0.49 (1.0)	0.97 (1.5)	2.60 (2.0)	5.16 (1.6)
October 14, 1996	0.45 (5.3)	0.87 (7.0)	2.43 (1.4)	4.43 (6.0)
NO₃⁻				
Expected concentration	0.5	1	2.5	5
September 17, 1996	0.46 (4.2)	0.88 (6.4)	2.37 (2.7)	4.80 (2.0)
September 27, 1996	0.51 (1.0)	0.90 (5.3)	2.57 (1.4)	4.80 (2.0)
October 14, 1996	0.46 (4.2)	0.78 (12)	2.44 (1.2)	3.72 (15)
SO₄²⁻				
Expected concentration	1	2	5	10
September 17, 1996	0.93 (3.6)	1.92 (2.0)	4.80 (2.0)	9.64 (1.8)
September 27, 1996	1.05 (2.4)	2.04 (1.0)	5.23 (2.2)	9.88 (0.6)
October 14, 1996	0.94 (3.1)	1.89 (2.8)	4.77 (2.4)	9.01 (5.2)

Table A1.6: Repeat analyses (mg/L) of anion standard AN2.

	Cl ⁻	NO ₂ ⁻	NO ₃ ⁻	SO ₄ ²⁻
Expected concentration	0.94	0.5	0.5	1.0
Repeat No.				
1	0.90	0.50	0.43	0.84
2	0.93	0.50	0.49	0.85
3	0.94	0.54	0.46	1.19
4	0.94	0.52	0.48	0.96
5	0.90	0.53	0.47	0.95
6	0.93	0.53	0.49	0.96
7	0.90	0.54	0.58	0.93
8	0.91	0.53	0.57	0.97
9	0.91	0.52	0.48	0.96
10	0.94	0.53	0.50	0.96
Mean	0.920	0.524	0.493	0.956
SD	0.017	0.013	0.044	0.091
% RSD (measured)	1.8	2.6	8.9	9.5
% RSD_r (expected)	8.1	8.9	8.9	8.0

Note: % RSD (measured) = $100 \times \frac{SD}{\text{mean}}$; % RSD_r (expected) = $C^{-0.1505}$ where C = expected concentration (mg/L x 10⁻⁶) (Horwitz and Albert, 1993).

Table A1.7: Duplicate HPIC analyses for some of the Barbrook water samples. Numbers in parentheses represent the percentage difference between the duplicate values.

Cations (mg/L):	BW4A	BW4B	BW6A	BW6B	BW19A	BW19B
Na ⁺	285	281 (0.7)	3.73	3.73 (0.0)	13.3	13.2 (0.4)
NH ₄ ⁺	27.9	27.2 (1.3)			38.6	38.7 (0.1)
K ⁺	43.3	43.3 (0.0)	0.385	0.375 (2.7)	5.38	5.37 (0.1)
Mg ²⁺	102	99.5 (1.2)	4.22	4.32 (1.2)	93.4	96.6 (1.7)
Ca ²⁺	318	318 (0.0)	2.14	2.19 (1.2)	102	101 (0.5)

Anions (mg/L):	BW14A	BW14B	BW18A	BW18B	BW26A	BW26B
Cl ⁻	17.3	15.2 (6.5)	4.54	4.49 (0.6)	4.20	4.16 (0.5)
NO ₂ ⁻	76.9	73.9 (2.0)				
NO ₃ ⁻	43.0	40.6 (2.9)	0.48	0.49 (1.0)	1.17	1.16 (0.4)
SO ₄ ²⁻	1436	1431 (0.2)	9.41	9.46 (0.3)	5.36	5.32 (0.4)

Table A1.8: Anion-cation charge balance results for the Barbrook water samples.

Sample No.	BW1	BW2	BW3	BW4	BW5	BW6	BW7
Cations (mmol_c/L):							
Na ⁺	0.149	4.24	5.18	12.31	0.233	0.162	0.131
NH ₄ ⁺	0.342		1.13	1.53			0.145
K ⁺	0.522	0.374	0.183	1.11	0.014	0.010	0.020
Mg ²⁺	1.51	6.91	5.07	8.30	0.946	0.351	0.361
Ca ²⁺	0.924	16.88	4.99	15.88	0.646	0.108	0.203
Total cations	3.45	28.40	16.55	39.13	1.84	0.631	0.860
Anions (mmol_c/L):							
F ⁻	0.004	0.007	0.008	0.003			
HCO ₃ ⁻	2.85	0.727	3.92	1.37	0.829	0.453	0.535
Cl ⁻	0.583	1.03	1.21	0.416	0.148	0.122	0.120
NO ₂ ⁻							
NO ₃ ⁻	0.009	1.21	0.020	0.982	0.121	0.017	0.004
SO ₄ ²⁻	0.084	26.57	10.14	29.40	0.617	0.064	0.115
PO ₄ ³⁻			0.727				
Total anions	3.53	29.54	16.03	32.17	1.72	0.656	0.774
% Difference	-1.29	-1.97	1.60	9.76	3.45	-1.94	5.56

Sample No.	BW8	BW9	BW10	BW11	BW12	BW13	BW14
Cations (mmol_c/L):							
Na ⁺	0.135	8.32	13.93	5.69	6.90	2.08	27.91
NH ₄ ⁺						0.562	3.72
K ⁺	0.005	0.186	0.195	0.095	0.072	0.988	3.84
Mg ²⁺	0.306	12.02	12.53	7.11	9.00	12.75	7.40
Ca ²⁺	0.292	4.29	6.52	6.80	2.27	14.92	11.75
Total cations	0.738	24.82	33.18	19.69	18.24	31.30	54.63
Anions (mmol_c/L):							
F ⁻		0.023	0.018	0.015	0.023	0.004	
HCO ₃ ⁻	0.531	7.33	9.17	4.98	5.57	1.46	3.93*
Cl ⁻	0.127	5.51	8.67	2.85	3.95	0.336	0.489
NO ₂ ⁻		0.472					1.67
NO ₃ ⁻	0.004	0.086	0.047			0.750	0.693
SO ₄ ²⁻	0.096	9.22	9.77	9.00	9.20	23.50	29.90
Total anions	0.758	22.64	27.68	16.85	18.74	26.05	36.68
% Difference	-1.34	4.59	9.04	7.77	-1.35	9.15	19.66

Table A1.8: (continued)

Sample No.	BW15	BW16	BW17	BW18	BW19	BW20	BW21
Cations (mmol_c/L):							
Na ⁺	29.28	0.100	0.134	0.370	0.575	1.84	1.34
NH ₄ ⁺	2.08				2.14	0.637	0.738
K ⁺	0.870	0.007	0.008	0.029	0.137	0.976	0.985
Mg ²⁺	8.22	0.225	0.119	1.21	7.82	14.94	17.90
Ca ²⁺	11.50	0.080	0.230	1.23	5.07	16.05	20.44
Total cations	51.96	0.412	0.491	2.84	15.74	34.44	41.40
Anions (mmol_c/L):							
F ⁻					0.003	0.003	
HCO ₃ ⁻	2.55	0.280	0.337	2.58	1.81	1.05	2.32
Cl ⁻	0.920	0.102	0.109	0.127	0.225	0.360	0.385
NO ₂ ⁻	0.210				0.167		
NO ₃ ⁻	1.02	0.010	0.017	0.008	3.03	1.33	1.11
SO ₄ ²⁻	32.85	0.019	0.027	0.196	7.70	29.86	37.45
Total anions	37.55	0.411	0.490	2.91	12.94	32.60	41.26
% Difference	16.09	0.111	0.102	-1.27	9.76	2.74	0.169

Sample No.	BW22	BW23	BW24	BW25	BW26
Cations (mmol_c/L):					
Na ⁺	0.322	0.368	0.071	0.127	0.153
NH ₄ ⁺	0.636	0.904	0.005		
K ⁺	0.073	0.073	0.017	0.002	0.008
Mg ²⁺	6.85	7.21	1.16	0.354	0.416
Ca ²⁺	3.43	3.34	0.637	0.174	0.199
Total cations	11.31	11.89	1.89	0.657	0.776
Anions (mmol_c/L):					
F ⁻					
HCO ₃ ⁻	1.44	1.84	0.131	0.442	0.486
Cl ⁻	0.142	0.157	0.067	0.116	0.118
NO ₂ ⁻	0.031	0.027			
NO ₃ ⁻	1.47	2.55	0.185	0.002	0.019
SO ₄ ²⁻	7.12	7.27	1.36	0.054	0.111
Total anions	10.20	11.84	1.74	0.614	0.734
% Difference	5.16	0.211	4.13	3.38	2.78

Although Murray and Wade (1996) state that anion-cation differences of ± 2 to 5% are acceptable for an anion range of 10 to 800 mmol_c/L, differences of $\leq 10\%$ are considered acceptable for the purposes of this study. As only two samples, BW14 and BW15, have charge balances outside this limit (refer to Chapter 3 for further details), the HPIC data for the Barbrook water samples are therefore considered to be of acceptable quality.

A1.6 Silica concentrations

Silica concentrations (Table A1.9) were determined using the heteropoly blue method (Standard Methods, 1985; p. 460-461) on water samples which had been passed

through 0.2 μm Millipore filter membranes. The procedure involved adding, in quick succession, 0.5 mL 1:1 HCl and 1.0 mL ⁽¹⁾ammonium molybdate reagent to each 25 mL sample. The solutions were mixed thoroughly by inverting at least six times, and then allowed to stand for 5 to 10 minutes prior to the addition of 1.0 mL ⁽²⁾oxalic acid solution and further mixing. The solutions were allowed to stand for a further 2 to 15 minutes prior to mixing with 1.0 mL ⁽³⁾aminonaphtholsulfonic acid reducing agent. The individual reagents were prepared as follows:

⁽¹⁾10 g $(\text{NH}_4)_6\text{Mo}_7\text{O}_{24}\cdot 4\text{H}_2\text{O}$ dissolved in 100 mL deionised water and adjusted to pH = 7 to 8 with NaOH

⁽²⁾7.5 g $\text{H}_2\text{C}_2\text{O}_4\cdot\text{H}_2\text{O}$ dissolved in 100 mL deionised water

⁽³⁾500 mg 1-amino-2-naphthol-4-sulfonic acid and 1 g Na_2SO_3 dissolved in 50 mL deionised water and added to a solution of 30 g $\text{Na}_2\text{S}_2\text{O}_5$ in 150 mL deionised water.

According to Standard Methods (1985), the underlying principle to the heteropoly blue method is that, at a pH of ~ 1.2 , the ammonium molybdate reacts with the silica to produce heteropoly acids. The addition of oxalic acid destroys the molybdophosphoric acid but not the yellow molybdosilicic acid which is then reduced to heteropoly blue by the addition of the aminonaphtholsulfonic acid. Five minutes after the addition of the reducing agent, a blue colour developed and the absorbance at 815 nm within each solution was measured using a Sequoia-Turner model 340 spectrophotometer with a light path of 1 cm. The minimum detectable silica concentration using the heteropoly blue method is $\sim 20 \mu\text{g/L}$.

A range of standard solutions containing SiO_2 concentrations of 0, 20, 40, 60, 80 and 100 $\mu\text{g}/55 \text{ mL}$ final volume (all standard solutions were prepared using double quantities of standard and reagent solutions) was analysed in order to derive a calibration curve (Figure A1.1) from which sample SiO_2 concentrations (mg/L) were determined.

A comparison of SiO_2 values obtained via the heteropoly blue method with total Si values obtained for seven of the Barbrook water samples via inductively coupled plasma-atomic emission spectrometry (ICP-AES: Section A1.8) is presented in Table A1.9. Whereas the difference between the results of the two methods for six of these samples is $<7\%$, sample BW21 has a significantly higher ICP-AES total Si content (2.49 mg/L) compared to SiO_2 measured by colorimetric analysis (1.90 mg/L). Although this may be due to the failure of the colorimetric method to detect any monomeric Si in solution, the low SiO_2 content of this sample may also have contributed to a poor result via colorimetric analysis. An examination of RSD values for all of the colorimetric SiO_2 results indicates good precision (RSD $<5\%$), although samples with $<1.5 \text{ mg SiO}_2/\text{L}$ do have reduced precision compared to those samples with higher SiO_2 contents. Standard Methods (1985) also cites a decrease in precision with decreasing SiO_2 concentration for repeat colorimetric analyses of synthetic samples with SiO_2 contents of 5 mg/L and 30 mg/L. Although precision (4.9% RSD) and accuracy (5.1% relative error) were good for the 30 mg SiO_2/L sample, the precision (27.2% RSD) associated with 11 measurements of the 5 mg SiO_2/L sample was poor although the accuracy was still good (3.0% relative error).

Table A1.9: Silica results for the Barbrook water samples. Total Si ICP-AES values are provided for comparison; values in parentheses represent percentage difference between the results of the two analytical methods.

Sample	Dilution	Absorbance (815 nm)	SiO ₂ (mg/L)	Mean ± SD SiO ₂ content (mg/L)	% RSD	ICP-AES Si (mg/L)																																																																																																																																																																																																																		
BW1	1:10	0.319	2.92	2.95 ± 0.04	1.20	7.24 (5.1)																																																																																																																																																																																																																		
		0.322	2.97				BW2	1:10	0.650	6.50	6.54 ± 0.06	0.86	0.654	6.58	BW3	1:10	0.617	6.14	6.20 ± 0.08	1.26	0.625	6.25	BW4	1:10	0.164	1.50	1.47 ± 0.04	2.89	0.158	1.44	BW5	1:10	0.513	4.98	4.94 ± 0.06	1.13	0.504	4.88	0.508	4.90	0.506	4.99	BW6	1:10	0.441	4.16	4.14 ± 0.03	0.68	0.439	4.12	BW7	1:10	0.477	4.57	4.61 ± 0.06	1.23	0.486	4.65	BW8	1:5	0.885	4.80	4.81 ± 0.01	0.15	0.889	4.81	BW9	1:5	0.690	3.50	3.51 ± 0.01	0.200	0.695	3.51	BW10	1:10	0.739	7.59	7.61 ± 0.02	0.28	0.742	7.62	BW11	1:10	0.304	2.80	2.79 ± 0.01	0.51	0.301	2.78	BW12	1:10	0.488	4.68	4.70 ± 0.02	0.45	0.491	4.71	BW13	1:10	0.187	1.70	1.75 ± 0.07	4.04	0.198	1.80	BW14	1:10	0.241	2.21	2.25 ± 0.06	2.51	0.249	2.29	0.248	2.27	BW15	1:10	0.129	1.18	1.22 ± 0.05	4.34	0.139	1.28	0.131	1.20	BW16	1:10	0.380	3.50	3.46 ± 0.06	1.63	0.372	3.42	BW17	1:10	0.418	3.90	3.97 ± 0.06	1.57	0.425	3.99	0.430	4.02	BW18	1:10	0.775	8.06	8.12 ± 0.08	1.04	0.781	8.18	0.776	8.10	BW19	1:10	0.517	5.00	5.02 ± 0.02	0.42	0.519	5.03	BW20	1:10	0.139	1.28	1.32 ± 0.05	3.59	0.149	1.37	0.141	1.30	BW21	1:10	0.206	1.89	1.90 ± 0.01	0.74	0.209	1.91	BW22	1:10	0.354	3.28	3.29 ± 0.01	0.43	0.357	3.30	BW23	1:10	0.411	3.81	3.82 ± 0.01	0.37	0.412	3.83	BW24	1:10	0.194	1.76	1.77 ± 0.01	0.80	0.196	1.78	BW25	1:10	0.458	4.32	4.40 ± 0.11	2.57	0.469	4.48	BW26	1:10	0.436	4.10
BW2	1:10	0.650	6.50	6.54 ± 0.06	0.86																																																																																																																																																																																																																			
		0.654	6.58				BW3	1:10	0.617	6.14	6.20 ± 0.08	1.26	0.625	6.25	BW4	1:10	0.164	1.50	1.47 ± 0.04	2.89	0.158	1.44	BW5	1:10	0.513	4.98	4.94 ± 0.06	1.13	0.504	4.88			0.508	4.90			0.506	4.99	BW6	1:10	0.441	4.16	4.14 ± 0.03	0.68	0.439	4.12	BW7	1:10	0.477	4.57	4.61 ± 0.06	1.23	0.486	4.65	BW8	1:5	0.885	4.80	4.81 ± 0.01	0.15	0.889	4.81	BW9	1:5	0.690	3.50	3.51 ± 0.01	0.200	0.695	3.51	BW10	1:10	0.739	7.59	7.61 ± 0.02	0.28	0.742	7.62	BW11	1:10	0.304	2.80	2.79 ± 0.01	0.51	0.301	2.78	BW12	1:10	0.488	4.68	4.70 ± 0.02	0.45	0.491	4.71	BW13	1:10	0.187	1.70	1.75 ± 0.07	4.04	0.198	1.80	BW14	1:10	0.241	2.21			2.25 ± 0.06	2.51			0.249	2.29	0.248	2.27			BW15	1:10			0.129	1.18	1.22 ± 0.05	4.34	0.139	1.28	0.131	1.20	BW16	1:10	0.380	3.50			3.46 ± 0.06	1.63			0.372	3.42	BW17	1:10			0.418	3.90			3.97 ± 0.06	1.57	0.425	3.99	0.430	4.02	BW18	1:10	0.775	8.06	8.12 ± 0.08	1.04			0.781	8.18			0.776	8.10	BW19	1:10	0.517	5.00	5.02 ± 0.02	0.42	0.519	5.03	BW20	1:10	0.139	1.28	1.32 ± 0.05	3.59	0.149	1.37	0.141	1.30	BW21	1:10	0.206	1.89	1.90 ± 0.01	0.74	0.209	1.91	BW22	1:10	0.354	3.28	3.29 ± 0.01	0.43	0.357	3.30	BW23	1:10	0.411	3.81	3.82 ± 0.01	0.37	0.412	3.83	BW24	1:10	0.194	1.76
BW3	1:10	0.617	6.14	6.20 ± 0.08	1.26																																																																																																																																																																																																																			
		0.625	6.25																																																																																																																																																																																																																					
BW4	1:10	0.164	1.50	1.47 ± 0.04	2.89																																																																																																																																																																																																																			
		0.158	1.44																																																																																																																																																																																																																					
BW5	1:10	0.513	4.98	4.94 ± 0.06	1.13																																																																																																																																																																																																																			
		0.504	4.88																																																																																																																																																																																																																					
		0.508	4.90																																																																																																																																																																																																																					
		0.506	4.99																																																																																																																																																																																																																					
BW6	1:10	0.441	4.16	4.14 ± 0.03	0.68																																																																																																																																																																																																																			
		0.439	4.12																																																																																																																																																																																																																					
BW7	1:10	0.477	4.57	4.61 ± 0.06	1.23																																																																																																																																																																																																																			
		0.486	4.65																																																																																																																																																																																																																					
BW8	1:5	0.885	4.80	4.81 ± 0.01	0.15																																																																																																																																																																																																																			
		0.889	4.81																																																																																																																																																																																																																					
BW9	1:5	0.690	3.50	3.51 ± 0.01	0.200																																																																																																																																																																																																																			
		0.695	3.51																																																																																																																																																																																																																					
BW10	1:10	0.739	7.59	7.61 ± 0.02	0.28																																																																																																																																																																																																																			
		0.742	7.62																																																																																																																																																																																																																					
BW11	1:10	0.304	2.80	2.79 ± 0.01	0.51																																																																																																																																																																																																																			
		0.301	2.78																																																																																																																																																																																																																					
BW12	1:10	0.488	4.68	4.70 ± 0.02	0.45																																																																																																																																																																																																																			
		0.491	4.71																																																																																																																																																																																																																					
BW13	1:10	0.187	1.70	1.75 ± 0.07	4.04																																																																																																																																																																																																																			
		0.198	1.80																																																																																																																																																																																																																					
BW14	1:10	0.241	2.21	2.25 ± 0.06	2.51																																																																																																																																																																																																																			
		0.249	2.29																																																																																																																																																																																																																					
		0.248	2.27																																																																																																																																																																																																																					
BW15	1:10	0.129	1.18	1.22 ± 0.05	4.34																																																																																																																																																																																																																			
		0.139	1.28																																																																																																																																																																																																																					
		0.131	1.20																																																																																																																																																																																																																					
BW16	1:10	0.380	3.50	3.46 ± 0.06	1.63																																																																																																																																																																																																																			
		0.372	3.42																																																																																																																																																																																																																					
BW17	1:10	0.418	3.90	3.97 ± 0.06	1.57																																																																																																																																																																																																																			
		0.425	3.99																																																																																																																																																																																																																					
		0.430	4.02																																																																																																																																																																																																																					
BW18	1:10	0.775	8.06	8.12 ± 0.08	1.04																																																																																																																																																																																																																			
		0.781	8.18																																																																																																																																																																																																																					
		0.776	8.10																																																																																																																																																																																																																					
BW19	1:10	0.517	5.00	5.02 ± 0.02	0.42																																																																																																																																																																																																																			
		0.519	5.03																																																																																																																																																																																																																					
BW20	1:10	0.139	1.28	1.32 ± 0.05	3.59																																																																																																																																																																																																																			
		0.149	1.37																																																																																																																																																																																																																					
		0.141	1.30																																																																																																																																																																																																																					
BW21	1:10	0.206	1.89	1.90 ± 0.01	0.74																																																																																																																																																																																																																			
		0.209	1.91																																																																																																																																																																																																																					
BW22	1:10	0.354	3.28	3.29 ± 0.01	0.43																																																																																																																																																																																																																			
		0.357	3.30																																																																																																																																																																																																																					
BW23	1:10	0.411	3.81	3.82 ± 0.01	0.37																																																																																																																																																																																																																			
		0.412	3.83																																																																																																																																																																																																																					
BW24	1:10	0.194	1.76	1.77 ± 0.01	0.80																																																																																																																																																																																																																			
		0.196	1.78																																																																																																																																																																																																																					
BW25	1:10	0.458	4.32	4.40 ± 0.11	2.57																																																																																																																																																																																																																			
		0.469	4.48																																																																																																																																																																																																																					
BW26	1:10	0.436	4.10	4.13 ± 0.04	1.03																																																																																																																																																																																																																			
		0.441	4.16																																																																																																																																																																																																																					

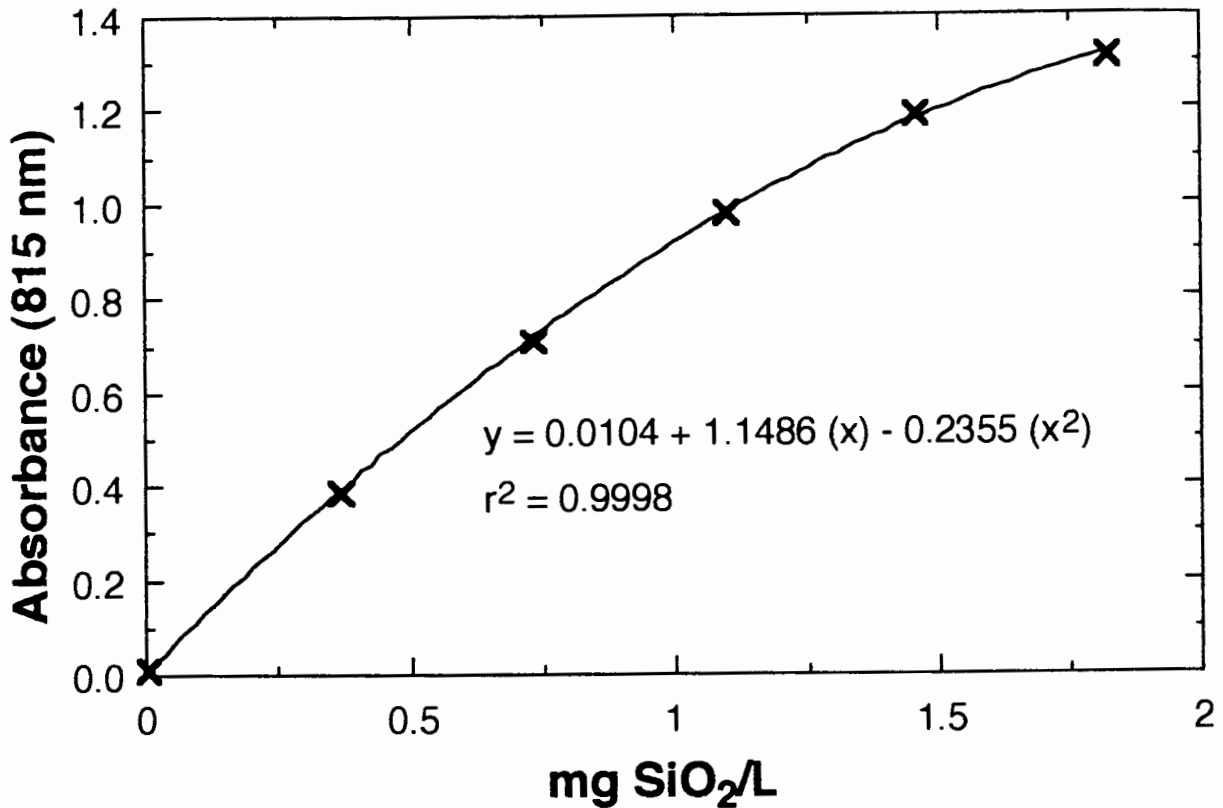


Figure A1.1 Silica calibration curve derived for the standard solutions.

A1.7 Phosphorus concentrations

Phosphorus concentrations were determined using the ascorbic acid colorimetric method of Murphy and Riley (1962), as described in Standard Methods (1985; p.448-451). Following filtration through 0.2 μm Millipore filter membranes, each sample was tested with 0.05 mL phenolphthalein indicator in order that any resulting red colour could be dispelled via the dropwise addition of 5M H₂SO₄. The actual analytical procedure involved mixing 4.0 mL of a mixed reagent (100 mL reagent = 50 mL ⁽¹⁾5M H₂SO₄ + 5.0 mL ⁽²⁾potassium antimonyl tartrate solution + 15 mL ⁽³⁾ammonium molybdate solution + 30 mL ⁽⁴⁾0.01M ascorbic acid solution) with 25 mL of each water sample plus a range of standard phosphate solutions. The individual components of the mixed reagent were prepared as follows:

- (1) 70 mL conc. H₂SO₄ made up to 500 mL in deionised water
- (2) 1.3715 g K(SbO)C₄H₄O_{1/2}H₂O dissolved in 500 mL deionised water
- (3) 20 g (NH₄)₆Mo₇O₂₄·4H₂O dissolved in 500 mL deionised water
- (4) 1.76 g ascorbic acid dissolved in 100 mL deionised water

All glassware was soaked overnight in 1:1 HCl and rinsed thoroughly in Milli-Q deionised water prior to use in order to minimise phosphate contamination. Absorbance at 880 nm

within each of the sample and standard solutions was measured between 10 and 30 minutes after addition of the mixed reagent.

According to Standard Methods (1985), the ammonium molybdate and potassium antimonyl tartrate within the mixed reagent reacts with orthophosphate within an acid medium to produce phosphomolybdic acid. This heteropoly acid is then reduced by ascorbic acid to form an intense blue colour. A Sequoia-Turner model 340 spectrophotometer with a light path of 1 cm was used to measure absorbance at 880 nm within each of the sample and standard solutions. The minimum detectable P concentration using this method is reported as 0.01 mg P/L (Standard Methods, 1985).

Standard solutions containing P concentrations of 0, 0.2, 0.4, 0.6, 0.8, 1.0 and 1.2 mg/L were analysed in order to derive a calibration curve (Figure A1.2). The P contents (mg/L) of the Barbrook water samples could then be calculated from the standard calibration curve using the equation:

$$\text{mg P/L} = \frac{\text{absorbance} - 0.0196}{0.6219} \times \text{dilution factor}$$

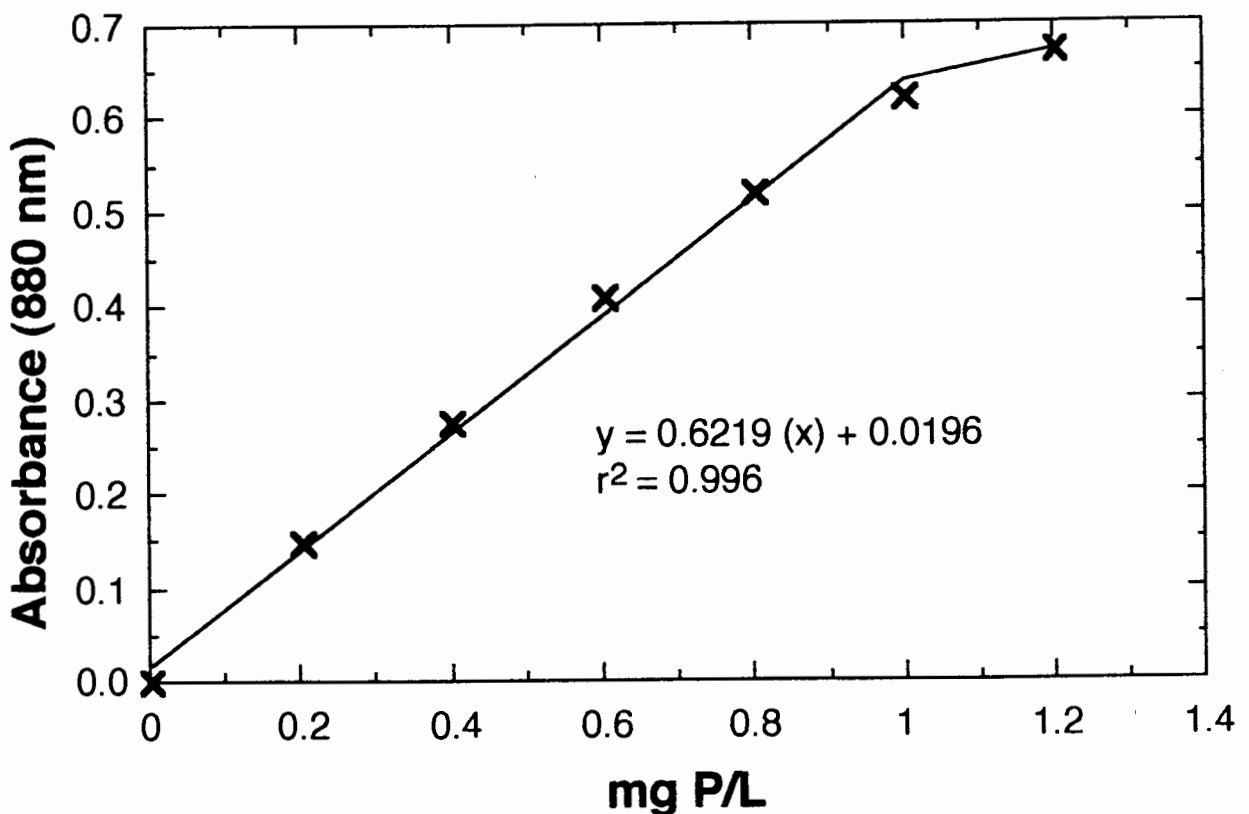


Figure A1.2 Phosphorus calibration curve derived for the standard phosphate solutions using the method of Murphy and Riley (1962). As predicted by the Beer-Lambert law, absorbance is not directly proportional to P concentration at high concentrations. Therefore, the value for the 1.2 mg/L standard was ignored in deriving the calibration curve.

Phosphorus was only detected within one of the Barbrook water samples (BW3: absorbance at 880 nm = 0.069; P content = 0.08 mg/L). However, arsenates can also react with the ammonium molybdate solution to produce a similar blue colour change to that observed with P (Standard Methods, 1985). Although the presence of 1.64 mg As/L in sample BW3 suggests that some As interference may therefore have occurred, samples BW4 and BW14 also contain >1 mg As/L but no detectable P.

A1.8 ICP-AES analyses

A range of elements were analysed in seven of the Barbrook water samples by inductively coupled plasma-atomic emission spectrometry (ICP-AES) on a Joby Yvon 70C (JY70C) spectrometer in the Chemistry Department at the University of Cape Town. Approximate detection limits are listed in Table A1.10. Duplicate analyses of sample BW10 (Table A1.10) indicate relative precision within 5% for most elements above detection limit, although the reproducibility for Co is significantly lower. Potts (1987) states that although the accuracy of ICP-AES analysis for major elements such as Si, Fe and Mn is $\pm 3.6\%$, it is more variable for trace element (e.g. Zn) analysis with accuracy estimated at 5 to 10%.

Table A1.10: Results of duplicate ICP-AES analyses for Barbrook water sample BW10; all elemental data in mg/L.

Element	LLD	BW10		% RSD
		1	2	
Zn	0.1	nd	nd	
Pb	0.5	nd	nd	
Co	0.1	0.229	0.201	9.21
Ni	0.2	0.257	nd	
Si	0.1	7.97	8.20	2.01
Mn	0.05	3.82	3.57	4.78
Fe	0.1	0.371	0.360	2.13
Cr	0.1	nd	nd	
Al	0.5	nd	nd	
Cu	0.2	nd	nd	

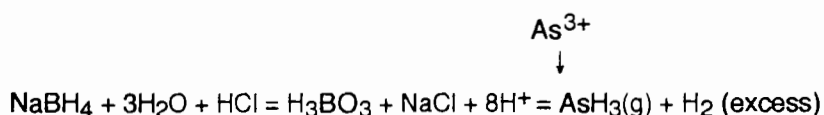
Note: LLD = lower limit of detection; nd = below detection limit

A1.9 Arsenic concentrations

Arsenic concentrations within the Barbrook water samples were determined by hydride generation-atomic absorption spectroscopy (HG-AAS) on undigested samples. These analyses were performed at the Scientific Services department of the Cape Town City Council, using a GBC 902 double beam atomic absorption spectrophotometer with a Varian VGA 76 vapour generation accessory. All samples were filtered through 0.2 μm Millipore filter

membranes and acidified via the addition of 1 mL 10M HNO₃ to each 100 mL of sample. Initially, several samples were analysed following HNO₃ digestion and the results were compared to those of the undigested samples. Since no significant differences were found between the two sets of analytical results, it was assumed that no significant organic As is present in the Barbrook waters.

Prior to arsenic analysis via HG-AAS, 5 mL conc. HCl and 1 mL 15% KI were added to each 45 mL sample in order to ensure that all of the As(V) was reduced to As(III). Hydride generation involved the use of the conc. HCl as well as a 0.6% (w/v) NaBH₄ solution stabilised in a 0.5% (w/v) NaOH solution. This results in the conversion of all As to an arsine gas (AsH₃) via the reaction (Lajunen, 1992):



Results were measured in µg As/L following machine calibration using standards containing 10, 20, 50 and 100 µg As/L. Sample dilution was undertaken at the discretion of the analyst in order to achieve As concentrations within the calibration range. The lower limit of detection was 0.001 mg As/L.

In addition to the 26 Barbrook water samples, two hidden standard solutions were also included for analysis by Scientific Services. Both standards were prepared using a 10 mg/L As(V) standard solution diluted with Milli-Q deionised water to 0.05 mg As/L (BST1) and 0.01 mg As/L (BST2). The results of the standard analyses (Table A1.11) indicate that accuracy was ≤2.5% relative, whereas the RSD for 6 analyses of each standard was ≤9%. As a further indication of analytical precision the results of replicate analyses for 14 of the Barbrook water samples are presented in Table A1.12. The precision for these analyses is ≤13% RSD.

Table A1.11: Results (µg As/L) of replicate analyses of two As standard solutions, as analysed by HG-AAS.

	Expected	Measured mean ± SD (n=6)	% difference	% RSD (n=6)
Standards:				
BST1	50	47.57 ± 3.20	2.49	6.73
BST2	10	10.28 ± 0.89	1.38	8.66

Table A1.12: Results of replicate As analyses of the Barbrook water samples, as performed by HG-AAS.

Sample	As ($\mu\text{g/L}$)				Mean	SD	% RSD
	1	2	3	4			
BW2	150	167	166	182	166	13	7.86
BW3	1620	1688	1620	1620	1637	34	2.08
BW4	1575	1530	1780	1790	1669	135	8.12
BW5	11.0	11.0	10.8		10.9	0.12	1.06
BW13	13.0	11.2	10.8	11.5	11.6	0.96	8.26
BW14	4272	3960			4116	221	5.36
BW15	450	400	420		423	25	5.94
BW18	11.8	13.0			12.4	0.85	6.85
BW19	11.0	12.8	9.5	10.5	11.0	1.38	12.6
BW20	23.8	25.0	20.0	22.5	22.8	2.14	9.39
BW21	17.5	17.5			17.5		
BW22	4.0	3.4			3.70	0.42	11.5
BW23	4.0	3.5			3.75	0.35	9.43
BW24	23.0	19.8			21.4	2.26	10.6

A1.10 Fluoride concentrations

The fluoride concentrations of the Barbrook water samples were determined using the ion selective electrode method, whereby a selective ion sensor containing a lanthanum fluoride (LaF_3) crystal is used to measure the activity of fluoride in solution (Standard Methods, 1985: p. 357-359). Each 10 mL filtered water sample was mixed with 10 mL of a total ionic strength adjustment buffer (TISAB) prior to analysis. The TISAB solution was prepared by combining 57 mL glacial acetic acid, 58 g NaCl and 4 g CDTA (1,2 cyclohexylenediaminetetraacetic acid) in ~500 mL deionised water, which was then adjusted to pH 5.3 to 5.5 with 6M NaOH prior to being made up to a total volume of 1L with deionised water. The addition of this reagent maintains the sample solution at $\text{pH} > 5$ in order to minimise HF complex production and prevent hydroxide interference. The addition of TISAB also ensures that the samples all have the same ionic strength which is necessary as the activity coefficient of F^- is proportional to ionic strength. The CDTA in the reagent acts as a chelating agent which preferentially complexes with aluminium ions to ensure that the fluoride occurs as free ions in solution rather than complexing with aluminium to form AlF_6^{3-} and AlF_2^+ . The use of a chelating agent such as CDTA may be rendered less efficient in the presence of high Al concentrations (≥ 0.7 mg/L), however, necessitating sample pre-treatment with an organic complexing agent (Nicholson and Duff, 1981). The negligible Al contents of the Barbrook water samples ($< \text{LLD}$ of 0.5 mg/L by ICP-AES; Section A1.8) dictated that such pre-treatment was not required.

Fluoride concentrations (ppm) were measured with a fluoride ion selective electrode attached to a Corning ion analyzer 255 following a three-point calibration using standards containing 0.1, 1 and 10 ppm F^- . The lower limit of detection using this method is 0.05 ppm F^- (McCaffrey, 1996). Duplicate analyses of three samples indicated that precision was $\leq 1.5\%$ (RSD).

APPENDIX 2

Analytical methods used for the Barbrook soil and sediment samples

A2.1 pH measurements

In order to determine the pH values of the Barbrook soil and sediment samples, two separate solutions were prepared for each sample using water or KCl. The preparation of these solutions involved mixing 10 g of ground, sieved (<2 mm) and air-dried soil or sediment with either 25 mL Milli-Q deionised water or 25 mL 1MKCl. Both mixtures were then agitated for 10 minutes using a horizontal shaker, and left to stand for a further 30 minutes prior to measuring the pH of the supernatant. Determination of pH was achieved using a Metrohm 691 pH meter which comprises a combined electrode (glass indicator electrode plus reference electrode). The pH meter was calibrated before use with buffer solutions of pH 7.02 and 4.00. All sample measurements were performed at room temperature (18.3°C). Further details regarding the principles of soil pH measurement are presented in McLean (1982); information regarding the analytical precision of pH measurement is presented in Section A1.2.

A2.2 Calcium carbonate content

The CaCO₃ content of each soil and sediment sample was determined using the Karbonat-Bombe method of Birch (1981) on aliquots which had been ground in a carbon steel swing mill. The analytical method involved reacting 5 mL conc. HCl with a known sample aliquot in a sealed plexiglass cylinder and recording the attached manometer pressure reading (KPa) once effervescence has ceased and all CO₂ has been liberated. Sample analyses were performed in duplicate using 2 g sample aliquots. Every five to six sample analyses were interspersed with the analysis of 1 g of pure CaCO₃ powder, representing a 100% CaCO₃ standard. Manometer readings for each sample analysis were recalculated to % CaCO₃ (Table A2.1) using the equation:

$$\% \text{ CaCO}_3 \text{ in sample} = \frac{100\%}{\text{CaCO}_3 \text{ standard manometer reading}} \times \text{sample manometer reading}$$

Birch (1981) states that the precision of the analytical method decreases with decreasing CaCO₃ content, whereby the relative precision of 2% for CaCO₃ contents >5% decreases to <4% for lower CaCO₃ contents. However, the precision of the duplicate analyses of the Barbrook soil and sediment samples was variable and not simply a function of CaCO₃ content, with RSD values of up to 15% for samples with >5% CaCO₃ (Table A2.1). According to Birch (1981), the absolute accuracy of the Karbonat-Bombe method is 2% for CaCO₃ contents >10% and 3% for lower CaCO₃ contents.

Table A2.1: Results of duplicate CaCO₃ measurements for the Barbrook soil and sediment samples; raw results were divided in half to account for the use of 2 g sample powder aliquots.

Sample	Manometer reading (KPa)		% CaCO ₃ Mean ± SD	% RSD
	1	2		
1 g CaCO ₃	151			
BS1A	10	8	3.0 ± 0.46	15.4
BS1B	8	9	2.8 ± 0.25	8.7
BS2	9	9	3.0	
1 g CaCO ₃	155			
BS3	21	21	6.8	
BS4	18	18	5.8	
1 g CaCO ₃	155			
BS5	8	8	2.6	
BS6	9	9	2.9	
BS7	25	22	7.6 ± 0.67	8.9
1 g CaCO ₃	156			
BS8	10	10	3.2	
BS9	9	9	2.9	

A2.3 Extractable arsenic concentrations

Arsenic was extracted from the Barbrook soil and sediment samples using the sodium bicarbonate method, as described in Olsen and Sommers (1982) for phosphorus extraction. This method involved shaking 5 g of ground, sieved (<2 mm) and air-dried soil or sediment with 100 mL 0.5M NaHCO₃ which had been adjusted to a pH of 8.5 via the dropwise addition of 1M NaOH. Samples were then filtered through Whatman No. 40 ashless filter paper prior to As analysis by inductively coupled plasma - mass spectrometry (ICP-MS) at the Institute for Soil, Climate and Water (ISCW) in Pretoria. Measured sample data in mg/L were recalculated to mg/kg soil using the following equations:

$$\text{mg As/5 g soil} = \frac{\text{mg As/L}}{1000} \times 100 \text{ mL}$$

$$\text{mg As/kg soil} = \frac{\text{mg As/5 g soil}}{5} \times 1000$$

In order to examine the accuracy of the analytical procedure, two hidden standards were included with the samples sent for ICP-MS As analysis. These standards were prepared

by diluting a commercially available 1000 mg/L As standard solution to 5 mg/L (200 x dilution = sample ST1) and 0.5 mg/L (2000 x dilution = sample ST2) in a matrix solution of 0.5M NaHCO₃ which had been adjusted to a pH of 8.5. The results of the standard analyses (Table A2.2) indicate that accuracy was $\leq 2\%$ relative. As a measure of analytical precision, duplicate extractions and analyses were performed on three samples, the results of which indicate precision of $< 6.5\%$ relative (Table A2.2).

Table A2.2: Results of the standard and duplicate sample As analyses by ICP-MS.

	Expected As content (mg/L)	Measured As content (mg/L)	% difference
Standards:			
ST1	5.0	4.80	2.04
ST2	0.5	0.508	0.79
Duplicate As analyses (mg/kg soil)			
	1	2	% RSD
Samples:			
BS1A	0.454	0.471	2.60
BS6	6.59	7.20	6.25
BS9	3.46	3.44	0.41

A2.4 XRFS major and trace element determinations

Total major and trace element concentrations within the Barbrook soil and sediment samples were determined by X-ray fluorescence spectrometry (XRFS) within the Department of Geological Sciences at the University of Cape Town according to the method of Norrish and Chappell (1977). Sample preparation involved grinding 60 to 80 g of completely air-dried soil within a carbon steel swing mill for two to three minutes to produce a fine powder ($\leq 70 \mu\text{m}$ particle size). Approximately 6 g of this soil powder was then combined with 6 drops Mowiol binder, if necessary, and pressed into a powder briquette with a boric acid backing. Samples were analysed using a Philips X'Unique II PW1480 spectrometer which was calibrated using international standards, blanks and specpure compounds (silica and oxides). Instrumental conditions are presented in Table A2.3. Results for international standard reference materials, BIR-1 and BHVO-1 (Table A2.4), provide an indication of the accuracy of trace element data measured on the Philips PW1480 spectrometer. The XRFS determination of major element concentrations is usually performed on glass fusion discs prepared according to the method of Norrish and Hutton (1969). Time limitations, however, dictated the use of powder briquettes to measure Fe, Al and Ca in the Barbrook soil and sediment samples. This method results in reduced accuracy, in the order of $\pm 10\%$ of the concentration determined.

Detection limits for XRFS analysis are calculated using the equation:

$$\text{LLD (ppm)} = \frac{6}{m} \left(\frac{b}{I_{\text{total}}} \right)^{1/2}$$

where m = net peak/concentration, I_b = background count rate under the peak in cps and $T_{total} = T_p + T_b$ where T_p = counting time for peak in seconds and T_b = total counting time for background in seconds. Although the precision (counting statistics) depends on the concentration of the element being measured, it is generally ≤ 2 ppm (1σ) for most elements.

Table A2.3: Instrumental conditions for routine XRF trace element analysis using the Philips PW1480 spectrometer within the Department of Geological Sciences at the University of Cape Town.

Element	Emission Line	X-ray tube		Crystal
		Target	kV - mA	
Fe	K α	Mo/Sc	100 - 25	LiF 220
Al	K α	Mo/Sc	40 - 65	PE 002
Ca	K α	Mo/Sc	40 - 65	LiF 200
As	K α	Mo/Sc	100 - 25	LiF 220
Zn	K α	Au	60 - 45	LiF 220
Cu	K α	Au	60 - 45	LiF 220
Ni	K α	Au	60 - 45	LiF 220
Co	K α	Au	50 - 55	LiF 220
Mn	K α	Au	50 - 55	LiF 220
Cr	K α	Au	50 - 55	LiF 220
V	K α	Au	50 - 55	LiF 220
Pb	L β_1	Rh	80 - 35	LiF 200

Table A2.4: Trace element data for two international standard reference materials, BIR-1 and BHVO-1 as measured on the Philips PW1480 spectrometer in the Department of Geological Sciences at the University of Cape Town (Willis, 1996).

Element	BHVO-1		BIR-1	
	Accepted	Measured	Accepted	Measured
Zn	105	106	71	69
Cu	136	139	126	132
Ni	121	127	166	170
Co	45	44	51	52
Mn	1300	1290	1320	1280
Cr	289	312	382	404
V	317	314	313	306

A2.5 Exchangeable acidity and exchangeable cation concentrations

The potassium chloride method of Thomas (1982) was combined with automated potentiometric titration to determine the exchangeable acidity of the Shortlands soil sample BS5. The method involved agitating a mixture of 25 mL 1M KCl and 10 g of ground, sieved (<2 mm) and air-dried soil for 10 minutes using a horizontal shaker. The mixture was then left to stand for 30 minutes prior to filtration through Whatman No. 1 filter paper. Filtration involved the use of a further five 25 mL increments of 1M KCl, resulting in a final ratio of 10 g soil: 150 mL 1M KCl ratio. The KCl extract of sample BS5 was prepared in duplicate (samples

BS5 A and BS5 B) and three 5 mL replicates of each filtrate were titrated to an end-point pH of 8.3 using 0.01M NaOH and a Radiometer DTS 800 multi-titration system. Instrument calibration was ensured prior to sample measurements using a buffer solution of pH 7.02. Results were obtained in units of mmol/L and were recalculated to cmol exchangeable acidity/kg soil (Table A2.5) using the following equations:

$$\text{mmol/10 g soil} = \text{mmol/150 mL} = \frac{\text{mmol/L}}{1000} \times 150 \text{ mL}$$

$$\text{cmol/kg soil} = \frac{\text{mmol/10 g soil}}{10} \times 100$$

The average blank measurement for the 1M KCl solution (0.053 cmol/kg soil) was subtracted from the average value for BS5 (0.0827 cmol/kg soil) to give a final mean value for KCl exchangeable acidity of 0.0297 cmol/kg soil.

The results presented in Table A2.5 for replicate analyses indicate good analytical precision with RSD values of $\leq 4\%$.

Table A2.5: Results of replicate blank and sample KCl extractable acidity measurements on Shortlands soil sample BS5.

	Replicate analyses			mean	SD	% RSD
	1	2	3			
Blank						
mmol/L	36.1×10^{-3}	34.9×10^{-3}		35.5×10^{-3}	0.8×10^{-3}	
cmol/kg	0.054	0.052		0.053	0.001	2.7
BS5 A						
mmol/L	56.0×10^{-3}	57.3×10^{-3}	53.4×10^{-3}	55.6×10^{-3}	2.0×10^{-3}	
cmol/kg	0.084	0.086	0.080	0.083	0.003	3.7
BS5 B						
mmol/L	56.0×10^{-3}	56.0×10^{-3}	52.0×10^{-3}	54.7×10^{-3}	2.3×10^{-3}	
cmol/kg	0.084	0.084	0.078	0.082	0.003	4.2

Concentrations of the exchangeable cations Ca^{2+} and Mg^{2+} in the filtered BS5 KCl extracts were measured by flame-atomic absorption spectroscopy (AAS) on a Spectra Varian AA-30 spectrometer in the Department of Chemical Engineering at the University of Cape Town. Dilutions (Table A2.6) were undertaken at the discretion of the analyst in order to achieve cation concentrations within the ranges of the standards used during analysis: 0, 1, 2 and 4 ppm for Ca^{2+} and 0, 5, 10 and 20 ppm for Mg^{2+} . The detection limits for Mg^{2+} and Ca^{2+} via AAS are 0.12 ppm and 0.6 ppm, respectively (Potts, 1987). Measured AAS cation results were given in ppm and recalculated to cmol_c/kg soil (Table A2.6) using the following sequence of equations:

$$\text{mg/10 g soil} = \frac{\text{ppm cation} \times \text{lab dilution factor}}{1000} \times 150 \text{ mL}$$

$$\text{mg/kg soil} = \frac{\text{mg/10 g soil}}{10} \times 1000$$

$$\text{cmol}_c/\text{kg soil} = \left(\frac{\text{mg/kg soil}}{\text{atomic weight}} \times \text{ionic charge} \right) \div 10$$

In a review of some of the literature regarding the accuracy and precision of the flame-AAS analytical technique, Potts (1987) states that long-term precision of most major elements under controlled conditions is likely to be within 3 to 5% (coefficient of variation) whereas short-term precision is normally within the range of 1 to 3%. The Mg^{2+} results for duplicate analyses of sample BS5 indicate lower precision, however, with an RSD value of 8.3%.

Table A2.6: Measured (ppm) and recalculated (cmol_c/kg) AAS cation results for Shortlands soil sample BS5. Each measured value represents the mean of four absorbance readings.

Sample	Ca^{2+} (ppm)	Ca^{2+} (cmol_c/kg)	Mg^{2+} (ppm)	Mg^{2+} (cmol_c/kg)
BS5 A	2.79 (x 25 dilution)	11.4	9.20 (x 10 dilution)	5.22
BS5 B	3.92 (x 20 dilution)	11.7	9.46 (x 10 dilution)	5.87
Mean		11.5		5.54
SD		0.23		0.46
% RSD		1.84		8.29

A2.6 Organic carbon content

The organic C content of the Shortlands soil sample BS5 was determined using the rapid dichromate oxidation-titration method of Walkley and Black (1934), as described in Nelson and Sommers (1982). This method involved grinding the air-dried soil with an agate mortar and pestle so that it passed through a 0.53 mm sieve. Duplicate 0.5 g aliquots of sample BS5 were then thoroughly mixed with 10 mL potassium dichromate (0.167M $\text{K}_2\text{Cr}_2\text{O}_7$) and 20 mL conc. H_2SO_4 and left to cool for 30 minutes in a 500 mL wide-mouthed Erlenmeyer flask. Immediately prior to titration, the soil solutions were further mixed with 150 mL Milli-Q deionised water, 10 mL conc. H_3PO_4 and 5 drops ferroin indicator solution. Titration of the sample soil solution was achieved via the dropwise addition of 0.5M iron (II) ammonium sulphate solution ($\text{Fe}(\text{NH}_4)_2(\text{SO}_4)_2$) until the brown endpoint colour was reached.

The results of the titrations, including those of two blank solutions which were prepared by exactly the same method, and the subsequent calculations are presented in

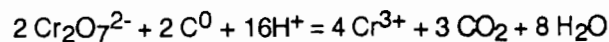
Table A2.7. The % organic C concentrations of the soils were calculated using the following equation:

$$\% C = \frac{[\text{mL Fe(NH}_4)_2(\text{SO}_4)_2 \text{ in blank} - \text{mL Fe(NH}_4)_2(\text{SO}_4)_2 \text{ in sample}] \times M \times 0.3 \times f}{\text{soil mass (g)}}$$

$$\text{where } M = \text{concentration of Fe(NH}_4)_2(\text{SO}_4)_2 \text{ in mol/L} = \frac{10 \text{ mL K}_2\text{Cr}_2\text{O}_7 \times 0.167 \times 6}{\text{mL Fe(NH}_4)_2(\text{SO}_4)_2}$$

and f = average recovery factor = 1.3

According to Nelson and Sommers (1982) the Walkley-Black method for the determination of organic C in soil is based on the proposal of Schollenberger (1927) that organic matter in soil can be oxidised by treatment with a hot mixture of $\text{K}_2\text{Cr}_2\text{O}_7$ and H_2SO_4 according to the equation:



Following the completion of this reaction, the excess dichromate is titrated with $\text{Fe(NH}_4)_2(\text{SO}_4)_2 \cdot 6\text{H}_2\text{O}$ and the dichromate reduced during the reaction with the soil is assumed to equal the amount of organic C in the sample, assuming that organic C has an average valence state of zero. The Walkley-Black method stipulates that no external heat source is applied to the soil - H_2SO_4 - $\text{K}_2\text{Cr}_2\text{O}_7$ mixture, thereby constituting a so-called heat of dilution method. As a result of the experimental findings of Walkley and Black (1934) that an average of only 76% of the organic C in 20 soils was recovered by heat of dilution alone, a recovery factor (f) features in the equation used to calculate percentage organic C content. This recovery factor is supposed to account for unrecovered organic C. However, Nelson and Sommers (1982) discuss the results of a number of experiments which indicate that unless an appropriate f value is determined experimentally for a particular soil, the Walkley-Black method will only provide approximate or semi-quantitative estimates of soil organic C content. Other possible problems associated with the dichromate method used here include interferences by soil constituents such as Cl^- , Fe^{2+} and MnO_2 and the assumption that the average oxidation state of the organic C is zero (Nelson and Sommers, 1982). The precision associated with the duplicate BS5 analyses is <10% relative (Table A2.7).

Table A2.7: Results obtained for sample BS5 during the determination of soil organic C content via the method of Walkley and Black (1934).

	Blank	BS5 A	BS5 B	Mean \pm SD	% RSD
mL $\text{Fe(NH}_4)_2(\text{SO}_4)_2$	20.5	16.4	16.8		
M		0.611	0.596		
% organic C		0.489	0.430	0.46 \pm 0.04	9.07

A2.7 Soluble salt concentrations

In order to determine the concentrations of soluble salts within the Shortlands soil sample BS5 at a standardised water content, a saturated paste extract was prepared by mixing Milli-Q deionised water with 250 g of ground, sieved (<2 mm) and air-dried soil until the soil was uniformly saturated. As stipulated by Rhoades (1982a), saturation was considered to have been achieved when the sample glistened as it reflected light, flowed only slightly when tipped, and consolidated easily by tapping or jarring the container after forming a trench through the mixture with the side of a spatula. The sample was then sealed and allowed to equilibrate overnight prior to extraction of the supernatant using a Büchner filter funnel attached to a vacuum pump.

Following extraction and prior to refrigeration, the saturated paste extract was measured for pH and electrical conductivity (EC). Determination of pH at room temperature (18.3°C) was achieved using a Metrohm 691 pH meter, as described in Section A2.1. The EC of the saturated paste extract was determined using a CRISON microCM 2201 conductivity meter, as described in Section A1.1. The RSD value obtained for three EC readings was 0.12%, indicating excellent analytical precision.

The saturated paste extract was analysed for soluble salt concentrations using high performance ion chromatography (HPIC) and inductively coupled plasma-atomic emission spectroscopy (ICP-AES). Details of these analytical procedures are provided in Sections A1.5 and A1.8, respectively. Sample preparation for both analytical procedures involved centrifugation for 10 minutes at 6000 rpm and filtration using 0.2 µm Millipore filter membranes in order to remove any suspended solids. No dilution was required for HPIC analysis as the mean EC value for the saturated paste extract was 49.23 µS/cm. The anion-cation charge balance difference of 0.46 % (Table A2.8) for the saturated paste extract HPIC analyses indicates good quality data.

Table A2.8: Anion-cation charge balance (Murray and Wade, 1996) results for the HPIC analyses of the saturated paste extract prepared for Barbrook soil sample BS5.

Sample No.	BS5
Cations (mmol_c/L):	
Na ⁺	0.230
K ⁺	0.012
Mg ²⁺	0.018
Ca ²⁺	0.067
Total cations	0.327
Anions (mmol_c/L):	
F ⁻	0.003
Cl ⁻	0.162
NO ₃ ⁻	0.122
SO ₄ ²⁻	0.037
Total anions	0.324
% Difference	0.46

A2.8 Separation of the clay fraction and XRD mineralogical analysis

The dominant clay mineralogy of the Shortlands soil sample BS5 was determined using X-ray diffractometry (XRD) following separation of the clay fraction (<2 μm effective spherical diameter) via a method of dispersion and fractionation. The method used involved placing a 1 g subsample of ground, sieved (<2 mm) and air-dried soil in a 250 mL plastic bottle which was then three-quarters filled with deionised water and shaken to produce a liquid slurry. The dropwise addition of 1M NaOH to this slurry continued until the pH was stabilised at a value of ~9. The sample was then shaken mechanically for three hours prior to transfer into a 3L plastic jar which was filled with deionised water, stirred and left covered overnight at room temperature (22°C). The stipulated depth to which the supernatant suspension should be siphoned off after 16 hours is 18 cm, whereby Stoke's Law should ensure that particles >2 μm would have settled below the 20 cm mark, thereby leaving only the clay fraction in suspension. Depending on the length of time that the slurry actually remained untouched, the depth of siphoning (cm) was calculated as:

$$\text{cm supernatant to be siphoned} = \frac{\text{time slurry left standing}}{16} \times 18$$

After initial siphoning of the supernatant, the 3L jar containing the original soil slurry was refilled with pH 9.8 to 10.2 Na₂CO₃ solution and stirred thoroughly before being left again to settle overnight prior to siphoning. This entire procedure of stirring, settling and siphoning was repeated until the supernatant was clear. Meanwhile, the decanted suspension was accumulated in a large bucket to which 1M HCl was added in a dropwise manner to maintain the pH at a value between 5 and 7.

In order to flocculate the clay within the decanted suspension, a large excess of NaCl crystals were added and the solution was left overnight. The clear supernatant was removed once the clay fraction had settled out of suspension. The clay fraction was then centrifuged at 1000 rpm for ~2 minutes prior to further removal of any remaining clear supernatant. The resulting clay concentrate was transferred with a small amount of water into a length of dialysis tubing which was equilibrated overnight in a bucket of continuously running tap water. Following two further overnight dialyses involving deionised water, the bathing water within the bucket was checked for salt content. This involved testing for the presence of chloride using a silver nitrate solution, whereby the formation of a white precipitate indicated that further dialysis with deionised water was required. Once the centrifuged supernatant obtained from the dialysed clay suspension tested free of chloride, the suspension concentration (mg/mL) was determined gravimetrically. This was achieved by adding 5 to 10 mL of the dialysed clay suspension into an oven-dried and tared porcelain crucible prior to drying overnight at ~110°C. The dried clay fraction was then weighed and the suspension concentration was adjusted to 20 mg/mL.

In preparation for the semi-quantitative determination of clay mineral content within sample BS5 via XRD, a glass slide was thoroughly cleaned with acetone and completely covered with an approximately 2 mL pipetted aliquot of the clay suspension. The slide was allowed to air dry such that the clay particles could settle out of suspension onto their basal planes and thereby provide orientated samples within which the characteristic d-spacings of individual crystals could be determined. X-ray diffractometry was performed on each of the clay samples using the Philips PW3890 diffractometer within the Department of Geological Sciences at the University of Cape Town. The diffractometer was fitted with a Cu X-ray tube and operated at an accelerating voltage of 40 kV and a beam current of 20 mA. The scanning range used was 4 to 70° (2θ angle) at steps of 1°.

A2.9 Soil water content

In order to determine the soil water content (%) of Shortlands soil sample BS5, a ~20 g subsample of ground, sieved (<2 mm) and air-dried soil was weighed and dried in an oven overnight at a temperature of 110°C. The sample was then reweighed and the weight loss (g) was assumed to represent soil water loss (Table A2.9). The percentage soil water content was calculated using the equation:

$$\%H_2O = 100 \frac{(\text{wt of undried container + sample}) - (\text{wt of dried container + sample})}{(\text{wt of undried container + sample}) + (\text{wt of dried container + sample})}$$

Table A2.9: Soil water content results obtained for BS5.

Sample	Prior to oven-drying		After oven-drying		% difference
	container (g)	container + sample (g)	container + sample (g)	difference (g)	
BS5	14.131	34.159	33.855	0.304	0.45

A2.10 Extractable Fe, Al and Mn

Two methods were used to determine extractable Fe, Al and Mn in the Shortlands soil sample BS5 at ISCW in Pretoria. The first method involved extracting all three elements using the dithionite-citrate-bicarbonate method (Non-Affiliated Soil Analysis Work Committee, 1990). This extraction procedure involved adding 40 mL 0.3M Na₃C₆H₆O₇·2H₂O (sodium citrate) and 5 mL 1M NaHCO₃ to 4 g soil which had been crushed to pass through a 0.18 mm sieve. The mixture was placed in a waterbath and allowed to equilibrate at a temperature of 77±2°C before adding 1g Na₂S₂O₄ (sodium dithionite). Following 15 minutes of intermittent stirring while still in the waterbath, the sample was

centrifuged at 1500 to 3000 rpm for 10 minutes and the supernatant was decanted. The entire extraction procedure was then repeated. A further 60 mL of deionised water was added to the residue in the centrifuge tube, heated to 77°C, centrifuged at 1500 to 3000 rpm for 10 minutes and decanted into the beaker containing the previous two aliquots of supernatant. The volume in this beaker was made up to 200 mL with deionised water. If necessary, further centrifuging was undertaken in order to derive a clear solution. An aliquot of this extract solution was diluted (4:1 ratio) with a KCl solution containing 2500 mg K/L prior to analysis for Fe, Al and Mn using flame-AAS. The readings were matched against calibration curves derived using standard solutions prepared with the dithionite-bicarbonate-citrate and KCl solutions and containing 0 to 50 mg Al/L, 0 to 50 mg Fe/L and 0 to 10 mg Mn/L. Results were calculated using the following equation:

$$\% \text{ Fe (or Al or Mn)} = \frac{a \times 200 \times 5}{\text{mass soil (g)}} \times 10^{-4}$$

where a = mg Fe (or Al or Mn)/L in soil extract.

The second extraction method, used for Fe and Al alone, was the sodium pyrophosphate method (Non-Affiliated Soil Analysis Work Committee, 1990). This involved adding 100 mL 0.1M Na₄P₂O₇·10H₂O (sodium pyrophosphate solution adjusted to pH 10 using NaOH) to a 1 g subsample of ground, sieved (<2 mm) and air-dried soil and shaking the mixture overnight on a horizontal shaker at 180 oscillations per minute. The sample was then centrifuged, either with 0.4 mL 0.1% superfloc solution at 1500 to 2000 rpm or without superfloc at 13 000 rpm, for 10 minutes and the supernatant was decanted and filtered if necessary. The Fe and Al contents of the extract were determined using flame-AAS following 1:4 dilution with a 2500 mg K/L solution of KCl. The readings were matched against calibration curves derived using standard solutions prepared with the sodium pyrophosphate and KCl solutions and containing 0 to 50 mg Al/L and 0 to 50 mg Fe/L. Results were calculated using the following equation:

$$\text{mg Fe (or Al)/kg soil} = \frac{a \times \text{volume of extractant (mL)} \times 5}{\text{mass soil (g)}}$$

where a = mg Fe (or Al)/L in soil extract.

A2.11 Phosphorus sorption index

The phosphorus sorption index of Shortlands soil sample BS5 was determined at ISCW in Pretoria. The method used involved adding 200 mL of a 100 ppm P solution to an 8 g aliquot of ground, sieved (<2 mm) and air-dried soil. The mixture was then shaken on an end-over-end shaker at 40 rpm for 24 hours. A constant temperature of 20°C was maintained. Following filtration through Whatman No. 40 ashless filter paper, the P content of the supernatant was determined using the ascorbic acid colorimetric method of Murphy and

Riley (1962). The amount of P sorbed by the soil was expressed as a percentage and calculated as follows:

$$\% P = P \text{ sorbed (mg P/kg soil)} = (\text{initial P concentration} - P \text{ in equilibrium solution}) \times \frac{200}{8}$$

A2.12 Particle size distribution

Particle size distribution was determined on the Shortlands soil sample BS5 at ISCW in Pretoria. The hydrometer method, used to determine the relative percentages of sand, silt and clay, is described in Gee and Bauder (1986). The method involved overnight soaking of an accurately weighed aliquot (10 to 100 g) of ground, sieved (<2 mm) and air-dried soil in 250 mL deionised water and 100 mL of a 50 g/L sodium-hexametaphosphate (HMP) solution prior to mechanical mixing. The suspension was then transferred to a sedimentation cylinder and the volume brought up to 1 L with deionised water. Once the suspension was equilibrated thermally, it was mixed thoroughly and a calibrated hydrometer was inserted. A hydrometer reading (R) was taken after 30 and 60 seconds (for calculation of the sand fraction) and repeated after 1.5 and 24 hours (for calculation of the clay fraction), with the hydrometer being removed and cleaned in between each reading. Readings were also taken at 3, 10, 30, 60 and 120 minutes in order to derive a summation percentage curve. The temperature and the hydrometer reading of a blank solution (R_L) was recorded at the time of each sample reading. At the completion of the readings, the sand fraction was separated by passing the suspension through a 53 μm sieve, and the filtered sand fraction was dried at 105°C and weighed. The calculations used to determine the percentage of each size fraction are detailed in Gee and Bauder (1986) as follows:

Clay fraction:

$$P_{2\mu\text{m}} = m \ln \left(\frac{2}{X_{24}} \right) + P_{24}$$

where X_{24} = mean particle diameter in suspension at 24 hours; P_{24} = summation percentage at 24 hours; $m = \frac{P_{1.5} - P_{24}}{\ln(X_{1.5}/X_{24})}$ = slope of summation percentage curve between X at 1.5 hours and X at 24 hours; $X_{1.5}$ = mean particle diameter in suspension at 1.5 hours; and $P_{1.5}$ = summation percentage at 1.5 hours

where $P = \frac{C}{C_0} \times 100$; $C = R - R_L$; and C_0 = oven-dry weight of the soil sample
and $X = \theta t^{-1/2}$; θ = sedimentation parameter ($\mu\text{m min}^{1/2}$); and t = time in minutes.

Sand fraction:

The $P_{50\mu\text{m}}$ summation percentage is calculated as for the $P_{2\mu\text{m}}$ summation percentage but using the hydrometer readings at 30 and 60 seconds instead of 1.5 and 24 hours. The $P_{50\mu\text{m}}$ value is then subtracted from 100 to obtain % sand.

Silt fraction:

$$\% \text{ silt} = 100 - (\% \text{ sand} + \% \text{ clay})$$

A2.13 Specific surface area

In order to quantify the reactive surface of the Shortlands soil sample BS5, the specific surface area was determined using a Micrometrics Accelerated Surface Area and Porosimetry (ASAP) 2000 machine in the Particle Technology Centre of the Department of Chemical Engineering at the University of Cape Town. The method involved determining external surface area by measuring the adsorption of nitrogen gas, and calculating the number of adsorbate molecules in a monolayer via the BET equation (Carter *et al.*, 1986):

$$\frac{P}{V(P_0 - P)} = \frac{1}{V_m C} + \frac{(C - 1)P}{V_m C P_0}$$

where V = volume of gas adsorbed at pressure P ; V_m = volume of gas required for a single molecular layer over the entire adsorbent surface; P_0 = gas pressure required for saturation at the temperature of the experiment; and $C = \exp \frac{[E_1 - E_2]}{RT}$ where E_2 = heat of liquefaction of the gas, E_1 = heat of adsorption of the first layer of adsorbate, R = gas constant, and T = absolute temperature.

Carter *et al.* (1986) state that, in addition to a number of assumptions associated with the use of the BET equation, the fact that the calculated area per molecule is dependent on the density used means that there is a degree of uncertainty in the absolute surface area measured. They also state that nitrogen gas is only weakly adsorbed and will therefore not penetrate the interlayer surfaces of minerals such as montmorillonite, resulting in a measurement of external surface area only.

APPENDIX 3

Analytical methods used for the Barbrook rock and mineral samples

A3.1 Calcium carbonate content

The CaCO₃ content of the waste rock samples were determined using the Karbonat-Bombe method of Birch (1981), as described in Section A2.2. The results for duplicate analyses (Table A3.1) indicate relative precision of <3%, in keeping with the findings of Birch (1981) that the relative precision of this method is ~2% for CaCO₃ contents >5%.

Table A3.1: Results of duplicate CaCO₃ measurements for the Barbrook waste rock samples; raw results were divided in half to account for the use of 2 g sample powder aliquots.

Sample	Manometer reading (KPa)		% CaCO ₃ Mean ± SD	% RSD
	1	2		
1 g CaCO ₃	154	151		
BR2	34	35	11.3 ± 0.25	2.18
BR3	30	29	9.67 ± 0.25	2.56

A3.2 XRFS major and trace element determinations

Total major and trace element concentrations within the Barbrook waste rock samples were determined by X-ray fluorescence spectrometry (XRFS) within the Department of Geological Sciences at the University of Cape Town, as described in Section A2.4.

A3.3 Toxicity characteristic leaching procedure (TCLP)

The toxicity characteristic leaching procedure (TCLP) was performed on two samples from the Barbrook waste rock pile at the Anglo American Research Laboratories in Johannesburg. Samples were submitted as ~500 g of fine powder following milling in a carbon steel swing mill for 4 minutes. The leaching procedure used was the United States Environmental Protection Agency (EPA) Method 1311 TCLP procedure (EPA, 1993) whereby the samples were leached for 24 hours using an acetate buffer solution at pH 5.0

and the rolling bottle technique. The mass/mass ratio was 20:1 liquid to solids. A range of elements were analysed in the TCLP extract by inductively coupled plasma - optical emission spectrometry (ICP-OES) to a 0.5 mg/L detection limit. Arsenic, Se and Te were analysed by inductively coupled plasma - mass spectrometry (ICP-MS) to a detection limit of 0.05 mg/L.

A3.4 Electron microprobe sulphide mineral analysis

The chemical compositions of individual sulphide minerals from the Barbrook ore rock were determined by wavelength-dispersive spectrometry (WDS) using the Cameca Camebax electron microprobe in the Department of Geological Sciences, University of Cape Town. The microprobe was operated at an accelerating voltage of 15 kV and samples were analysed as carbon-coated polished thin sections. The lower limit of detection was 0.1 ppm.

A3.5 SEM secondary mineral analysis

Secondary minerals resulting from oxidation of the ore and waste rock at Barbrook were analysed using a Leica Stereoscan 440 scanning electron microscope (SEM) in the Physics Department at the University of Cape Town. Selected rock chips were mounted, photographed and carbon-coated prior to analysis. The instrument was operated at an accelerating voltage of 20 kV and the samples were maintained under vacuum at between 10^{-4} and 10^{-6} torr. Energy dispersive spectrometry (EDS) was used to obtain spot semi-quantitative chemical analyses, whereas high-resolution morphological images were obtained from the secondary and backscattered electrons emitted.

APPENDIX 4

Methods used for the arsenic and phosphorus sorption experiments

A4.1 Phosphorus sorption experiment

Prior to commencement of the P sorption experiment, all glassware and other equipment to be used in sample/standard preparation were soaked overnight in 1:1 HCl and rinsed thoroughly with Milli-Q deionised water. A standard P solution containing 500 mg P/L (= 0.5 mg/mL) was prepared by dissolving 2.291 g Na₂HPO₄ in 0.1M NaCl. The pH of the solution, using the method described in Section A1.2, was 8.94. The electrical conductivity (EC) of the solution, using the method described in Section A1.1, was 11.22 mS/cm. As the appropriate concentration range of P to be added to the soil was unknown at the start, the P sorption experiment was performed in two parts. The initial procedure involved weighing out ten individual 2.5 g aliquots of ground, sieved (<2 mm) and air-dried soil into centrifuge tubes, to each of which was added a 25 mL solution made up using the standard P solution diluted with 0.1M NaCl to one of the following P concentrations (mg/L): 0 (blank), 5, 10, 20, 40, 60, 80, 100, 250 and 500. These suspensions were then equilibrated at room temperature via shaking on a horizontal shaker at a constant speed over a 24 hour period. Prior to filtering through Whatman No. 1 filter paper, the samples were centrifuged at maximum rpm for 5 minutes and the pH and EC of each supernatant was measured.

The P concentrations of each of the ten filtrates obtained for sample BS5 were determined using the ascorbic acid colorimetric method of Murphy and Riley (1962), as described in Section A1.7. Standard solutions containing P concentrations of 0, 0.2, 0.4, 0.6, 0.8, 1.0 and 1.2 mg/L were prepared by diluting an intermediate P solution (representing a 50 x dilution of the original 500 mg P/L standard and containing 10 mg P/L = 0.01 mg P/mL), with appropriate amounts of 0.1M NaCl. Analysis of this set of standard solutions enabled the derivation of a calibration curve (Figure A4.1) from which the equilibrium P contents (mg P/L) of the BS5 filtrates could be calculated using the equation:

$$\text{Equilibrium P (mg/L)} = \left(\frac{\text{absorbance} - 0.0227}{0.6126} \times \text{dilution factor} \right) - \text{measured P}_{\text{blank}}$$

Sorbed P concentrations (mg/L) were then calculated for each of the solutions as follows:

$$\text{sorbed P (mg/kg soil)} = \text{initial P (mg/L)} - (\text{equilibrium P}) \times 10$$

where 10 = solution:soil ratio

Absorbance readings and equilibrium P results for the BS5 filtrates are presented in Table A4.1.

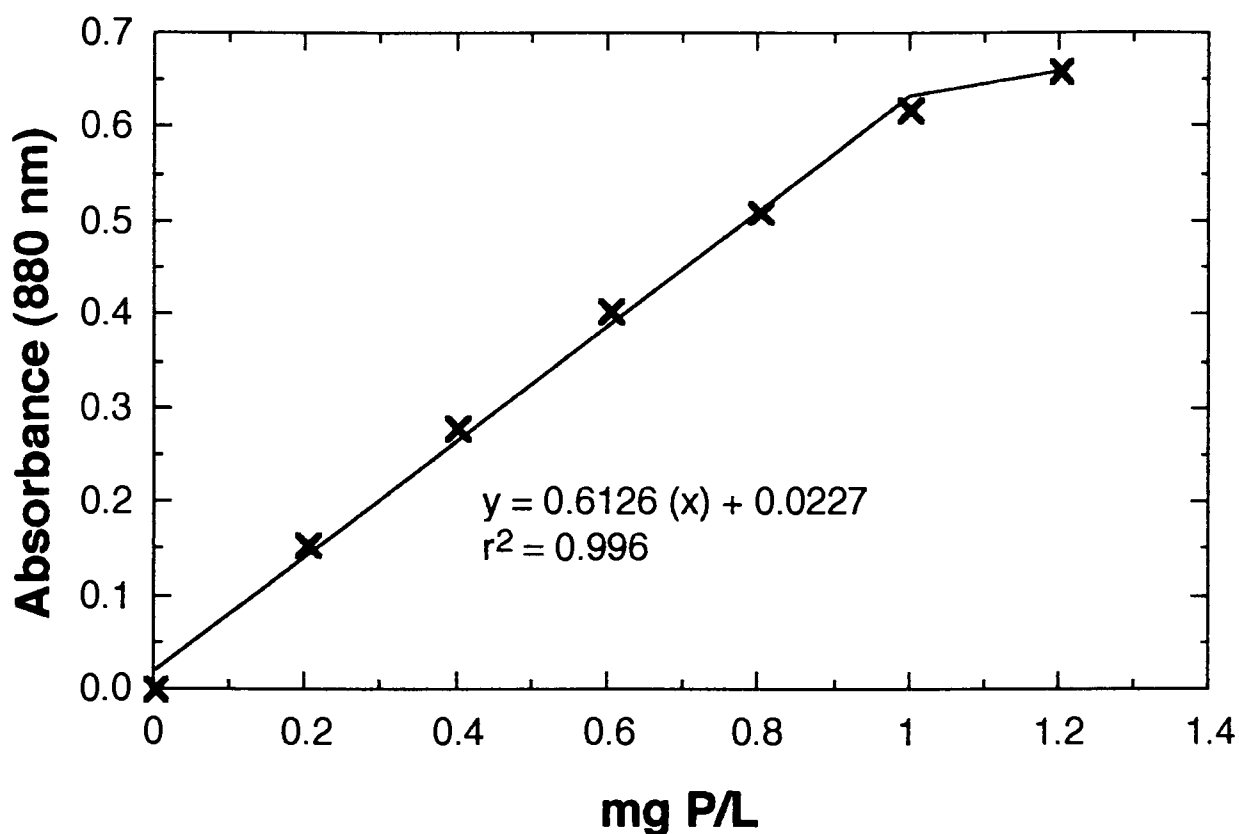


Figure A4.1: Phosphorus calibration curve derived for the standard phosphate solutions using the method of Murphy and Riley (1962). The value for the 1.2 mg/L P standard was ignored in deriving the calibration curve.

Table A4.1: Measured P sorption results for the BS5 filtrates.

Initial P (mg/L)	Absorbance (880 nm)	Dilution	Equilibrium P (mg/L)
0	0.013	-	0
5	0.015	-	0
10	0.020	-	0
20	0.022	-	0
40	0.124	-	0.165
60	0.261	1:2	0.778
80	0.175	1:10	2.49
100	0.164	1:25	5.77
250	0.251	1:250	93.2
500	0.411	1:500	317

Based on the first set of P sorption results, it was decided that interim points were required for the P sorption curve. Therefore, a second P sorption experiment was undertaken involving initial P concentrations of 0 (blank), 150, 200, 250, 300, 400 and 500 mg/L. The same analytical procedure was strictly followed and a new calibration curve was derived (Figure A4.2) in order that the equilibrium P contents (mg P/L) of the second set of BS5 filtrates could be calculated using the equation:

$$\text{equilibrium P (mg/L)} = \frac{\text{absorbance} - 0.0196}{0.6119} \times \text{dilution factor} - \text{measured P}_{\text{blank}}$$

Absorbance readings and equilibrium P results for the second set of BS5 filtrates are presented in Table A4.2.

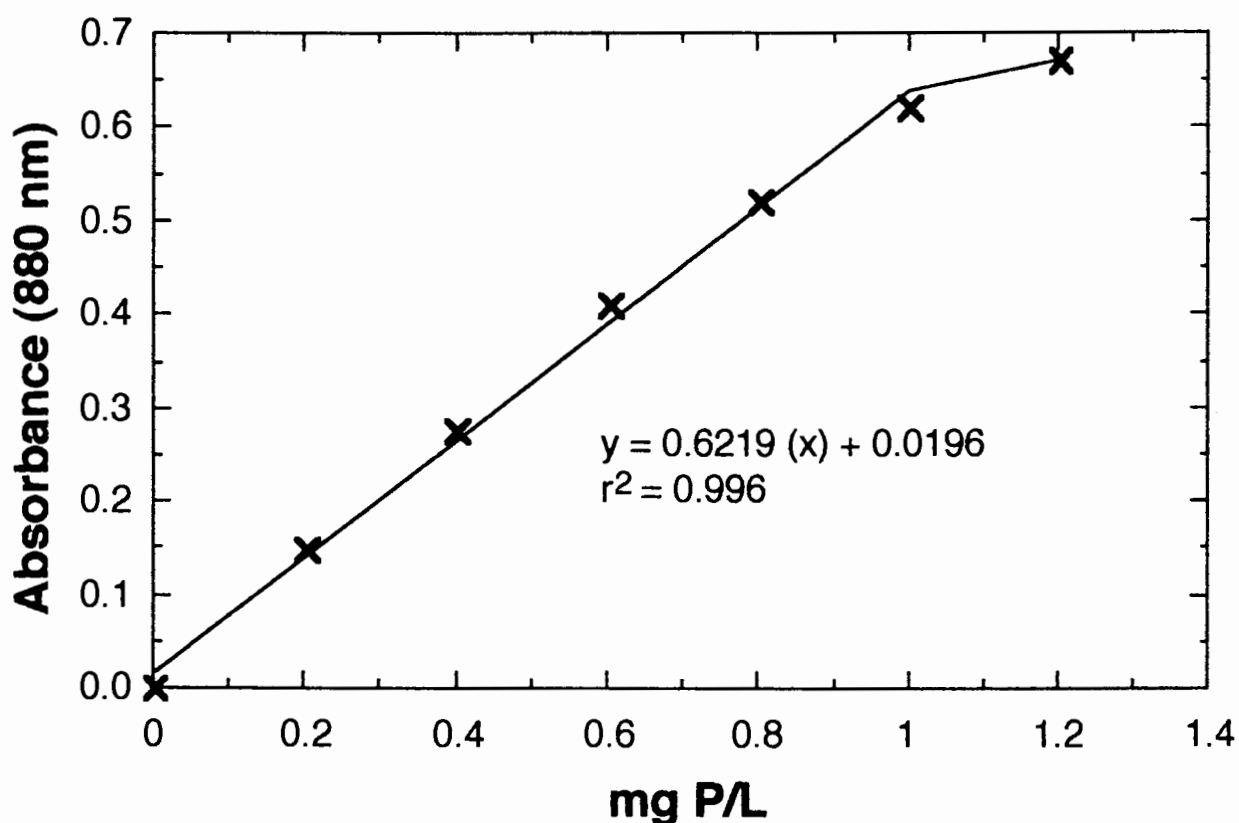


Figure A4.2: Phosphorus calibration curve derived for the second set of standard phosphate solutions using the method of Murphy and Riley (1962). The value for the 1.2 mg/L standard was again ignored in deriving the calibration curve.

Table A4.2: Measured P sorption results for the BS5 filtrates.

Initial P (mg/L)	Absorbance (880 nm)	Dilution	Equilibrium P (mg/L)
0*	0.019	-	0
150	0.351	1:50	26.6
200	0.363	1:100	55.2
250*	0.267	1:250	99.5
300	0.352	1:250	134
400	0.297	1:500	223
500*	0.367	1:500	287

Note: * indicates repeat values

A4.2 Arsenic sorption experiment

Prior to commencement of the As sorption experiment, all glassware and other equipment to be used in sample/standard preparation were soaked overnight in 1:1 HCl and rinsed thoroughly with Milli-Q deionised water. Since one of the intentions of the experimental work was to compare As and P sorption in the Shortlands soil, a standard As solution containing 1209.43 mg As/L was prepared in order to take into account the different atomic weights of As and P when comparing initial adsorbate concentrations. The As standard solution, prepared by dissolving 5.0366 g $\text{Na}_2\text{HAsO}_4 \cdot 7\text{H}_2\text{O}$ in 0.1M NaCl, had a pH of 8.94 and an EC value of 11.19 mS/cm. These values were virtually identical to the values obtained for the P standard solution.

The method used to determine As sorption was identical to that employed for the P sorption study, whereby a 25 mL solution, made up using the standard As solution diluted with 0.1M NaCl to one of the following As concentrations (mg/L): 0 (blank), 44, 97, 145, 194, 242, 363, 484, 605, 726, 968 or 1209 was added to each 2.5 g aliquot of ground, sieved (<2 mm) and air-dried soil. The suspensions were equilibrated via shaking with a horizontal shaker at a constant speed over a 24 hour period. Prior to filtering through Whatman No. 1 filter paper, the samples were centrifuged at maximum rpm for 5 minutes and the pH and EC of each supernatant was measured. The As content of each filtrate was analysed by inductively coupled plasma - mass spectrometry (ICP-MS) at ISCW in Pretoria. Data reported as equilibrium As concentrations (mg/L) were recalculated to sorbed As (mg/kg soil) concentrations as follows:

$$\text{sorbed As (mg/kg soil)} = \text{initial As (mg/L)} - (\text{measured As} - \text{measured As}_{\text{blank}}) \times 10$$

where 10 = solution:soil ratio

In order to examine the accuracy of the analytical procedure, three hidden standards were included with the samples sent to ISCW for As analysis. These standards were prepared by diluting the As standard solution with 0.1M NaCl to 120.9 mg As/L (BAS 10), 12.09 mg As/L (BAS 7) and 1.21 mg As/L (BAS 4). The results of the standard analyses

(Table A4.3) indicate that good accuracy was achieved, with a difference between expected and measured standard values of $\leq 5\%$.

Table A4.3: Results of the standard As analyses by ICP-MS.

	Expected As content (mg/L)	Measured As content (mg/L)	% difference
Standards:			
BAS 4	120.9	122.5	0.66
BAS 7	12.09	13.44	5.29
BAS 10	1.21	1.27	2.42